Dynamic, Stochastic, and Coordinated Optimization for Synchromodal Matching Platforms

Guo, W.

DOI
10.4233/uuid:6806500b-6ed9-4d94-a4d7-17965cfc9ca0

Publication date
2020

Document Version
Final published version

Citation (APA)
Guo, W. (2020). *Dynamic, Stochastic, and Coordinated Optimization for Synchromodal Matching Platforms*. [Dissertation (TU Delft), Delft University of Technology]. TRAIL Research School. https://doi.org/10.4233/uuid:6806500b-6ed9-4d94-a4d7-17965cfc9ca0

Dynamic, Stochastic, and Coordinated Optimization for Synchromodal Matching Platforms

W. Guo

Dynamic, Stochastic, and Coordinated Optimization for Synchromodal Matching Platforms

Proefschrift

ter verkrijging van de graad van doctor
aan de Technische Universiteit Delft,
op gezag van de Rector Magnificus prof. dr. ir. T.H.J.J. van den Hagen,
voorzitter van het College voor Promoties,
in het openbaar te verdedigen op vrijdag 13 November 2020 om 12:30 uur
door

Wenjing GUO

Master of Science in Traffic and Transportation Engineering,
Wuhan University of Technology, Wuhan, China
geboren te Qianjiang, Hubei, China.

Dit proefschrift is goedgekeurd door de promotoren:
Prof. dr. R.R. Negenborn
Dr. W.W.A. Beelaerts van Blokland
Dr. B. Atasoy

Samenstelling promotiecommissie:

Rector Magnificus	voorzitter
Prof. dr. R.R. Negenborn	Technische Universiteit Delft, promotor
Dr. W.W.A. Beelaerts van Blokland	Technische Universiteit Delft, copromotor
Dr. B. Atasoy	Technische Universiteit Delft, copromotor

Onafhankelijke leden:

Prof. T.G. Crainic	Université du Québec à Montréal
Prof. dr. R.A. Zuidwijk	Erasmus University
Prof. dr. ir. Z. Lukszo	TBM, Technische Universiteit Delft
Prof. dr. ir. L.A. Tavasszy	TBM, Technische Universiteit Delft

The research described in this thesis was supported by the China Scholarship Council under grant 201606950003.

TRAIL Thesis Series T2020/16, The Netherlands TRAIL Research School
P.O. Box 5017
2600 GA Delft
The Netherlands
E-mail: info@rsTRAIL.nl

Published and distributed by: W. Guo
Cover design: W. Guo,
E-mail: guowenjing1111@gmail.com

ISBN 979-90-5584-273-5

Keywords: Global synchrmodal transportation, dynamic shipment matching, spot request uncertainty, travel time uncertainty, coordinated planning.

Printed in the Netherlands

"*Strengthen self without stopping, and hold world with virtue.*"
–Book of Changes

Preface

When I recall the whole PhD journey, my feeling is so complicated. To be honest, the PhD life is not as what I expected. But if you ask me that do I regret came to the Netherlands, my answer is of course not. Because if I didn't come here, how can I met these people that are so brilliant, kind, and different. Therefore, I would like to use this chance to thank all the people that helped me during my PhD journey.

First of all, I would like to thank my master supervisor Prof. Wenfeng Li who supported me in applying for the PhD position from TU Delft and the grant from China Scholarship Council. Thank you so much for always being supportive and encouraging. Your scientific way of thinking and professional guidance not only supported my master project but also inspired me to become an independent researcher during my PhD journey.

Besides, I would like to thank the China Scholarship Council for funding my PhD study. I am also grateful to Prof. Gabriël Lodewijks for giving me the chance to join the Section of Transportation Engineering and Logistics.

Next, I would like to show my sincere gratitude to my PhD promoter Prof. Rudy R. Negenborn. Dear Rudy, thanks so much for giving me the chance to conduct my PhD research under your supervising. Your patience, enthusiasm, critical thinking, and expert knowledge constantly guide me to achieve the required level of quality. I am grateful for the time and efforts that you spent on reviewing my work and providing valuable feedback. The monthly discussions we had are always insightful and helpful. Moreover, I really appreciate your help in speeding up the final procedures of my PhD project.

The next person I have to express my appreciation is my co-promoter Dr. Wouter Beelaerts van Blokland. Dear Wouter, thanks for your support during the whole PhD journey. I am grateful for the freedom that you gave me to explore my research interests on the one hand. On the other hand, you always protect me to be on the right track. I will always remember the mountain figure that you drew for me to guide me in achieving the peak point step-by-step. Thanks for your trust and support in the past four years.

My great appreciation goes to my daily supervisor Dr. Bilge Atasoy. Dear Bilge, thanks so much for coming to TU Delft and for joining my supervisory team. I am always thinking that how lucky I am to have such a perfect supervisor. Your timely feedback, detailed comments, and valuable discussions are crucial for my academic achievements. Your keen mind on methodologies, numerical experiments, and managerial insights helped me to become a better researcher. Your constant trust and support keep me always motivated and continuously breaking my limits. Without you, I don't think I can finish my draft thesis within three months with the same quality level. Moreover, I want to thank you for organizing the internal academic seminars where I learned and enjoyed a lot. Also, thanks for giving me the chance to join the Synchromodality project where I learned a lot from industrial scientists.

Besides my supervisors, I would like to thank all the committee members. Dear Prof. Crainic, Prof. Zuidwijk, Prof. Lukszo, and Prof. Tavassay, thanks for the time and efforts that you devoted to reviewing and commenting on my draft thesis. I am looking forward to our discussions during the defence and after that. Especially, I would like to thank Prof. Crainic for providing me the postdoc position in your team. Looking forward to our collaboration in Canada!

Many thanks to the colleagues and friends in the TEL section and beyond for the happy times during my PhD. Dear Xiao, Xiaojie, Rie, Breno, Johan, and Frederik, having you as colleagues was a blessing. I enjoyed and learned so much from our discussions about intermodality vs synchromodality, model predictive control vs rolling horizon approach, combinatorial optimization, reinforcement learning, collaborative planning, and distributed approaches. Our general talks during coffee breaks and lunch times are also valuable memories during my PhD life. Dear Xiao, Kai, Qingsong, Linyin, Guangming, Jie, Zhe, Yimeng, Zhikang, Yi, Meng, Daniella, Thais, and Fayezeh, thanks for the great times we had together in traveling, cycling, walking, badminton, table tennis, barbecues, hotpots, and board games. Besides, I would like to thank Dick for translating my thesis summary into Samenvaatting. Many thanks to our secretaries, especially Patty, for always being kind and helpful during my PhD journey.

Finally, I want to thank my closest family. Dear father, mother, and sister, thanks so much for your love and support throughout my life. Thanks for giving me the strength to chase my dreams. Your unconditional love is the light that supports me going through the hardest times during my PhD journey.

Wenjing Guo,
Delft, October 2020

Contents

List of Figures

List of Tables

List of notations

Below follows a list of the most frequently used notations in this thesis.

A_{ri}	arrival time of shipment r at terminal i
b_i	the i^{th} breakpoint of time-dependent travel time functions of truck services, $i = \{1, 2, ..., I\}$
c^{emission}	activity-based carbon tax charged by institutional authorities
c_i^{storage}	storage cost at terminal i per container per hour
c_r^{delay}	delay cost of request $r \in R$ per container per hour overdue
c_s	travel cost of service $s \in S$ per container
c_{rp}	the total cost of matching request $r \in R$ with path $p \in P$
d_r	destination terminal of request $r \in R, d_r \in N$
d_s	destination terminal of service $s \in S, d_s \in N$
e_s^k	carbon emissions of service $s \in S$ per container with type $k \in K$
f_{ri}	transshipment cost of request $r \in R^t \cup \bar{R}^t$ at terminal $i \in N$ per container
f_{ri}^+	loading cost of request $r \in R$ at terminal $i \in N$ per container
f_{ri}^-	unloading cost of request $r \in R$ at terminal $i \in N$ per container
h	time stage indices
H	length of the prediction horizon
$\mathbb{H}$	prediction stages after decision epoch t, $\mathbb{H} = \{t+1, ..., \max\{t+H, T\}\}$
i	terminal indices
I_v	itinerary of vehicle $v \in V \backslash V^{\text{truck}}$
I_v^n	the n^{th} service of vehicle $v \in V \backslash V^{\text{truck}}, I_v^n \in S \backslash S^{\text{truck}}$
k	container type indices
K	container types, $K = \{\text{dry}, \text{ reefer}\}$
l_{sq}	a binary variable equal to 0 if service s is the preceding service of service q, otherwise 1
L	the largest number of services in a path
m	mode indices
M	modes, $M = \{\text{ship}, \text{ barge}, \text{ train}, \text{ truck}\}$
$\mathbf{M}$	a large number used for binary constraints
n	iteration indices
n_{rs}	an integer variable used for normalizing departure time of truck service $s \in S^{\text{truck}}$ with request $r \in R$
N	terminals
N^1	terminals within the export hinterland network

N^2	terminals within the intercontinental network
N^3	terminals within the import hinterland network
N^{exp}	export terminals, $N^{\text{exp}} = N^1 \cap N^2$
N^{imp}	import terminals, $N^{\text{imp}} = N^2 \cap N^3$
$N^{\text{iteration}}$	maximum number of iteration
o_r	origin terminal of request $r \in R$, $o_r \in N$
o_s	origin terminal of service $s \in S, o_s \in N$
o	operator indices
O	set of local operators, $O = \{1,2,3\}$
p	path indices
p_r	freight rate of request $r \in R$
P	set of feasible paths
P_{ij}^l	set of feasible paths with $l \in \{1,...,L\}$ services that depart from terminal $i \in N$ and arrive at terminal $j \in N$
r	shipment request indices
R	shipment requests, $R = R^0 \cup R^1 ... \cup R^T$
R^0	requests received before the planning horizon
R^{0k}	requests received before the planning horizon with container type k
R^t	requests received during time interval $(t-1,t], t > 0$
R^{tk}	requests received during time interval $(t-1,t], t > 0$ with container type k
$\bar{R}^t$	accepted requests that require reoptimization at decision epoch t due to infeasible transshipments, $t > 0$
$\bar{R}^{tk}$	accepted requests that require reoptimization at decision epoch t due to infeasible transshipments, $t > 0$ with container type $k \in K$
$\hat{R}^t$	requests received before stage t and will expire before stage $t+1$
$\acute{R}^t$	requests received before stage t and will expire after t
s	transport service indices
S	services, $S = S^{\text{ship}} \cup S^{\text{barge}} \cup S^{\text{train}} \cup S^{\text{truck}}$
S^o	services belong to operator o
S^m	services with mode $m \in M$
S_i^+	services departing at terminal $i \in N$, $S_i^+ = S_i^{+\text{ship}} \cup S_i^{+\text{barge}} \cup S_i^{+\text{train}} \cup S_i^{+\text{truck}}$
S_i^{+m}	services departing at terminal $i \in N$ with mode $m \in M$
S_i^-	services arriving at terminal $i \in N$, $S_i^- = S_i^{-\text{ship}} \cup S_i^{-\text{barge}} \cup S_i^{-\text{train}} \cup S_i^{-\text{truck}}$
S_i^{-m}	services arriving at terminal $i \in N$ with mode $m \in M$
S^{+t}	services departing at origin terminals during time interval $(t-1,t]$
S^{-t}	services arriving at destination terminals during time interval $(t-1,t]$
t	decision epoch indices
t_s	scheduled travel time of service $s \in S$
$\bar{t}_s$	actual travel time of service $s \in S$
$\tilde{t}_s$	travel time of service $s \in S$, $\tilde{t}_s \sim N(\mu_s, \sigma_s^2)$
t_{rs}^{truck}	travel time of service $s \in S^{\text{truck}}$ with request $r \in R$
$t_s(\tau)$	time-dependent travel time function of truck service s with departure time τ
t_{ri}^-	arrival time of request r at export and import terminal $i \in N^{\text{exp}} \cup N^{\text{imp}} \backslash \{o_r, d_r\}$
t_{ri}^+	departure time of request r at export and import terminal $i \in N^{\text{exp}} \cup N^{\text{imp}} \backslash \{o_r, d_r\}$
T	length of the planning horizon

T^m	the m^{th} time period within a day, $T^m = [b_m, b_{m+1}]$, $m = \{1,2,...,I-1\}$
$\mathbb{T}_r^{\text{announce}}$	announce time of request $r \in R$
$\mathbb{T}_r^{\text{release}}$	release time of request $r \in R$
$\mathbb{T}_r^{\text{due}}$	due time of request $r \in R$
$\mathbb{T}_r^{\text{delay}}$	delay of request $r \in R^t \cup \bar{R}^t$ at destination terminal d_r in deterministic models
$\tilde{\mathbb{T}}_r^{\text{delay}}$	delay of request $r \in R^t \cup \bar{R}^t$ at destination terminal d_r in stochastic models
u_r	container volume of request $r \in R$
U_s	free capacity of service $s \in S$
U_s^t	free capacity of service $s \in S$ at decision epoch t
U_s^{tk}	free capacity of service $s \in S$ at decision epoch t for container type $k \in K$
V	vehicles $V = V^{\text{ship}} \cup V^{\text{barge}} \cup V^{\text{train}} \cup V^{\text{truck}}$
V^m	vehicles with mode $m \in M$
w_{ri}	storage time of request $r \in R^t \cup \bar{R}^t$ at terminal $i \in N$ in deterministic models
$\tilde{w}_{ri}$	storage time of request $r \in R^t \cup \bar{R}^t$ at terminal $i \in N$ in stochastic models
x_{rs}	binary variable; 1 if request $r \in R$ is matched with service $s \in S$, 0 otherwise
x_{rs}^t	binary variable; 1 if request $r \in R^t \cup \bar{R}^t$ is matched with service $s \in S$ at decision epoch t, 0 otherwise
$\hat{x}_{rs}^{\gamma h}$	binary variable; 1 if sample request $r \in \omega^{\gamma h}$ is matched with service $s \in S$ at decision epoch t, 0 otherwise
y_r^t	binary variable; 1 if request $r \in R^t$ is accepted at decision epoch t
$\hat{y}_r^{\gamma h}$	binary variable; 1 if sample request $r \in \omega^{\gamma h}$ is accepted at decision epoch t
z_{rp}	binary variable; 1 if request $r \in R$ is matched with path $p \in P$, 0 otherwise
z_{rp}^t	binary variable; 1 if request $r \in R^t \cup \bar{R}^t$ is matched with path $p \in P$, 0 otherwise
$\hat{z}_{rp}^{\gamma h}$	binary variable; 1 if sample request $r \in \omega^{\gamma h}$ is matched with path $p \in P$ at decision epoch t, 0 otherwise
z_{rsq}^t	binary variable; 1 if request $r \in R^t \cup \bar{R}^t$ is matched with service $s \in S$, $x_{rs} = 1$ and service $q \in S$, $x_{rq} = 1$, 0 otherwise
CT_r	container type of request $r \in R, CT_r \in K$
IR_r	itinerary of request $r \in R^t \cup \bar{R}^t$ consists of matched services
lc_i^m	loading/unloading cost per container at terminal $i \in N$ with mode $m \in M$
lt_i^m	loading/unloading time at terminal $i \in N$ with mode $m \in M$
LD_r	lead time of request $r \in R$, $LD_r = \mathbb{T}_r^{\text{due}} - \mathbb{T}_r^{\text{release}}$
MT_s	mode of service $s \in S, MT_s \in M$
$MT_v^{'}$	mode of vehicle $v \in V$
TA_s	scheduled arrival time of service $s \in S \backslash S^{\text{truck}}$
$\bar{T}A_s$	actual arrival time of service $s \in S \backslash S^{\text{truck}}$
$\tilde{T}A_s$	arrival time of service $s \in S \backslash S^{\text{truck}}$, $\tilde{T}A_s \sim N(\mu_s^-, \sigma_s^{-2})$
TD_{rs}	departure time of truck service $s \in S^{\text{truck}}$ with request $r \in R^t \cup \bar{R}^t$
TD_s	scheduled departure time of service $s \in S \backslash S^{\text{truck}}$
$\bar{T}D_s$	actual departure time of service $s \in S \backslash S^{\text{truck}}$
$\tilde{T}D_s$	departure time of service $s \in S \backslash S^{\text{truck}}$, $\tilde{T}D_s \sim N(\mu_s^+, \sigma_s^{+2})$
$TD_v^{'}$	departure time of vehicle $v \in V \backslash V^{\text{truck}}$ at its origin terminal
α	confidence level

β	traffic congestion coefficients
δ	optimization interval
Γ	number of scenarios
$\omega^{\gamma h}$	sampled requests under scenario $\gamma \in \{1, ..., \Gamma\}$ at stage $h \in \mathbb{H}$
Ω^t	entire populations of shipment requests after stage t
μ_s	mean of the travel time of service $s \in S$
μ_s^+	mean of the departure time of service $s \in S$
μ_s^-	mean of the arrival time of service $s \in S$
σ_s	standard deviation of the travel time of service $s \in S$
σ_s^+	standard deviation of the departure time of service $s \in S$
σ_s^-	standard deviation of the arrival time of service $s \in S$
ξ_s^-	preceding service of service s operated by the same vehicle
ξ_s^+	succeeding service of service s operated by the same vehicle
θ_s^m	the slope of the travel time function of truck service s for time period T^m
η_s^m	the intersection of the travel time function of truck service $s \in S^{\text{truck}}$ for time period T^m
τ_{rs}	departure time of truck service $s \in S^{\text{truck}}$ with request $r \in R$
$\tau_{rs}^{'}$	normalized departure time of truck service $s \in S^{\text{truck}}$ with request $r \in R$, $0 \leq \tau_{rs}^{'} \leq 24$
ζ_{rs}^k	a continuous variable used for linearizing the time-dependent travel time function of truck service $s \in S^{\text{truck}}$, $0 \leq \zeta_{rs}^k \leq 1$
ξ_{rs}^m	a binary variable used for linearizing the time-dependent travel time function of truck service $s \in S^{\text{truck}}$
Φ	set of feasible matches
λ	Lagrangian multipliers
ρ	penalty parameters

Chapter 1

Introduction

This thesis focuses on dynamic, stochastic, and coordinated approaches for shipment matching in global synchromodal transportation. In this chapter, the research background, the research challenges, the research objectives and questions, the contributions, and the outline of this thesis are described. This chapter is structured as follows. In Section 1.1, the research background in global container transportation is introduced. Section 1.2 presents the research challenges. Section 1.3 formulates the research questions and approaches of this thesis. Finally, the contributions and the outline of this thesis are presented in Section 1.4 and Section 1.5, respectively.

1.1 Research background

Global freight transportation involves the movement of cargoes between inland locations in different continents by road, rail, air, water or any combination of them [55], as shown in Figure 1.1. It consists of three segments: hinterland transportation in continent A, intercontinental transportation between continent A and B, and hinterland transportation in continent B. The handling activities (e.g., unloading, loading) between different modes at transshipment terminals can be facilitated by using standardized loading units (i.e., containers) [87]. With the increasing rate of containerization in global trades, efficient global container transport planning becomes more and more important in the management of global supply chains.

Traditionally, global container transportation is organized by multiple stakeholders (e.g., inland carriers, ocean carriers) independently without information and resource sharing, which causes high logistics costs, long delivery delays, and heavy carbon emissions. To improve the competitiveness in global trade, more and more stakeholders turn to form alliances to provide transport services integrally from vertical level as well as horizontal level [9], namely synchromodal transportation. While horizontal integration refers to the collaboration among competing carriers doing similar activities (e.g., transport services with different modes), vertical integration indicates the collaboration among carriers operating at different levels of the same transport chain (e.g., the collaboration between an inland railway company and an ocean carrier). The vertical and horizontal integration brings a larger and more complex global network, as shown in Figure 1.2. Synchromodality is the pro-

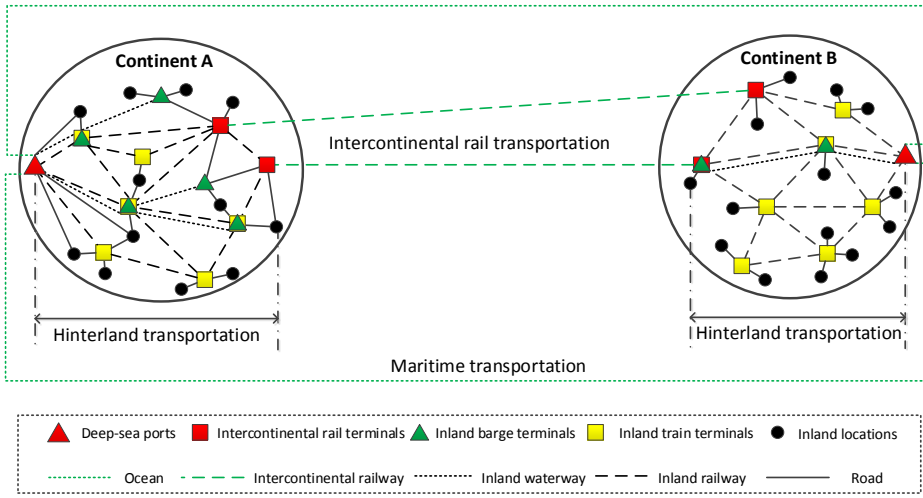

Figure 1.1: Topology of global freight transport network.

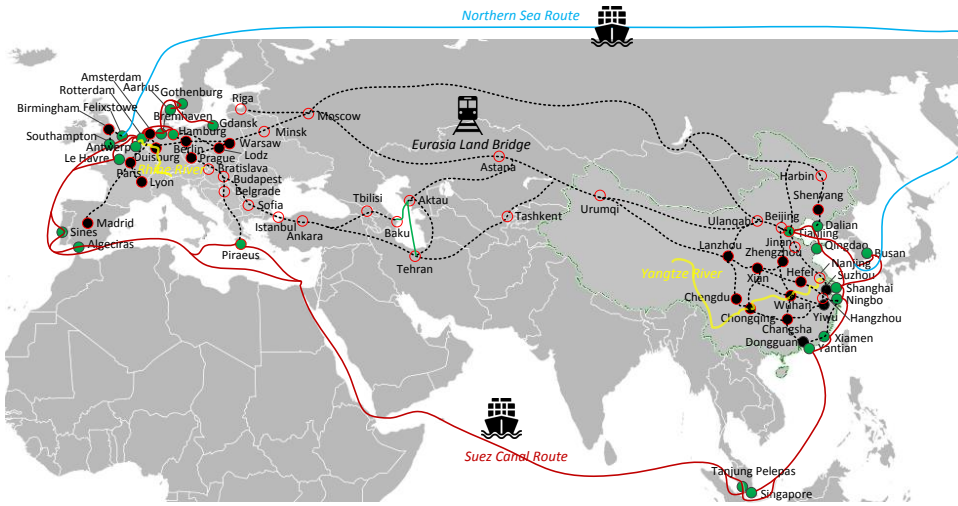

Figure 1.2: Map of the integrated global network representing our vision.

vision of efficient, reliable, flexible, and sustainable services through the coordination and cooperation of stakeholders and the synchronization of operations in integrated networks driven by information and communication technologies and intelligent transportation system technologies [30].

A synchromodal transport system consists of several types of entities that interact with each other, mainly including shippers, carriers, and network operators [99]. Shippers represent the entities who are searching for services to transport their shipments. Examples of shippers include freight forwarders and third party logistics (3PL) companies. Carriers are the entities that provide transport services for part of the transport chain (e.g., for mar-

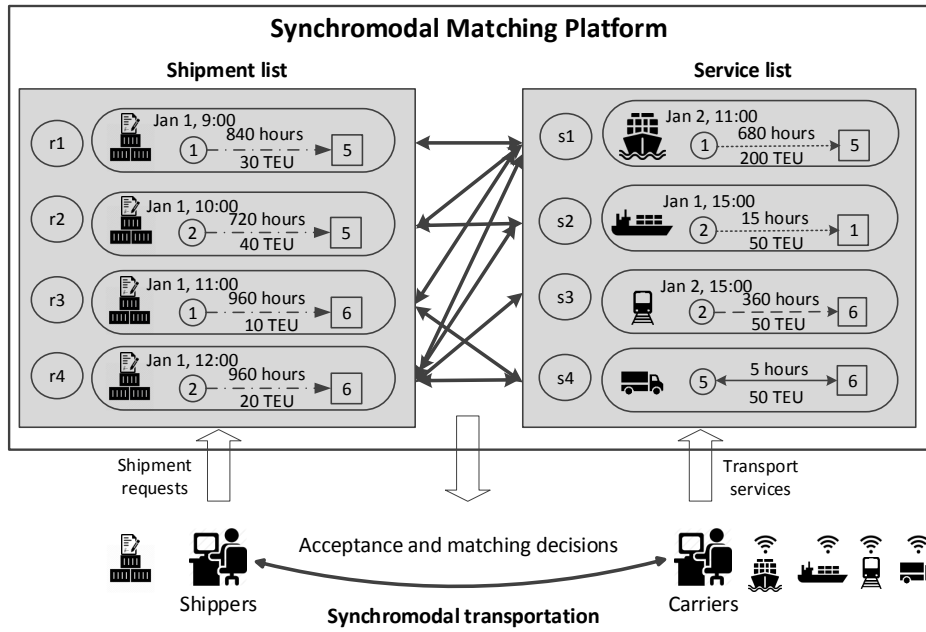

Figure 1.3: Synchromodal matching platform.

itime transportation or inland railway transportation). Carriers could be drayage operators, railway companies, or shipping lines. In this thesis, we use network operators to represent the alliances formed by multiple carriers who operate integrated networks. Specifically, network operators receive shipment requests (including shipments' origin, destination, release time, lead time, and volume) from shippers and receive transport services (including services' origin, destination, departure time, arrival time, and capacity) from carriers. The network operators aim to provide integrated transport plans.

With the development of digitalization, increasing companies in logistics industries have evolved in providing online booking platforms that support real-time decisions, such as Saloodo!, Sjipit, Uber Freight, Quicargo, Maersk. In this thesis, we consider a synchromodal matching platform owned by a network operator that receives real-time shipment requests from shippers, and receives real-time travel times of multimodal services from carriers, as shown in Figure 1.3. The platform aims to provide optimal acceptance and matching decisions in an integrated network. A match between a shipment request and a transport service represents that the shipment will be transported by the service from the service's origin to the service's destination. The platform combines the matched services into itineraries to provide integrated transport for shipments. For example, request r4 might be transported by barge service s2 from origin 2 to terminal 1, and further transported by ship service s1 from terminal 1 to 5, and finally transported by truck service s4 from terminal 5 to destination 6.

This thesis develops methodologies for synchromodal matching platforms to optimize the matches between shipment requests with specific time windows and transport services with specific time schedules considering the trade-off between logistics costs, delays, and carbon emissions.

1.2 Research challenges

The synchromodal matching platforms support the efficiency of emerging operational and business models for transportation and logistics (e.g., City Logistics, Physical Internet, and Synchromodality) that aim to jointly achieve economic, environmental, and societal objectives [17]. However, due to the existing challenges, operating a synchromodal matching platform is very complex. The five aspects of challenges are briefly discussed as follows:

RC1. Synchromodal shipment matching with time-dependent travel times

In the literature, the intermodal routing choice (IRC) problem is most similar to the synchromodal shipment matching (SSM) problem proposed in this thesis. However, the majority of IRC problems focus on the assignment of modes to commodities. Therefore, the IRC models are typically developed at the container flow level [49]. In comparison, the SSM problem focuses on the matches between services with specific time schedules and shipments with specific time windows. Besides, due to the limited capacity of transport infrastructures, traffic congestion exists during several times of a day [90]. Travel speed of transport services is thus affected by traffic conditions, which results in time-dependent travel times. In synchromodal transportation, ignoring the time-dependent travel times of services might result in suboptimal solutions or even infeasible transport plans because of the transshipment operations between different services. However, in the literature, the majority of the models considering time-dependent travel times are designed for vehicle routing problems [42, 91]. How to design shipment matching with time-dependent travel times in synchromodal transportation leads to one of the research challenges.

RC2. Real-time shipment requests

The trend towards spot markets and digitalization in container transportation increases the need for online synchromodal matching platforms. In the literature, most of the existing studies assume that container shipments are only collected from large shippers based on long-term contracts. These contractual shipment requests are often fixed and known over a given planning period. Recently, quite a few studies [105, 106] have pointed out the trend towards spot markets in container transportation. Different from the former contracted requests, spot shipment requests arrive in real-time and require receiving transport solutions as soon as possible. Thanks to the development of digitalization and advanced information and communication technologies in logistic industries, information can be collected in real-time, and decisions can be made online [68]. Nevertheless, these new trends also introduce complexity in synchromodal transport planning, unveiling the need for decision support systems adapted to dynamic contexts.

RC3. Spot request uncertainty

The advance of information and communication technologies as well as the growing amount of available historical data makes it possible to gather stochastic information of random variables for advanced decision-making in freight transportation [75]. Decisions with the consideration of uncertainties have been proved to have better performance in many research domains, such as resource allocation problems [109], service

network design problems [77], and pickup and delivery problems [31]. By incorporating stochastic information of spot requests into online decision-making processes, the synchromodal matching platform might hold some capacity for future requests which are predicted to be more "important." In this way, decisions made for current requests might be suboptimal but the global performance over the planning horizon might be "optimal." The SSM problem is therefore not only dynamic but also stochastic. The challenge faced by dynamic and stochastic problems is known as the curse of dimensionality. How to solve dynamic and stochastic shipment matching problem in synchromodal transportation is another research challenge.

RC4. Travel time uncertainty

The travel times of transport services are quite uncertain in real-world [29]. The reason can be explained by traffic congestion, limited handling capacities of terminals, and external disruption events (e.g., port closure due to high wind, poor weather such as fog and wind) [18]. Due to travel time uncertainty and the utilization of multimodal services, the matches made for accepted requests might become suboptimal or even infeasible at transshipment terminals. Thanks to the development in data analytics, probability distributions of uncertainties are often available to transport systems [29]. However, while stochastic approaches that incorporating stochastic information of travel times in decision-making processes have been well investigated in vehicle routing problems [21, 51] and pickup and delivery problems [56, 83], the stochastic approach for the SSM problem in synchromodal transportation under travel time uncertainty is still missing.

RC5. Coordinated planning

In the literature, the majority of studies assume a centralized controller that provides integrated decisions in synchromodal transportation [30]. However, in practice, a large number of entities are involved in global container transport and they may not all be willing to give authority to a centralized platform [46]. To deal with this issue, the coordination mechanism among them and incentives to stimulate cooperation need to be deployed. Under coordinated planning, a synchromodal transport system will be decomposed into several sub-systems. These sub-systems are optimized separately under local constraints as well as under the incentives imposed by cooperative systems to meet the constraints in interconnections. In this way, these local decision makers cooperate to achieve global optimum. While extensive coordination mechanisms and incentives have been proposed in vehicle routing problems [28], only a few studies investigated in intermodal transportation [25, 50, 71]. The coordination mechanisms for global synchromodal transportation with dynamic and stochastic shipment matching is still missing.

1.3 Research questions and approaches

The overall research question of this thesis is **how to develop methodologies that support the decision-making processes of synchromodal matching platforms under dynamic, stochastic, and distributed environments**. To address each of the research challenges we have specific research questions (RQs) for each, presented as follows:

RQ1. How to model shipment matching with time-dependent travel times in hinterland synchromodal transportation? (**RC1**)

To address research question **RQ1**, a mathematical model for synchromodal shipment matching with time-dependent travel times is developed in Chapter 3.

RQ2. How to deal with real-time shipment requests in hinterland synchromodal transportation? (**RC2**)

To address research question **RQ2**, a dynamic approach and a heuristic algorithm to deal with real-time shipment requests in hinterland synchromodal transportation are developed in Chapter 4.

RQ3. How to address spot request uncertainties in hinterland synchromodal shipment matching? (**RC3**)

To address research question **RQ3**, a stochastic approach to address spot request uncertainty in hinterland dynamic shipment matching is proposed in Chapter 5.

RQ4. How to address travel time uncertainties in global synchromodal shipment matching? (**RC4**)

To address research question **RQ4**, a hybrid stochastic approach to address spot request and travel time uncertainties simultaneously in global synchromodal transportation is developed in Chapter 6.

RQ5. How to design coordinated mechanisms that facilitate cooperative planning in global synchromodal transport? (**RC5**)

To address research question **RQ5**, distributed approaches to facilitate coordinated planning in global synchromodal transportation are proposed in Chapter 7.

1.4 Thesis contributions

The main contributions of this dissertation are as follows:

- A mixed integer linear programming model for synchromodal shipment matching with time-dependent travel times is developed in [39] (see also Chapter 3). The model formulates binary variables to indicate the matches between specific shipments and services and applies time-dependent travel time functions for truck services. The model helps network operators to achieve efficient, effective, and sustainable transport planning.

- A rolling horizon approach is proposed to handle newly arrived shipment requests in [37] (see also Chapter 4). The implementation of the rolling horizon approach relies on an optimization algorithm that can generate timely matching decisions at each decision epoch. Thus, a heuristic algorithm is developed to solve the SSM problem. With the proposed approaches, the use of barges, trains, and trucks can be managed more effectively taking into account their impact on transport time, costs, and emissions together with different time sensitivities of shipments.

- A Markov decision process model is proposed to describe the SSM problem in hinterland transportation. Due to the curse of dimensionality, a stochastic approach is proposed to solve the problem under realistic instances in [33] (see also Chapter 5). The stochastic approach uses a sample average approximation method to approximate expected objective functions and applies a progressive hedging algorithm to get solutions at each decision epoch of a rolling horizon framework. This approach enables to consider a large set of scenarios to more accurately represent the stochasticity and this in turn increases the benefits of incorporating stochastic information in dynamic decision-making processes.

- A Markov decision process model that integrates acceptance and matching decisions is proposed to describe the SSM problem with spot request uncertainty and travel time uncertainty in global transportation. To solve the problem, a hybrid stochastic approach that integrates a rolling horizon framework, a chance-constrained programming model, and a sample average approximation method with a preprocessing-based heuristic algorithm is developed in [35] (see also Chapter 6). With the proposed approach, the global synchromodal matching platform can achieve better performance in logistics costs, delays, and carbon emissions.

- Three distributed optimization approaches are proposed to deal with interconnecting constraints between local operators in [34] (see also Chapter 7). Theses approaches contribute significantly to synchronizing different operations in synchromodal transport chains. In turn, these approaches not only improve the efficiency of operations within each operator but also help to avoid large delays at destination terminals. Under the proposed coordination schemes, the cooperation among local operators is at the level of information exchange among local operators and each operator shares only a limited amount of information with others.

1.5 Thesis outline

Hinterland transportation, as a key component of global transportation, has different time scales, transport modes, and network topology from intercontinental transportation. In this thesis, relevant methodologies that support the decision-making processes of synchromodal matching platforms are developed for hinterland and global transportation, respectively. Specifically, mathematical models, dynamic and stochastic approaches are discussed for hinterland synchromodal transportation from a more centralized perspective in Chapters 3, 4, and 5. Then, these methodologies combined with distributed approaches are discussed for global synchromodal transportation in Chapters 6 and 7. Figure 1.4 presents the outline of the thesis. The main contents of Chapters 2-8 are as follows:

In Chapter 2, a survey on opportunities and challenges faced by decision makers in synchromodal transportation is presented.

In Chapter 3, a mixed integer linear programming (MILP) model is developed to describe the synchromodal shipment matching problem in hinterland transportation. Time-dependent travel times of truck services have been considered in the MILP model.

To deal with real-time shipment requests, a rolling horizon approach is proposed for hinterland synchromodal transportation in Chapter 4. The implementation of the RHA relies

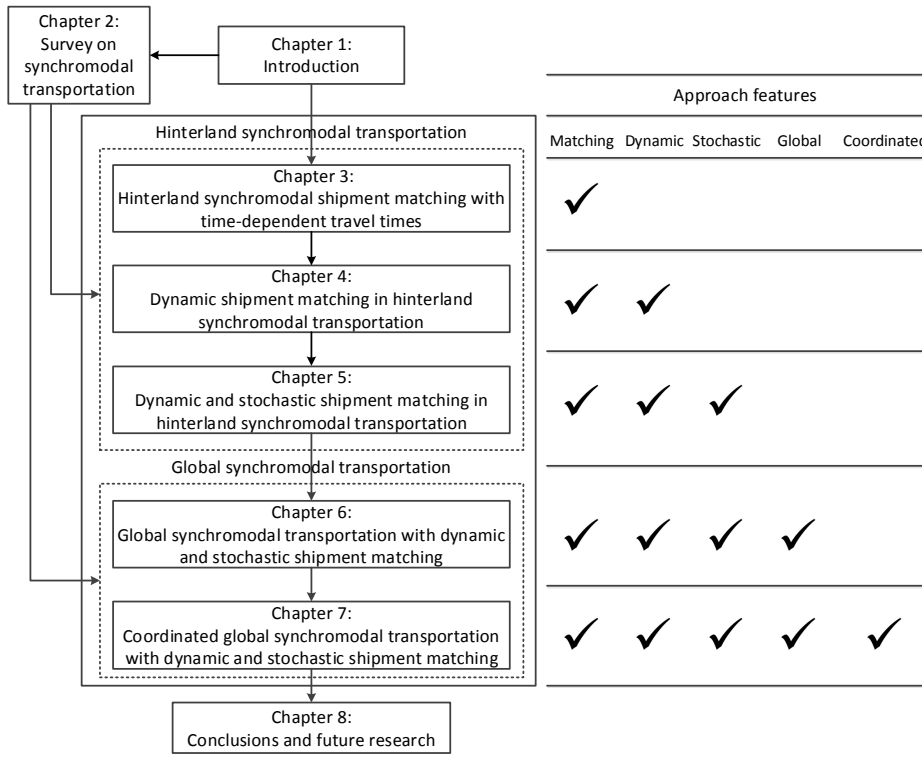

Figure 1.4: Outline of the thesis and main features of the approaches proposed.

on an optimization algorithm that generates timely solutions at each decision epoch. A heuristic algorithm is therefore designed to solve the MILP model proposed in Chapter 3.

To investigate the benefits of incorporating stochastic information of spot requests, in Chapter 5, we propose an anticipatory approach for dynamic shipment matching in hinterland synchromodal transportation. Compared with the myopic approach proposed in Chapter 4, the anticipatory approach proposed in Chapter 5 has better performance in total costs, delays, and carbon emissions.

In terms of dynamic shipment matching in global synchromodal transportation, in Chapter 6, we develop a hybrid stochastic approach to address spot request and travel time uncertainties integrally. Specifically, the approach consists of a rolling horizon framework that handles real-time information, a chance-constrained programming model that deals with travel time uncertainty, a sample average approximation method that addresses spot request uncertainty, and a preprocessing-based heuristic algorithm that generates timely solutions at each decision epoch.

Due to the distributed nature of global synchromodal transport systems, the local operators may not all be willing to give authority to a centralized platform. To stimulate cooperative planning among local operators, three distributed optimization approaches are developed in Chapter 7.

Chapter 8 states the main conclusions of the thesis and presents recommendations for future research.

Chapter 2

Survey on synchromodal transportation

In Chapter 1, this thesis was placed in the literature of synchromodal transport planning. It was shown that the research on dynamic, stochastic, and coordinated synchromodal shipment matching problems is limited. What's more, none of the existing studies investigated the benefits of incorporating stochastic information in dynamic shipment matching under coordinated synchromodal transport systems. While some studies lie in hinterland synchromodal transportation, only a few investigated global synchromodal transportation. This thesis aims to contribute to that literature by studying the dynamic, stochastic, and coordinated shipment matching in global synchromodal transportation.

To define the contribution of this thesis in the literature of synchromodal transportation, this chapter presents a structured overview of the recent literature. In Section 2.1, the definition of synchromodal transportation and its development are discussed. In Section 2.2, the critical success factors are illustrated. After that, we analyze the network-wide synchromodal planning problems at strategic, tactical, and operational level, respectively. The strategic infrastructure network design problem is described in Section 2.3. Section 2.4 analyzes the tactical service network design problem. Operational intermodal routing choice problem is discussed in Section 2.5. Finally, overall conclusions are provided in Section 2.6.

Parts of this chapter have been published in [38]: "W. Guo, W. Beelaerts van Blokland, G. Lodewijks. Survey on characteristics and challenges of synchromodal transportation in global cold chains. In *Proceedings of the 8th International Conference on Computational Logistics*, pages 420-434, Southampton, UK, 2017."

2.1 Introduction

With the increasing volume of containers in global trade, intermodal transportation has been developed for integrated transport in the last decades [99]. The International Transport Forum defined intermodal transportation as: multimodal transport of goods, in the same transport unit by successive modes of transport without handling of goods themselves when changing modes [43]. Compared with truck transportation, intermodal transportation can

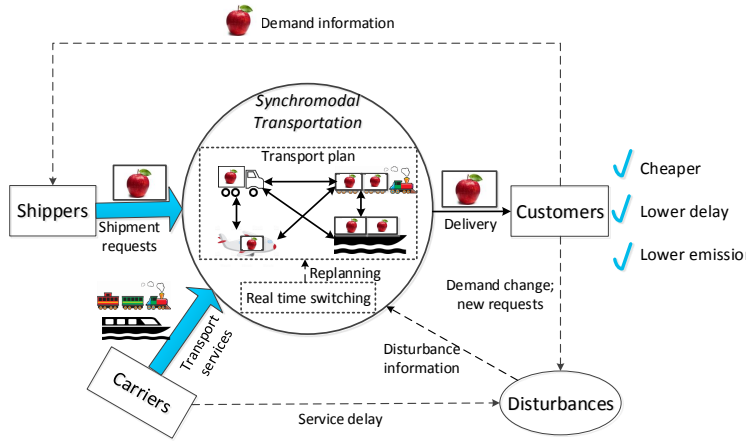

Figure 2.1: A framework of synchromodal transportation.

largely reduce logistics costs and emissions but has less flexibility for disturbances [103]. The capacity sharing of services among different shippers contributes to cost reduction, and the utilization of barges and trains brings about less emissions. However, in global container transport, multiple uncertainties might exist during the transportation from origin to destination. The impact of disturbances (such as service delay and traffic congestion) for shipments in intermodal transportation is very critical. A dynamic and stochastic intermodal transport plan is therefore needed. However, current intermodal transport planning models tend to be static and deterministic, resulting in less flexibility for disturbances [87].

Although intermodality has been discussed for decades, truck transportation still occupies the largest share in hinterland transportation, which causes transport congestion and environmental pollution. The main reason is that current intermodal transport systems do not have good performance under dynamic and stochastic environments. According to the statistics, in 2014 about 75.4% of total freight transportation in European Union countries were transported via road, around 18% via rail, and 6.6% via inland waterways. The Netherlands has better performance, with 56.1%, 4.9%, and 39%, respectively [23]. Recently, global supply chains are confronted with increasing consumer demands on sustainability [97]. Sustainability commonly refers to how the needs of the present human generation can be met without compromising the ability of future generations to meet their needs [112]. In terms of sustainable transportation, it generally relates to less carbon emissions. Increasing the utilization of barges and trains in hinterland transportation can reduce emissions on one side. On the other side, the mathematical models become more complex due to the transshipment operations between different modes [18].

Synchromodal transportation, as an extension of intermodal transportation, is a potential method for global supply chains to reach better performance, first proposed by Tavasszy in 2010 [74]. It refers to creating an effective, efficient, and sustainable transport plan for all shipments by using real-time information [99], as shown in Figure 2.1. Under synchromodality, the transport services for shipments can be changed before or during the transportation in case of disturbances. The capacity of barges and trains will be better used in hinterland transportation for reducing logistics costs and emissions. The main objectives

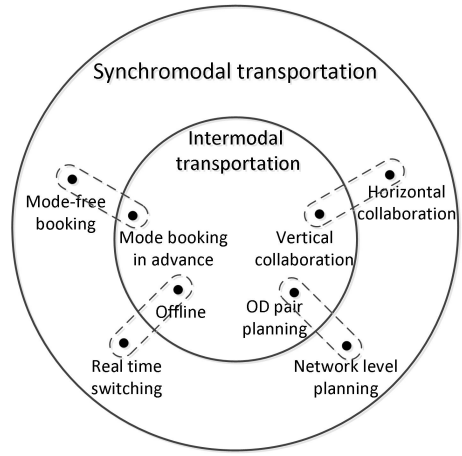

Figure 2.2: Synchromodality versus intermodality.

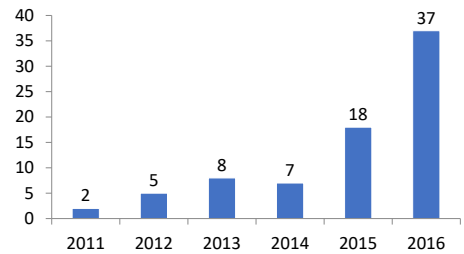

Figure 2.3: Publication trends of synchromodal transportation.

of synchromodal transportation focus on reducing logistics costs, emissions, and delays in delivery [62]. Therefore, this new transport concept has benefits for both economy, society, and environment aspects.

Compared with intermodality, synchromodality has several distinct features, as shown in Figure 2.2. Firstly, it aims at horizontal collaboration as well as vertical collaboration. Horizontal collaboration can promote information sharing among different carriers, avoiding vicious competition. Secondly, the mode booking pattern is mode-free booking rather than mode-fixed booking. Shippers only specify shipments' origin, destination, time window, and volume, leaving the choice of transport services to network operators. Thirdly, instead of planning on corridors, synchromodal transportation refers to network-wide planning, which includes all the shipments and services involved in the transport network. Most importantly, it focuses on real-time switching in case of disturbances to guarantee service efficiency, operational effectiveness, and less environmental impact [95].

As a new concept, limited articles have been published about synchromodal transportation, especially for global supply chains. By 2016, 77 articles of synchromodal transportation are found using research databases, such as Web of Science. Nevertheless, this research area has an increasing trend, as illustrated in Figure 2.3. However, none of them provide an integral analysis about the characteristics and challenges of synchromodal transportation in global supply chains. The objective of this chapter is therefore to thoroughly analyze it.

Table 2.1: Critical success factors of synchromodal transportation.

References	Behdani et al. [9]	Tavasszy et al. [95]	Van Riessen et al. [99]	Singh et al. [85]	Pfoser et al. [67]
Legal and political issues				✓	✓
Physical infrastructure				✓	✓
Mind shift		✓	✓		✓
Information technology		✓		✓	✓
Horizontal collaboration	✓	✓		✓	✓
Service-based pricing strategy	✓		✓		✓
Integrated planning	✓	✓	✓	✓	✓
Real-time switching	✓	✓	✓		

2.2 Critical success factors

Although synchromodal transportation is a promising idea, it is hard to realize it in practice. Until now, only several successful pilot studies are known in the Netherlands. Almost all the case studies that exist in the literature are based on the network of European Gateway Services, which includes Rotterdam port and at least 20 hinterland terminals in Europe [99]. Critical success factors analysis is an effective method to identify the key enablers of synchromodality [67].

According to the literature review, we find that synchromodal transportation mainly includes eight factors, as shown in Table 2.1. Legal and political issues and physical infrastructure investment are decided by governments, such as tax incentives for sustainable logistics and new hub construction. In terms of shippers' mode booking pattern, the benefits of synchromodality, like cost receiving and environmentally friendly, can promote customers' mind shift. Advanced information technology and horizontal collaboration are the foundation, while service-based pricing strategy plays as an incentive. Integrated planning is the core of synchromodal transportation, which will be further discussed at strategic, tactical, and operational level respectively. Real-time switching is the key factor which responses to dynamic events and disturbances. As the first three factors are determined by governments or high level organizations, next, we focus on the last five factors.

2.2.1 Information technology

Information technology mainly refers to information sharing, track and trace, and communication technologies [85]. Regarding reefer containers, radio frequency identification is a critical technology for monitoring environmental data, such as temperature and moisture. Real-time position of services and container shipments can be attained by using global positioning systems. Information and communications technology can promote information sharing and communication among different operators. In summary, advanced information technology is the foundation of synchromodal transportation in global supply chains.

2.2.2 Horizontal collaboration

Horizontal collaboration is another basic factor in realizing synchromodal transportation. It refers to the cooperative relationship between actors at the same level, whereas vertical collaboration refers to different levels. For example, the relationship among competing carriers with different modes belongs to horizontal collaboration, while inland carries and ocean carries build vertical collaboration. For switching flexibility among different services, horizon-

tal collaboration among carriers turns out to be essential. Shippers also establish horizontal cooperation to achieve lower costs by sharing the capacity of services. The collaboration contract between them used to be long term, static, and offline. However, due to the dynamic characteristic of the global shipment market, dynamic and online contracts become more suitable. What's more, considering the private safety of different actors, fully information sharing is unpractical. Real-time decisions based on limited information are still challenging. Distributed optimization is an effective method for promoting collaboration among stakeholders with coupling constraints [25].

2.2.3 Pricing strategy

In terms of pricing strategy, synchromodal transportation shows distinct characteristics from intermodal transportation [99]. Intermodality adopts mode-based pricing strategies, price is determined by the mode used. Mode choice for shipments is decided before the transportation, thus the price is fixed. With respect to synchromodality, the mode booking pattern is mode-free booking. The mode choices might be changed before or during transport in case of disturbances, such as service delay. The mode-based pricing strategy is thus unsuitable for synchromodal transportation. The pricing strategy in synchromodal transportation should be differentiated for different far classes [101]. For the same mode choice, the price can be different according to the time windows of shipments. Considering the credits of customers, different price for different credits is an effective motivation. Based on the above analysis, we can see that the pricing strategy of synchromodal transportation is still challenging and thus deserves further research.

2.2.4 Integrated planning

An effective planning model is the core of synchromodal transportation. While intermodal transportation focuses on one OD pair planning, synchromodal transportation aims at integrated planning at a network level [9]. Under synchromodality, all the services belong to different carriers are assumed to be in a large resource pool and all the arriving shipment requests will be allocated simultaneously. Due to the complexity of planning models, most researches focus on centralized planning of synchromodal transportation. However, the entities in global supply chains are often geographically distributed. It is thus very difficult to apply a central coordinator to manage the whole system [25]. Moreover, when the computation size becomes large enough, a distributed system promotes better computation performance. To improve operational efficiency, service effectiveness, and reduce environmental impact, the key performance indicators of synchromodal transportation are logistics cost, delays, and emissions [62]. Therefore, an integrated objective function combining the logistics cost with delay costs and carbon tax is required for transport planning.

2.2.5 Real-time switching

With the development of information technology, real-time information becomes available for intermodal operators. Due to the occurrences of dynamic events (e.g., newly arrived shipment requests) and variety disturbances during transportation (e.g., service delay), real-time switching is essential for improving service reliability. An integrated planning model

is the prerequisite of real-time switching [100]. To realize real-time switching, researchers have proposed different methods, like rolling horizon strategy, model predictive control, decision tree, and approximate dynamic programming. Under the rolling horizon strategy [1], shipment requests arrive continuously in different planning horizons. The planning horizon is rolled forward to include more known information. Decisions are made at the deadline of the requests. Regarding the model predictive control approach [54], it is an effective method to obtain an ideal output by controlling the inputs. For instance, to keep banana's shelf life, both the container's temperature and mode choice will be controlled by the system operators in real-time. As for decision tree [100], it can be used in a decision support system for instantaneously allocating incoming requests to suitable services, without the requirement of continuous planning updates. Approximate dynamic programming (ADP) is a framework that contains several methods to modify Bellman's equation with a series of components and algorithmic manipulation. It determines the values and policies of decision making before the execution of the transport plan [76]. As real-time switching requires short responses of disturbances, the computation efficiency indicates significant means. Optimization algorithms that can generate timely solutions are essential to realize real-time switching [99].

2.2.6 Discussions

According to the discussions above, we know that under government support, based on advanced information technology and horizontal collaboration as well as attractive pricing strategy, synchromodal transport can be realized in global supply chains by combining real-time switching with effective planning models. Next, we further analyze the characteristics and challenges of synchromodal transport planning at the strategic, tactical, and operational level, respectively.

2.3 Strategic infrastructure network design

The strategic level focuses on long term decisions. The infrastructure network design (IND) problem in synchromodal transportation refers to investment decisions on hub locations [87]. Under synchromodal transport, different shippers' shipments are bundled together in hubs for large container flow. To reduce total transport costs, the allocation of hubs depends on the service demands in different areas. The connection between hubs can be a highway, railway, or waterway.

The IND problem mainly depends on the availability of infrastructure, transport assets, and the adequacy of cargo flow in a specific corridor [9]. Typically, this problem can be described by using mixed-integer linear programming models which include both binary decision variables and continuous decision variables. Binary decision variables are related to whether the hub is used or not, while continuous decision variables illustrate bundled flow [2]. The objective of the IND used to be simply focused on cost. As delay in deliveries deeply affects customer satisfaction degrees, it should be considered as another important objective. With respect to environmental impact, proper network design maximizes the utilization of green modes which produce less emissions. Thus, for global supply chains, the objectives of the IND should include both logistics cost, delays, and emissions.

2.4 Tactical service network design

The tactical level focuses on middle term decisions. It optimally utilizes the given infrastructure by choosing services and associated transportation modes, allocating their capacities to shipments, and planning their itineraries and frequency. Service network design (SND) is the major problem at the tactical level. It mainly gives decisions on choosing the transportation services and modes for predicted customer demands, and the frequency and capacity of each mode on certain corridor [87]. Here, service is characterized by its origin, destination, and intermediate terminals, its transportation mode, route, time schedules, and its service capacity. Likewise, a mode is characterized by its loading capacity, speed, and cost, which means that different services may have the same mode. To improve operational efficiency, service effectiveness, and environmental sustainability, the objectives of the SND problem should include logistics cost, delays, and emissions. The availability and capacity of infrastructure networks or terminals are the primary resource constraints [9].

Regarding global supply chains, transport distance tends to be very long. The modes in global transportation include ships, trains, barges, and trucks. Different models have different characteristics, and therefore need to be considered separately. However, the majority of studies only consider modes in hinterland transportation instead of global transportation [77, 102]. Besides, transshipment operations between different modes bring more chances to the utilization of barges and trains, which result in less emissions and costs. However, it also takes additional costs and time at transshipment terminals. Thus, transfer and storage costs and time should be considered in synchromodal SND [87].

In the literature, SND problems can be divided into static and dynamic groups [87]. Van Riessen et al. [102] proposed a static SND model, demand and travel times are assumed as static parameters based on expectations. However, a time-varying network is more practical, because traffic condition normally changes with time, and shipment requests tend to be arriving in real-time. Li et al. [49] proposed a dynamic SND model in synchromodal transportation based on a model predictive control approach. However, their work lies in hinterland transportation. The dynamic SND model for global synchromodal transport is still missing.

Compared with centralized planning systems, decentralized systems are more practical for global container transportation. Information sharing is crucial for centralized planning. However, it is difficult to realize among different entities, especially for stakeholders with a competitive relationship. Li et al [50] proposed a distributed service network design approach to support cooperative synchromodal transport planning among multiple local operators in different and interconnected service networks, however, this approach is applied in hinterland transport. Distributed optimization for global synchromodal transportation is a promising future research direction.

In summary, the synchromodal SND problem in global transportation is still challenging owing to its multi-objective, long-distance, dynamic, and distributed features. To our best knowledge, only Van Riessen et al. [102], Rivera et al. [77] and Li et al. [50] proposed SND models for synchromodal transport. But none of them considered the characteristics of global transport. Therefore, there still have lots of research opportunities in global synchromodal SND.

2.5 Operational intermodal routing choice problem

The operational level deals with dynamic problems that are not explicitly addressed at the strategic and tactical levels [87]. At the operational level, the main issue is the determination of the best choice of services and the best itineraries for newly arrived shipment requests, which called the intermodal routing choice (IRC) problem in the literature [12]. Although the SND models have many similarities with the IRC models, there have many differences. In IRC, demand is actual demand rather than predicted demand, and constraints include time windows of shipments and service capacity limitations rather than the availability of infrastructures. While the tactical SND determines routes, frequency, and capacity of services, the operational IRC considers the selection of specific transport services for specific shipments [9].

The objectives of the IRC problem include reducing logistics costs, delays, and carbon emissions. This problem thus belongs to a multi-objective planning problem. Multi-objective planning is more complex than single objective planning. One method is to assign different weights for different objectives, and then summarizes these objectives as a single objective [12]. Another method is to solve all the single objectives respectively while others are assigned as constrains. Pareto optimum solutions can be attained by optimization and composition method [13].

Typically, the IRC models in the literature are static and deterministic [100]. The planning horizon used to be one day. These intermodal transport systems assume that all the information on shipments and services are accessed before the planning horizon [8]. However, in practice, it is difficult to achieve or predict all the information in advance [9]. Thus, dynamic and stochastic transport planning models are critical to realize synchromodal transportation [100]. Furthermore, the stakeholders in global container transportation tend to be distributed worldwide, distributed optimization models are more practical. However, none of the studies in the literature consider both the aspects of dynamic, stochastic, distributed, and global networks, as shown in Table 2.2. Therefore, we conclude that efficient synchromodal transport planning models at the operational level are still challenging.

2.6 Conclusions

In this chapter, we have analyzed the characteristics and challenges of global synchromodal transportation. We have discussed the critical success factors at first. We found that information technology and horizontal collaboration are the foundation factors, and service-based pricing strategy plays as an incentive. Integrated planning models are essential, and real-time switching is the most challenging factor.

After that, we have further discussed the planning problems at three different levels. The strategic infrastructure network design problem refers to hub locations. The tactical service network design decides mode routes and the frequency of services. The operational intermodal routing choice problem aims at the selection of transport services for specific shipments with time windows. While extensive transport planning models have been investigated in intermodal transportation under static and deterministic environments, the synchromodal transport planning models with dynamic, stochastic, and distributed features are still missing.

This thesis addresses the above mentioned gaps in the literature with dynamic, stochastic, and coordinated models. Specifically, in Chapter 3, we develop a shipment matching model with time-dependent travel times in hinterland synchromodal transportation. In Chapter 4, a rolling horizon approach is proposed to handle real-time shipment requests. Chapter 5 proposed an anticipatory approach to incorporate stochastic information of spot requests in online decision-making processes of a hinterland synchromodal matching platform. In Chapter 6, a hybrid stochastic approach is proposed to deal with spot request and travel time uncertainties integrally in global synchromodal transportation. Finally, in Chapter 7, we developed three distributed approaches to stimulate cooperative planning in global synchromodal transportation. Thanks to the developed methodologies, the proposed synchromodal matching platforms can support decision makers to optimize the matching of shipments and services considering the trade-off among logistics costs, delays, and carbon emissions under dynamic, stochastic, and decentralized environments.

Table 2.2: Articles related to operational synchromodal transport planning.

Articles	Network	Dynamic events	Uncertainties	Decentralized decision-making	Objectives	Transfer	Time-dependent travel times
Moccia et al. [63]	Inland				Costs	✓	
Behdani et al. [9]	Inland				Costs, delays		
Van Riessen et al. [103]	Inland				Costs, delays	✓	
Sun et al. [93]	Inland				Costs, emissions	✓	
Chapter 3	*Inland*				*Costs, emissions, time*	✓	✓
Li et al. [49]	Inland	Container flow, travel time			Costs	✓	
Mes et al. [62]	Inland	Shipment request			Costs, delays, emissions	✓	
Van Heeswijk et al. [98]	Inland	Shipment request			Costs, delays, emissions	✓	
Qu et al. [72]	Inland	Release time, container flow, travel time			Costs	✓	
Chapter 4 [37]	*Inland*	*Shipment request*			*Costs, delays, emissions*	✓	✓
Zuidwijk et al. [117]	Inland		Release time, travel time		Costs		
Hrušovský et al. [41]	Inland		Travel time		Costs, delays, emissions	✓	
Demir et al. [18]	Inland		Travel time, container flow		Costs, delays, emissions	✓	
Sun et al. [92]	Inland		Service capacity		Costs, delays, emissions	✓	✓
Van Riessen et al. [100]	Inland	Shipment request	Container flow		Costs, delays		
Rivera et al. [76]	Inland	Shipment request	Shipment request		Costs		
Steadieseifi [88]	Inland	Container flow	Container flow		Costs		
Chapter 5 [33, 36]	*Inland*	*Shipment request*	*Shipment request*		*Costs, delays, emissions*	✓	✓
Dong et al. [20]	Maritime		Container flow		Costs	✓	
Chang [12]	Global				Costs, time	✓	
Ayar et al. [7]	Global				Costs	✓	
Meng et al. [60]	Global				Costs	✓	
Liu et al. [55]	Global				Costs	✓	
Tran et al. [96]	Global				Costs, emissions	✓	
Wei et al. [111]	Global				Costs, time	✓	
Chapter 6 [35]	*Global*	*Shipment request, travel time*	*Shipment request, travel time*		*Costs, delays, emissions*	✓	
Febbraro et al. [25]	Inland	Shipment request		✓	Costs, delays	✓	
Li et al. [50]	Inland	Container flow, travel time		✓	Costs	✓	
Puttettmann et al. [71]	Global		Container flow	✓	Costs	✓	
Chapter 7	*Global*	*Shipment request, travel time*	*Travel time*	✓	*Costs, delays*	✓	

Chapter 3

Hinterland sychromodal shipment matching

In Chapter 2, we have classified eight critical success factors for realizing synchromodal transportation. Integrated planning, as the core of synchromodality, has been further divided into three levels: strategic, tactical, and operational level. This chapter proposes a shipment matching model with time-dependent travel times for hinterland synchromodal transportation at the operational level.

This chapter is structured as follows. Section 3.1 gives a detailed introduction of hinterland synchromodal transportation. In Section 3.2, a literature review of the shipment matching problem is presented. Section 3.3 describes the details of hinterland synchromodal shipment matching. After that, time-dependent travel times and matching formulations are presented in Section 3.4. In Section 3.5, we conduct numerical experiments and analyze experimental results. We discuss the main conclusions in Section 3.6.

Parts of this chapter have been published in [39]: "W. Guo, W. Beelaerts van Blokland, G. Lodewijks, and R. R. Negenborn. Multi-Commodity Multi-Service Matching Design for Container Transportation Systems. In *Proceedings of the 97th Annual meeting of the Transportation Research Board*, Washington, DC, 2018."

3.1 Introduction

Hinterland intermodal transportation is the movement of shipments between deep-sea ports and inland terminals by using barges, trains, trucks, or any combination of them [26]. It plays an important role in improving the competitiveness of global supply chains. However, recently, network operators (such as European Gateway Services) face increasing pressure from road traffic congestion, less flexibility, low reliability, and serious environmental impacts in hinterland transport. As we discussed in Chapter 2, synchromodal transportation aims at creating an efficient, effective, and sustainable transportation plan for network operators by using the available flexibility. While efficiency refers to the reduction of logistics costs by improving the utilization of barges and trains, effectiveness guarantees service quality and sustainable transportation promotes the reduction of carbon emissions.

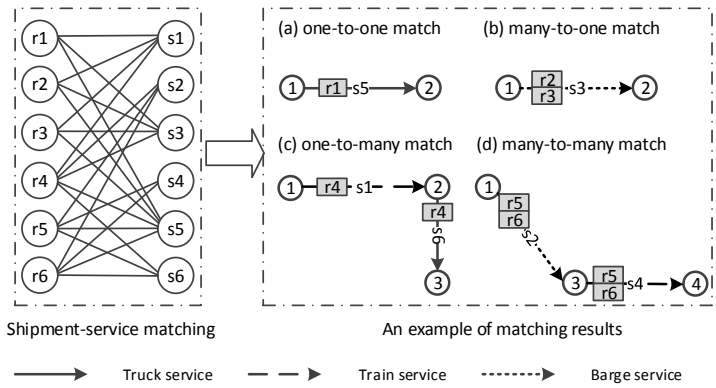

Figure 3.1: Hinterland synchromodal shipment matching.

Synchromodal transportation is in practice a further optimization of intermodal transportation [62]. It relies on the design of differentiated transportation services, mode-free booking, horizontal collaboration, integrated planning, and real-time switching [38]. By mode-free booking, network operators have the flexibility to assign different transportation services to shippers with differentiated prices. With regard to horizontal collaboration, entities with competitive relationships will cooperate together for a system-wide optimum. While integrated planning is the core of hinterland synchromodal transportation, real-time switching guarantees the flexibility of transport plans under dynamic and stochastic environments. This chapter focuses on the operational integrated planning design.

We consider a hinterland synchromodal transport system owned by a network operator that receives shipment requests from shippers and receives transport services from carriers. Shippers are the entities who are searching for services to transport their shipments, such as freight forwarders. Carriers are the entities that provide transportation services, such as barge carriers. We assume network operator as the alliances formed by multiple carriers that collaborate with each other. Under synchromodality, shippers only specify shipments' origin, destination, container volume, and time windows, leaving the service choices to the network operator. Carriers provide service information to the network operator, including services' origin, destination, time schedule, capacity, and transport cost. The network operator aims to provide integrated optimal matches between shipments and services. A match between a shipment and a service represents that the shipment will be transported by the service from the service's origin to the service's destination. In synchromodal transportation, a shipment might be matched with multiple services, a service might be matched with multiple shipments, as shown in Figure 3.1. Here, shipment r4 is matched with train service s1 and truck service s6; barge service s3 is matched with shipment r2 and r3.

Due to the limited capacity of road networks, traffic congestion exists during several times of a day [90]. Travel speed of truck services is thus affected by traffic conditions, which results in time-dependent travel times. In synchromodal transportation, ignoring the time-dependent travel times of truck services might result in infeasible transportation plans and suboptimal solutions [92]. The matching of shipments with multimodal services under time-dependent hinterland networks gives rise to a new problem. In this chapter, we define this problem as a hinterland synchromodal shipment matching (HSSM) problem.

Table 3.1: Comparison between ride matching and synchromodal shipment matching.

	Ride matching	Hinterland synchromodal shipment matching
Supply		
Stakeholder	Drivers	Carriers
Entity	Private cars	Multimodal services
Capacity	Ride limits	Container slot limits
Path	Flexible	Fixed
Time	Time window	Time schedules
Demand		
Stakeholder	Passengers	Shippers
Entity	Riders	Shipments
Service time	Waiting and transit time	Loading/unloading, storage, and transport time
Service quality	Detour, travel time, success rate	Costs, time, carbon emissions
System		
Decision	Matching, vehicle route	Matching
Objective	System-wide optimum	System-wide optimum

3.2 Literature review

The studies related to the shipment matching problem can be divided into two groups: ride matching problem; intermodal routing choice problem.

3.2.1 Ride matching problem

Ride matching systems, which aim to bring together travelers with similar itineraries and time schedules, provide significant societal and environmental benefits by reducing the number of cars used for personal travel and improving the utilization of available seat capacity [1, 4, 58, 64, 89, 105]. The ride-matching problem has many similarities but also differences with the HSSM problem, as shown in Table 3.1. In terms of the supply side, the stakeholders are drivers in a ride matching system and carriers in a HSSM system. Here, drivers are individual person who drives private cars, while carriers are individual companies that operator transport services. Regarding private cars, they drive from origins to destinations with limited rides and flexible path under fixed time windows. By contrast, multimodal services transport from its origin to destination with limited capacities and fixed path under scheduled timetables.

With respect to the demand side, the stakeholders are passengers in a ride matching system and shippers in a HSSM system. In a ride matching system, passengers propose requests on rides. The service time consists of waiting time at locations, and transit time during the trip. The service quality is measured by detours, travel time, and matching success rates. By contrast, shippers in a HSSM system propose requests on transport services. Shipments will get loading/unloading and storage operations at terminals, and transport services from origins to destinations. The transport performance is measured by cost savings, transport time, and carbon emissions.

From the system perspective, the decision of ride matching systems includes matching decisions and vehicles routing decisions under system-wide optimum objective. For the HSSM system, the decision only includes matching decisions due to fixed paths of transport services. The objective of the HSSM is also global optimum.

Table 3.2: Formulation Characteristics of related articles in synchromodal transportation.

Formulation characteristics			Chang [12]	Moccia et al. [63]	Ayar et al. [7]	Behdani et al. [9]	van Riessen et al. [103]	Sun et al. [93]	**This chapter**
Service pattern	Committed services		✓	✓			✓		✓
	Uncommitted services			✓	✓	✓	✓	✓	✓
Shipment integrity	Unsplittable			✓	✓			✓	✓
	Splittable		✓			✓	✓		
Network state	Time-constant travel times		✓	✓	✓	✓	✓	✓	
	Time-dependent travel times								✓
Optimization criterion	Logistics cost	Transport cost	✓	✓	✓	✓	✓	✓	✓
		Transfer cost					✓	✓	✓
		Storage cost			✓	✓		✓	✓
	Carbon emissions							✓	✓
	Transport time		✓						✓

3.2.2 Intermodal routing choice problem

Intermodal routing choice (IRC) problem is developed to select optimal routes to move shipments from their origins to destinations within specified time windows in an intermodal transport network [94]. From the perspective of mathematical formulation, the HSSM problem is very similar to the IRC problems, as shown in Table 3.2.

With regard to the service pattern, it consists of committed services and uncommitted services. Most of the researches only consider uncommitted services [7, 9, 93] in which cost structures are container-based costs, such as 7.54 € per container. For committed services, the cost structure is service-based cost, such as 300 € per barge. Thus, based on the economy of scale theory, more shipments sharing one committed service results in less transport costs distributed to per shipment. Under synchromodality, both committed services and uncommitted services might exist in hinterland transport networks. Therefore, this chapter considers both of them in the HSSM model.

In terms of shipment integrity, it can be distinguished as unsplittable shipments and splittable shipments. Unsplittable shipments indicate that each shipment is not allowed to be split into several batches. Thus, each shipment will only be assigned to one route. Therefore, the decision variables are binary variables [7, 63, 93]. Regarding the splittable shipment, it suggests that one shipment can be split into several batches. Then, these batches can be assigned to different routes, the total flow of batches equal to the total container volume of a shipment [9, 12, 103]. Under synchromodality, a match between a shipment and a service is indicated by a binary variable. Therefore, shipments are assumed unsplittable in the HSSM model.

The third aspect is network state which refers to time-constant travel times and time-dependent travel times. Here, time-dependent travel time means that the travel time of services changes over time. In practice, road traffic conditions change over time. The travel time of truck services, in turn, changes over time. Therefore, it is necessary to consider time-dependent travel times. Otherwise, the transport plan received from time-constant models will be suboptimal or even infeasible in practice. However, none of the IRC models consider time-dependent travel times.

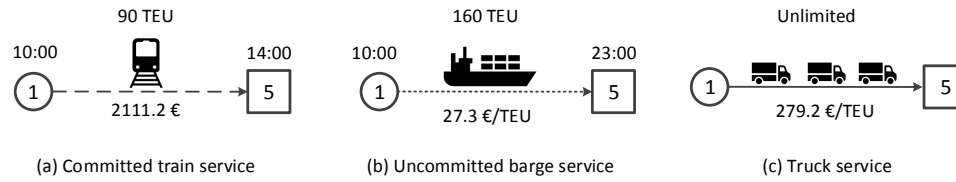

Figure 3.2: Examples of committed and uncommitted services.

In terms of optimization criterion, it can be divided into three groups: logistics costs, carbon emissions, and transport time. Here, logistics cost includes transport cost, transfer cost, and storage cost. Specifically, transfer cost consists of loading and unloading cost at terminals [93, 103]. Due to the fixed time schedules of barge and train services, storage cost is produced when shipments are stored at terminals waiting for departure or transfer [7, 9, 93]. In addition, transportation contributes to a large part of gas emissions every year. Recently, carbon tax has been proposed by governments to control carbon emissions in the transportation sector [93]. In the literature, only Sun et al. [93] considered carbon tax in the IRC model. Regarding service reliability, only Chang [12] considered transport time as an objective in the IRC models. However, none of the IRC models considered logistics costs, carbon emissions, and transport time simultaneously.

3.2.3 Contributions

The contribution of this chapter is twofold. First, we develop a shipment matching model with time-dependent travel times in hinterland synchromodal transportation taking into account logistics costs, transport time, and carbon emissions. Second, we conduct extensive experiments to analyze the sensitivity of parameters.

3.3 Problem description

The HSSM problem defined in this chapter contains two sets of participants. The first set is shippers that are searching for services to transport their shipments. Shipment $r \in R$ is characterized by container volume u_r, origin terminal o_r and destination terminal d_r, the earliest departure time $\mathbb{T}_r^{\text{release}}$ at origin terminal and the latest arrival time $\mathbb{T}_r^{\text{due}}$ at destination terminal.

Another set is carriers who provide weekly service schedules to network operators. According to the contracts between network operators and carriers, services can be divided into two groups:

(1) *Committed services*. The network operator has long term contracts with carriers who provide barge or train services for committed capacity. Thus, the network operator needs to pay fixed costs per service and has no additional costs per used slot. Furthermore, committed services have fixed time schedules and limited capacities, as shown in Figure 3.2 (a). Specifically, each committed service $q \in Q$ is characterized by its departure time TD_q at origin terminal o_q, arrival time TA_q at destination terminal d_q, capacity U_q, transport cost c_q, transport time t_q, transport distance D_q, and carbon emissions e_q.

(2) *Uncommitted services*. The network operator can use uncommitted capacities of barge or train services from carriers at a slot cost per TEU (twenty-foot equivalent unit). Uncommitted barge or train services have fixed time schedules and limited capacities, as shown in Figure 3.2 (b). Each uncommitted scheduled service $s \in S^{\text{barge}} \cup S^{\text{train}}$ is characterized by its departure time TD_s at origin terminal o_s, arrival time TA_s at destination terminal d_s, transport cost c_s, transport time t_s, transport distance D_s, capacity U_s, and carbon emissions e_s. In addition, the network operator can also use uncommitted capacity from truck companies at slot-based costs. We view each truck service as a fleet of trucks that has flexible time schedules and unlimited capacity, as shown in Figure 3.2 (c). Thus, a truck service might have multiple departure times. Each truck service $s \in S^{\text{truck}}$ is characterized by its origin terminal o_s, destination terminal d_s, travel time t_s, travel cost c_s, travel distance D_s, and carbon emissions e_s. Due to the existence of traffic congestion at several time periods within a day, the travel time of truck services is time-dependent.

A match $\langle r,s \rangle$ is defined as a combination of shipment $r \in R$ and service $s \in \{Q,S\}$. A match $\langle r,s \rangle$ is feasible only if r and s satisfy spatial, capacity, and time window constraints. Regarding spatial constraints, each shipment must be matched with a service leaving its origin node, and a service entering its destination node. In terms of capacity constraints, for service $s \in S \cup Q$, the total volume of shipments that matched with s cannot exceed the capacity limitations of s. Concerning time window constraints, the departure time of service $s \in S \cup Q$ in match $\langle r,s \rangle$ is later than the arrival time of shipment r plus the loading/unloading time at terminal o_s, and the arrival time of service s is earlier than the latest arrival time of shipment r minus the loading/unloading time at terminal d_r.

To achieve efficient, effective, and sustainable synchromodal transport planning, the objective of the network operator is to minimize logistics costs, transport time, and carbon emissions. The HSSM problem is thus a multi-objective planning problem.

3.4 Time-dependent matching model

In this section, we establish formulations to express the objective and constraints of the HSSM. We define N as the set of terminals. Without loss of generality, we assume that the loading/unloading cost coefficient lc, loading/unloading time lt, and storage cost coefficient c^{storage} at each terminal are the same. The carbon tax coefficient is set as c^{emission}. In this chapter, we assume shipments have hard time window. To ensure customers receive their shipments as a whole, each shipment can only be matched with one route.

3.4.1 Time-dependent travel times

In practice, road traffic condition changes over time. The travel time of truck services, in turn, changes over time. Therefore, it is necessary to consider time-dependent travel times. Thus, a truck service that is matched with different shipments might have different departure times and in turn, have different travel times. Let TD_{rs} be the departure time of truck service $s \in S^{\text{truck}}$ with shipment $r \in R$; let t_{rs}^{truck} be the travel time of truck service $s \in S^{\text{truck}}$ with shipment $r \in R$. We denote c^{truck} as the travel cost coefficient of truck services. Althought the travel times are time-dependent, we assume the travel time functions are known beforehand and deterministic.

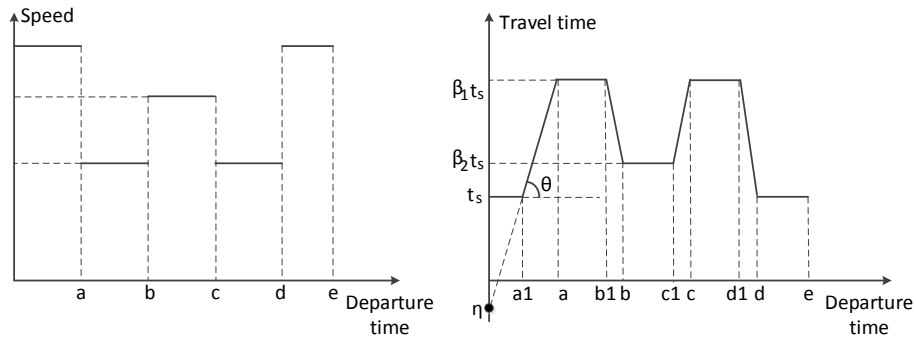

Figure 3.3: Time-dependent speed and travel times.

To describe the time-dependent travel time, we introduce the classical functions proposed by Ichoua et al. [42]. The core idea is that the travel speed changes when the boundary between two consecutive time periods is crossed. The travel time functions follow the first-in-first-out rule, which ensures that the earlier the truck departure, the earlier the truck arrival. Figure 3.3 describes a time-dependent speed profile and the corresponding travel time function of a truck service s. β_1 and β_2 are traffic congestion coefficients. The travel time functions are piecewise linear and can be represented by breakpoints. Specifically, we let $\mathbb{T}$ represent the set of time periods within a day. A time period $T^m \in \mathbb{T}$ can be defined by two consecutive breakpoints. For time period $T_2 = [a1, a]$, given the values $a1, a, t_s, \beta_1 t_s$, we can calculate the slope θ of the function and the intersection η with the y-axis. Therefore, $t_s(\tau) = \theta_s^m \tau + \eta_s^m \quad \forall \tau \in T^m$. Because of the FIFO property of travel time functions, a later departure should result in a later arrival, thus, $\theta \geq -1$.

3.4.2 Matching model

Let x_{rs} indicate the match between shipment $r \in R$ and service $s \in S \cup Q$. We denote w_{rs} as the storage time of match $\langle r, s \rangle$ and A_{ri} as the arrival time of shipment r at terminal i. The objective of the matching model is to minimize total cost and transport time. The mathematical model is presented as follows:

Minimize

$$J = J_1 + J_2 + J_3 + J_4 + wJ_5 \tag{3.1}$$

where

$$J_1 = \sum_{q \in Q} c_q l_q + \sum_{r \in R} \sum_{s \in S^{\text{barge}} \cup S^{\text{train}}} c_s u_r x_{rs} + \sum_{r \in R} \sum_{s \in S^{\text{truck}}} c^{\text{truck}} t_{rs}^{\text{truck}} u_r x_{rs}$$

$$J_2 = \sum_{r \in R} \sum_{s \in Q \cup S^{\text{barge}} \cup S^{\text{train}}} 2lcu_r x_{rs}$$

$$J_3 = \sum_{r \in R} \sum_{s \in Q \cup S^{\text{barge}} \cup S^{\text{train}}} w_{rs} c^{\text{storage}} u_r$$

$$J_4 = \sum_{r \in R} \sum_{s \in Q \cup S} c^{\text{emission}} e_s u_r x_{rs}$$

$$J_5 = \sum_{r \in R} (A_{rd_r} - \mathbb{T}_r^{\text{due}}) u_r$$

In the objective function (3.1), J_1 represents the total transport cost of shipments R matching with committed services Q, and uncommitted services S. As the cost structure of uncommitted services is container-based cost, the transport cost of match $\langle r,s \rangle$ depends on the transport cost coefficient of service $s \in S$ and the volume of shipment r. In contrast, the transport cost structure of committed services is service-based cost, the transport cost of match $\langle r,q \rangle$ depends on the total volume of shipments matched with service $q \in Q$, i.e. $c_{rq} = \frac{c_q}{\sum_{r \in R} x_{rq} u_r} x_{rq} u_r$. Let l_q be the binary variable which equals 1 if $\sum_{r \in R} x_{rq} > 0$. Therefore,

$$l_q \geq x_{rq}, \qquad \forall q \in Q, r \in R. \tag{3.2}$$

Since t_{rs}^{truck} and x_{rs} are both decision variables, to linearize the objective function, we design $TX_{rs} = t_{rs}^{\text{truck}} x_{rs}$. Thus, J_1 changes to:

$$J_1 = \sum_{q \in Q} c_q l_q + \sum_{r \in R} \sum_{s \in S^{\text{barge}} \cup S^{\text{train}}} c_s u_r x_{rs} + \sum_{r \in R} \sum_{r \in R} c^{\text{truck}} u_r T X_{rs} \tag{3.3}$$

The second term J_2 in equation (3.1) denotes the total loading and unloading cost of shipments R matching with committed services Q, uncommitted barge services S^{barge}, and uncommitted train services S^{train}. We assume that no loading/unloading cost exists for match $\langle r,s \rangle$, $\forall r \in R$, $s \in S^{\text{truck}}$.

The third term J_3 in equation (3.1) indicates the total storage cost of shipments R matching with services Q, S^{barge} and S^{train}. Specifically, the storage time of match $\langle r,s \rangle$ between shipment $r \in R$ and service $s \in Q \cup S^{\text{barge}} \cup S^{\text{train}}$ equal to the departure time of s minus the arriving time of r at the origin terminal of s minus the loading time. Thus,

$$w_{rs} = (TD_s - A_{ro_s} - lt) x_{rs}, \qquad \forall r \in R, s \in Q \cup S^{\text{barge}} \cup S^{\text{train}}. \tag{3.4}$$

The fourth term J_4 of the objective function represents the total carbon emissions of shipments R matching with services Q and S.

The fifth term J_5 represents the total transport time. The transport time of each shipment is calculated by the arrival time at its destination terminal minus the departure time at its origin terminal. Here, w represents the weight coefficient of the total transport time.

Regarding the constraints, the matching model is confined by the following three sets of constraints: spatial constraints, capacity constraints, and time constraints.

- Spatial constraints:

$$\sum_{q \in Q_{o_r}} x_{rq} + \sum_{s \in S_{o_r}} x_{rs} = 1, \qquad \forall r \in R, \tag{3.5}$$

where $Q_{o_r} = \{q | o_q = o_r, q \in Q\}, S_{o_r} = \{s | o_s = o_r, s \in S\}$.

$$\sum_{q \in Q_{d_r}} x_{rq} + \sum_{s \in S_{d_r}} x_{rs} = 1, \qquad \forall r \in R, \tag{3.6}$$

where $Q_{d_r} = \{q | d_q = d_r, q \in Q\}, S_{d_r} = \{s | d_s = d_r, s \in S\}$.

$$\sum_{q\in Q_i^+} x_{rq} + \sum_{s\in S_i^+} x_{rs} = \sum_{q\in Q_i^-} x_{rq} + \sum_{s\in S_i^-} x_{rs}, \quad \forall r \in R, i \in N\backslash\{o_r, d_r\}, \tag{3.7}$$

where $Q_i^+ = \{q|o_q = i, q \in Q\}, S_i^+ = \{s|o_s = i, s \in S\}, Q_i^- = \{q|d_q = i, q \in Q\}, S_i^- = \{s|d_s = i, s \in S\}$.

Constraints (3.5-3.7) are imposed to find the feasible matches between shipments and services based on the spatial information (i.e., origins and destinations). Constraints (3.5) ensure that only one service carries shipment r leaving origin o_r. Constraints (3.6) ensure only one service carries shipment r arriving destination d_r. Constraints (3.7) ensure flow conservation.

- Capacity constraints:

$$\sum_{r\in R} x_{rs} u_r \leq U_s, \qquad \forall s \in Q \cup S^{\text{barge}} \cup S^{\text{train}}. \tag{3.8}$$

Constraints (3.8) ensure that the total volumes of shipments carried by service $s \in Q \cup S^{\text{barge}} \cup S^{\text{train}}$ do not exceed the capacity limitation of service s.

- Time constraints:

$$A_{ro_r} = \mathbb{T}_r^{\text{release}}, \qquad \forall r \in R, \tag{3.9}$$

$$A_{rd_r} \leq \mathbb{T}_r^{\text{due}}, \qquad \forall r \in R, \tag{3.10}$$

$$(A_{ri} - TA_s - lt)x_{rs} = 0, \qquad \forall r \in R, i \in N\backslash\{o_r\}, s \in Q_i^- \cup S_i^{-\text{barge}} \cup S_i^{-\text{train}}, \tag{3.11}$$

$$\left(A_{ri} - (A_{ro_s} + t_{rs}^{\text{truck}})\right) x_{rs} = 0, \qquad \forall r \in R, i \in N\backslash\{o_r\}, s \in S_i^{-\text{truck}}, \tag{3.12}$$

$$t_{rs}^{\text{truck}} = t_s(A_{ro_s}), \qquad \forall r \in R, s \in S^{truck}, \tag{3.13}$$

$$(TD_s - lt - A_{ri})x_{rs} \geq 0, \qquad \forall r \in R, i \in N\backslash\{d_r\}, s \in Q_i^+ \cup S_i^{+\text{barge}} \cup S_i^{+\text{train}}. \tag{3.14}$$

Constraints (3.9) assume that the arrival time of shipment r at origin terminal is the earliest departure time. Constraints (3.10) ensure that the arrival time of shipment r at destination terminal is earlier than the latest arrival time. Constraints (3.11) ensure that the arrival time of shipment r at terminal i is the arrival time of service $s \in Q_i^- \cup S_i^{-\text{barge}} \cup S_i^{-\text{train}}$ plus unloading time, if shipment r is transported by service s entering terminal i, $i \in N\backslash\{o_r\}$. Constraints (3.12) ensure that the arrival time of shipment r at terminal i is the sum of arrival time of shipment r at terminal o_s, and travel time of truck service $s \in S_i^{-\text{truck}}$, if shipment r is transported by truck service s entering terminal i, $i \in N\backslash\{o_r\}$. Constraints (3.13) calculate the travel time of truck service r with shipment r based on the time-dependent travel time function and the departure time at origin terminal o_s. Constraints (3.14) ensure that the arrival time of shipment r at terminal i is earlier than the departure time of service $s \in Q_i^+ \cup S_i^{+\text{barge}} \cup S_i^{+\text{train}}$ minus loading time, if shipment r is transported by service s leaving terminal i, $i \in N\backslash\{d_r\}$.

3.4.3 Linearization of nonlinear constraints

To improve the computational efficiency, the nonlinear constraints discussed above need to be linearized. The linearization of nonlinear constraints are presented as follows:

- Nonlinear constraint (3.4) $w_{rs} = (TD_s - lt - A_{ro_s})x_{rs} \quad \forall r \in R, s \in S, w_{rs} \in \mathbb{R}^+, x_{rs} \in \{0,1\}, lt \in \mathbb{C}, TD_s \in \mathbb{C}, 0 \leq A_{ri} \leq \mathbf{M}$ under minimum objective can be linearized as following:

$$w_{rs} \geq TD_s - A_{ro_s} - lt + \mathbf{M}(x_{rs} - 1), \qquad \forall r \in R, s \in S, \tag{3.15}$$

  where $\mathbf{M}$ is a large enough number used for binary constraints.

- Nonlinear constraint (3.11) $(A_{ri} - TA_s - lt)x_{rs} = 0, \forall r \in R, i \in N \backslash \{o_r\}, s \in S_i^-, x_{rs} \in \{0,1\}, TA_s \in \mathbb{C}, 0 \leq A_{ri} \leq \mathbf{M}$ can be linearized as following:

$$A_{ri} \leq (TA_s + lt)x_{rs} + \mathbf{M}(1 - x_{rs}), \qquad \forall r \in R, i \in N \backslash \{o_r\}, s \in S_i^-, \tag{3.16}$$

$$A_{ri} \geq (TA_s + lt)x_{rs} + \mathbf{M}(x_{rs} - 1), \qquad \forall r \in R, i \in N \backslash \{o_r\}, s \in S_i^-. \tag{3.17}$$

- Nonlinear constraint (3.12) $(A_{ri} - (A_{ro_s} + t_{rs}^{\text{truck}}))x_{rs} = 0, \forall r \in R, i \in N \backslash \{o_r\}, s \in S_i^{-\text{truck}}$, $x_{rs} \in \{0,1\}, A_{ro_s} \in \mathbb{C}, t_{rs}^{\text{truck}} \in \mathbb{C}, 0 \leq A_{ri} \leq \mathbf{M}$ can be linearized as following:

$$A_{ri} \leq A_{ro_s} + TX_{rs} + \mathbf{M}(1 - x_{rs}), \qquad \forall r \in R, i \in N \backslash \{o_r\}, s \in S_i^{-\text{truck}}, \tag{3.18}$$

$$A_{ri} \geq A_{ro_s} + TX_{rs} + \mathbf{M}(x_{rs} - 1), \qquad \forall r \in R, i \in N \backslash \{o_r\}, s \in S_i^{-\text{truck}}, \tag{3.19}$$

$$TX_{rs} \leq \mathbf{M}x_{rs}, \qquad \forall r \in R, s \in S_i^{-\text{truck}}, \tag{3.20}$$

$$TX_{rs} \leq t_{rs}^{\text{truck}} + \mathbf{M}(1 - x_{rs}), \qquad \forall r \in R, s \in S_i^{-\text{truck}}, \tag{3.21}$$

$$TX_{rs} \geq t_{rs}^{\text{truck}} + \mathbf{M}(x_{rs} - 1), \qquad \forall r \in R, s \in S_i^{-\text{truck}}. \tag{3.22}$$

- Nonlinear constraint (3.14) $(TD_s - lt - A_{ri})x_{rs} \geq 0, \forall r \in R, i \in N \backslash \{d_r\}, s \in S_i^+, x_{rs} \in \{0,1\}, lt \in \mathbb{C}, 0 \leq A_{ri} \leq \mathbf{M}$ can be linearized as following:

$$A_{ri} \leq (TD_s - lt)x_{rs} + \mathbf{M}(1 - x_{rs}), \qquad \forall r \in R, i \in N \backslash \{d_r\}, s \in S_i^+. \tag{3.23}$$

3.5 Numerical experiments

To assess the potential of the matching models, we conduct numerical experiments based on a port-hinterland network by using CPLEX 12.6.3, on a desktop computer with Intel Core i5-6500 3.2 GHz processor and 8 GB of RAM.

3.5.1 Hinterland synchromodal transport network

The topology of a hinterland synchromodal transport network is adapted from Li et al. [49], as shown in Figure 3.4, which includes 6 nodes and 15 arcs.

According to Qu et al. [73] and Li et al. [49], the parameters for different modalities are shown in Table 3.3. For committed barge and train services, the data of modality, origin, destination, capacity, departure time, arrival time, transport time, transport cost, transport distance, and carbon emissions are shown in Table 3.4. For uncommitted barge and train services, the data of modality, origin, destination, capacity, departure time, arrival time,

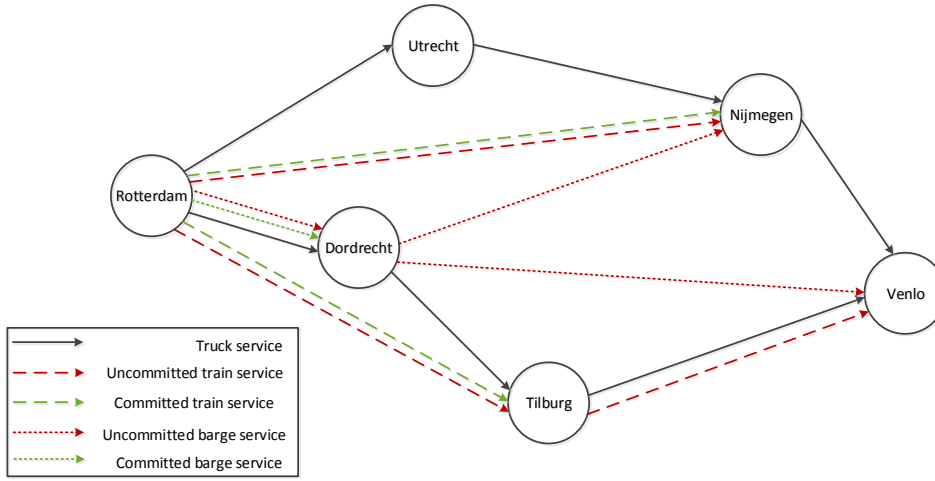

Figure 3.4: Topology of a hinterland synchromodal transport network.

Table 3.3: Parameters used in experiment.

Modality	Speed (km/h)	Transport cost coefficient (€/TEU-h)	Carbon emission coefficient (kg/TEU-km)
Truck	60	30.98	0.8866
Train	35	7.54	0.3146
Barge	15	0.6122	0.2288

Table 3.4: Committed barge and train services.

Service. ID	1	2	3	4	5	6
Modality	Barge	Barge	Train	Train	Train	Train
Origin	Rotterdam	Rotterdam	Rotterdam	Rotterdam	Rotterdam	Rotterdam
Destination	Dordrecht	Dordrecht	Tilburg	Tilburg	Nijmegen	Nijmegen
Capacity (TEU)	200	200	100	100	100	100
Departure time	4	16	4	16	4	16
Arrival time	8	20	8	20	8	20
Transport time (h)	4	4	4	4	4	4
Transport cost (€)	343	343	2111.2	2111.2	2111.2	2111.2
Transport distance(km)	60	60	140	140	140	140
Carbon emissions (kg/TEU)	13.728	13.728	44.044	44.044	44.044	44.044

transport time, transport cost, transport distance, and carbon emissions are shown in Table 3.5. For truck services, the data of origin, destination, transport time, transport cost, transport distance, and carbon emissions are shown in Table 3.6. Loading/unloading cost and time are assumed to be 11.945 €/TEU and 1 hour for barge and train services. The storage cost at each terminal is 1 €/TEU-h. The carbon tax of carbon emissions is 8 €/ton. Regarding the terminal operating hours, we assume all the terminals operate 24 hours every day. The planning horizon is assumed to be one day. The capacity of truck services is assumed to be unlimited.

Table 3.5: Uncommitted barge and train services.

Service. ID	1	2	3	4	5	6
Modality	Barge	Train	Train	Barge	Barge	Train
Origin	Rotterdam	Rotterdam	Rotterdam	Dordrecht	Dordrecht	Tilburg
Destination	Dordrecht	Tilburg	Nijmegen	Nijmegen	Venlo	Venlo
Capacity (TEU)	30	65	30	37	51	47
Departure time	6	6	9	13	12	17
Arrival time	10	10	13	20	23	20
Transport time (h)	4	4	4	7	11	3
Transport cost (€/TEU)	2.45	30.16	30.16	4.29	6.73	22.62
Transport distance (km)	60	140	140	105	165	105
Carbon emissions (kg/TEU)	13.728	44.044	44.044	24.024	37.752	33.033

Table 3.6: Truck services.

Service. ID	7	8	9	10	11	12
Origin	Rotterdam	Rotterdam	Utrecht	Dordrecht	Tilburg	Nijmegen
Destination	Utrecht	Dordrecht	Nijmegen	Tilburg	Venlo	Venlo
Transport time (h)	2	1	1.5	1	1.5	1
Transport cost (€/TEU)	61.96	30.98	46.47	30.98	46.47	30.98
Transport distance(km)	120	60	90	60	90	60
Carbon emissions (kg/TEU)	106.392	53.196	79.794	53.196	79.794	53.196

Table 3.7: Shipments.

Shipments	Origin	Destination	Volume (TEU)	Earliest departure time	Latest arrival time
1	Rotterdam	Utrecht	12	3	24
2	Rotterdam	Utrecht	14	5	24
3	Rotterdam	Utrecht	16	7	24
4	Rotterdam	Utrecht	18	9	24
5	Rotterdam	Dordrecht	14	3	24
6	Rotterdam	Dordrecht	17	5	24
7	Rotterdam	Dordrecht	18	7	24
8	Rotterdam	Dordrecht	19	9	24
9	Rotterdam	Tilburg	17	3	24
10	Rotterdam	Tilburg	18	5	24
11	Rotterdam	Tilburg	19	7	24
12	Rotterdam	Tilburg	20	9	24
13	Rotterdam	Nijmegen	10	3	24
14	Rotterdam	Nijmegen	14	5	24
15	Rotterdam	Nijmegen	17	7	24
16	Rotterdam	Nijmegen	19	9	24
17	Rotterdam	Venlo	13	3	24
18	Rotterdam	Venlo	16	5	24
19	Rotterdam	Venlo	19	7	24
20	Rotterdam	Venlo	20	9	24

The demand data between the Port of Rotterdam and 5 inland terminals are described in Table 3.7. Each shipment is characterized by its origin terminal, destination terminal, container volumes, earliest departure time, and latest arrival time. We assume all the information of shipments is received in advance.

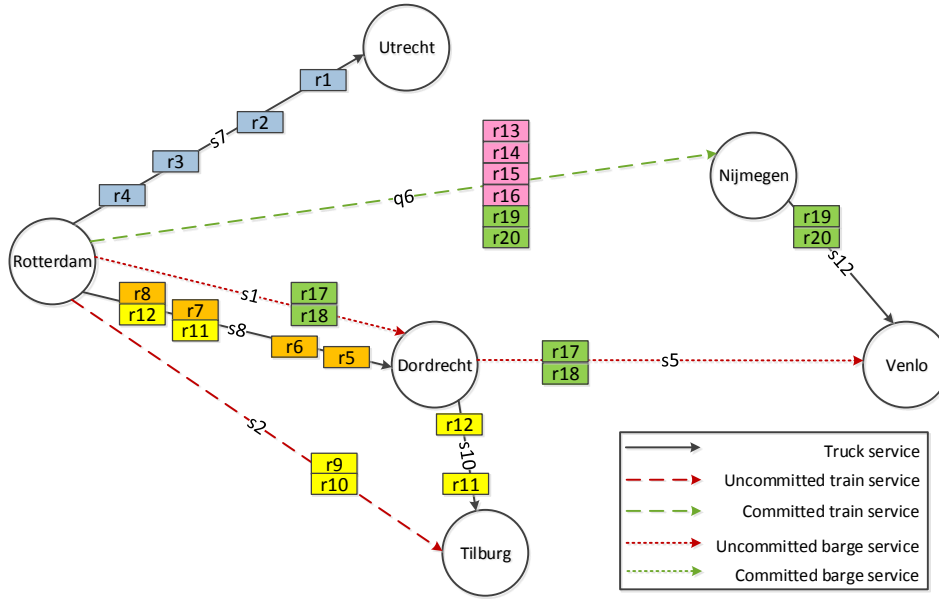

Figure 3.5: Matching results of the HSSM model with time-constant travel times.

3.5.2 Matching results analysis

We set traffic congestion coefficients $\beta_1 = \beta_2 = 1$, weight coefficient $w = 0$. Based on the demand and supply data, the matching result of the HSSM model with time-constant travel times is shown in Figure 3.5. It shows that shipments r1, r2, r3, and r4 are matched with truck service s7. Shipments r5, r6, r7, and r8 are matched with truck service s8. Shipments r9 and r10 are matched with uncommitted train service s2. Shipments r11 and r12 are matched with truck service s8 and s10. Regarding shipments r13, r14, r15, and r16, both of them are matched with committed train service q6. Shipments r17 and r18 are matched with uncommitted barge service s1 and s5 by transferring at Dordrecht terminal. Shipments r19 and r20 are matched with committed train service s6 and truck service s12 by transferring at Nijmegen terminal. From Figure 3.5, we can see that half of the shipments are matched with truck services due to hard time windows of shipments and fixed time schedules and capacity limitations of barge and train services.

Figure 3.6 shows that the truck transport cost occupies the largest share in total logistics costs. The transfer cost is even higher than the barge and train transportation cost, while storage cost and carbon tax are negligible. The reason is that the storage cost coefficient and carbon tax coefficient are much lower than the loading/unloading cost coefficient in the experiment setting.

Sensitivity analysis

To analyze the influence of parameter setting, we varied the values of the loading cost coefficient, loading time, storage cost coefficient, and carbon tax coefficient. For network operators, cost saving is still the primary goal, and modal split belongs to government ob-

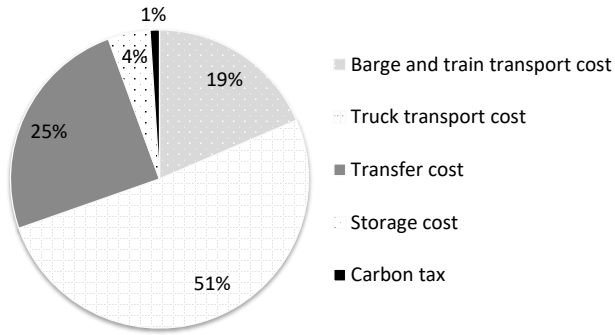

Figure 3.6: Cost distribution of the matching results.

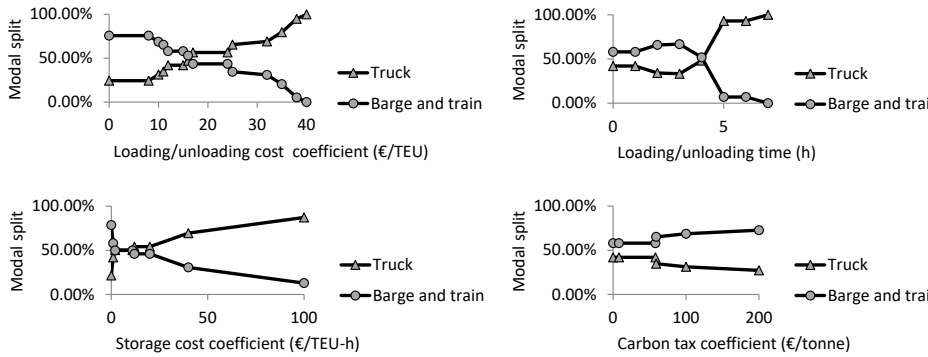

Figure 3.7: Sensitivity analysis.

jective. We view modal split as a post performance indicator to describe the effects. We calculate the modal split of intermodal services and truck services as follows:

Modal split of barge and train services=

$$\frac{\sum_{r\in R}\sum_{q\in Q} x_{rq}u_r D_q + \sum_{r\in R}\sum_{s\in S^{\text{barge}}\cup S^{\text{train}}} x_{rs}u_r D_s}{\sum_{r\in R}\sum_{q\in Q} x_{rq}u_r D_q + \sum_{r\in R}\sum_{s\in S} x_{rs}u_r D_s},$$

Modal split of truck services=

$$\frac{\sum_{r\in R}\sum_{s\in S^{\text{truck}}} x_{rs}u_r D_r}{\sum_{r\in R}\sum_{q\in Q} x_{rq}u_r D_q + \sum_{r\in R}\sum_{s\in S} x_{rs}u_r D_s}.$$

Figure 3.7 shows that the utilization of barge and train services will decrease with the increasing of loading cost coefficient. If the loading cost declines, the utilization of barge and train services will increase. Increasing the loading time, the modal split of barge and train services rises at first and decreases after reaching a certain point. The reason is that a tiny increase in the loading time will decrease the storage time which in turn increasing the utilization of barge and train services.

Table 3.8: Cost distribution of three different scenarios.

Scenarios	Total cost	Barge and train transport cost	Truck transport cost	Transfer cost	Storage cost	Carbon tax
Integrated planning	18500	3433	9449	4587	842	189
Sequential planning	20216	1976	14057	3536	430	228
Decentralized planning	19425	3071	11912	3894	335	213

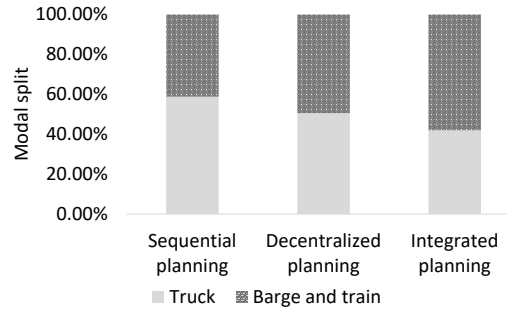

Figure 3.8: Modal split of three different scenarios.

In terms of the storage cost coefficient, the modal split of barge and train services falls with the growth of the storage cost coefficient. Because the utilization of barge and train services produces storage costs at terminals. Regarding the carbon tax coefficient, we can see that the modal split of barge and train services will increase only when the carbon tax coefficient is larger than 50 €/ton.

Different scenarios comparison

The hinterland synchromodal shipment matching problem belongs to an operational integrated planning problem. To verify its benefits, this chapter compares it with sequential planning and decentralized planning. With respect to sequential planning, we assume that shipments arrive one-by-one, so sequential planning is based on the first-in-first-out algorithm. The capacity of barge and train services will be assigned to shipments arriving earlier to the system. For decentralized planning, we assume there exist three carriers. Carrier 1 owns all the barge services, carrier 2 has all the train services, and carrier 3 has all the truck services. Both carriers 1 and 2 collaborate with carrier 3. However, carriers 1 and 2 have a competitive relationship and thus do not share capacity or change requests with each other. Here, we assume shipments r1 to r10 are received by carrier 1, and shipments r11 to r20 are received by carrier 2.

Table 3.8 indicates that integrated planning has the best performance. While sequential planning focuses on local optimum, integrated planning aims at global optimum, the experiment results demonstrate the value of information in transport planning. Compared with decentralized planning, the cost savings achieved by integrated planning show the benefits of horizontal collaboration among carriers in synchromodal transportation.

Figure 3.8 presents the modal split of three different scenarios. The modal split of barge and train services under integrated planning is the largest. Compared with sequential planning, decentralized planning has better performance on the modal split of barge and train services in the designed case.

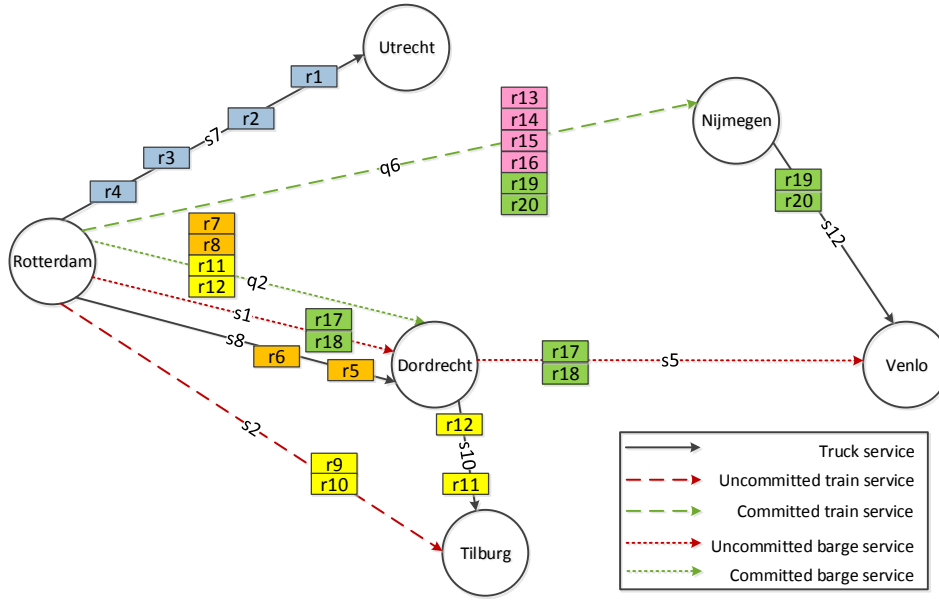

Figure 3.9: Matching results of the HSSM model with time-dependent travel times.

3.5.3 Impact of time-dependent travel times

In this section, we aim to investigate the matching results under time-dependent travel times. We set traffic congestion coefficient $\beta_1 = \beta_2 = 2$. Breaking points $a1 = 5$, $a = 7$, $d1 = 15$, $d = 19$, and $e = 24$. Figure 3.9 presents the matching result of the matching model with time-dependent travel times. Compared with Figure 3.5, shipments r7, r8, r11, and r12 are matched with committed barge service q2 rather than truck service s8 in Figure 3.9. The reason is that the transport cost of truck service s8 is higher than barge service q2 under traffic congestion. Shipments r5 and r6 keep original choice, because their departure time is during the off-peak hour. The results indicate that under the time-varying network, the matching results of the time-constant matching model become suboptimal.

To evaluate the performance of the matching model with time-dependent travel times (TD) under different traffic conditions, we generated 6 instances with different traffic congestion coefficient β_1, varying from 2 to 4.5. We set $a1 = 5, a = 7, b1 = 9, b = c1 = 13, c = 17, d1 = 19, d = 21, e = 24, \beta_2 = 1.5$. We use the matching model with time-constant travel times (TC) as the benchmark. Due to traffic congestion, the matching decisions generated by the TC model might be infeasible. In this case, shipments might be switched from barge or train services to truck services, and shipments might be delayed. We assume the cost of overdue delivery is 50 €/TEU-h.

Figure 3.10 shows that the higher the traffic congestion coefficient, the larger the number of infeasible matches generated by the TC model. By increasing the traffic congestion coefficient, the gap between the TC and TD models also increases in terms of total costs. Therefore, it is shown that the TD model outperforms the TC model when travel times change during the day in hinterland synchromodal transportation.

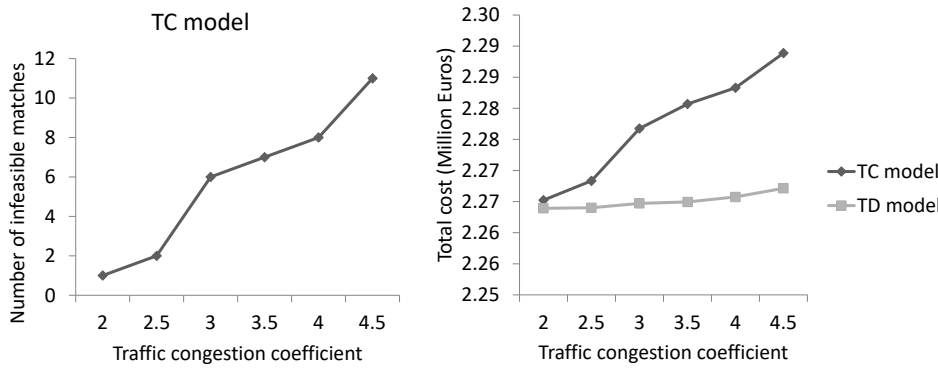

Figure 3.10: Comparison between the TC and TD model.

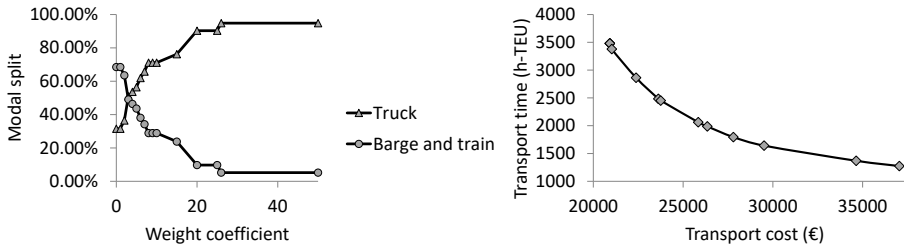

Figure 3.11: Impact of time weight coefficient.

3.5.4 Multi-objective analysis

To analyze the trade-off between transport cost and time, we varied the weight coefficient w from 0 to 50. Figure 3.11 shows that the modal split of barge and train services decreases with the rising of the time weight coefficient. Because barge and train services generally have longer transport time than truck services for the same OD pair. In addition, the right plot of Figure 3.11 indicates that the changes of transport cost and time have opposite directions. The higher the transport cost, the lower the transport time. For shipments with perishable characteristics, the transport time is more important, the time weight coefficient should be set higher.

3.6 Conclusions

This chapter answers research question **RQ1** by investigating a hinterland synchromodal shipment matching problem in which a network operator aims to provide optimal matches between shipments with specific time windows and multimodal services with time schedules. Due to the existence of road traffic congestion, the travel time of truck services is time-dependent. To solve the problem, we have proposed a matching model with time-dependent travel times.

We have conducted numerical experiments to test the performance of the model. The experimental results show that the integrated matching model has better performance than a sequential model and a decentralized model in total costs. Besides, we have tested the impact of different traffic conditions. The matching model with time-dependent travel times has shown to have better performance than the model with time-constant travel times, and the gap between these two models increases with the increasing degree of traffic congestion. Regarding the multi-objective function, the experiment result indicates that the weight coefficient of the total transport time has a high influence on the matching results.

The matching model designed in this chapter assumes that all the requests and services are received in advance. However, in practice, the information of requests arrives dynamically or even in real-time, and the service information might change over time due to disturbances. Possible future work can be to develop online approaches that handle dynamic events and disturbances in synchromodal transport. Chapter 4 in particular, develops dynamic approaches to handle real-time shipment requests.

Chapter 4

Dynamic shipment matching

In Chapter 3, a static shipment matching model was developed to support operational hinterland synchromodal transport planning. The model assumes all the information of shipments and services are received in advance. However, in practice, shipment requests from spot markets arrive in real-time. Therefore, dynamic approaches that support online decision-making processes are required in hinterland synchromodal transportation.

This chapter is structured as follows. In Section 4.1, a dynamic shipment matching problem in hinterland synchromodal transportation is introduced. We discuss the relevant literature in Section 4.2. In Section 4.3, we formally describe the dynamic shipment matching problem. In Section 4.4, we explain the implementation of dynamic approaches. In Section 4.5, we present optimization algorithms. In Section 4.6, we describe the generation of instances and present the experiment results. Finally, Section 4.7 ends the chapter with conclusions.

Parts of this chapter have been published in [37]: "W. Guo, B. Atasoy, W. Beelaerts van Blokland, and R. R. Negenborn. A dynamic shipment matching problem in hinterland synchromodal transportation. *Decision Support Systems*, 134, 113289, 2020."

4.1 Introduction

Hinterland intermodal transportation is the movement of containers between deep-sea ports and inland terminals by using trucks, trains, barges, or any combination of them [87]. Compared with unimodal transportation, intermodal transportation has the flexibility to use different modes considering the specific characteristics of containers and in turn achieves better performance in costs, delays, and emissions [18]. However, due to the utilization of multiple modes, operating an intermodal transportation system is very complex. In intermodal transportation, barge and train services normally follow fixed time schedules and have limited free capacity [18]. Conversely, truck services are usually not scheduled and have time-dependent travel times as a result of road traffic congestion [91]. Therefore, constraints such as time compatibility between different services and capacity limitations of barge and train services need to be considered in intermodal transport planning.

Synchromodal transportation, as discussed in Chapter 2, is an extension of intermodal transportation. It refers to transport systems with dynamic updating of planning by incor-

porating real-time information [30]. The trend towards spot markets and digitalization in hinterland transportation increases the need for such online synchromodal transport systems. In the literature, most of the existing studies assume that container shipments are only collected from large shippers based on long-term contracts. These contractual shipment requests are often fixed and known over a given planning period. Recently, quite a few studies [e.g., 105, 106] have pointed out the trend towards spot markets in container transportation. Different from the former contracted requests, spot shipment requests arrive in real-time and require receiving transport solutions as soon as possible. Thanks to the development of digitalization and advanced information and communication technologies in logistic industries, information can be collected in real-time, and decisions can be made online [68]. Nevertheless, these new trends also introduce complexity in intermodal transport planning, unveiling the need for decision support systems adapted to dynamic contexts.

In this chapter, we investigate a dynamic shipment matching (DSM) problem in which a platform provides online matches between shipment requests and transport services. We consider an online synchromodal matching platform that receives contractual and spot shipment requests from shippers, and receives transport services from carriers, as shown in Figure 4.1. Shippers are the entities that are searching for services to transport their shipments. Examples of shippers include freight forwarders and ocean carriers. Carriers are the entities that provide transport services. Carriers could be truck, train or barge companies. We consider a network operator as the owner of the platform. A network operator could be a logistics service provider or an alliance formed by multiple carriers. The recent developments in information technologies such as cloud computing and Internet of Things allow real-time information sharing and container tracking, which facilitates the adoption of such a platform in practice.

The objective of the platform is to minimize the total cost of matching shipment requests and transport services over a given planning horizon. Due to the capacity limitation of barge and train services, decisions made for current requests may influence the decisions for future requests. Therefore, dynamic approaches that create online matching decisions for current requests are required. In this chapter, we design a rolling horizon approach to handle dynamically revealed shipment requests and develop a heuristic algorithm to solve the DSM problem in a computationally efficient way.

4.2 Literature review

Over the past decades, different freight transport concepts have been proposed in the literature and in the industry: multimodality, intermodality, co-modality, and synchromodality [30]. Although these concepts are often used interchangeably, there are subtle differences between these terms: multimodality focuses on the utilization of multiple modes; intermodality emphasizes the integration between different modes by using standard loading units; co-modality aims to have efficient utilization of resources; synchromodality, as an extension of intermodality, adds dynamic updating of transport plans over a network to benefit from real-time information [5]. In this section, the studies related to the DSM problem have been divided into two categories: hinterland intermodal transportation and synchromodality.

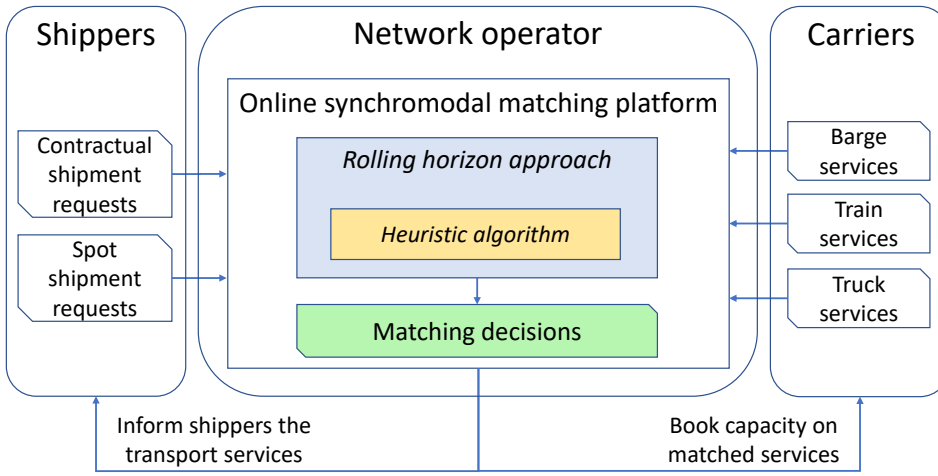

Figure 4.1: Illustration of an online synchromodal matching platform. The platform provides online matches between shipment requests received from shippers and transport services received from carriers thanks to the developed rolling horizon approach.

4.2.1 Hinterland intermodal transportation

Hinterland intermodal transportation is the provision of efficient, reliable, and sustainable services through integrated strategic and tactical planning at a network level. Strategic planning concerns the design of transportation network topologies, such as direct link, corridor, or hub-and-spoke [16]. Konings et al. [45] investigate the benefits of a hub-and-spoke network for hinterland transportation in turnaround times, waiting times, and the reliability of barge services. Containers at a seaport terminal that have different destinations in the hinterland would be transported together to the hub and after being regrouped and bundled with containers originate from other seaport terminals would continue their trip to their inland destination.

Tactical planning refers to optimally utilizing the given network by choosing transportation services, allocating their capacity to customer demands, and planning their itineraries and frequency [87]. Bhattacharya et al. [10] propose a mixed integer programming model to optimize schedules for an intermodal transport network by taking into account the road traffic flow estimation. Zuidwijk et al. [117] propose a single period model to allocate containers to a truck or barge and schedule the barge departure time considering container release time uncertainty and service transit time uncertainty. Crainic et al. [14] propose a service network design model to decide the optimal schedules for the services operated by a fleet of shuttles on the railway network connecting seaport terminals and inland terminals. Demir et al. [18] investigate a service network design problem with travel time uncertainty to decide on the routing of containers and the departure time of transport services.

4.2.2 Synchromodality

While intermodality focuses on offline planning in which all forms of input information are required in advance and decisions are made before the start of transportation, synchromodality , as discussed in Chapter 2, emphasizes online planning in which real-time information about the current state of the transport system can be taken into account in online planning processes [19]. Specifically, synchromodal transport planning deals with dynamic events that are not explicitly addressed in intermodal transportation, including the representation of real-time data, decisions, and system states [16]. The most common dynamic events are the arrival of new shipment requests, but container flows and travel times are possible dynamics as well.

In the literature, Fazi et al. [24] develop a decision support system for the optimal allocation of import containers to a heterogeneous fleet composed of barges and trucks. van Riessen et al. [100] design a decision tree to derive real-time decision rules for suitable allocation of containers to services. Rivera et al. [77] propose an algorithm based on approximate dynamic programming to assign newly arrived containers to either a barge or a truck. Although the above studies considered the utilization of multiple modes, none of them take into account the transshipment operations between different services. Research that models transshipment in synchromodal transportation, such as Li et al. [49] and Qu et al. [72], are usually designed for container flows. However, in practice, shippers would like to receive their shipments as a whole. Therefore, in this chapter, we investigate the DSM problem from shipment requests' perspective, namely, decisions are designed as binary variables indicating the allocation of a specific shipment request to a specific service. Mes et al. [62] propose a greedy approach to select the cheapest services for dynamically arrived shipment requests but without the consideration of road traffic congestion. Due to the limited capacity of road infrastructures, traffic congestion exist during several periods of a day [91]. The variation of road travel times has been well investigated in the literature and therefore can be incorporated in the online synchromodal matching process.

4.2.3 Contributions

In the literature, the work most similar to our work is Li et al. [49], which proposes a rolling horizon approach to control container flows in a hinterland intermodal network by considering time-dependent truck travel times and time-schedules for trains and barges. In contrast to our work, Li et al. [49] focuses on aggregated container flows instead of specific shipment requests with time windows, and therefore uses the value of time instead of delay costs in the objective function to push containers move to their destinations.

The main contributions of this chapter are as follows. First, we propose a rolling horizon approach to handle newly arrived shipment requests. The implementation of the rolling horizon approach relies on an optimization algorithm that can generate timely matching decisions at each decision epoch. In particular, we develop a heuristic algorithm to solve the DSM problem. Third, we conduct extensive experiments to assess the performance of the heuristic algorithm in comparison to an exact algorithm, and the performance of the rolling horizon approach in comparison to a greedy approach from practice. Briefly, we design, operationalize and validate an online matching platform in the context of synchromodal transportation.

4.3 Problem description

Let N be the set of terminals. Without loss of generality, we assume that the loading/unloading cost coefficient of barges lc^{barge}, trains lc^{train}, and trucks lc^{truck}, the loading/unloading time of barges lt^{barge}, trains lt^{train}, and trucks lt^{truck}, and the storage cost coefficient c^{storage} at different terminals are the same.

Let R be the set of shipment requests. Each shipment request $r \in R$ is characterized by its announce time $\mathbb{T}_r^{\text{announce}}$ (i.e., the time when the platform receives the request), release time $\mathbb{T}_r^{\text{release}}$ (i.e., the time when the shipment is available for hinterland transportation) at origin terminal o_r, due time $\mathbb{T}_r^{\text{due}}$ (i.e., the time that the shipment needs to be delivered) at destination terminal d_r, and container volume u_r (i.e., the number of containers). Delay in delivery is available but with a delay cost coefficient per container per hour overdue c_r^{delay}. The lead time of shipment request r is represented as, $LD_r = \mathbb{T}_r^{\text{due}} - \mathbb{T}_r^{\text{release}}$.

Shipment requests can be divided into two groups: contractual requests R^{contract} and spot requests R^{spot}. For a contractual request $r \in R^{\text{contract}}$, the network operator has long-term contracts with shippers. Therefore, the announce time of contractual request r is, $\mathbb{T}_r^{\text{announce}} = 0$. All the information $\{o_r, d_r, u_r, \mathbb{T}_r^{\text{release}}, \mathbb{T}_r^{\text{due}}, c_r^{\text{delay}}\}$ is known in a given planning horizon. Conversely, for a spot request $r \in R^{\text{spot}}$, the platform receives the request from spot markets in real-time. The information of the spot request $\{o_r, d_r, u_r, \mathbb{T}_r^{\text{release}}, \mathbb{T}_r^{\text{due}}, c_r^{\text{delay}}\}$ is unknown before its announce time.

Let S be the set of transportation services. According to the type of modes, services can be divided into two groups: time-scheduled barge and train services, and departure time flexible truck services.

Barge and train services have limited capacity and fixed time schedules but can help generating economies of scale. Each barge or train service $s \in S^{\text{barge}} \cup S^{\text{train}}$ is characterized by its origin terminal o_s, destination terminal d_s, free capacity in terms of loading units (i.e., containers) U_s, departure time (at origin terminal) TD_s, arrival time (at destination terminal) TA_s, transport cost c_s, and generation of carbon emissions e_s.

Truck services have unlimited capacity, flexible departure times, and time-dependent travel times $t_s(\tau) = \theta_s^m \tau + \eta_s^m, \forall \tau \in T^m$, as shown in Figure 4.2. Here, θ_s^m and η_s^m are the slope and intersection of the travel time function for truck service s at time period m; τ represents the departure time of truck services; $\mathbb{T}$ represents the set of time periods within a day; t_s is the travel time at non-peak periods; β_1 and β_2 are traffic congestion coefficients. Each truck service $s \in S^{\text{truck}}$ is characterized by its origin o_s, destination d_s, time-dependent travel time $t_s(\tau)$, transport cost c_s, and generation of carbon emissions e_s.

As spot shipment requests arrive in real-time, the platform provides online matches between shipment requests and transport services. A match is defined as a combination of a shipment and a service, which means the shipment will be transported by the service from the service's origin to the service's destination. Each shipment might be matched with multiple services, each service might be matched with multiple shipments. An illustrative example of shipment matching in synchromodal transportation is shown in Figure 4.3. Matching decision $\langle r1, s4 \rangle$ means shipment $r1$ will be transported by service $s4$ from terminal 1 to terminal 5; matching decision $\langle r2, s1 \rangle, \langle r2, s3 \rangle, \langle r2, s7 \rangle$ means shipment $r2$ will be transported by service combination $[s1, s3, s7]$ from terminal 1 to terminal 6.

To model this problem, we make the following five assumptions. First, we assume the platform is centralized and the contracts among carriers, shippers, terminal operators, and

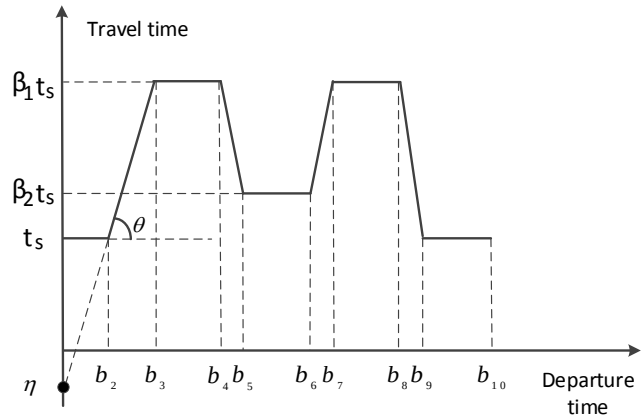

Figure 4.2: Time-dependent travel times of truck services.

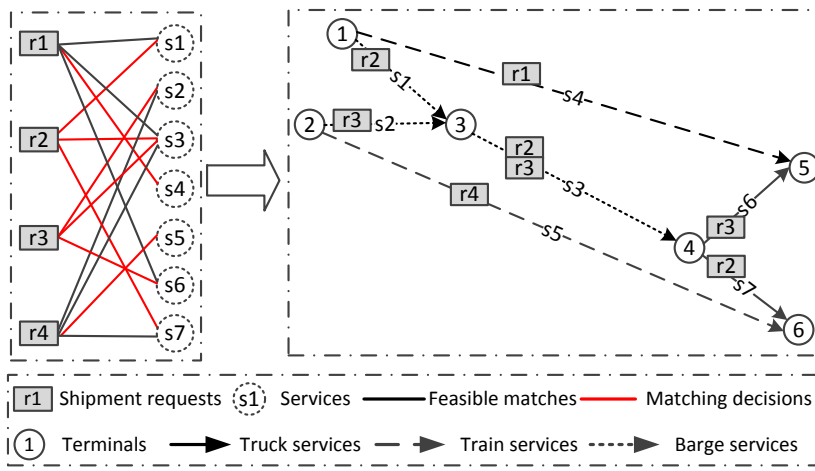

Figure 4.3: Illustrative example of shipment matching in synchromodal transportation.

the network operator have been made. Therefore, we do not consider fairness, pricing, and contracting strategies among players. Second, we do not model the accept/reject decisions and consider only the accepted spot requests by the platform. Third, we assume that shippers require their shipments to be transported as a whole, thus shipments are unsplittable. Fourth, we assume shippers require to receive matching decisions before the release time of shipments. Therefore, the response time of request r is $\Delta\mathbb{T}_r = \mathbb{T}_r^{\text{release}} - \mathbb{T}_r^{\text{announce}}$. Fifth, we assume the capacity of truck services is unlimited. Therefore, the synchromodal matching system always has feasible matches for newly arrived shipment requests. Last, we do not consider stochasticity of travel times in this chapter. Instead, we use deterministic travel times for all services, and consider time-dependent travel times for trucks, since the road traffic patterns have been well investigated in the literature [91].

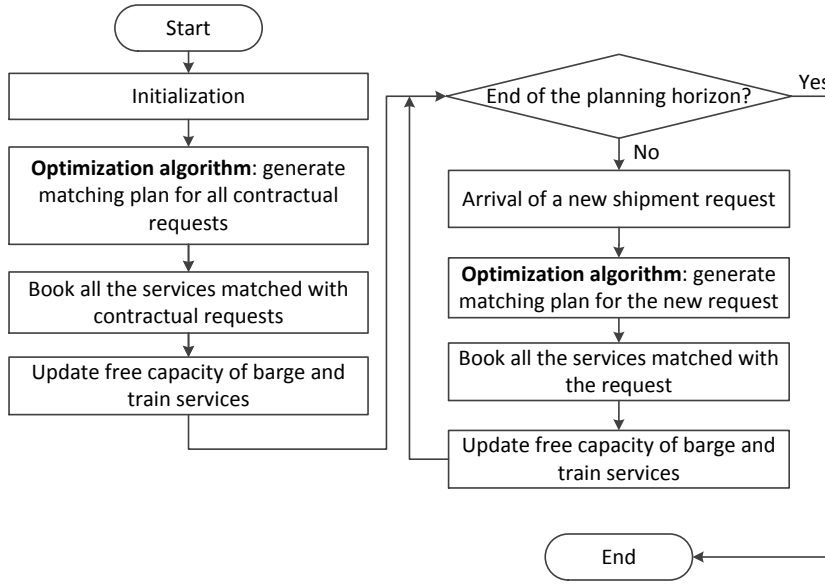

Figure 4.4: Flow chart of the greedy approach.

4.4 Dynamic approaches

To handle newly arrived shipment requests, we need to design methodologies that can update the decisions based on dynamically revealed information. This chapter proposes a rolling horizon approach for the DSM problem and uses a greedy approach as the benchmark. While the greedy approach makes matching decisions for each newly arrived shipment request and the decisions are fixed once they are made, the rolling horizon approach makes decisions at fixed time points for all active requests including newly received requests at the current time interval and the requests received at previous time intervals which have not expired yet, and the decisions are fixed only when the response for the request cannot be further postponed, namely, the request will expire before the next decision epoch.

4.4.1 Benchmark: greedy approach

Greedy approach (GA) is a simple, intuitive algorithm that makes fixed decisions at each step. In practice, a GA is often used for container transport planning [100]. By using the GA, a shipment request is assigned to the cheapest feasible service at the time of request arrival. Figure 4.4 presents the flow chart of the GA applied in dynamic shipment matching. Specifically, the platform provides matches for all the contractual requests received before the planning horizon. After that, the platform books all the services matched with the contractual requests and updates the free capacity of barges and trains. A dynamic event, that is the arrival of a spot shipment request before the end of the planning horizon, triggers a new optimization process. After that, the platform books all the services matched with the spot shipment request, and updates the free capacity of barges and trains.

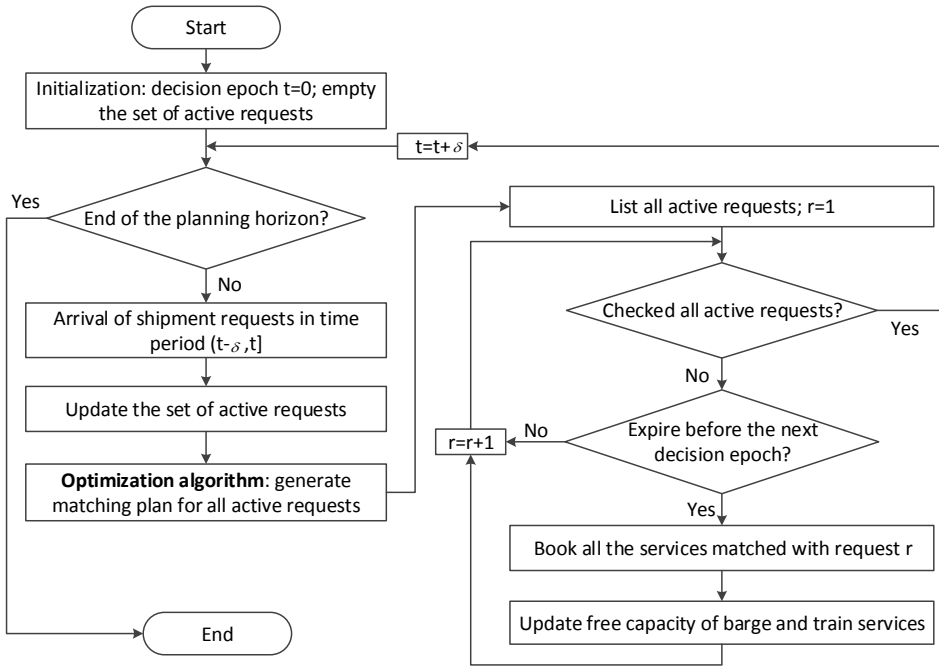

Figure 4.5: Flow chart of the rolling horizon approach.

4.4.2 Rolling horizon approach

Rolling horizon approach (RHA) is a periodic reoptimization approach, which has been applied in many research fields, such as ride-sharing problems [64] and parcel delivery problems [6]. Under a RHA, the system is optimized periodically at pre-specified points in time called *optimization times*. The length between two consecutive optimization times is called *the optimization interval*, δ. The RHA is therefore executed at a given set of time points $\{0, \delta, 2\delta, ..., T\}$. Here, T is the length of the planning horizon.

Under the RHA, plans are made using all known information within a planning horizon, but decisions are not finalized until necessitated by a deadline. Re-optimizing the system allows for enhancing the reliability of the system and improving its performance by incorporating the latest information. The flow chart of the RHA applied in the DSM problem is presented in Figure 4.5. At each decision epoch, the system determines the matches for all active shipments. At time point t, shipment r is active if its announce time is earlier than t, and its release time is later than t. The matching plan for active shipment r made at time point t is fixed only if its release time is earlier than $t+\delta$, namely, the shipment request will expire before the next decision epoch. Thus, the system books all the services matched with this request, and updates the free capacity of barge and train services.

4.5 Optimization algorithms

In this section, we present two optimization algorithms to solve the DSM problem: an exact algorithm and a heuristic algorithm. While the exact algorithm aims to generate optimal solutions, the heuristic algorithm is designed to generate timely solutions.

4.5.1 Exact algorithm

In this section, we present a mixed integer linear programming model (MILP) for the DSM problem. The MILP model is solved by an exact algorithm which is the CPLEX solver. The objective function (4.1) minimizes the total costs for the matching of all shipments with services. The total costs consist of logistics costs (including transport costs, transfer costs, and storage costs), delay costs, and carbon tax. We include delay costs to address the level of services (i.e., delayed deliveries). Considering carbon tax follows the trend towards sustainability in the transport industry. In the literature, there exist several models for calculating emission charges. However, most of the models require detailed input data (e.g., the mass of the vehicle, air, and rolling resistance) which is in many cases not available. As an alternative, the activity-based method that multiplies the number of containers with the CO_2 emission factor yields better feasibility in transportation practice and has been applied in many studies [18, 91]. Therefore, this chapter uses the activity-based method to charge CO_2 emissions. We denote c^{emission} as the CO_2 emissions-related cost coefficient.

Minimize

$$\begin{aligned}&\sum_{r\in R}\sum_{s\in S} x_{rs}u_r c_s + \sum_{r\in R}\sum_{i\in N}\left(f_{ri}^{+}+f_{ri}^{-}\right)u_r + \sum_{r\in R}\sum_{i\in N} w_{ri}u_r c^{\text{storage}}\\ &+\sum_{r\in R}\mathbb{T}_r^{\text{delay}}u_r c_r^{\text{delay}}\\ &+\sum_{r\in R}\sum_{s\in S} x_{rs}e_s u_r c^{\text{emission}}\end{aligned} \tag{4.1}$$

subject to

$$\sum_{s\in S_{or}^{+}} x_{rs} = 1, \quad \forall r\in R, \tag{4.2}$$

$$\sum_{s\in S_{dr}^{-}} x_{rs} = 1, \quad \forall r\in R, \tag{4.3}$$

$$\sum_{s\in S_i^{+}} x_{rs} = \sum_{s\in S_i^{-}} x_{rs}, \quad \forall r\in R, i\in N\backslash\{o_r,d_r\}, \tag{4.4}$$

$$\sum_{r\in R} x_{rs}u_r \le U_s, \quad \forall s\in S^{\text{barge}}\cup S^{\text{train}}, \tag{4.5}$$

$$f_{ri}^{+} = \sum_{s\in S_{i^+}^{\text{barge}}} x_{rs}lc^{\text{barge}} + \sum_{s\in S_{i^+}^{\text{train}}} x_{rs}lc^{\text{train}} + \sum_{s\in S_{i^+}^{\text{truck}}} x_{rs}lc^{\text{truck}}, \ \forall r\in R, i\in N\backslash\{d_r\}, \tag{4.6}$$

$$f_{ri}^{-} = \sum_{s\in S_{i^-}^{\text{barge}}} x_{rs}lc^{\text{barge}} + \sum_{s\in S_{i^-}^{\text{train}}} x_{rs}lc^{\text{train}} + \sum_{s\in S_{i^-}^{\text{truck}}} x_{rs}lc^{\text{truck}}, \ \forall r\in R, i\in N\backslash\{o_r\}, \tag{4.7}$$

$$A_{ro_r} = \mathbb{T}_r^{\text{release}}, \quad \forall r\in R, \tag{4.8}$$

$$A_{ri} \leq \left(TA_s + lt^{\text{barge}}\right) x_{rs} + M\left(1 - x_{rs}\right), \quad \forall r \in R, i \in N \backslash \{o_r\}, s \in S_{i^-}^{\text{barge}}, \tag{4.9}$$

$$A_{ri} \geq \left(TA_s + lt^{\text{barge}}\right) x_{rs} + M\left(x_{rs} - 1\right), \quad \forall r \in R, i \in N \backslash \{o_r\}, s \in S_{i^-}^{\text{barge}}, \tag{4.10}$$

$$A_{ri} \leq \left(TA_s + lt^{\text{train}}\right) x_{rs} + M\left(1 - x_{rs}\right), \quad \forall r \in R, i \in N \backslash \{o_r\}, s \in S_{i^-}^{\text{train}}, \tag{4.11}$$

$$A_{ri} \geq \left(TA_s + lt^{\text{train}}\right) x_{rs} + M\left(x_{rs} - 1\right), \quad \forall r \in R, i \in N \backslash \{o_r\}, s \in S_{i^-}^{\text{train}}, \tag{4.12}$$

$$A_{ri} \leq \tau_{rs} + t_{rs}^{\text{truck}} + lt^{\text{truck}} x_{rs} + M\left(1 - x_{rs}\right), \quad \forall r \in R, i \in N \backslash \{o_r\}, s \in S_{i^-}^{\text{truck}}, \tag{4.13}$$

$$A_{ri} \geq \tau_{rs} + t_{rs}^{\text{truck}} + lt^{\text{truck}} x_{rs} + 2M\left(x_{rs} - 1\right), \quad \forall r \in R, i \in N \backslash \{o_r\}, s \in S_{i^-}^{\text{truck}}, \tag{4.14}$$

$$A_{ri} \leq \left(TD_s - lt^{\text{barge}}\right) x_{rs} + M\left(1 - x_{rs}\right), \quad \forall r \in R, i \in N \backslash \{d_r\}, s \in S_{i^+}^{\text{barge}}, \tag{4.15}$$

$$A_{ri} \leq \left(TD_s - lt^{\text{train}}\right) x_{rs} + M\left(1 - x_{rs}\right), \quad \forall r \in R, i \in N \backslash \{d_r\}, s \in S_{i^+}^{\text{train}}, \tag{4.16}$$

$$A_{ri} \leq \tau_{rs} - lt^{\text{truck}} x_{rs} + M\left(1 - x_{rs}\right), \quad \forall r \in R, i \in N \backslash \{d_r\}, s \in S_{i^+}^{\text{truck}}, \tag{4.17}$$

$$\tau_{rs}^{'} = \tau_{rs} - 24 n_{rs}, \quad \forall r \in R, s \in S^{\text{truck}}, \tag{4.18}$$

$$\tau_{rs}^{'} = \sum_k \zeta_{rs}^k b_k, \quad \forall r \in R, s \in S^{\text{truck}}, \tag{4.19}$$

$$\sum_k \zeta_{rs}^k = 1, \quad \forall r \in R, s \in S^{\text{truck}}, \tag{4.20}$$

$$t_{rs}^{\text{truck}} = \sum_k \zeta_{rs}^k \left(\theta_s^m b_k + \eta_s^m\right), \quad \forall r \in R, s \in S^{\text{truck}}, \tag{4.21}$$

$$\sum_m \xi_{rs}^m = 1, \quad \forall r \in R, s \in S^{\text{truck}}, \tag{4.22}$$

$$\zeta_{rs}^1 \leq \xi_{rs}^1, \quad \forall r \in R, s \in S^{\text{truck}}, \tag{4.23}$$

$$\zeta_{rs}^k \leq \xi_{rs}^{k-1} + \xi_{rs}^k, \quad \forall r \in R, s \in S^{\text{truck}}, k \in \{2, 3, \ldots K-1\}, \tag{4.24}$$

$$\zeta_{rs}^K \leq \xi_{rs}^{K-1}, \quad \forall r \in R, s \in S^{\text{truck}}, \tag{4.25}$$

$$w_{ri} \geq \left(TD_s - lt^{\text{barge}}\right) x_{rs} - A_{ri}, \quad \forall r \in R, i \in N \backslash \{d_r\}, s \in S_{i^+}^{\text{barge}}, \tag{4.26}$$

$$w_{ri} \geq \left(TD_s - lt^{\text{train}}\right) x_{rs} - A_{ri}, \quad \forall r \in R, i \in N \backslash \{d_r\}, s \in S_{i^+}^{\text{train}}, \tag{4.27}$$

$$w_{ri} \geq \tau_{rs} - lt^{\text{truck}} x_{rs} + M(x_{rs} - 1) - A_{ri}, \quad \forall r \in R, i \in N \backslash \{d_r\}, s \in S_{i^+}^{\text{truck}}, \tag{4.28}$$

$$\mathbb{T}_r^{\text{delay}} \geq A_{rd_r} - \mathbb{T}_r^{\text{due}}, \quad \forall r \in R, \tag{4.29}$$

where f_{ri}^+ and f_{ri}^- are the loading and unloading cost of request $r \in R$ at terminal $i \in N$ per container; w_{ri} is the storage time of request r at terminal i; $\mathbb{T}_r^{\text{delay}}$ is the delay of request r at destination terminal d_r; M is a large number used for linearizing binary constraints; τ_{rs} represents the departure time of truck service $s \in S^{\text{truck}}$ with request $r \in R$; $\tau_{rs}^{'}$ is the normalized departure time of truck service s with request r, $0 \leq \tau_{rs}^{'} \leq 24$; n_{rs} denotes an integer variable used for normalizing departure time of truck service s with request r; ζ_{rs}^k is a continuous variable used for linearizing the time-dependent travel time function of truck service $s \in S^{\text{truck}}$, $0 \leq \zeta_{rs}^k \leq 1$; ξ_{rs}^m is a binary variable used for the linearization.

Constraints (4.2)-(4.4) manage the inflow of shipments at their origin terminal, outflow at destination terminal, and flow conservation at transshipment terminal. Constraints (4.5) ensure that the total container volumes of shipments carried by service $s \in S^{\text{barge}} \cup S^{\text{train}}$

do not exceed its free capacity. Constraints (4.6)-(4.7) represent the loading and unloading cost of request r per container generated at terminal i. Constraints (4.8) assume that the arrival time of request r at origin terminal is the release time. Constraints (4.9)-(4.12) ensure that the arrival time of request r at terminal i is the arrival time of service $s \in S^{\text{barge}} \cup S^{\text{train}}$ plus unloading time, if request r is transported by service s entering terminal i. Constraints (4.13)-(4.14) ensure that the arrival time of request r at terminal i is the sum of departure time of service $s \in S^{\text{truck}}$ with request r at terminal o_s, travel time of truck service s, and unloading time, if request r is transported by truck service s entering terminal i. In constraints (4.14), we use $2M$ instead of M in the right-hand side to make sure the value of A_{ri} will not be influenced by the constraints when $x_{rs} = 0$ and $\tau_{rs} = M$. Constraints (4.15-4.17) ensure that the arrival time of request r at terminal i is earlier than the departure time of service $s \in S$ minus loading time, if request r is transported by service s leaving terminal i. Constraints (4.18)-(4.25) are imposed to linearize the time-dependent travel time functions of truck services. Constraints (4.26)-(4.28) ensure that the storage time of request r at terminal i is the departure time of service s minus the arrival time of request r at terminal i and minus loading time, if request r is transported by service s leaving terminal i. Constraints (4.29) are imposed to calculate the late deliveries of request r at destination terminal d_r. We do not penalize earlier deliveries but only late deliveries.

4.5.2 Heuristic algorithm

Due to the computational complexity of the matching problem, the exact algorithm proposed in Section 4.5.1 cannot generate feasible solutions for realistic instances. Therefore, this chapter proposes a preprocessing-based heuristic algorithm to reduce the computational complexity. The algorithm consists of three steps: preprocessing of path generation in which no request-specific characteristics are taken into account, preprocessing of feasible matches in which request-specific characteristics (i.e., release time and due time) are considered, and binary integer programming to generate 'optimal' solutions.

Preprocessing of path generation

We define a path as a combination of services. A path p can consist of a single service or multiple services. For example, a path p consists of a barge service s_1 and a truck service s_2, thus, $p = [s_1, s_2]$. We define L as the largest number of services in a path. Due to fixed schedules of barge and train services, some of the service combinations are infeasible. Let P_{ij}^{l} be the set of feasible paths with l services that depart at terminal $i \in N$ and arrive at terminal $j \in N$, $l \in \{1,...,L\}$. A path $p \in P_{ij}^{l}$ is feasible only if all the services in path $p = [s_1,...,s_l]$ satisfies spatial and time compatibility: for service $s_n, s_{n+1} \in p, n \in \{1,...,l-1\}$, the destination terminal of service s_n should be the same as the origin terminal of service s_{n+1}; the arrival time of s_n plus unloading and loading time at the transshipment terminal should be earlier than the departure time of service s_{n+1}.

Based on the above principles, feasible paths with maximum L services are generated by using the offline preprocessing algorithm presented in Algorithm 4.1. The algorithm starts with determining the feasible paths for each origin-destination pair with just one service, and subsequently combines these paths with a single service to create feasible paths with two services, three services, and so on. For each feasible path, we record the virtual

Algorithm 4.1 Path generation algorithm.

Input: Set of transportation services S, set of terminals N, the largest number of services in a path L, index $l \in \{1,2,...,L\}$.

Output: Set of feasible paths $P = P^1 \cup ...P^l \cup ...P^L$, $P^l_{ij} \subseteq P^l$ represents the set of feasible paths with l services that depart at node i, and arrive at node j. Auxiliary time points $MT^l_p = \left[MT^{l1}_p, ..., MT^{l(2l)}_p\right]$.

Initialize: Let $P \leftarrow \emptyset, MT^l_p \leftarrow [0], l \leftarrow 1$.

```
for node i ∈ N, node j ∈ N do
  for service s ∈ S do
    if origin o_s = i and destination d_s = j then
      p ← [s]
      P^l_ij ← P^l_ij ∪ {p}
      MT^l_p ← AUXILIARYTIMEPOINTS(p)
l ← l + 1
while l ≤ L do
  for node i ∈ N, node j ∈ N do
    for service s ∈ S do
      if origin o_s ≠ i and destination d_s = j then
        for feasible path p ← [s_1, ..., s_{l-1}] ∈ P^{l-1}_{io_s} do
          if TIMECOMPATIBLE1(p, s) = 1 then
            p' = [s_1, ..., s_{l-1}, s]
            P^l_ij ← P^l_ij ∪ {p'}
            MT^l_{p'} ← AUXILIARYTIMEPOINTS(p')
  l ← l + 1
```

departure and arrival time points of all the services in the path by calling the AUXILIARYTIMEPOINTS as described in Algorithm 4.2. The virtual departure (arrival) time points of barge and train services are the departure (arrival) time of these services minus (plus) loading (unloading) time. Instead of determining the departure time of truck services to avoid traffic congestion, we define the virtual departure time points of truck services as the virtual arrival time points of their previous services to reduce computational complexity. The time-dependent travel time of truck services is calculated based on the virtual departure time point plus loading time. To examine whether a path $p' = [s_1, ..., s_{l-1}, s] \in P^l_{ij}$ is feasible, we check the time compatibility between path $p = [s_1, ..., s_{l-1}] \in P^{l-1}_{io_s}$ and service $s \in S^-_j$ by calling the TIMECOMPATIBLE1 as described in Algorithm 4.3.

Preprocessing of feasible matches

A match $\langle r, p \rangle$ is defined as a combination of shipment $r \in R$ and path $p = [s_1, ..., s_l]$, $p \in P$, which means shipment r will be transported by the services included in path p. The match $\langle r, p \rangle$ is feasible only if it satisfies spatial and time compatibility: the origin of shipment r should be the same as the origin of service s_1, the destination of shipment r should be the same as the destination of service s_l; the release time of shipment r should be earlier than the virtual departure time point of service s_1.

Algorithm 4.2 AUXILIARYTIMEPOINTS.

Input: Feasible path $p = [s_1, ..., s_l]$.

Output: Auxiliary time points $MT_p^l = \left[MT_p^{l1}, ..., MT_p^{l(2n)}, ..., MT_p^{l(2l)}\right], n \in \{1, ..., l\}$.

Initialize: Let $MT_p^l \leftarrow [0], n \leftarrow 1$.

while $n \leq l$ **do**
  if $s_n \in S^{\text{truck}}$ **then**
    if $n = 1$ **then**
      $MT_p^{l(2n-1)} \leftarrow 0$
    else
      $MT_p^{l(2n-1)} \leftarrow MT_p^{l(2n-2)}$
    Travel time of truck service $s_n \leftarrow$ calculate the time-dependent travel time function
    $MT_p^{l(2n)} \leftarrow MT_p^{l(2n-1)}$ plus loading time plus travel time of truck service s_n plus unloading time
  else
    $MT_p^{l(2n-1)} \leftarrow$ departure time of service $s_n \in S^{\text{barge}} \cup S^{\text{train}}$ minus loading time
    $MT_p^{l(2n)} \leftarrow$ arrival time of service $s_n \in S^{\text{barge}} \cup S^{\text{train}}$ plus unloading time
  $n \leftarrow n + 1$

Algorithm 4.3 TIMECOMPATIBLE1.

Input: node $i \in N$, service $s \in S \backslash S_i^+$, feasible path $p = [s_1, ..., s_{l-1}] \in P_{io_s}^{l-1}$.
Output: z, equal to 1 if path p and service s is time compatible, 0 otherwise.
Initialize: Let $z \leftarrow 0$.

if $s \in S^{\text{barge}} \cup S^{\text{train}}$ **then**
  if $MT_p^{2(l-1)} \leq$ departure time of service s minus loading time **then**
    $z \leftarrow 1$, return z
else
  $z \leftarrow 1$, return z

We define Φ as the set of feasible matches, c_{rp} as the cost of matching shipment r with path p. Algorithm 4.4 is designed to create the feasible matches. For shipment r and path $p = [s_1, ..., s_l] \in P_{o_r d_r}^l$, the time compatibility between r and p is checked by calling TIMECOMPATIBLE2, as presented in Algorithm 4.5. If $s_1, ..., s_n$ are truck services, the virtual departure and arrival time points of these truck services need to be updated sequentially. After the updating, if the virtual arrival time point of s_n is less than the virtual departure time point of service $s_{n+1} \in S^{\text{barge}} \cup S^{\text{train}}$, match $\langle r, p \rangle$ is feasible. If s_1 is a barge or train service, and the release time of shipment r is less than the virtual departure time point of service s_1, then match $\langle r, p \rangle$ is feasible.

Binary integer programming

Based on the above preprocessing procedures, the objective function is updated to minimize the total costs for the matching of shipments with feasible paths. Let z_{rp} be a binary decision variable equal to 1 if shipment r is matched with path p, and 0 otherwise. The mathematical formulation translates into a binary integer programming (BIP) model:

Algorithm 4.4 Feasible match generation algorithm.

Input: Set of feasible paths P, set of shipment requests R, the largest number of services in a path L, index $l \in \{1,2,...,L\}$, set of auxiliary time points MT, objective function (4.1).
Output: Set of feasible matches $\Phi = \Phi_1 \cup \Phi_2 ... \cup \Phi_r ... \cup \Phi_R$.
Initialize: Let $\Phi \leftarrow \emptyset, l \leftarrow 1$.

for shipment request $r \in R$ **do**
  for $l \in \{1,2,...,L\}$ **do**
    for feasible path $p = [s_1, s_2, ..., s_l] \in P^l_{o_r d_r}$ **do**
      if TIMECOMPATIBLE2$(r,p) = 1$ **then**
        $\Phi_r \leftarrow \Phi_r \cup \{p\}$
        $c_{rp} \leftarrow$ Calculate the objective function

Algorithm 4.5 TIMECOMPATIBLE2.

Input: shipment request $r \in R$, feasible path $p = [s_1, ..., s_l] \in P^l_{o_r d_r}$, auxiliary time points $MT^l_p = \left[MT^{l1}_p, ..., MT^{l(2n)}_p, ..., MT^{l(2l)}_p\right], n \in \{1, ..., l\}$.
Output: z, equal to 1 if r and p is time compatible, 0 otherwise.
Initialize: Let $z \leftarrow 0, n \leftarrow 2$.

if $s_1 \in S^{\text{truck}}$ **then**
  update $MT^{l1}_p \leftarrow$ release time of shipment request r
  update travel time of truck service $s_1 \leftarrow$ calculate time-dependent travel time function truck service s_1
  update $MT^{l2}_p \leftarrow MT^{l1}_p$ plus loading time plus travel time of truck service s_1 plus unloading time
  while $n \leq l$ **do**
    if $s_n \in S^{\text{truck}}$ **then**
      update $MT^{l(2n-1)}_p \leftarrow MT^{l(2n-2)}_p$
      update travel time of truck service $s_n \leftarrow$ calculate time-dependent travel time function truck service s_n
      update $MT^{l(2n)}_p \leftarrow MT^{l(2n-1)}_p$ plus loading time plus travel time of truck service s_n plus unloading time
    else
      if $MT^{l(2n-2)}_p \leq MT^{l(2n-1)}_p$ **then**
        $z \leftarrow 1$, return z
      else
        return z
    $n \leftarrow n+1$
else
  if release time of shipment request $r \leq MT^{l1}_p$ **then**
    $z \leftarrow 1$, return z

Minimize

$$\sum_{r \in R} \sum_{p \in \Phi_r} c_{rp} z_{rp} \tag{4.30}$$

subject to

$$\sum_{p\in\Phi_r} z_{rp} = 1, \quad \forall r \in R, \tag{4.31}$$

$$\sum_{r\in R}\sum_{p\in\Phi_{rs}} z_{rp}u_r \leq U_s, \quad \forall s \in S^{\text{barge}} \cup S^{\text{train}}. \tag{4.32}$$

where $\Phi_{rs} = \{p \in \Phi_r | s \in p\}$.

Constraints (4.31) ensure that only one feasible path will be assigned to each shipment. Constraints (4.32) ensure that the total volume of shipments assigned to service $s \in S^{\text{barge}} \cup S^{\text{train}}$ does not exceed its free capacity.

4.6 Numerical experiments

In this section, we first evaluate the performance of the optimization algorithms and compare the GA with the RHA. Then, we investigate the impact of different objective functions and optimization intervals. All algorithms were implemented in MATLAB R2017a, and all experiments were performed on a computer with 2.50 GHz Intel Core i5-7200U CPU and 8 GB RAM. CPLEX 12.6.3 was used as an IP solver.

4.6.1 Generation of test instances

In practice, different companies have different network sizes. For example, Combi Terminal Twente (https://www.ctt-twente.nl/en/, accessed: 2020-03-16) provides container transports from the port of Rotterdam to 3 inland terminals in the Netherlands and Germany with 7 barges, 3 trains and 40 trucks per week. European Gateway Services (EGS, https://www.europeangatewayservices.com/en, accessed: 2020-03-16) offers above 40 trains and 30 barges per week between the Ports of Rotterdam and Antwerp and 11 inland terminals in the Netherlands, Belgium, Germany, and Austria. Every year, approximately 1000000 TEU is transported within the EGS network. To show the application of the model, we consider a hinterland intermodal network in Europe to carry out the numerical experiments, as shown in Figure 4.6. The network consists of three deep-sea terminals (nodes 1, 2, 3) and seven inland terminals (nodes 4, 5, 6, 7, 8, 9, 10) which are connected by 116 transport services, including 49 barges, 33 trains, and 34 trucks. The length of the planning horizon was set to one week. The coefficients used in the experiments were derived from Riessen et al. [102] and Li et al. [49], as shown in Table 4.1. Here, the transport cost of services is a linear function of the transport time t and distance d.

We generated several instances to represent different characteristics of shipments within the given network. We use $\text{EU}-n_1-n_2$ to represent an instance with n_1 contractual requests and n_2 spot requests. The average container volume of contractual requests is 20 TEU, and the average container volume of spot requests is 5 TEU. We set the arrival frequency to 20, 10, 6 and 4 minutes for instances with 400, 800, 1200 and 1600 spot requests, respectively. Regarding the time-dependent travel times, we set $b_1 = 0, b_2 = 5, b_3 = 7, b_4 = 9, b_5 = 13, b_6 = 17, b_7 = 19, b_8 = 21, b_9 = 24, \beta_1 = 2, \beta_2 = 1.5$. The detailed information of services and instances used in this chapter is available at http://doi.org/10.4121/uuid:512169a0-5a69-43a9-a85b-105dd351cc74.

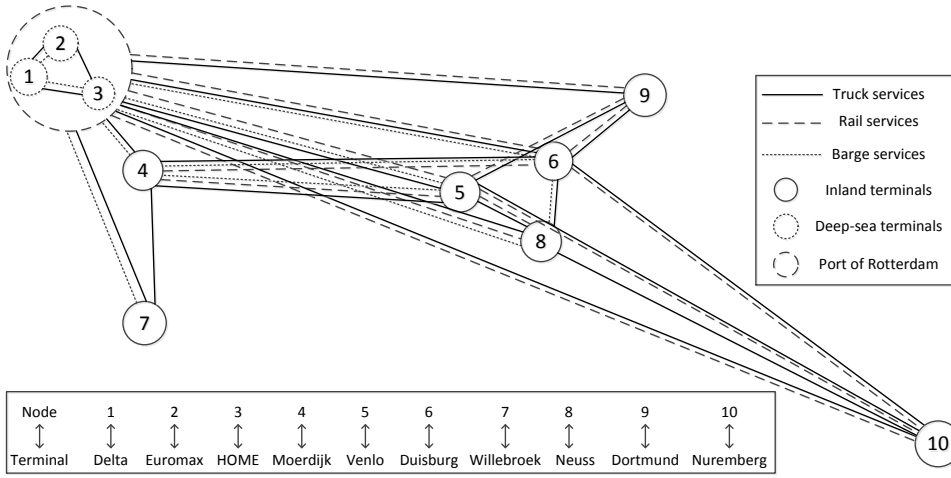

Figure 4.6: The topology of an intermodal network in Europe.

Table 4.1: Experimental setting.

Coefficient	Truck	Barge	Train
Transport cost (€/TEU-km-h)	30.98t+0.2758d	0.6122t+0.0213d	7.54t+0.0635d
Carbon emission (kg/TEU-km)	0.8866	0.2288	0.3146
Loading/unloading cost (€/TEU)	3	18	18
Loading/unloading time (h)	0	1	1
Carbon tax (€/ton)	8	8	8
Storage cost (€/TEU-h)	1	1	1

4.6.2 Performance of the heuristic algorithm

To compare the performance of the heuristic algorithm presented in Section 4.5.2 with the exact algorithm presented in Section 4.5.1, we generated 8 instances of the DSM problem with different numbers of shipment requests. In the exact algorithm, we set the large enough number M to 168. In the heuristic setting, we let the largest number of services in a path L be 1, 2, 3 and 4, respectively. We use heuristic-L to represent the heuristic algorithm with setting L. The number of variables (i.e., N.var) and constraints (i.e., N.con) for the instances under different algorithms is presented in Table 4.2.

We consider two performance indicators: total costs (obj: €) and computation time (CPU: seconds). The computation time of heuristics includes the time of generating feasible matches and the time of solving the BIP model. We use 'gap' to represent the %gaps in total costs between different algorithms, which is given by (objective value - benchmark value)*100/benchmark value. Table 4.3 summarizes the performance for all instances. It shows that the small instances with up to 30 contractual requests are still solvable by using the exact algorithm. However, the computation time increases dramatically from 27 to 5647 seconds. In comparison, extending L from 1 to 3, the gaps in total cost between the heuristic algorithm and the exact algorithm decreases to 0.00%. The computation time of the heuristic algorithm with a maximum of 3 services in a path (Heuristic-3) is no more than 1 second.

Table 4.2: Number of variables and constraints for the instances under different algorithms.

Instances	Exact algorithm		Heuristic-1		Heuristic-2		Heuristic-3		Heuristic-4	
	N.var	N.con	N.var	N.con	N.var	N.con	N.var	N.con	N.var	N.con
EU-5-0	4185	4221	26	18	54	25	66	25	68	25
EU-10-0	8370	8408	28	24	209	63	684	82	944	82
EU-20-0	16740	16676	84	61	428	85	1125	91	1488	91
EU-30-0	25110	24963	112	66	564	104	1646	105	2235	105
EU-700-0	585900	580996	2504	767	13725	780	36449	781	56777	781
EU-1000-0	837000	829916	3279	1067	18108	1082	49908	1082	79805	1082
EU-1300-0	1088100	1079016	4473	1367	25377	1380	69202	1381	109758	1381
EU-1600-0	1339200	1327942	6032	1667	33742	1680	91020	1681	143859	1681

Table 4.3: Performance of the heuristic algorithm with different L.

Instances	Exact algorithm		Heuristic-1		Heuristic-2		Heuristic-3		Heuristic-4		
	obj	CPU	%gap	CPU	%gap	CPU	%gap	CPU	obj	%gap	CPU
EU-5-0	4386	27.01	0.00	0.05	0.00	0.15	0.00	0.60	4386	0.00	0.28
EU-10-0	25988	213.06	32.89	0.03	0.00	0.11	0.00	0.45	25988	0.00	0.80
EU-20-0	44198	1704.98	29.56	0.02	0.05	0.13	0.00	0.43	44198	0.00	0.65
EU-30-0	65126	5647.03	28.52	0.02	0.00	0.13	0.00	0.60	65126	0.00	0.94
EU-700-0	Out of memory		17.49	1.37	0.17	8.21	0.00	25.47	1060077		38.43
EU-1000-0			18.37	2.60	0.25	16.46	0.00	45.22	1017669		78.94
EU-1300-0			19.03	6.12	0.42	34.15	0.00	94.62	1042481		158.57
EU-1600-0			18.36	10.55	0.17	63.22	0.00	176.24	1020075		302.41

For instances with above 700 total requests, we cannot obtain feasible solutions with the exact algorithm. The limitation in these instances is not the computation time but rather the memory since the size of the problems becomes too large to read. In contrast, all these large instances can be solved by using the heuristic algorithm with a maximum of 3 services in a path within 176.24 seconds, and the gaps in total costs between heuristic-3 and heuristic-4 are 0.00%.

4.6.3 Performance of the dynamic approaches

In this section, we aim to compare the performance of two dynamic approaches: the GA and the RHA. Both of them work with Heuristic-3. We set the length of the optimization interval under the RHA to 1 hour.

We generated 4 groups of instances with different demand densities represented by the ratio between demand and supply: EU-100-400 (40%), EU-200-800 (80%), EU-300-1200 (120%), and EU-400-1600 (160%). Here, demand is the total container volumes of shipments, supply is the total free capacity of barge and train services. Each group includes 10 instances with the same ratio between demand and supply. We use the GA as the benchmark. Figure 4.7 (a) shows that the RHA has lower total costs in all the groups of instances, and the reduction in total costs increases with the demand density. The reason is that the higher the ratio between demand and supply, the competition between shipment requests is higher. The proposed RHA better allocates limited barge and train capacity to more suitable shipment requests which might arrive later in the system.

We generated another 4 groups of instances with different degrees of dynamism (DOD). In this chapter, we define the DOD as the ratio between the number of spot containers

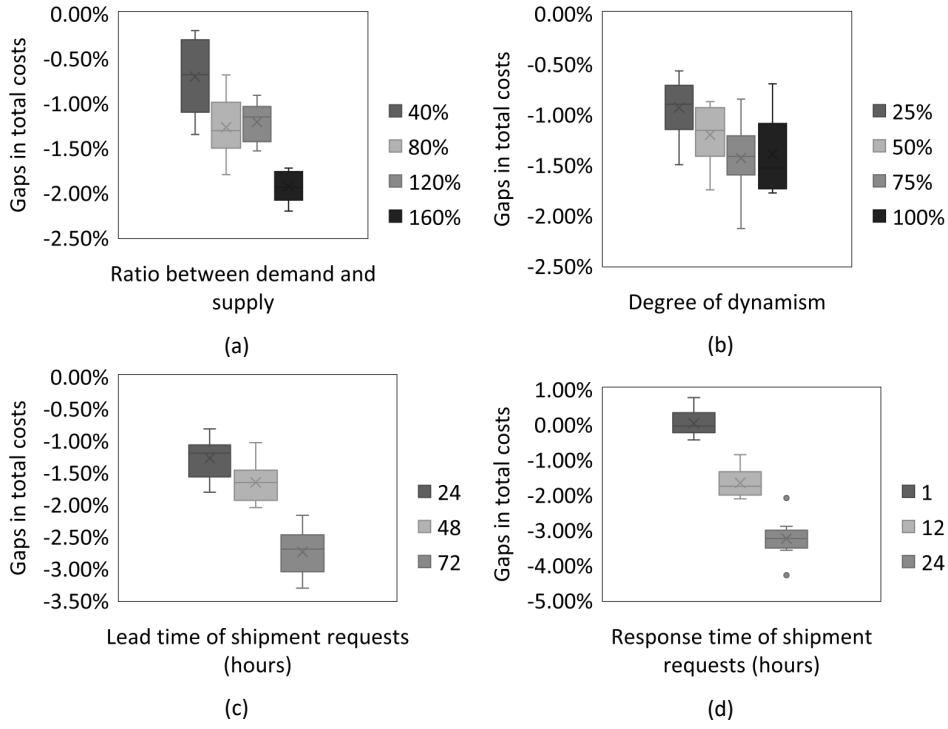

Figure 4.7: Comparison between the rolling horizon approach and the greedy approach.

and the number of total containers. For instance EU-300-400, its DOD is calculated as $(400*5)/(300*20+400*5) = 25\%$. The DOD for instance EU-300-400, EU-200-800, EU-100-1200, EU-0-1600 are therefore 25%, 50%, 75% and 100% respectively. Each group includes 10 instances with the same DOD. Figure 4.7 (b) shows that the RHA also has better performance in all the groups of instances compared to the GA, and the improvement is increasing further with a higher DOD. Interestingly, when the matching system is 100% dynamic, the variance of the performance of the RHA becomes the largest. The reason is when the system is fully dynamic, the performance of the reoptimization-based RHA becomes uncertain.

To investigate the performance of the GA and the RHA under different lead time scenarios, we generated 3 groups of instances with different lead times of spot requests: EU-100-1200 (24), EU-100-1200 (48), and EU-100-1200 (72). Each group consists of 10 instances with the same lead time setting. Figure 4.7 (c) shows that the RHA has better performance than the GA in terms of total costs for all groups of instances and the improvement is larger for longer lead times. Longer lead times provide more flexibility for the RHA to re-optimize the decisions as new requests are received and the capacity can be allocated more effectively.

Similarly, we varied the response time of shipment requests from 1 hour to 24 hours for 3 groups of instances: EU-100-1200 (1), EU-100-1200 (12), and EU-100-1200 (24). Figure 4.7 (d) shows that the larger the response time, the better the performance of the RHA is in reducing total costs since it has more time to update decisions for all requests until their release times.

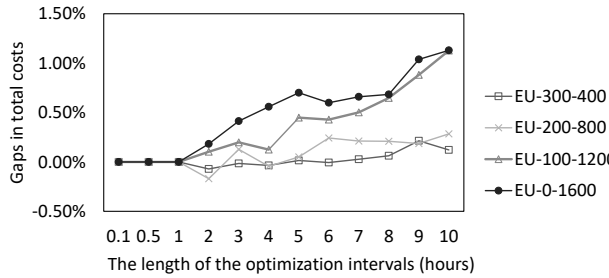

Figure 4.8: Impact of the length of the optimization interval.

4.6.4 Effects of objective functions and optimization intervals

Impact of different objective functions

We investigate the impact of different objective functions under instance EU-1000-0. The utilization of barges and trains is defined as the ratio between the utilized capacity of barge and train services multiplied by corresponding transport distances and the utilized total capacity of all services multiplied by corresponding distances. Table 4.4 shows that different objective functions generate different matching solutions. Comparing case 11 with cases 1 to 10, we observe that the total cost is the lowest when the objective function includes all elements. When we minimize the transport cost (case 1) or the carbon tax (case 5), the utilization of barges and trains is favored as they are cheaper and environmental friendlier than trucks. On the other hand, minimizing the transfer (case 2), storage (case 3) or delay (case 4) cost favors the utilization of trucks as they are faster in general and have flexible departure times. Comparing case 11 with cases 6 to 10, we see that the transport cost has the largest influence on the matching decisions while carbon tax has the smallest impact. However, it is predictable that the carbon tax coefficient will increase in the near future because of the increasing environmental issues and the enforced regulations. Under a restrict emission policy, such as case 14, including the carbon tax in the objective function can greatly affect the utilization of barges and trains. It is also interesting to observe that there is a clear trade-off between delay and carbon emissions as it is what is happening in real life.

Impact of the length of the optimization interval

To test the impact of the length of the optimization interval in the RHA, we used 4 instances with different DOD: EU-300-400 (25%), EU-200-800 (50%), EU-100-1200 (75%) and EU-0-1600 (100%). For each instance, we vary the length of the optimization interval δ from 0.1 to 10 hours.

We use optimization intervals of 1 hour as the benchmark. Figure 4.8 shows that reducing h allows the system to react more quickly to new information, which in turn leads to improved solutions. This is especially the case for instances with a high DOD. However, excessively reducing δ does not improve the performance of the RHA. It is seen that below 1 hour of optimization intervals does not bring values as expected since the response times are set as a minimum of 1 hour. Therefore, decision makers can improve the matching quality by choosing a proper δ-value.

Table 4.4: Impact of different objective functions.

Case	Carbon tax coefficient (€/ton)	Objective function[1] (Min.)	Total cost (€)	OF1 (€)	OF2 (€)	OF3 (€)	OF4 (€)	OF5 (€)	Delay (TEU-h)	Carbon emission (kg)	Utilization of barges and trains (%)	Utilization of trucks (%)
1		OF1	4478714	**598864**	328458	137798	3406214	7379	39170	922429	71.47	28.53
2		OF2	1473382	1411229	**47622**	0	0	14530	0	1816311	0.00	100.00
3		OF3	1618747	1499961	103374	**0**	0	15412	0	1926482	0.04	99.96
4		OF4	1617409	1495824	105960	245	**0**	15379	0	1922413	0.42	99.58
5		OF5	4432293	601621	324498	144863	3353948	**7364**	40167	920491	72.06	27.94
6	8	OF2,3,4,5	1473382	1411229	47622	0	0	14530	0	1816311	0.00	100.00
7		OF1,3,4,5	1042644	648402	313266	72066	1112	7799	11	974863	67.96	32.04
8		OF1,2,4,5	1028388	668393	270732	80338	972	7953	10	994084	65.78	34.22
9		OF1,2,3,5	1803565	656501	260772	69829	808619	7844	8624	980454	66.71	33.29
10		OF1,2,3,4	1017693	695156	252702	60783	880	8172	9	1021544	**63.76**	36.24
11		Total cost	**1017675**	692118	254448	62114	850	8145	9	1018154	64.05	35.95
12	100	Total cost	1110869	684140	260790	64039	972	100929	10	1009287	64.78	35.22
13	500	Total cost	1507925	658359	284862	72431	1162	491111	12	982222	66.94	33.06
14	1000	Total cost	1995063	643700	298386	78945	8159	965872	88	965872	**68.48**	31.52

[1] OF1: Transport cost; OF2: Transfer cost; OF3: Storage cost; OF4: Delay cost; OF5: Carbon tax; OF2,3,4,5: Transfer cost + Storage cost + Delay cost + Carbon tax; OF1,3,4,5: Transport cost + Storage cost + Delay cost + Carbon tax; OF1,2,4,5: Transport cost + Transfer cost + Delay cost + Carbon tax; OF1,2,3,5: Transport cost + Transfer cost + Storage cost + Carbon tax; OF1,2,3,4: Transport cost + Transfer cost + Storage cost + Delay cost

4.7 Conclusions

This chapter answers research question **RQ2** by introducing an online synchromodal matching problem in which a platform aims to provide optimal matches between shipment requests and transport services. We proposed a rolling horizon approach and a heuristic algorithm to support the online decision-making process. We validated the heuristic algorithm and the rolling horizon approach on an intermodal network in Europe. The results indicate that the heuristic algorithm is efficient in large instances of the matching problem, and can be used under dynamic contexts. The rolling horizon approach has been proved to outperform a greedy approach in reducing total costs under various scenarios.

In conclusion, the proposed online matching platform will support decision makers to optimize the matching of shipments and services considering the trade-off between logistics costs, delays, and carbon emissions thanks to the developed rolling horizon approach. In other words, with the proposed approach, the use of barges, trains, and trucks can be managed more effectively taking into account their impact on logistics costs, delays, and emissions together with different time sensitivities of shipments.

This work can be extended in several directions. During the day, the number of trucks available to the matching platform is quite dynamic. Therefore, combining the dynamics of truck services in the synchromodal matching model is a further research direction. Considering the multiple uncertainties that exist in synchromodal transportation, future research can be carried out on *stochastic and dynamic* shipment matching. Chapter 5 in particular, incorporates the stochastic information of spot requests in online shipment matching processes. Furthermore, the origins and destinations of containers are usually located in different countries. Thus, looking into models with an *integrated* network combining intercontinental and inland transport is a promising research direction. This is the subject of Chapter 6. Besides, in this chapter, the online matching platform is controlled in a centralized way. However, in practice, multiple operators are present and they may not all be willing to give authority to a central platform. The *coordination mechanism* among them and *incentives* to stimulate cooperation are part of future research. This will be investigated in Chapter 7.

Chapter 5

Dynamic and stochastic shipment matching

In Chapter 4, a dynamic shipment matching model was developed for hinterland synchromodal transportation. In order to investigate the benefits of incorporating stochastic information of spot requests in the online shipment matching process, this chapter focuses on dynamic and stochastic shipment matching in hinterland synchromodal transportation.

This chapter is structured as follows. Section 5.1 introduces the motivations and challenges faced by network operators in hinterland synchromodal transportation. We briefly review the relevant literature and specify our contributions in Section 5.2. In Section 5.3, we describe the dynamic and stochastic shipment matching problem, design the preprocessing procedures, and present the Markov decision process model. In Section 5.4, we design the rolling horizon framework, the sample average approximation method, and the progressive hedging algorithm. In Section 5.5, we describe the experimental setup, and present the experimental results. Finally, in Section 5.6, some concluding remarks are provided.

Parts of this chapter have been submitted to a journal: "W. Guo, B. Atasoy, W. Beelaerts van Blokland, and R. R. Negenborn. Anticipatory approach for dynamic and stochastic shipment matching in hinterland synchromodal transportation. Submitted to a journal, 2020."

5.1 Introduction

Hinterland synchromodal transportation is the movement of shipments (i.e., a batch of containers) between deep-sea ports and inland terminals by trucks, trains, barges, or any combination of them [87]. Typically, a hinterland synchromodal transportation system is made up of multiple stakeholders that interact with each other, including network operators, shippers, carriers, terminal operators, and institutional authorities [17]. Network operators (e.g., logistics service providers and alliances formed by multiple carriers) control the synchromodal transport system. Shippers (e.g., manufacturers, ocean carriers, and freight forwarders) generate the freight transportation demand and outsource transport activities to network operators. Carriers (e.g., truck, train, and barge companies) provide transporta-

tion services and supply timely transport capacity to network operators. Terminal operators handle transshipment operations at terminals. Institutional authorities (e.g., governments and public administrations) charge tax, give incentives, and regulate transport activities to network operators, such as the charging of carbon emissions.

As shippers become more time-sensitive that require shipments to be delivered within tight time windows, trucks are used more often which contributes to road traffic congestion, transport costs, and carbon emissions [18]. However, due to the increasing environmental issues and the enforced regulations, companies in the transport industry are required to control carbon emissions [18]. The main advantage of synchromodal transportation is the ability to manage different types of shipments considering the trade-off among costs, delays, and emissions [62]. For example, for time-sensitive shipments, network operators can assign trucks for transportation; but if time available, barges, trains or barge-truck can be assigned taking into account their impact on logistics costs, time, and emissions.

The growing trend towards digitalization in freight transportation gives rise to dynamic and stochastic problems in which part or all of the input is unknown and revealed dynamically over a planning horizon, but exploiting stochastic information of random variables is viable with the help of data analytics [75]. In this chapter, we consider a synchromodal matching platform owned by network operators (e.g., European Gateway Services) that receives real-time shipment requests from shippers, receives weekly multimodal services from carriers, and receives timely transshipment services from terminal operators. The handling capacity at transshipment terminals is assumed unlimited, while the capacity of transport services is limited. The platform aims to provide optimal online matches between shipment requests and multimodal services over a planning horizon under future request uncertainty. The stochastic information of future requests (i.e., probability distributions) is available from historical data. We define the optimization problem as a dynamic and stochastic shipment matching (DSSM) problem in hinterland synchromodal transportation.

The complexity of the DSSM problem lies in three aspects. First, the time-space compatibility between shipments and services needs to be considered. Second, due to the capacity limitation of barge and train services, the matching decisions made for current requests will affect the ability to make good matches for future requests. Third, incorporating stochastic information in online decision-making processes can improve the system's performance over a planning horizon but increase the computational complexity.

In response to the complexities, we present preprocessing procedures to generate feasible matches between shipments and multimodal services, model the DSSM problem as a Markov decision process, and propose an anticipatory approach to solve the problem under realistic instances in a reasonable time. The anticipatory approach consists of a rolling horizon approach to deal with dynamic events that arrive over a planning horizon, a sample average approximation method to approximate expected objective functions and a progressive hedging algorithm to solve the deterministic formulations at each decision epoch.

5.2 Literature review

In the past decades, because of economic factors and environmental concerns, different management concepts have appeared in the literature and in the logistics industry: multimodal, intermodal, co-modal and synchromodal transportation. While multimodality refers

to the utilization of multiple modes, intermodality emphasizes the utilization of standardized loading units (i.e., containers), namely the vertical integration of different modes [87]. Co-modality focuses on the optimal and sustainable utilization of different modes on their own or in combination, namely the horizontal integration of different modes. Synchromodality, as an extension of intermodality, focuses on the (real-time) flexibility in planning when disturbances happen [30]. Compared with multimodal, intermodal, and co-modal, transportation, synchromodal transportation is the most advanced concept and includes all the notions [9]. Therefore, in this chapter, we use synchromodal transportation to represent the utilization of multiple modes, the utilization of standard loading units, the horizontal and vertical integration of transport services, and the flexibility in planning.

The implementation of synchromodal transportation relies on collaboration among stakeholders, information technologies, and integrated planning at different decision levels. Typically, synchromodal transport planning can be divided into three levels: strategic, tactical, and operational level. While strategic and tactical planning focus on physical network design (e.g., hub location) and service network design (e.g., service selection, service frequency) in long and medium time horizons, operational planning deals with the optimal allocation of resources (e.g., services, empty containers, handling equipment) that requires optimization in dynamic and stochastic environments [30].

In the literature, the majority of the studies [e.g., 7, 12, 63, 103] related to synchromodal transport planning are conducted in a static and deterministic environment, namely, all the inputs are known beforehand and decisions do not change once they are set. However, in practice, there are many sources of uncertainties in synchromodal transportation. With the growing amount of historical data, the stochastic information about uncertainties is available. Incorporating stochastic information in decision-making processes has been proven to have better performance than the corresponding myopic approaches in many fields, such as vehicle routing problems [3] and dial-a-ride problems [82].

In the field of stochastic synchromodal transport planning, Demir et al. [18] studied a green intermodal service network design problem with demand and travel time uncertainties. In this study, the origins, destinations, time windows of shipments are known in advance, but the actual demand (i.e, the number of containers) is uncertain. A sample average approximation method was proposed to generate robust plans. Hrusovsky et al. [41] proposed a hybrid approach combining a deterministic model with a simulation model to investigate an intermodal transportation planning problem with travel time uncertainty. Sun et al. [90] established a fuzzy chance-constrained mixed integer nonlinear programming model to describe rail service capacity uncertainty and road traffic congestion. Generally, stochastic transportation planning problems have a probability distribution of the random variables and the optimization process is performed before their realization. The transport plan will not be updated after the realization, thus, it is often referred to as a-priori optimization [75].

The trend towards digitalization in transportation allows gathering real-time information and thus dynamic decision making. In synchromodal transportation, some input data are revealed during the execution of the plan. The most common dynamic events are the arrival of new shipment requests (also called transport orders), but demands and travel times are possible dynamics as well. In the literature, Li et al. [49] presented a receding horizon intermodal container flow control approach to deal with the dynamic transport demands and dynamic traffic conditions. Mes et al. [62] considered the real-time planning of shipment

requests under a synchromodal network with the objective to minimize costs, delays, and carbon emissions. van Heeswijk et al. [98] proposed an online planning algorithm to schedule the transport of less than truckload freight via intermodal networks. Since dynamic transport planning problems require online decisions, a compromise between reactiveness and decision quality needs to be found. In addition, the degree of dynamism and the flexibility of updating decisions in execution have an influence on the choice of methods to respond to dynamic events.

The advances in information and communication technologies as well as the computing power allow the incorporation of stochastic information of future events in dynamic decision-making processes. Approaches for dynamic and stochastic transport planning problems can be divided into two categories: methods based on preprocessed decisions and methods based on online decisions. Solution approaches in the first group (preprocessed decisions) determine the values and policies of decision making before the execution of the transport plan [75]. Therefore, possible states need to be constructed in advance and evaluated based on possible dynamic events and stochastic information over a planning horizon. For example, van Riessen [100] designed a decision tree to derive real-time decision rules for suitable allocation of shipment requests to services. Rivera et al. [76] proposed an algorithm based on approximate dynamic programming to tackle the curse of dimensionality of a Markov decision process model. The second group (online decisions) focuses on the computation when a dynamic event occurs. Specifically, decisions are made online with respect to the current system state and the available stochastic information. SteadieSeifi [88] proposed a rolling horizon approach to handle dynamic demands. At each iteration of the rolling horizon framework, the author proposed a scenario-based two-stage stochastic programming model to incorporate the stochastic information of future demands.

In this chapter, we investigate a dynamic and stochastic shipment matching (DSSM) problem in hinterland synchromodal transportation at the operational level. The formulation characteristics of the DSSM problem include: (1) real-time shipment requests; (2) stochastic information of future requests; (3) unsplittable shipments, i.e., a shipment should be delivered as a whole; (4) soft time windows, i.e., delay in delivery is available but with a penalty; (5) capacitated and time-scheduled barge and train services; (6) departure time-flexible truck services with time-dependent travel times; (7) transshipment operations at terminals; (8) minimizing generalized costs which consist of logistics costs, delay costs, and carbon tax over a planning horizon. The formulation characteristics, solution approaches and experiment size of related articles are summarized in Table 5.1.

Table 5.1: Formulation characteristics, solution approaches and experiment size of related articles.

Articles	Dynamic information[1]	Stochastic information[1]	Integrity	Time windows	Barge/train services [2]	Truck services	Transshipment	Objectives[3]	Methods[4]	Maximum instance size[5]
Demir et al. [18]	-	Demand, travel times	Splittable	Soft	Capacitated	Flexible	✓	C, D, E	SAA	I-20-250-5
Hruovsky et al. [41]	-	Travel times	Splittable	Soft	Capacitated	Flexible	✓	C, D, E	SO	I-20-250-20
Sun et al. [90]	-	Service capacity	Unsplittable	Soft	Capacitated	Flexible, time-dependent	✓	C,D,E	MILP	I-12-25-10
Li et al. [49]	Demand, travel times	-	Splittable	-	Capacitated	Flexible	✓	C	RHA	I-6-54-1
Mes et al. [62]	Shipment requests	-	Unsplittable	Soft	Capacitated	Flexible	✓	C, D, E	GA	I-6-110-1728
van Heeswijk et al. [98]	Shipment requests	-	Unsplittable	Hard	Uncapacitated	Flexible	✓	C, D, E	CA	I-37-110-1006
van Riessen et al. [100]	Shipment requests	demand	Splittable	Soft	Capacitated	Flexible	-	C, D	DT	I-2-4-20
Rivera et al. [76]	Shipment requests	Shipment requests	Splittable	Hard	Capacitated	Flexible	-	C	ADP	I-12-29-40
SteadieSeifi [88]	Demand	Demand	Splittable	Hard	Capacitated	Scheduled	-	C	RHA, STSP	I-20-400-200
This chapter	Shipment requests	Shipment requests	Unsplittable	Soft	Capacitated	Flexible, time-dependent	✓	C, D, E	RHA, SAA, PHA	I-10-116-1600

[1] Information of shipment requests consists of shipments' origin, destination, container volume (i.e., demand), announce time, release time, and due time
[2] All the articles consider time-scheduled barge or train services
[3] C: Costs; D: Delays; E: Emissions
[4] SAA: Sample average approximation method; SO: Simulation-optimization; HA: Hybrid algorithm; MILP: Mixed integer linear programming; RHA: Rolling horizon approach; GA: Greedy approach; CA: Consolidation algorithm; DT: Decision trees; ADP: Approximate dynamic programming; STSP: Scenario-based two-stage stochastic programming; PHA: Progressive hedging algorithm
[5] Instances follow naming convention of I-a-b-c where a represents the number of terminals, b is the number of services, and c is the number of shipment requests

Our work has three main contributions to the literature. First, we propose a Markov decision process model to describe the DSSM problem in hinterland synchromodal transportation. Second, we propose an anticipatory approach to solve the problem under realistic instances in a reasonable time. The anticipatory approach uses a sample average approximation method to approximate expected objective functions and applies a progressive hedging algorithm to get solutions at each decision epoch of a rolling horizon framework. This approach enables to consider a large set of scenarios (within 1 minute of computation time) to more accurately represent the stochasticity and this in turn increases the benefits of incorporating stochastic information in dynamic decision-making processes. Third, thanks to the above developed methodologies we propose a platform in which companies can manage different types of shipments (e.g., time-sensitive shipments) under a synchromodal network considering the trade-off among costs, delays, and emissions. Such a platform provides the means for a more efficient, effective and sustainable decision-making framework for transportation systems.

5.3 Problem description and formulation

In this section, we first describe the DSSM problem, and then design the preprocessing procedures to reduce the solution space. After that, we present the Markov decision process model for the problem.

5.3.1 Problem description

We consider an online matching platform that receives real-time shipment requests from shippers, receives weekly multimodal services from carriers, and receives timely handling services (i.e., loading and unloading) from terminal operators. Let N be the set of terminals. Without loss of generality, we assume that the loading/unloading cost coefficient of barge services lc^{barge}, train services lc^{train} and truck services lc^{truck}, the loading/unloading time of barge services lt^{barge}, train services lt^{train} and truck services lt^{truck}, and the storage cost coefficient c^{storage} at different terminals are the same. The CO_2 emissions-related cost coefficient is set as c^{emission}.

Let R be the set of shipment requests. Each shipment request $r \in R$ is characterized by its announce time $\mathbb{T}_r^{\text{announce}}$ (i.e., the time when the platform receives the request), release time $\mathbb{T}_r^{\text{release}}$ (i.e., the time when the shipment is available for hinterland transportation) at origin terminal o_r, due time $\mathbb{T}_r^{\text{due}}$ (i.e., the time that the shipment needs to be delivered) at destination terminal d_r, expiry date $\mathbb{T}_r^{\text{expire}}$ (i.e., the time that the matching decisions for request r cannot be further postponed), and container volume u_r. Delay in delivery is available but with a delay cost coefficient per container per hour overdue c_r^{delay}. Request r is unknown before its announce time. However, the probability distributions $\{\pi_o, \pi_d, \pi_u, \pi_{\mathbb{T}^{\text{announce}}}, \pi_{\mathbb{T}^{\text{release}}}, \pi_{\mathbb{T}^{\text{due}}}, \pi_{\mathbb{T}^{\text{expire}}}\}$ of future requests' origin, destination, volume, announce time, release time, due time, and expiry date are available from historic data. In addition, shippers require their shipments to be transported as a whole, and ask to receive the transport plan before shipments' release time, namely the expiry date is equal to the release time, $\mathbb{T}_r^{\text{release}} = \mathbb{T}_r^{\text{expire}}$.

Let S be the set of multimodal services, all the services are received before the planning horizon. According to the modalities in hinterland transportation, services can be divided into two groups:

- *Barge and train services*. Each barge or train service $s \in S^{\text{barge}} \cup S^{\text{train}}$ is characterized by its departure time TD_s at origin terminal o_s, arrival time TA_s at destination terminal d_s, free capacity U_s, transport cost c_s and carbon emissions e_s.
- *Truck services*. We view each truck service as a fleet of trucks which has flexible departure times and an unlimited capacity. Thus, a truck service might have multiple departure times for different shipments. Due to traffic congestion at several time periods throughout a day, the travel time of truck services is time-dependent [42]. Therefore, each truck service $s \in S^{\text{truck}}$ is characterized by its origin terminal o_s, destination terminal d_s, time-dependent travel time function $t_s(\tau)$, transport cost c_s, and carbon emissions e_s.

The objective of the platform is to provide optimal online matches in total costs between shipment requests and multimodal services over a planning horizon T. The total costs consist of transport costs generated by using services, transfer costs and storage costs generated at transshipment terminals, delay costs caused by delay in delivery, and carbon tax charged for services' carbon emissions.

5.3.2 Preprocessing procedures

In this section, we present the preprocessing procedures that aim to reduce the computational complexity of the DSSM problem by identifying infeasible matches between shipments and services. It consists of two steps: the preprocessing of path generation and the preprocessing of feasible matches.

- *Preprocessing of path generation*. We define a path p as a combination of one or more services in sequence. A path p is feasible if the services inside a combination satisfy time-spatial compatibility. Specifically, for two consecutive services s_i, s_{i+1} within path p, the destination of service s_i must be the same as the origin of service s_{i+1}; the arrival time of service s_i must be earlier than the departure time of service s_{i+1} minus loading and unloading time at transshipment terminal d_{s_i}. The set P denotes the collection of feasible paths.
- *Preprocessing of feasible matches*. A match $\langle r, p \rangle$ means shipment r will be transported by path p from its origin to its destination. A match between request $r \in R$ and path $p = [s_1, ..., s_l] \in P$ is feasible if it satisfies time-spatial compatibility:
  - *Spatial compatibility*. The origin terminal of shipment request r should be the same as the origin of service s_1; the destination of request r should be the same as the destination of service s_l.
  - *Time compatibility*. The release time of request r should be earlier than the departure time of service s_1 minus loading time at origin terminal o_r.

  Let P_r be the set of feasible paths for request r, and let c_{rp} denote the costs of matching request r with path p including logistics costs, delay costs and carbon tax. The details of the preprocessing procedures are presented in Guo et al. [37].

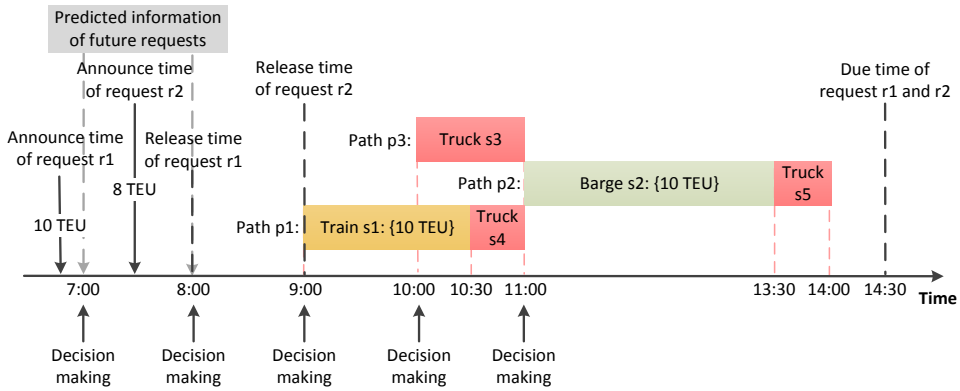

Figure 5.1: An illustrative example of the DSSM problem.

5.3.3 Illustrative examples

An illustrative example of the DSSM problem is shown in Figure 5.1. At time period 1 (6:00-7:00), the platform receives shipment request r_1 with 10 TEU (twenty-foot equivalent units). Path $p_1 = [s_1, s_4]$ (i.e., train-truck service combination), path $p_2 = [s_2, s_5]$ (i.e., barge-truck service combination), and path $p_3 = [s_3]$ (i.e., truck service) are all feasible for request r_1. At time period 2 (7:00-8:00), the system receives request r_2 with 8 TEU. Path $p_2 = [s_2, s_5]$ and path $p_3 = [s_3]$ are feasible for request r_2 while path $p_1 = [s_1, s_4]$ is infeasible because the departure time of s_1 (9:00) minus loading time (1 hour) is earlier than the release time of request r_2 (9:00). The probability information of requests that will arrive in time period 2 and 3 is available. The platform needs to create matches for request r_1 at time stage 1 (7:00), and create matches for request r_2 at time stage 2 (8:00).

An illustrative example of the dynamic and stochastic shipment matching process is shown in Figure 5.2. The number on the arcs means the cost of matching requests with services. At time stage 1 (7:00), the platform creates matches for current received request r_1 incorporating the information of predicted future request r_2. Path p_1 will be assigned to request r_1 instead of path p_2 since $70\langle r_1, p_1\rangle + 50\langle r_2, p_2\rangle < 50\langle r_1, p_2\rangle + 100\langle r_2, p_3\rangle$. At time stage 2, decision for request r_2 is made incorporating the information of predicted future request r_3. Here, request r_2 is assigned to path p_2, since $40\langle r_2, p_2\rangle + 50\langle r_3, p_3\rangle < 80\langle r_2, p_3\rangle + 25\langle r_3, p_2\rangle$. The total cost of matching for request r_1 and r_2 is $70 + 40 = 110$. In comparison, if only dynamic information is used for decision making (without the information of future requests), the platform will assign p_2 to request r_1 at time stage 1 (local 'optimal'). Since the free capacity of path p_2 has already been assigned to request r_1, request r_2 can be only matched with path p_3 at time stage 2. Then the total cost of matching without the utilization of stochastic information is $50 + 80 = 130 > 110$.

5.3.4 Markov decision process model

In this section, we formulate the optimization problem as a Markov decision process (MDP) model. There are seven fundamental elements in the MDP model: stages, state variables, exogenous information, decision variables, the transition function, costs, and the objective

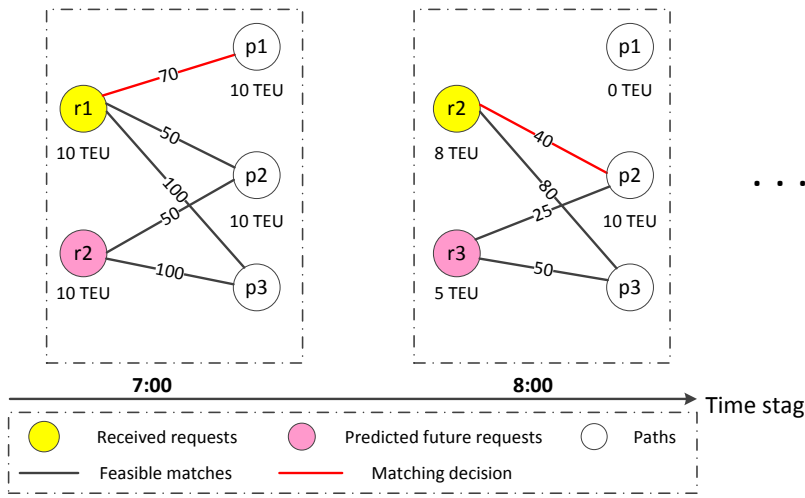

Figure 5.2: An illustrative example of the dynamic and stochastic matching process.

function [70]. A brief summary of these elements is as follows:

- **Stages**. We define t as the points in time at which decisions are made, $t \in \{0,1,...,T\}$. Therefore, the planning horizon is divided into T consecutive time intervals.

- **State variables**. The state $\mathbf{F}^t$ of the synchromodal matching system contains all the information that is necessary and sufficient to model the system at decision epoch t. We distinguish between the initial state $\mathbf{F}^0$ and the dynamic state $\mathbf{F}^t$ for $t > 0$. The initial state contains all the deterministic parameters $\{R^0, S, P, N, c_{rp}, T\}$, initial values of dynamic parameters $U^0 = \left[U_s^0\right]_{\forall s \in S^{\text{barge}} \cup S^{\text{train}}}$, and probability distributions of unknown parameters $\{\pi_o, \pi_d, \pi_u, \pi_{\mathbb{T}^{\text{announce}}}, \pi_{\mathbb{T}^{\text{release}}}, \pi_{\mathbb{T}^{\text{due}}}, \pi_{\mathbb{T}^{\text{expire}}}\}$. The dynamic state $\mathbf{F}^t$ contains the information that is evolving over time. We define $\mathbf{F}^t$ as the set of free capacity of multimodal services at stage t namely $\mathbf{F}^t = U^t$.

- **Exogenous information**. The exogenous information $\mathbf{W}^t$ at stage t consists of all the new information that first becomes known at stage t. We define $\mathbf{W}^t = R^t$, where $R^t = \{r | t-1 < \mathbb{T}_r^{\text{announce}} \leq t\}$ is the set of requests received during time interval $(t-1, t]$, $t > 0$.

- **Decision variables**. At stage t, the platform needs to decide the matching decision z^t for shipment requests that are received before t and will expire before $t+1$, namely $\forall r \in \hat{R}^t = \{r | r \in R^{0...t}, \mathbb{T}_r^{\text{announce}} \leq t, t < \mathbb{T}_r^{\text{expire}} \leq t+1\}$. The decisions are restricted by the capacity of multimodal services at stage t. Let p_{rs} be the set of feasible paths for shipment request r including service s, $P_{rs} = \{p | p \in P_r, s \in p\}$, the total container volumes of shipments assigned to service $s \in S^{\text{barge}} \cup S^{\text{train}}$ within paths P_{rs} cannot exceed its free capacity at stage t. We use the binary variable z_{rp}^t to represent the match between request $r \in \hat{R}^t$ and path $p \in P$. The decision z^t consists of all the decision variables at stage t as seen in (5.1), subject to constraints (5.2-5.4), which define the feasible decision space Z^t.

$$z^t = \left[z_{rp}^t\right]_{\forall r \in \hat{R}^t, p \in P} \tag{5.1}$$

subject to

$$\sum_{p\in P_r} z_{rp}^t = 1, \quad \forall r \in \hat{R}^t, \tag{5.2}$$

$$\sum_{r\in\hat{R}^t}\sum_{p\in p_{rs}} u_r z_{rp}^t \le U_s^t, \quad \forall s \in S^{\text{barge}} \cup S^{\text{train}}, \tag{5.3}$$

$$z_{rp}^t \in \{0,1\}, \quad \forall r \in \hat{R}^t, p \in P. \tag{5.4}$$

- **Transition function**. Following decision z^t from state $\mathbf{F}^t$ with exogenous information $\mathbf{W}^t$, the system transitions to a new state. We denote the transition function by $\mathbf{F}^{t+1} = f(\mathbf{F}^t, \mathbf{W}^t, z^t)$. Specifically, the free capacity of service $s \in S^{\text{barge}} \cup S^{\text{train}}$ at stage $t+1$ is decided by the free capacity of service s at stage t and the matching decisions made for shipment requests $\hat{R}^t$, as shown in constraints (5.5).

$$U_s^{t+1} = U_s^t - \sum_{r\in\hat{R}^t}\sum_{p\in p_{rs}} u_r z_{rp}^t, \qquad \forall s \in S^{\text{barge}} \cup S^{\text{train}}. \tag{5.5}$$

- **Costs**. Based on the state $\mathbf{F}^t$, the exogenous information $\mathbf{W}^t$, and the decision z^t, the costs at stage t can be defined as a function of $\mathbf{F}^t$, $\mathbf{W}^t$ and z^t, as shown in (5.6).

$$C(\mathbf{F}^t, \mathbf{W}^t, z^t) = \sum_{r\in\hat{R}^t}\sum_{p\in P_r} c_{rp} z_{rp}^t. \tag{5.6}$$

- **Objective functions**. Due to the capacity limitation of multimodal services, decisions made for current requests will influence the decisions for future requests. Therefore, the objective of the MDP model is to minimize the expected costs over the planning horizon. Thus, we write the objective function as follows.

$$\min_{z^{0\ldots T}} \mathbb{E}_{\mathbf{F}^0}\mathbb{E}_{\mathbf{W}^1,\ldots,\mathbf{W}^T|\mathbf{F}^0}\{\sum_{t=0}^{T} C^t(\mathbf{F}^t, \mathbf{W}^t, z^t)|\mathbf{F}^0\}. \tag{5.7}$$

We refer to the objective function in (5.7) as the cumulative formulation. Using Bellman's principle of optimality, the optimal costs can be computed through a set of recursive equations, as seen in (5.8).

$$\textbf{P0} \quad Q^t(U^t, \hat{R}^t, z^t) = \min_{z^t} \sum_{r\in\hat{R}^t}\sum_{p\in P_r} c_{rp} z_{rp}^t + E_{\Omega^t}[Q^{t+1}(U^{t+1}, \hat{R}^{t+1}, z^{t+1})] \tag{5.8}$$

5.4 Solution approaches

The recursive formulation presented above requires enumerating all states, exogenous information, and decisions in the future time stages which are known as the three curses of dimensionality. In this section, we propose an anticipatory approach (AA) to solve the DSSM problem and use a myopic approach (MA) as a benchmark. Both the AA and the MA are implemented under a rolling horizon framework. However, the MA is based on deterministic information only while the AA incorporates stochastic information at each decision epoch, as shown in Figure 5.3.

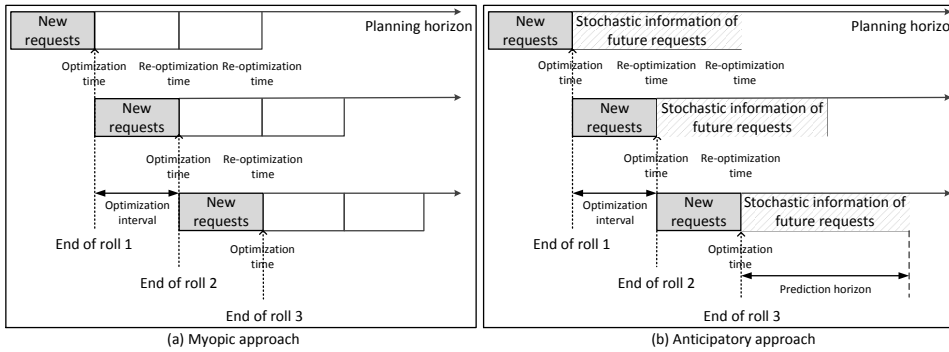

Figure 5.3: Illustration of the myopic approach and the anticipatory approach.

5.4.1 Myopic approach

The MA is known as an efficient periodic re-optimization approach for dynamic problems [e.g., 6, 64, 108, 114]. The planning horizon is rolled forward to incorporate the dynamically released information, and the process continuous until the end of the horizon. Under the MA, the system is optimized periodically at pre-specified points in time called *optimization times* (i.e., decision epochs). At decision epoch t, decisions for all active shipment requests $\acute{R}^t$ are made. Request r is active if it is already announced but not expired yet, formally $\acute{R}^t = \{r | r \in R^{0\ldots t}, \mathbb{T}_r^{\text{announce}} \leq t, \mathbb{T}_r^{\text{expire}} > t\}$. However, the decision for request $r \in \acute{R}^t$ is fixed only if $r \in \hat{R}^t = \{r | r \in R^{0\ldots t}, \mathbb{T}_r^{\text{announce}} \leq t, t < \mathbb{T}_r^{\text{expire}} \leq t+1\}$, namely the request will expire before the next decision epoch. The platform will inform shippers the decisions only if a match is fixed for them. Thus, only the matches fixed at stage t have effects on the free capacity of service $s \in S^{\text{barge}} \cup S^{\text{train}}$ at stage $t+1$.

Under the MA, the objective function is to minimize the total costs of the current-stage decisions made for active requests $\acute{R}^t$. The formulation of the DSSM problem at stage $t \in \{0, 1, ..., T\}$ under the MA is:

$$\textbf{P1} \quad \min_{z^t} \sum_{r \in \acute{R}^t} \sum_{p \in P_r} c_{rp} z_{rp}^t \tag{5.9}$$

subject to

$$\sum_{p \in P_r} z_{rp}^t = 1, \quad \forall r \in \acute{R}^t, \tag{5.10}$$

$$\sum_{r \in \acute{R}^t} \sum_{p \in p_{rs}} u_r z_{rp}^t \leq U_s^t, \quad \forall s \in S^{\text{barge}} \cup S^{\text{train}}, \tag{5.11}$$

$$U_s^{t+1} = U_s^t - \sum_{r \in \hat{R}^t} \sum_{p \in p_{rs}} u_r z_{rp}^t, \quad \forall s \in S^{\text{barge}} \cup S^{\text{train}}, \tag{5.12}$$

$$z_{rp}^t \in \{0, 1\}, \quad \forall r \in \acute{R}^t, p \in P. \tag{5.13}$$

Constraints (5.10) ensure that each request will be matched with one feasible path only. Constraints (5.11) ensure that the total container volumes of shipments assigned to service $s \in S^{\text{barge}} \cup S^{\text{train}}$ does not exceed its free capacity at decision epoch t. Constraints (5.12)

Algorithm 5.1 Anticipatory approach.

Input: Set of transportation services $S = S^{\text{barge}} \cup S^{\text{train}} \cup S^{\text{truck}}$, free capacity $[U_s^0]$ for all $s \in S^{\text{barge}} \cup S^{\text{train}}$, set of shipment requests R^0, the length of planning horizon T, the length of prediction horizon H, probability distributions $\{\pi_o, \pi_d, \pi_u, \pi_{\mathbb{T}^{\text{announce}}}, \pi_{\mathbb{T}^{\text{release}}}, \pi_{\mathbb{T}^{\text{due}}}, \pi_{\mathbb{T}^{\text{expire}}}\}$, and the number of scenarios Γ.

Output: Matching decision $z^t = [z_{rp}^t]_{\forall r \in \hat{R}^t, p \in P}$

Initialize: Let $R^t \leftarrow \emptyset$ for $t > 0$, $\acute{R}^t \leftarrow \emptyset$, $\hat{R}^t \leftarrow \emptyset$, $U_s^t \leftarrow 0$ for $t > 0$.

1: generate set of feasible paths $P \leftarrow$ *preprocessing of path generation*
2: **for** decision epoch $t \in \{0, 1, ..., T\}$ **do**
3: receive shipment requests R^t
4: update $\acute{R}^t \leftarrow \{r \in R^{0...t} | \mathbb{T}_r^{\text{announce}} \leq t, \mathbb{T}_r^{\text{expire}} > t\}$
5: update $\hat{R}^t \leftarrow \{r \in R^{0...t} | \mathbb{T}_r^{\text{announce}} \leq t, t < \mathbb{T}_r^{\text{expire}} \leq t+1\}$
6: get sample requests for future H time stages $\{\omega^1, \omega^2, ..., \omega^\Gamma\} \leftarrow$ *Monte Carlo simulation*
7: generate feasible matches for request $r \in \acute{R}^t \cup \omega^1 \cup ... \cup \omega^\Gamma \leftarrow$ *preprocessing of feasible matches*
8: get approximate expected objective functions $\leftarrow$ *sample average approximation method*
9: obtain matching decision $z^t \leftarrow$ *progressive hedging algorithm*
10: update free capacity for service $s \in S^{\text{barge}} \cup S^{\text{train}}$:

$$U_s^{t+1} \leftarrow U_s^t - \sum_{r \in \hat{R}^t} \sum_{p \in P} u_r z_{rp}^t$$

represent that the free capacity of service $s \in S^{\text{barge}} \cup S^{\text{train}}$ at the next stage is only influenced by the free capacity of service s at the current stage and the matching decisions made for requests $\hat{R}^t$ which will expire before the next stage.

5.4.2 Anticipatory approach

In this section, we propose the AA to incorporate the stochastic information of future requests at each decision epoch of the rolling horizon framework, in contrast to the MA in which dynamic decisions are made based on deterministic information only. The implementation of the AA for a synchromodal matching system is shown in Algorithm 5.1. Before the planning horizon, the system applies the preprocessing of path generation to get the set of feasible paths. At each decision epoch of the rolling horizon framework, the system generates scenarios of future requests by using Monte Carlo simulation, applies the preprocessing procedure to obtain feasible matches for active requests and sampled requests, utilizes a sample average approximation method to approximate expected objective functions, and utilizes a progressive hedging algorithm to generate solutions. The state of the system is updated based on the decisions made for requests $\hat{R}^t$. Then the system is rolled forward to obtain the decisions for the next stage.

Sample average approximation method

The sample average approximation method is an approach for solving stochastic optimization problems by using Monte Carlo simulation. In this technique, the expected objective function is approximated by a sample average estimate derived from a random sample [104]. At decision epoch t, a sample $\{\omega^1, \omega^2, ..., \omega^\gamma, ..., \omega^\Gamma\}$ of Γ scenarios is generated ac-

cording to probability distributions $\{\pi_o, \pi_d, \pi_u, \pi_{\mathbb{T}^{\text{announce}}}, \pi_{\mathbb{T}^{\text{release}}}, \pi_{\mathbb{T}^{\text{due}}}, \pi_{\mathbb{T}^{\text{expire}}}\}$. Each scenario includes a realization of shipment requests from stage $t+1$ to stage $t+H$, $\omega^\gamma = \{\omega^{\gamma(t+1)}, \omega^{\gamma(t+2)}, ..., \omega^{\gamma(t+H)}\}$. Here, H is the prediction horizon that is just long enough to obtain good decisions at stage t. The expected cost E_{Ω^t} in (5.8) is approximated by the sample average function $\Gamma^{-1}\sum_{\gamma=1}^{\Gamma}$. In addition, $\Gamma^{-1}\sum_{\gamma=1}^{\Gamma}$ is an unbiased estimator of E_{Ω^t}, and converges to E_{Ω^t} with probability 1 as the sample size Γ goes to infinity and the prediction horizon $t+H=T$ [81]. We define $\mathbb{H}$ as the set of predicted time stages at decision epoch t, $\mathbb{H} = \{t+1, ..., \min\{t+H, T\}\}, \forall t \in \{0, 1, ..., T-1\}$; $\mathbb{H} = \emptyset$ when $t = T$. Let $\hat{z}_{rp}^{\gamma h}$ be the binary variable which equals to 1 if request $r \in \omega^{\gamma h}$ is matched with path $p \in P$ under scenario $\gamma \in \{1, .., \Gamma\}$ at stage $h \in \mathbb{H}$. The formulation of the DSSM problem at stage t changes to:

$$\textbf{P2} \quad \min_{z^t, \hat{z}^t} \sum_{r \in \acute{R}^t} \sum_{p \in P_r} c_{rp} z_{rp}^t + \frac{1}{\Gamma} \sum_{\gamma=1}^{\Gamma} \sum_{h \in \mathbb{H}} \sum_{r \in \omega^{\gamma h}} \sum_{p \in P_r} c_{rp} \hat{z}_{rp}^{\gamma h} \tag{5.14}$$

subject to

$$\sum_{p \in P_r} z_{rp}^t = 1, \quad \forall r \in \acute{R}^t, \tag{5.15}$$

$$\sum_{p \in P_r} \hat{z}_{rp}^{\gamma h} = 1, \quad \forall \gamma \in \{1, ..., \Gamma\}, h \in \mathbb{H}, r \in \omega^{\gamma h}, \tag{5.16}$$

$$\sum_{r \in \acute{R}^t} \sum_{p \in p_{rs}} u_r z_{rp}^t + \sum_{h \in \mathbb{H}} \sum_{r \in \omega^{\gamma h}} \sum_{p \in p_{rs}} u_r \hat{z}_{rp}^{\gamma h} \leq U_s^t, \forall \gamma \in \{1, ..., \Gamma\}, s \in S^{\text{barge}} \cup S^{\text{train}}, \tag{5.17}$$

$$U_s^{t+1} = U_s^t - \sum_{r \in \hat{R}^t} \sum_{p \in p_{rs}} u_r z_{rp}^t, \quad \forall s \in S^{\text{barge}} \cup S^{\text{train}}, \tag{5.18}$$

$$z_{rp}^t \in \{0, 1\}, \quad \forall r \in \acute{R}^t, p \in P, \tag{5.19}$$

$$\hat{z}_{rp}^{\gamma h} \in \{0, 1\}, \quad \forall \gamma \in \{1, ..., \Gamma\}, h \in \mathbb{H}, r \in \omega^{\gamma h}, p \in P. \tag{5.20}$$

In formulation **P2**, z^t is first-stage decision which does not depend on the scenarios, $\hat{z}^t$ is the second-stage decision which depends on the corresponding scenarios. However, only $[z_{rp}^t]_{r \in \hat{R}^t}$ will be implemented at each decision epoch, $[z_{rp}^t]_{r \in \acute{R}^t \setminus \hat{R}^t}$ and $\hat{z}^t$ will be released after the optimization.

Progressive hedging algorithm

Formulation **P2** is a large-scale deterministic binary integer program which is non-convex and highly complex to solve. In this section, we apply the progressive hedging algorithm (PHA) to solve the formulation. The PHA is first proposed by Rockafellar et al. [79] and has been implemented in many applications, such as stochastic network design problems [15] and stochastic resource allocation problems [110]. It is a horizontal decomposition method which decomposes **P2** by scenarios rather than by time stages, and iteratively solves penalized version of the scenario-based subproblems to gradually enforce implementability (also called non-anticipativity) [27].

In **P2**, the condition that the first-stage decision z^t must not depend on the realization of random variables is implicit. In the PHA scheme, we write the non-anticipativity constraints explicitly. We define $z_{rp}^{t\gamma}$ as the binary variable which equals to 1 if request $r \in \acute{R}^t$ is matched with path $p \in P$ under scenario γ. Let $\bar{z}^t$ be the 'overall design vector'. The DSSM problem

is then reformulated as:

$$\mathbf{P3}\ \min_{z^t,\hat{z}^t}\frac{1}{\Gamma}\sum_{\gamma=1}^{\Gamma}\left(\sum_{r\in\acute{R}^t}\sum_{p\in P_r}c_{rp}z_{rp}^{t\gamma}+\sum_{h\in\mathbb{H}}\sum_{r\in\omega^{\gamma h}}\sum_{p\in P_r}c_{rp}\hat{z}_{rp}^{\gamma h}\right) \tag{5.21}$$

subject to

$$\sum_{p\in P_r}z_{rp}^{t\gamma}=1,\quad \forall\gamma\in\{1,...,\Gamma\},r\in\acute{R}^t, \tag{5.22}$$

$$\sum_{p\in P_r}\hat{z}_{rp}^{\gamma h}=1,\quad \forall\gamma\in\{1,...,\Gamma\},h\in\mathbb{H},r\in\omega^{\gamma h}, \tag{5.23}$$

$$\sum_{r\in\acute{R}^t}\sum_{p\in p_{rs}}u_r z_{rp}^{t\gamma}+\sum_{h\in\mathbb{H}}\sum_{r\in\omega^{\gamma h}}\sum_{p\in p_{rs}}u_r\hat{z}_{rp}^{\gamma h}\le U_s^t,\forall\gamma\in\{1,...,\Gamma\},s\in S^{\text{barge}}\cup S^{\text{train}}, \tag{5.24}$$

$$z_{rp}^{t\gamma}=\bar{z}_{rp}^{t},\quad \forall\gamma\in\{1,...,\Gamma\},r\in\acute{R}^t,p\in P_r, \tag{5.25}$$

$$U_s^{t+1}=U_s^t-\sum_{r\in\acute{R}^t}\sum_{p\in p_{rs}}u_r\bar{z}_{rp}^{t},\quad \forall s\in S^{\text{barge}}\cup S^{\text{train}}, \tag{5.26}$$

$$z_{rp}^{t\gamma}\in\{0,1\},\quad \forall\gamma\in\{1,...,\Gamma\},r\in\acute{R}^t,p\in P, \tag{5.27}$$

$$\hat{z}_{rp}^{\gamma h}\in\{0,1\},\quad \forall\gamma\in\{1,...,\Gamma\},h\in\mathbb{H},r\in\omega^{\gamma h},p\in P. \tag{5.28}$$

Constraints (5.25) are the non-anticipatory constraints which stipulate that in all feasible solutions, the first-stage decisions are not allowed to depend on scenarios. Therefore, the newly added variables do not affect the optimal solution, and thus **P3** is equivalent to **P2**.

Following the PHA scheme, we drop off the constant coefficient Γ^{-1}, and move the non-anticipativity constraints (5.25) into the objective function based on augmented Lagrangian strategy, which yields the objective function as follows:

$$\begin{aligned}\mathbf{P4}\ \min_{z^t,\hat{z}^t}\sum_{\gamma=1}^{\Gamma}\Big(&\sum_{r\in\acute{R}^t}\sum_{p\in P_r}c_{rp}z_{rp}^{t\gamma}+\sum_{h\in\mathbb{H}}\sum_{r\in\omega^{\gamma h}}\sum_{p\in P_r}c_{rp}\hat{z}_{rp}^{\gamma h}\\&+\sum_{r\in\acute{R}^t}\sum_{p\in P_r}\lambda_{rp}^{t\gamma}\left(z_{rp}^{t\gamma}-\bar{z}_{rp}^{t}\right)+\frac{1}{2}\sum_{r\in\acute{R}^t}\sum_{p\in P_r}\rho_{rp}^{t\gamma}\left(z_{rp}^{t\gamma}-\bar{z}_{rp}^{t}\right)^2\Big)\end{aligned} \tag{5.29}$$

subject to Constraints (5.22-5.24, 5.26-5.28).

In formulation **P4**, $[\lambda_{rp}^{t\gamma}]$ are Lagrangian multipliers, $[\rho_{rp}^{t\gamma}]$ are penalty factors. Given the binary requirements for variables $z^t,\bar{z}^t$, the objective function can be further formulated as:

$$\begin{aligned}\mathbf{P5}\ \min_{z^t,\hat{z}^t}\sum_{\gamma=1}^{\Gamma}\Big(&\sum_{r\in\acute{R}^t}\sum_{p\in P_r}\left(c_{rp}+\lambda_{rp}^{t\gamma}+\frac{1}{2}\rho_{rp}^{t\gamma}-\rho_{rp}^{t\gamma}\bar{z}_{rp}^{t}\right)z_{rp}^{t\gamma}-\lambda_{rp}^{t\gamma}\bar{z}_{rp}^{t\gamma}+\frac{1}{2}\rho_{rp}^{t\gamma}\bar{z}_{rp}^{t}\\&+\sum_{h\in\mathbb{H}}\sum_{r\in\omega^{\gamma h}}\sum_{p\in P_r}c_{rp}\hat{z}_{rp}^{\gamma h}\Big)\end{aligned} \tag{5.30}$$

subject to Constraints (5.22-5.24, 5.26-5.28).

For a given overall design $\bar{z}^t$, the relaxed formulation **P5** is separable on a scenario basis. As it contains Γ scenarios, it can be broken down into Γ individual subproblems. An arbitrary subproblem indexed by $\gamma\in\{1,...,\Gamma\}$ by dropping constant terms has the following

Algorithm 5.2 Progressive hedging algorithm.

1: **Initialization**. Set iteration number $n = 0$; maximum iteration number $N^{\text{iteration}}$; Lagrangian multipliers $\lambda^t = [0]$; penalty factors $\rho^t = [0]$; overall design vectors $\bar{z}^t = [0]$; assign a small positive number to η and a constant greater than 0 to θ.
2: **Optimization**. Solve $P6$ for all $\gamma \in \{1, ..., \Gamma\}$, and obtain the scenario-based solution $z^{t\gamma}$ for the nth iteration.
3: **Aggregation**. Update the overall design value $\bar{z}^t_{rp} \leftarrow \lfloor \frac{1}{\Gamma} \sum_{\gamma=1}^{\Gamma} z^{t\gamma}_{rp} \rceil$ for all $r \in \acute{R}^t, p \in P$.
4: **Termination criteria**. The algorithm stops if either of the following criteria is satisfied:
- $\sum_{\gamma=1}^{\Gamma} \sum_{r \in \acute{R}^t} \sum_{p \in P} |z^{t\gamma}_{rp} - \bar{z}^t_{rp}| \leq \eta$.
- $n > N^{\text{iteration}}$.

5: **Modification**. Update the Lagrangian multiplier $\lambda^t_{rp} \leftarrow \lambda^t_{rp} + \rho^t_{rp} \left(z^{t\gamma}_{rp} - \bar{z}^t_{rp} \right)$ where $\rho^t_{rp} = \theta c_{rp}$ for all $r \in \acute{R}^t, p \in P$.
6: $n \leftarrow n + 1$, and go to step (2).

form:

$$\begin{aligned} \textbf{P6} \quad \min_{z^{t\gamma}, \hat{z}^{t\gamma}} & \sum_{r \in \acute{R}^t} \sum_{p \in P_r} \left(c_{rp} + \lambda^{t\gamma}_{rp} + \frac{1}{2} \rho^{t\gamma}_{rp} - \rho^{t\gamma}_{rp} \bar{z}^t_{rp} \right) z^{t\gamma}_{rp} \\ & + \sum_{h \in \mathbb{H}} \sum_{r \in \omega^{\gamma h}} \sum_{p \in P_r} c_{rp} \hat{z}^{\gamma h}_{rp} \end{aligned} \tag{5.31}$$

subject to

$$\sum_{p \in P_r} z^{t\gamma}_{rp} = 1, \quad \forall r \in \acute{R}^t, \tag{5.32}$$

$$\sum_{p \in P_r} \hat{z}^{\gamma h}_{rp} = 1, \quad \forall h \in \mathbb{H}, r \in \omega^{\gamma h}, \tag{5.33}$$

$$\sum_{r \in \acute{R}^t} \sum_{p \in p_{rs}} u_r z^{t\gamma}_{rp} + \sum_{h \in \mathbb{H}} \sum_{r \in \omega^{\gamma h}} \sum_{p \in p_{rs}} u_r \hat{z}^{\gamma h}_{rp} \leq U^t_s, \quad \forall s \in S^{\text{barge}} \cup S^{\text{train}}, \tag{5.34}$$

$$z^{t\gamma}_{rp} \in \{0, 1\}, \quad \forall r \in \acute{R}^t, p \in P, \tag{5.35}$$

$$\hat{z}^{\gamma h}_{rp} \in \{0, 1\}, \quad \forall h \in \mathbb{H}, r \in \omega^{\gamma h}, p \in P. \tag{5.36}$$

Formulation **P6** is a scenario-based binary integer program which can be solved by using commercial solvers within an acceptable computational time, such as CPLEX. For a given scenario subproblem γ, the Lagrangian multiplier $\lambda^{t\gamma}_{rp}$ and the penalty parameter $\rho^{t\gamma}_{rp}$ contribute to penalize the difference in terms of values between the local variable $z^{t\gamma}_{rp}$ and the current overall design $\bar{z}^t_{rp}$.

The pseudocode of the PHA at decision epoch $t \in \{0, 1, ..., T\}$ is shown in Algorithm 5.2. Each iteration of the PHA involves an optimization (Step 2) for scenario-based subproblems, an aggregation (Step 3) which corresponds to a projection of the individual scenario solutions onto the subspace of non-anticipative policies, a termination criteria (Step 4) to make sure the algorithm converges to within a tolerance, and a modification (Step 5) to update multipliers.

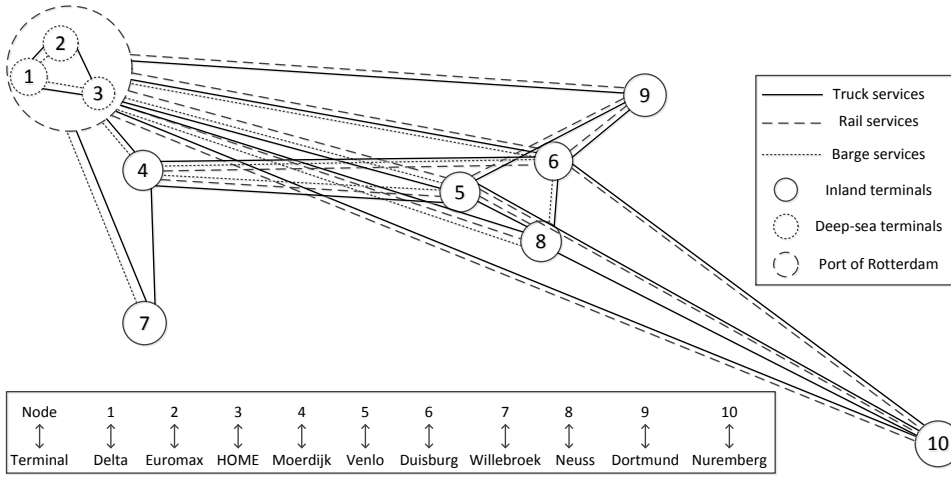

Figure 5.4: The topology of a hinterland synchromodal network in Europe.

Table 5.2: Experimental setting.

Coefficient	Truck	Barge	Train
Transport cost (€/TEU-km)	76.4+1.04d	0.14d	1.53+0.16d
Carbon emission (kg/TEU-km)	0.8866	0.2288	0.3146
Loading/unloading cost (€/TEU)	3	18	18
Loading/unloading time (h)	0	1	1
Carbon tax (€/ton)	8	8	8
Storage cost (€/TEU-h)	1	1	1

5.5 Numerical experiments

In this section, we evaluate the performance of the anticipatory approach (AA) in comparison with the myopic approach (MA) to investigate the benefits of incorporating stochastic information in dynamic decision-making processes. The approaches are implemented in MATLAB, and all experiments are executed on 3.70 GHz Intel Xeon processors with 32 GB of RAM. The optimization problems are solved with CPLEX 12.6.3.

5.5.1 Experimental setup

In this chapter, we use a hinterland synchromodal network in Europe for the numerical experiments, which includes 3 deep-sea terminals in the port of Rotterdam (i.e., node 1, 2, and 3) and 7 inland terminals in the Netherlands, Belgium, and Germany (i.e., node 4, 5, 6, 7, 8, 9, and 10), as shown in Figure 5.4. We design one week services of the network including 49 barge services, 33 train services, and 34 truck services. The detailed information of the services is presented in Appendix 5.A. The coefficients used in the experiments are derived from van Riessen et al. [102] and Qu et al. [73], as shown in Table 5.2. Here, the transport cost of services is a linear function of the transport distance d.

We generate several instances to represent different characteristics of shipment requests within a given planning horizon. Each shipment request is characterized by its origin, destination, container volume, announce time, release time, expiry date, and due time. We assume that:

- the origins of shipments are independent and identically distributed among $\{1,2,3\}$ with probabilities $\{0.66,0.2,0.14\}$;
- the destinations are independent and identically distributed among $\{4,5,6,7,8,9,10\}$ with probabilities $\{0.306,0.317,0.153,0.076,0.071,0.034,0.043\}$;
- the container volumes of shipment requests which arrive before the planning horizon (also called static requests) are drawn independently from a uniform distribution with range $[10,30]$, the average container volume of static requests $U_1^{\mathrm{AVE}} = 20$; the container volumes of dynamic requests are drawn independently from uniform distributions with range $[1,9]$, the average container volume of dynamic requests $U_2^{\mathrm{AVE}} = 5$;
- the announce time of static requests is 0, while the frequency of dynamic requests arriving in the system belongs to Poisson distributions with mean AT^{AVE};
- the release time of static requests is drawn independently from a uniform distribution with range $[1,120]$; the release time of dynamic requests is generated based on its announce time, $\mathbb{T}_r^{\mathrm{release}} = \lceil \mathbb{T}_r^{\mathrm{announce}} \rceil + \Delta\mathbb{T}$, $\Delta\mathbb{T}$ belongs to a uniform distribution with range $[1,6]$; the expiry date is equal to the release time;
- the due time of shipment requests is generated based on its release time and lead time, $\mathbb{T}_r^{\mathrm{due}} = \mathbb{T}_r^{\mathrm{release}} + LD_r$, the lead time of shipments is independent and identically distributed among $\{24,48,72\}$ (unit: hours) with probabilities $\{0.15,0.6,0.25\}$. The delay cost coefficients of shipments with lead time 24, 48, and 72 hours are 100, 70, and 50 €/h-TEU, respectively.

We use $\mathrm{EU}-n_1-n_2$ to represent an instance with n_1 static requests and n_2 dynamic requests. We set AT^{AVE} to 20, 10, 6, 5, and 4 minutes (i.e., about 0.33, 0.17, 0.1, 0.08, and 0.07 hours per request) for instances EU-300-400, EU-200-800, EU-100-1200, EU-50-1400, and EU-0-1600, respectively, as shown in Figure 5.5. The length of the planning horizon is set to one week (i.e., 168 hours) for all the instances. The length of the optimization interval is set to 1 hour in the MA and the AA.

5.5.2 Evaluation of the AA in comparison with the MA

To evaluate the performance of the AA with respect to the MA, we design 5 instances (EU-300-400, EU-200-800, EU-100-1200, EU-50-1400, and EU-0-1600) with different degrees of dynamism: 25%, 50%, 75%, 87.5%, and 100%. We define the degree of dynamism as the ratio between the number of containers from dynamic requests and the total number of containers over the planning horizon, namely, degree of dynamism=$\frac{n_2 * U_2^{\mathrm{AVE}}}{n1 * U_1^{\mathrm{AVE}} + n2 * U_2^{\mathrm{AVE}}}$. For example, the degree of dynamism of instance EU-100-1200 is (1200*5)/(100*20+1200*5)=75%. At each decision epoch of the AA, a sample is generated randomly based on the probability distributions presented above. In case of sample instability, for each instance, we replicate

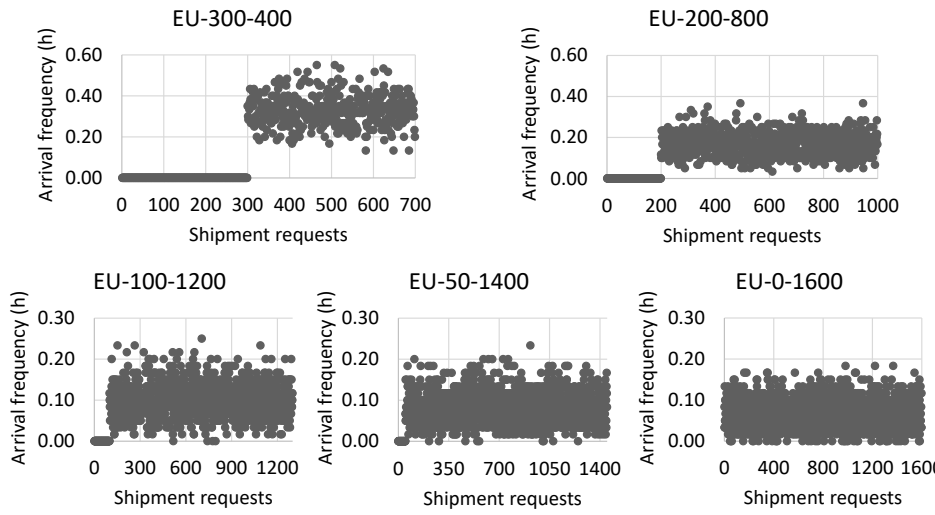

Figure 5.5: Arrival frequency of instances.

the optimization process 10 times under the AA. We use 'gaps in total costs' as the performance indicator which is given by (benchmark value - objective value)/benchmark value. Here, the total cost generated by the MA is the benchmark value, while the total cost generated by the AA is the objective value. Therefore, the higher the 'gaps in total costs', the better the performance of the AA in reducing total costs.

To test the influence of the degree of dynamism, we set the number of scenarios to 10, and the length of prediction horizon to 12 hours. Figure 5.6 shows that the AA has better performance than the MA in all the instances in reducing total costs, and the gap between the AA and the MA grows with the increasing of the degree of dynamism from 25% to 87.5%. Nevertheless, further increasing the degree of dynamism to 100%, the gap in total costs stays around 4%.

With regards to the number of scenarios, we set the degree of dynamism to 87.5% (i.e., instance EU-50-1400), and the length of prediction horizon to 12 hours. The number of scenarios is varied from 1 to 30. Figure 5.7 (a) shows that increasing the number of scenarios, the gap in total costs between the AA and the MA becomes larger. The reason is that the larger the number of scenarios, the more accurate the representation of the future. Moreover, we set the number of scenarios to 10, and vary the length of prediction horizon from 1 to 24 hours for instance EU-50-1400. Figure 5.7 (b) shows that the length of prediction horizon has high influences on the performance of the AA in reducing total costs. The longer the prediction horizon, the more stochastic information of future requests will be considered. The system thus reserves capacities for predicted future requests which are more 'valuable'. In turn, the performance of the system over the planning horizon becomes better.

To understand the differences in the matching process between the MA and the AA, we analyze the matching results of one instance at every time stage. Here, we use 'gaps in cumulated costs' to represent the differences in cumulated costs at previous stages between

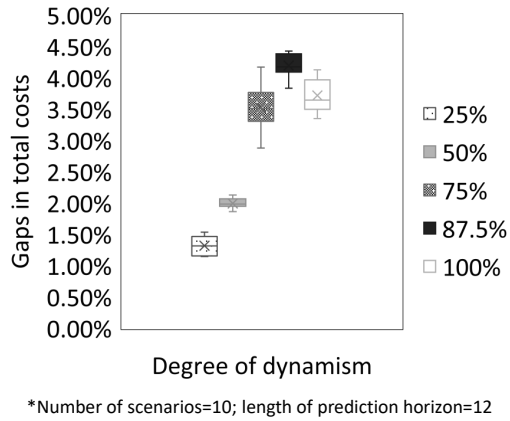

Figure 5.6: Comparison between the AA and the MA under instances with different degrees of dynamism.

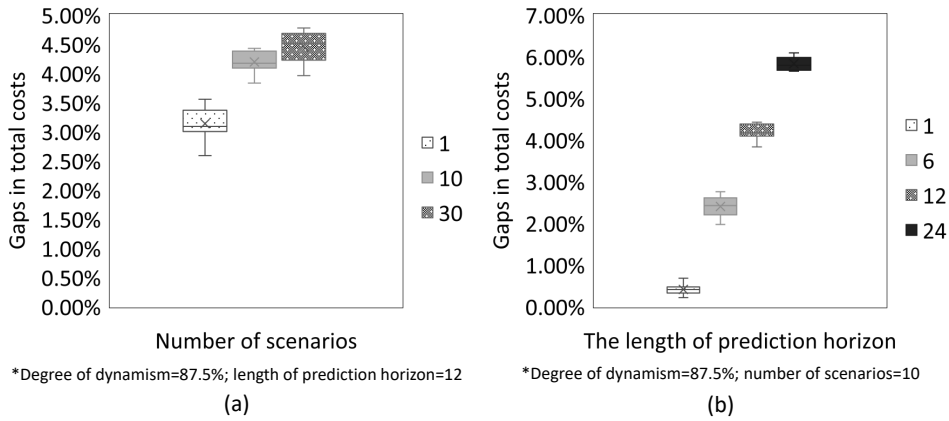

Figure 5.7: Comparison between the AA and the MA under instances with different number of scenarios and different length of prediction horizon.

the MA and the AA. The higher the 'gaps in cumulated costs', the better the performance of the AA. We use 'gaps in cumulated barge and train capacity utilization' to represent the differences in cumulated capacity utilization of barge and train services. Figure 5.8 shows that in earlier stages (before time stage 36), the MA tries to use as much barge and train capacity as possible, the cumulated cost is lower than the AA. However, in later stages (after time stage 104), the MA has no barge and train capacity that can be used. In comparison, the AA holds some capacity of barge and train services for requests arrived in later stages, the cumulated total cost over the planning horizon is lower than the MA; the cumulated capacity utilization of barge and train services over the planning horizon is higher than the MA. It is predictable that the longer the planning horizon, the better the performance of the AA since it anticipates the future.

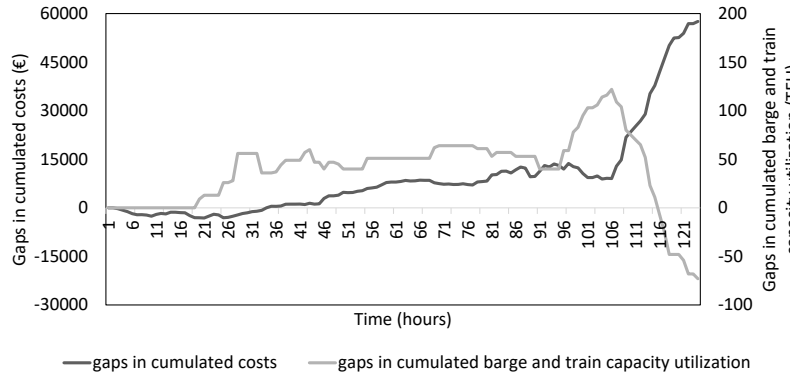

Figure 5.8: Differences in matching process between the MA and the AA.

5.5.3 Performance of the AA under extreme scenarios

In the instances presented so far, we assume the decision maker has the accurate probability distributions of future requests. Thus, the probability distributions used for sampling requests in the AA are the same as the probability distributions used in generating the above instances. However, due to uncertainties in demand during special periods (e.g., high inflation rate periods, Valentine's Day, Black Friday), the demand might be quite lower or higher than normal periods, namely under the 'extreme scenarios'.

In this section, we design another 5 instances with lower demand realizations drawn from a uniform distribution with range $[1,3]$, and another 5 instances with higher demand realizations drawn from a uniform distribution with range $[7,9]$, as shown in Figure 5.9(a). For each instance, we replicate the optimization process 10 times to get average solutions. We set the number of scenarios to 10, and the length of prediction horizon to 12 hours. Figure 5.9(b) shows that when realizations are quite lower than normal periods, the performance of the AA is almost the same as the MA in all the instances and even worse for instances with 100% degree of dynamism. The reason is that using the AA, the system will hold some capacity for future requests which actually have lower demand realizations than predictions. On the other hand, when the demand realizations are higher than normal periods, the AA still has better performance than the MA for all the instances. Interestingly, the gap between the AA under different demand realizations grows as the degree of the dynamism increases. This is expected since the larger the degree of dynamism, the larger the differences between the realizations and the predictions.

5.5.4 Performance of the progressive hedging algorithm

The experimental results of the AA presented above are based on the sample average approximation method to generate 'optimal solutions' for instances with a small sample size and short prediction horizon. Further increasing the number of scenarios or the length of prediction horizon makes the problem difficult to solve for the instances designed above. In this section, we test the performance of the AA based on the progressive hedging algorithm (PHA) for instances with larger sample sizes and longer prediction horizons.

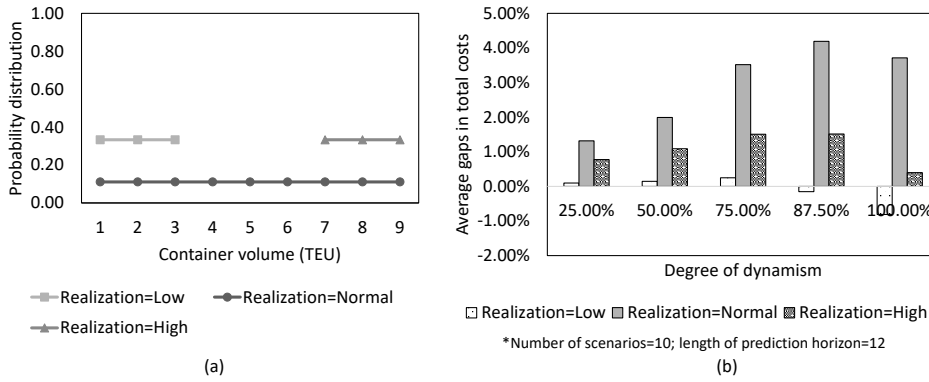

Figure 5.9: Performance of the AA under extreme scenarios.

Table 5.3: Comparison between the performance of the AA without the PHA and with the PHA for instance EU-100-1200.

MA		AA					
				without the PHA		with the PHA	
Total costs	Ave. CPU (s)	Sample size	Prediction horizon (h)	Total costs	Ave. CPU (s)	Total costs	Ave. CPU (s)
980743	0.42	10	24	936046	149.29	938995	5.21
		10	48	above 1 hour		931501	14.21
		10	72			931528	28.40
		30	24			936440	4.98
		30	48			928084	22.39
		30	72			925372	33.79
		100	24			936049	7.14
		100	48			922322	29.49
		100	72			**918225**	49.53

We set $N^{\text{iteration}} = 100, \theta = 1, \eta = 0.001$ for the PHA. The comparison between the performance of the AA without the PHA and with the PHA for instance EU-100-1200 with 75% degree of dynamism is shown in Table 5.3. We consider two performance indicators: the total costs (€) and the ave. CPU (s). The ave. CPU of the MA, the AA without the PHA, and the AA with the PHA is the average computation time per stage over the planning horizon (i.e., 168 time stages). Although the PHA needs to solve a large number of subproblems at each decision epoch due to the iteration of Lagrangian multipliers, applying the parallel computing techniques enables to use multiple CPUs to solve the subproblems in a single iteration of the PHA simultaneously. Table 5.3 shows that when the sample size (i.e., the number of scenarios) is larger than 10 and the length of prediction horizon is longer than 24 hours, the AA without the PHA cannot obtain any results within 1 hour (the length of the optimization interval) due to the large scale of the problem. By contrast, the AA with the PHA can generate better solutions within 1 minute at each decision epoch when the sample size is 100 and the length of prediction horizon is 72 hours. The total cost reduction of the AA with the PHA is 17821 € per week (i.e., about 1.90%) in comparison with the AA without the PHA, and 62518 € per week (i.e., about 6.37%) in comparison with the MA.

5.6 Conclusions

This chapter answers research question **RQ3** by introducing a dynamic and stochastic shipment matching problem in hinterland synchromodal transportation. The problem is dynamic since some shipment requests arrive in the system in real-time. The problem is stochastic since the probability distributions of future requests are available from historical data. We presented a Markov decision process model to describe the problem. Due to the curse of dimensionality, we developed an anticipatory approach (AA) to solve the problem. The AA uses a sample average approximation method to approximate expected objective functions and a progressive hedging algorithm (PHA) to generate solutions at each decision epoch of a rolling horizon framework.

We validated the performance of the AA in comparison with a myopic approach (MA) in which dynamic decisions are made based on deterministic information on a hinterland synchromodal network in Europe. The experimental results indicate that the AA has better performance than the MA in total cost savings up to 4.5% under different degrees of dynamism of the synchromodal matching system when the number of scenarios is set to 10 and the length of prediction horizon is set to 12 hours. Further increasing the number of scenarios or the length of prediction horizon has been proven to be able to further increase the performance of the AA. In addition, we tested the performance of the AA under 'extreme scenarios'. The results show that the AA almost has no improvement when realizations are lower than normal periods as it reserves capacity for future requests which have quite lower demand realization than predictions, but has better performance when realizations are quite higher than normal periods. Finally, we evaluated the performance of the AA with the PHA in comparison to the AA without the PHA. The results show that the AA with the PHA can obtain better results in total costs within 1 minute when the number of scenarios is 100 and the length of prediction horizon is 72 hours thanks to the parallel computing possibility of the PHA. Compared with the MA, the AA with the PHA can reduce total costs above 60000 € per week (around 6.5%) for the instance with 75% degree of dynamism of the synchromodal matching system. In conclusion, the proposed platform provides the means for a more efficient decision-making framework for transportation systems thanks to the developed anticipatory approach.

Future research can be conducted under three directions. First, due to the capacity limitation of road infrastructures, the number of trucks is limited in a synchromodal network. Therefore, the rejection of shipment requests can be considered in online matching processes to avoid infeasible solutions. Chapter 6 develops a matching model that integrates acceptance and matching decisions. Another research direction is to investigate the benefits of incorporating ad hoc services (i.e., dynamic services). Considering the excess capacity of services from carriers, the online matching of static requests, dynamic requests, dedicated services, and ad hoc services gives rise to a new variant of the dynamic shipment matching problem in synchromodal transportation. Third, due to the existence of traffic congestion and terminal congestion in synchromodal transportation, travel time of services and transfer time at terminals are usually uncertain. Combining multiple uncertainties in dynamic shipment matching is a promising research direction. Chapter 6 in particular, simultaneously considers spot request and travel time uncertainties in dynamic shipment matching processes.

Appendix 5.A

The detailed information of truck, barge, and train services used in Chapter 5 is presented in Table 5.4-5.6. We assume there exists a truck connection between all the terminals. The barge and train connections are derived from European Gateway Services (http://www.europeangatewayservices.com/en/). The distance of services used in Chapter 5 is obtained from European Gateway Services, InlandLinks (https://www.inlandlinks.eu/en), and Google maps.

Table 5.4: Truck services in the numerical experiments.

Truck services	Origin	Destination	Travel time (h)	Travel cost (€/TEU)	Distance (km)	Carbon emissions (kg/TEU)
1	Delta	Euromax	0.2	92.00	15	13.30
2	Delta	HOME	0.5	115.40	37.5	33.25
3	Delta	Moerdijk	1.0	154.40	75	66.50
4	Delta	Venlo	2.6	279.20	195	172.89
5	Delta	Duisburg	3.2	326.00	240	212.78
6	Delta	Willebroek	2.0	232.40	150	132.99
7	Delta	Neuss	3.5	349.40	262.5	232.73
8	Delta	Dortmund	4.0	388.40	300	265.98
9	Delta	Nuremberg	9.0	778.40	675	598.46
10	Euromax	HOME	0.6	123.20	45	39.90
11	Euromax	Moerdijk	1.2	170.00	90	79.79
12	Euromax	Venlo	2.8	294.80	210	186.19
13	Euromax	Duisburg	3.3	333.80	247.5	219.43
14	Euromax	Willebroek	2.2	248.00	165	146.29
15	Euromax	Neuss	3.6	357.20	270	239.38
16	Euromax	Dortmund	4.2	404.00	315	279.28
17	Euromax	Nuremberg	9.5	817.40	712.5	631.70
18	HOME	Moerdijk	0.6	123.20	45	39.90
19	HOME	Venlo	2.3	255.80	172.5	152.94
20	HOME	Duisburg	2.7	287.00	202.5	179.54
21	HOME	Willebroek	1.5	193.40	112.5	99.74
22	HOME	Neuss	3.0	310.40	225	199.49
23	HOME	Dortmund	3.4	341.60	255	226.08
24	HOME	Nuremberg	8.8	762.80	660	585.16
25	Moerdijk	Venlo	1.8	216.80	135	119.69
26	Moerdijk	Duisburg	2.4	263.60	180	159.59
27	Moerdijk	Willebroek	1.4	175.20	95	84.23
28	Venlo	Duisburg	0.8	138.80	60	53.20
29	Venlo	Neuss	0.9	146.60	67.5	59.85
30	Venlo	Dortmund	1.5	193.40	112.5	99.74
31	Venlo	Nuremberg	6.6	591.20	495	438.87
32	Duisburg	Neuss	0.5	115.40	37.5	33.25
33	Duisburg	Dortmund	0.9	146.60	67.5	59.85
34	Duisburg	Nuremberg	6	544.40	450	398.97

Table 5.5: Barge services in the numerical experiments.

Barge services	Origin	Destination	Capacity (TEU)	Departure time	Arrival time	Travel time (h)	Travel cost (€/TEU)	Distance (km)	Carbon emissions (kg/TEU)
1	Delta	Euromax	160	53	54	1	2.10	15	3.43
2	Delta	HOME	160	53	55.5	2.5	5.25	37.5	8.58
3	Delta	Moerdijk	160	3	8	5	10.50	75	17.16
4	Delta	Moerdijk	160	15	20	5	10.50	75	17.16
5	Delta	Moerdijk	160	27	32	5	10.50	75	17.16
6	Delta	Moerdijk	160	39	44	5	10.50	75	17.16
7	Delta	Moerdijk	160	51	56	5	10.50	75	17.16
8	Delta	Moerdijk	160	63	68	5	10.50	75	17.16
9	Delta	Moerdijk	160	75	80	5	10.50	75	17.16
10	Delta	Moerdijk	160	87	92	5	10.50	75	17.16
11	Delta	Moerdijk	160	99	104	5	10.50	75	17.16
12	Delta	Moerdijk	160	111	116	5	10.50	75	17.16
13	Delta	Moerdijk	160	123	128	5	10.50	75	17.16
14	Delta	Moerdijk	160	135	140	5	10.50	75	17.16
15	Delta	Moerdijk	160	147	152	5	10.50	75	17.16
16	Delta	Moerdijk	160	159	164	5	10.50	75	17.16
17	Delta	Venlo	160	12	25	13	27.30	195	44.62
18	Delta	Venlo	160	18	31	13	27.30	195	44.62
19	Delta	Venlo	160	36	49	13	27.30	195	44.62
20	Delta	Venlo	160	42	55	13	27.30	195	44.62
21	Delta	Venlo	160	60	73	13	27.30	195	44.62
22	Delta	Venlo	160	66	79	13	27.30	195	44.62
23	Delta	Venlo	160	90	103	13	27.30	195	44.62
24	Delta	Venlo	160	96	109	13	27.30	195	44.62
25	Delta	Venlo	160	120	133	13	27.30	195	44.62
26	Delta	Duisburg	160	82	98	16	33.60	240	54.91
27	Delta	Duisburg	160	102	118	16	33.60	240	54.91
28	Delta	Willebroek	160	68	79	11	23.10	165	37.75
29	Delta	Willebroek	160	98	109	11	23.10	165	37.75
30	Delta	Willebroek	160	146	157	11	23.10	165	37.75
31	Delta	Neuss	160	80	97	17	35.70	255	58.34
32	Euromax	Moerdijk	160	3	8.5	5.5	11.55	82.5	18.88
33	Euromax	Moerdijk	160	51	56.5	5.5	11.55	82.5	18.88
34	Euromax	Moerdijk	160	99	104.5	5.5	11.55	82.5	18.88
35	Euromax	Venlo	160	27	40.5	13.5	28.35	202.5	46.33
36	Euromax	Venlo	160	75	88.5	13.5	28.35	202.5	46.33
37	Euromax	Duisburg	160	103	119.5	16.5	34.65	247.5	56.63
38	Euromax	Willebroek	160	112	123.5	11.5	24.15	172.5	39.47
39	Euromax	Neuss	160	66	83.5	17.5	36.75	262.5	60.06
40	HOME	Moerdijk	160	5	8	3	6.30	45	10.30
41	HOME	Moerdijk	160	53	56	3	6.30	45	10.30
42	HOME	Moerdijk	160	101	104	3	6.30	45	10.30
43	HOME	Venlo	160	99	110	11	23.10	165	37.75
44	HOME	Venlo	160	126	137	11	23.10	165	37.75
45	HOME	Duisburg	160	51	66.5	15.5	32.55	232.5	53.20
46	HOME	Willebroek	160	20	30.5	10.5	22.05	157.5	36.04
47	Moerdijk	Venlo	160	95	105	10	21.00	150	34.32
48	Moerdijk	Duisburg	160	71	83	12	25.20	180	41.18
49	Duisburg	Neuss	160	120	122.5	2.5	5.25	37.5	8.58

Table 5.6: Train services in the numerical experiments.

Train services	Origin	Destination	Capacity (TEU)	Departure time	Arrival time	Travel time (h)	Travel cost (€/TEU)	Distance (km)	Carbon emissions (kg/TEU)
1	Delta	Venlo	90	16	20	4	30.33	180	56.63
2	Delta	Venlo	90	40	44	4	30.33	180	56.63
3	Delta	Venlo	90	9	13	4	30.33	180	56.63
4	Delta	Venlo	90	33	37	4	30.33	180	56.63
5	Delta	Venlo	90	57	61	4	30.33	180	56.63
6	Delta	Venlo	90	81	85	4	30.33	180	56.63
7	Delta	Venlo	90	105	109	4	30.33	180	56.63
8	Delta	Venlo	90	129	133	4	30.33	180	56.63
9	Delta	Duisburg	90	41	47	6	44.73	270	84.94
10	Delta	Duisburg	90	75	81	6	44.73	270	84.94
11	Delta	Duisburg	90	99	105	6	44.73	270	84.94
12	Delta	Duisburg	90	113	119	6	44.73	270	84.94
13	Delta	Neuss	90	110	115	5	37.53	225	70.79
14	Delta	Dortmund	90	88	95	7	51.93	315	99.10
15	Delta	Nuremberg	90	51	66	15	109.53	675	212.36
16	Delta	Nuremberg	90	99	114	15	109.53	675	212.36
17	Euromax	Venlo	90	78	82.5	4.5	33.93	202.5	63.71
18	Euromax	Venlo	90	102	106.5	4.5	33.93	202.5	63.71
19	Euromax	Duisburg	90	75	81.5	6.5	48.33	292.5	92.02
20	Euromax	Duisburg	90	99	105.5	6.5	48.33	292.5	92.02
21	Euromax	Neuss	90	77	82.5	5.5	41.13	247.5	77.86
22	Euromax	Dortmund	90	78	85.5	7.5	55.53	337.5	106.18
23	Euromax	Nuremberg	90	79	94.5	15.5	113.13	697.5	219.43
24	HOME	Venlo	90	86	89.5	3.5	26.73	157.5	49.55
25	HOME	Duisburg	90	27	32.5	5.5	41.13	247.5	77.86
26	HOME	Duisburg	90	75	80.5	5.5	41.13	247.5	77.86
27	Moerdijk	Venlo	90	75	78	3	23.13	135	42.47
28	Moerdijk	Duisburg	90	77	81	4	30.33	180	56.63
29	Venlo	Neuss	90	112	113.5	1.5	12.33	67.5	21.24
30	Venlo	Dortmund	90	113	115.5	2.5	19.53	112.5	35.39
31	Venlo	Nuremberg	90	114	125	11	80.73	495	155.73
32	Duisburg	Dortmund	90	121	122.5	1.5	12.33	67.5	21.24
33	Duisburg	Nuremberg	90	122	132	10	73.53	450	141.57

Chapter 6

Dynamic and stochastic global shipment matching

Hinterland transportation, as a key component of global transportation, has different time scales, transport modes, and network topology from intercontinental transportation. While Chapter 3, 4, and 5 have studied matching, dynamic, and stochastic models in hinterland synchromodal transportation, this chapter focuses on the dynamics and uncertainties in global synchromodal shipment matching.

This chapter is structured as follows. Section 6.1 introduces the motivations and challenges faced by network operators in global synchromodal transportation. We briefly review the relevant literature and specify our contributions in Section 6.2. In Section 6.3, we provide a detailed problem description, followed by a Markov decision process model in Section 6.4 and the hybrid stochastic approach in Section 6.5. In Section 6.6, we present the experimental results. Finally, the conclusions are given in Section 6.7.

Parts of this chapter have been submitted to a journal: "W. Guo, B. Atasoy, W. Beelaerts van Blokland, and R. R. Negenborn. Global synchromodal transportation with dynamic and stochastic shipment matching. Submitted to a journal, 2020."

6.1 Introduction

Global container transportation is the movement of containers between inland terminals located in different continents by using ships, barges, trains, trucks or any combination of them [113]. With the increasing volume of global trade, container transportation becomes more and more important in improving the efficiency of global supply chains. As the fastest-growing cargo segment, global containerized trade reached 152 million twenty-foot equivalent units (TEUs) in 2018 [97]. Traditionally, global container transportation is organized by multiple operators. For example, an inland operator in Asia transports containers from Chongqing Terminal to Shanghai Port; a shipping liner company manages the container transport from Shanghai Port to Rotterdam Port; an inland operator in Europe further transports containers from Rotterdam Port to Duisburg Terminal.

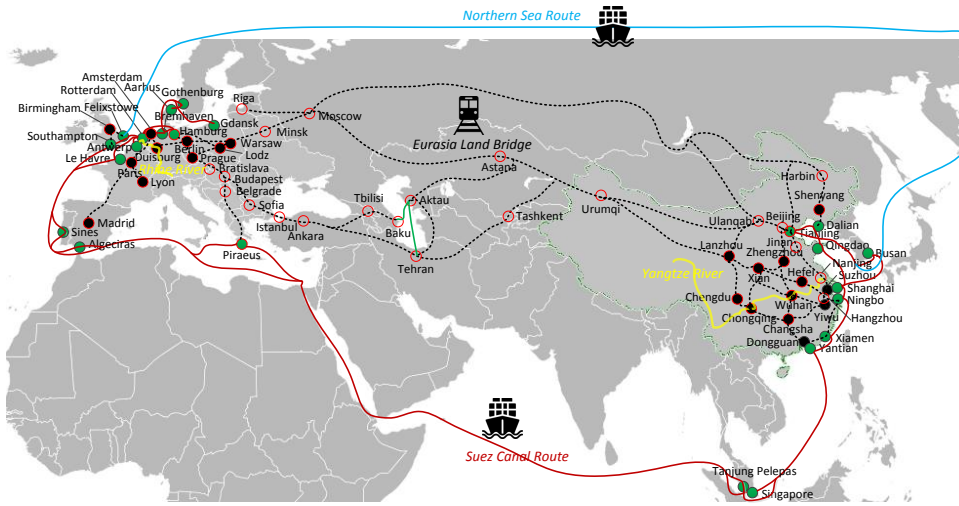

Figure 6.1: Map of the integrated global network representing our vision.

In the past decade, horizontal collaboration between shipping lines has been very popular by forming an alliance to improve the utilization of resources and increase service frequency and capacity [46]. Recently, port operators and shipping lines appear to be focusing more attention on vertical integration by expanding service networks to inland terminals, such as Maersk and COSCO Shipping Lines [97]. The vertical and horizontal collaboration among players in global container transport brings new challenges to global operators because of integrated planning in larger and more complex networks, as in Figure 6.1. In such a global network, we define the global operator as the integrator that collaborates with inland carriers, ocean carriers, and terminal operators.

Apart from integrated transportation, amodal booking and differentiated fare classes have also been introduced in container transportation [99]. Amodal booking implies that shippers do not select modes and routes for their shipments and leave the choices to a global operator. This increases the flexibility of the global operator to optimize the available capacities and to react effectively to disruptions by dynamically updating transport plans [30]. Differentiated fare classes have been proposed as incentives to promote the concept of amodal booking [101]. For each origin-destination (OD) pair, the global operator offers multiple fare classes to shippers. A fare class is characterized by a specific price, lead time, and delay cost. Once a booking request associated with a fare class is accepted by the global operator, the transport plan that assigns specific transport services to accepted requests needs to be created.

Furthermore, digitalization and online booking platforms enabled by advanced information technologies are being increasingly used by the container industry. For example, Maersk launched an online booking platform called Maersk Spot in 2018 that allows customers to check the real-time freight rates, book ship slots online, and track their bookings [61]. With Maersk Spot, the shipping company can instantly confirm whether to accept or reject a booking request and react dynamically to disturbances (e.g., service delays) by adjusting the transport plan.

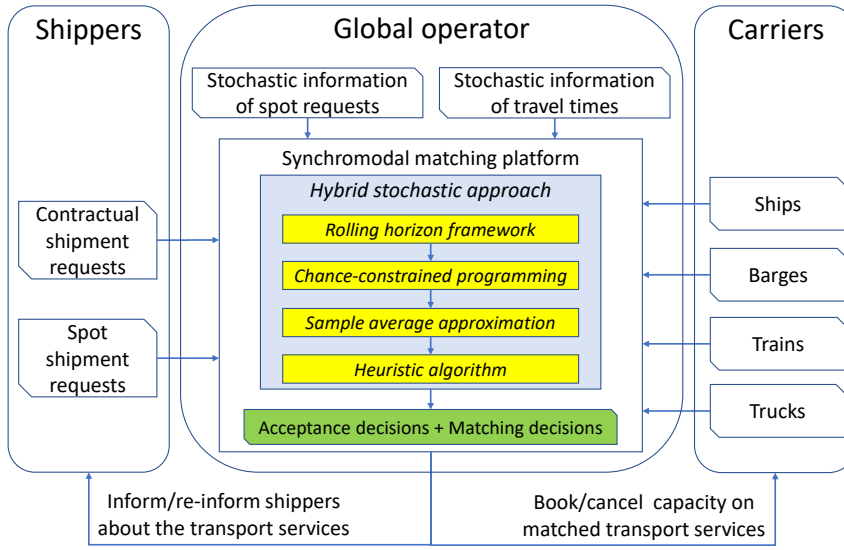

Figure 6.2: Illustration of a synchromodal matching platform. The platform provides online acceptance and matching decisions for shipment requests with multimodal services thanks to the developed hybrid stochastic approach.

The combined trend towards vertical and horizontal collaboration, amodal booking, differentiated fare classes, and digitalization gives rise to the concept of synchromodality in the container industry [99]. Synchromodality aims to reduce logistics costs, delays, and carbon emissions while improving the utilization of resources based on real-time information [30]. However, implementing synchromodality in practice is still challenging from several aspects, including pricing strategies and collaboration contracts at the strategical level, integrated service network design at the tactic level, and the allocation of resources to demands under a dynamic and stochastic environment at the operational level [30].

In this chapter, we investigate a dynamic and stochastic global shipment matching problem (DSGSM) under synchromodality. We consider a platform owned by a global operator that receives contractual and spot shipment requests from shippers and receives multimodal services from carriers. While the contractual requests are received before the planning horizon, the spot requests appear in the platform dynamically. The platform creates online decisions for shipment requests including acceptance and matching decisions in a global synchromodal network, as shown in Figure 6.2. A match between a request and a service represents that the request will be transported by the service from the service's origin to the service's destination. Due to spot request uncertainty and service capacity limitations, the decisions made for current requests might become suboptimal upon receiving new requests. Due to travel time uncertainty and the utilization of multimodal services, the matches made for accepted requests might become infeasible at transshipment terminals. The objective of the platform is to maximize the total profits over a given planning horizon taking into account logistics costs, delays, and carbon emissions.

Thanks to the development in data analytics, probability distributions of uncertainties are often available to online platforms. However, while dynamic and stochastic approaches

have been well investigated in vehicle routing problems [e.g., 75], resource allocation problems [e.g., 105], and inland container routing problems [e.g., 37], the dynamic and stochastic approach for global synchromodal transport is still missing in the literature. This chapter contributes to the literature by proposing a hybrid stochastic approach that incorporates stochastic information in online decision-making processes to solve the DSGSM problem. Specifically, we propose a rolling horizon framework to handle real-time information on requests and services. Travel time uncertainty is addressed by a chance-constrained programming model and spot request uncertainty is addressed by a sample average approximation method. Due to the computational complexity, we design a preprocessing-based heuristic algorithm to generate timely solutions at each decision epoch. Section 6.2.3 outlines the specific contributions of this chapter in more detail.

6.2 Literature review

The characteristics of the DSGSM problem under synchromodality mainly include: global synchromodal network consists of inland networks and intercontinental networks; online planning with acceptance and matching decisions; dynamic information of spot requests and travel times; stochastic information of spot requests and travel times; profits maximization over a given planning horizon. Studies related to the DSGSM problem are presented into two categories: global intermodal transportation; dynamic and stochastic container booking and routing models.

6.2.1 Global intermodal transportation

Intermodal transportation is the provision of efficient, effective, and sustainable transport services through integrated planning at a network level [18]. Global intermodal transportation consists of intercontinental transportation and inland transportation. In intercontinental transportation, containers are transported from export terminals to import terminals. In inland transportation, export containers are transported from inland origins to export terminals; import containers are transported from import terminals to inland destinations. While extensive studies investigated maritime transportation [59] and inland transportation [87] in the literature, only a few studies investigated global intermodal transportation [46].

Regarding global intermodal transport planning, Erera et al. [22] developed a multi-commodity network flow model to route loaded containers and reposition empty containers for global tank container management. Meng et al. [60] developed a global liner shipping network design model to facilitate multi-type container routing and repositioning. Liu et al. [55] proposed a holistic approach to solve a global intermodal liner shipping network design problem that covers both inland transport expenses and seaborne shipping costs. Tran et al. [96] considered not only the design of an optimal shipping route but also the inland connections between hinterlands and ports. Yang et al. [113] proposed a bi-level optimization model to reconstruct the shipping service network between Asia and Europe by considering the improvement of New Eurasian Land Bridge rail services and Budapest-Piraeus railway. Wei et al. [111] investigated a container routing problem in a new cross-border logistics network that connects the maritime network and inland network through dry ports.

In the literature, the existing global intermodal transport models assumed that all the input information is static and deterministic. However, in reality, multiple dynamic events and uncertainties exist in global intermodal transportation which highly affect the *feasibility* and *profitability* of transport plans. Synchromodal transportation, as an evolution of intermodal transportation, refers to transport systems with dynamically updating of plans by incorporating dynamic and stochastic information [30].

6.2.2 Dynamic and stochastic container booking and routing models

In container transportation, the dynamic and stochastic models related to the DSGSM problem mainly include container booking and container routing problems. While the former considers the acceptance of booking requests to maximize revenue, the latter emphasizes the decisions on assigning containers or shipments to specific transport services to minimize costs. A shipment is defined as a batch of containers with specific time windows, OD pairs, and fare classes that must be transported as a whole.

Dynamic and stochastic container booking models

Container booking control, also called slot allocation and capacity control, is one of the primary research topics in revenue management and is widely adopted by the airline industry [61]. Container booking control aims to maximize revenue in a stochastic environment by effectively deciding on the acceptance of booking requests. According to the network structure, studies on container booking control can be divided into two groups: single-leg level and network level. While the single-leg level models [e.g., 47, 107] consider services operating on a single corridor, the network level models study services that operate on a network with the possibility of transshipments [61].

Most network container booking control models study static environments with the main strategies of booking limits and bid-price. A booking limit represents the maximum number of containers that should be allocated to a service. For example, Zurheide et al. [118] proposed a slot allocation model for a liner shipping network to determine the booking limits for different booking classes (e.g. OD pair, container type, and service segment). van Riessen et al. [101] investigated a cargo fare class mix problem in an intermodal network to maximize revenue by determining the booking limits on each fare class. Under a bid-price strategy, the decision of whether to accept or reject a booking is made based on the lowest acceptable profit value or the marginal costs for the next unit of capacity. Zurheide et al. [119] developed a slot allocation model for a liner shipping company to decide the opportunity cost of a container slot as the bid-price and proved that the bid-price strategy outperforms the booking limit strategy due to the better utilization of capacity for profitable requests.

With the development of information technologies and digitalization in the container industry, researchers and industries have increasingly shifted their attention to dynamic models [61]. These models can better reflect the online container booking processes and therefore better manage resource capacity. Bilegan et al. [11] designed a load acceptance management system for rail container transport planning to dynamically accept requests or reject them in favor of future requests with potentially higher profit. Wang et al. [109] developed a probabilistic mixed integer programming optimization model to make acceptance

decisions with the objective to maximize the expected revenue of a barge carrier over a given planning horizon. Wang et al. [105] investigated a dynamic resource allocation problem, in which an intermodal operator attempts to determine the policy that characterizes the optimal quantities of each service product allowed to be sold during each time interval within a finite selling horizon.

In comparison to the DSGSM problem proposed in this chapter, the above-mentioned container booking models focus on the acceptance decisions of requests before the transport process by setting booking limits or bid-price to maximize revenue. However, we take into account the logistics costs, delays and carbon emissions generated for matching specific shipments with specific services during the transport process. Besides, our work considers the dynamic and stochastic information of spot requests and travel times in a global synchromodal network, and re-optimizes the transport plan when disturbances (i.e., infeasible transshipments) happen.

Dynamic and stochastic container routing models

In the literature, container routing models have been well investigated at the strategic and tactical levels under a static context [59]. Most of the studies integrate the container routing decision with other decisions such as empty container repositioning [e.g., 86] and service network design [e.g., 18, 20]. Recently, with the increasing interest towards synchromodality, several dynamic container routing models in synchromodal transportation have been proposed. Li et al. [49] proposed a rolling horizon approach to control and reassign container flows in an inland synchromodal freight transport network with dynamic transport demand and traffic conditions. Qu et al. [72] proposed a mixed-integer programming model to reschedule services and reroute shipment flows under the framework of synchromodality when unexpected dynamic events cause deviations from original plans. Guo et al. [37] investigated a dynamic shipment matching problem in which a platform provides online matches between shipment requests and transport services in a hinterland network.

The recent developments in information technologies and data analytics have facilitated the utilization of stochastic information in online decision-making processes [75]. With regards to dynamic and stochastic container routing problems, van Riessen et al. [100] proposed a decision tree to instantaneously allocate incoming containers to inland services by analyzing the solution structure of an optimization model on historical data of transport demand. Rivera et al. [76] proposed an adaptive approximate dynamic programming algorithm to assign the newly arrived containers to a barge or trucks incorporating the probability distributions of future requests, to achieve cost minimization over a multi-period horizon. Guo et al. [36] proposed an anticipatory optimization approach to create online matches between shipment requests and transport services in an inland synchromodal network by incorporating the probability distributions of future requests.

Compared with the DSGSM problem proposed in this chapter, the above-mentioned dynamic and stochastic container routing models focus on the routing/matching decisions for booking requests to minimize total costs without the consideration of acceptance decisions. Furthermore, none of them consider the dynamic and stochastic shipment requests and travel times simultaneously. Besides, while the above dynamic and stochastic container routing models are investigated in inland networks, the DSGSM problem focuses on global networks.

6.2.3 Contributions

In summary, the DSGSM problem investigated in this chapter differs from the existing literature in various ways: (i) we consider a global synchromodal transport network; (ii) we develop a dynamic and stochastic model that integrates the decisions of acceptance and matching; (iii) we simultaneously consider the uncertainty in spot requests and travel times; (iv) we formulate a Markov decision process to model the problem; (v) we develop a hybrid stochastic approach that integrates a rolling horizon framework, a chance-constrained programming model, and a sample average approximation method together with a preprocessing-based heuristic algorithm to solve the problem efficiently at each decision epoch; (vi) we evaluate the performance of our approach in comparison to a deterministic and a robust approach under a comprehensive set of experiments.

6.3 Problem description

We consider a platform owned by a global operator that receives contractual and spot shipment requests from shippers, and receives ship, barge, train, and truck services from carriers, as shown in Figure 6.2. We define the global operator as the coordinator that collaborates with shippers, carriers and terminal operators to provide integrated transport planning in a global synchromodal network. The global operator does not typically own any of the transport services used to move a shipment from its origin to its destination or any of the terminals used for transshipments. Instead, the global operator enters into contracts for transport services with carriers and loading/unloading and storage operations with terminal operators. The contract with carriers specifies the services that are available to the global operator with specific modalities, OD pairs, time schedules, available capacities, and costs. The global operators combine these services into itineraries to provide integrated transport for shipments. The global operator publishes the fare classes for each OD pair with specified freight rates, lead times, and delay costs. Shippers choose the fare classes for their shipments based on the value and urgency of commodities. After that, they initiate requests to the platform with specific OD pairs, container volumes, time windows, and fare classes, and leaves the choices of services to the platform.

6.3.1 Terminals

Let N be the set of terminals. Each terminal $i \in N$ is characterized by its loading/unloading cost lc_i^m, loading/unloading time lt_i^m with mode $m \in M = \{\text{ship, barge, train, truck}\}$, and storage cost per container per hour c_i^{storage}. We assume terminal operators provide unlimited loading/unloading and storage capacity to the global operator.

6.3.2 Shipment requests

Let R be the set of requests. Each request $r \in R$ is characterized by its container type CT_r (i.e., dry or reefer), origin terminal o_r, destination terminal d_r, container volume u_r, announce time $\mathbb{T}_r^{\text{announce}}$ (i.e., the time when the platform receives the request), release time $\mathbb{T}_r^{\text{release}}$ (i.e., the time when the shipment is available for transport process), and fare class including freight rate p_r, lead time LD_r, and delay cost c_r^{delay}. The due time of request

r is represented as, $\mathbb{T}_r^{\text{due}} = \mathbb{T}_r^{\text{release}} + LD_r$. Requests R consist of two groups: contractual requests R^0 and spot requests R^t. For a contractual request $r \in R^0$, the global operator has long-term contracts with shippers. Therefore, the announce time of contractual request r is, $\mathbb{T}_r^{\text{announce}} = 0$. All the information $\{CT_r, o_r, d_r, u_r, \mathbb{T}_r^{\text{release}}, \mathbb{T}_r^{\text{due}}, p_r, c_r^{\text{delay}}\}$ is known in advance. On a contrary, for a spot request $r \in R^t$, the platform receives the request from spot markets during time interval $(t-1,t]$. The information of the spot request $\{CT_r, o_r, d_r, u_r, \mathbb{T}_r^{\text{release}}, \mathbb{T}_r^{\text{due}}, p_r, c_r^{\text{delay}}\}$ is unknown before its announce time $\mathbb{T}_r^{\text{announce}}$. However, the probability distributions $\{\pi_{CT}, \pi_o, \pi_d, \pi_u, \pi_{\mathbb{T}^{\text{announce}}}, \pi_{\mathbb{T}^{\text{release}}}, \pi_{\mathbb{T}^{\text{due}}}, \pi_p, \pi_{c^{\text{delay}}}\}$ of spot requests are assumed available to the platform. In addition, shippers require their shipments to be transported as a whole, and ask to receive the transport plan as soon as possible. Besides, we do not consider cancellation of requests from shippers. The requests accepted by the platform will not be rejected in the future.

6.3.3 Transport services

Let S be the set of services. Each ship, barge or train service $s \in S^{\text{ship}} \cup S^{\text{barge}} \cup S^{\text{train}}$ is characterized by its mode $MT_s \in M$, origin terminal o_s, destination terminal d_s, free capacity U_s^{tk} in terms of container type $k \in K = \{\text{dry, reefer}\}$ at decision epoch t, total free capacity U_s^t, scheduled departure time TD_s, scheduled arrival time TA_s, estimated travel time t_s, travel cost c_s, and generation of carbon emissions e_s^k for container type k. Let $\bar{t}_s$, $\bar{T}D_s$ and $\bar{T}A_s$ be the actual travel, departure and arrival time of service s which are unknown before their realization. We consider ship, barge and train services as line services, namely, different services with the same mode might be operated by the same vehicle. We define ξ_s^- as the preceding service and ξ_s^+ as the succeeding service of service s. We define l_{sq} equals to 0 if service s is the preceding service of service q, otherwise equals to 1. Each truck service $s \in S^{\text{truck}}$ is characterized by its origin terminal o_s, destination terminal d_s, free capacity U_s^{tk} in terms of container type $k \in K$ at decision epoch t, total free capacity U_s^t, estimated travel time t_s, travel cost c_s, and generation of carbon emissions e_s^k for container type k. Let $\bar{t}_s$ be the actual travel time of service s which is unknown before its realization. Each truck service consists of a fleet of trucks that have flexible departure times. We define TD_{rs} as a variable that indicates the departure time of service $s \in S^{\text{truck}}$ with shipment $r \in R$. We assume the platform receives real-time information once a service $s \in S$ departs from or arrives to a terminal.

In practice, travel time uncertainties are quite common resulting from weather conditions and traffic congestions [18]. In this chapter, we assume the travel times $[\tilde{t}_s]_{\forall s \in S}$ are continuous random variables following normal distributions, and are statistically independent. Let $\tilde{t}_s \sim N(\mu_s, \sigma_s^2)$, in which μ_s is the mean travel time between terminal o_s and terminal d_s, and σ_s is the corresponding standard deviation. Due to the travel time uncertainties, the actual departure and arrival time of service $s \in S$ are also uncertain. The distribution of the departure time of service s is based on the distribution of the arrival time of its preceding service ξ_s^-; the distribution of the arrival time of service s is based on the distributions of the departure and travel time of service s. For vehicle $v \in V \backslash V^{\text{truck}}$, we define the itinerary of vehicle v as the sequence of services that the vehicle operated, and define I_v^n as the n^{th} service of vehicle v. Therefore, the departure time of service $s = I_v^n$ follows normal distribution given by:

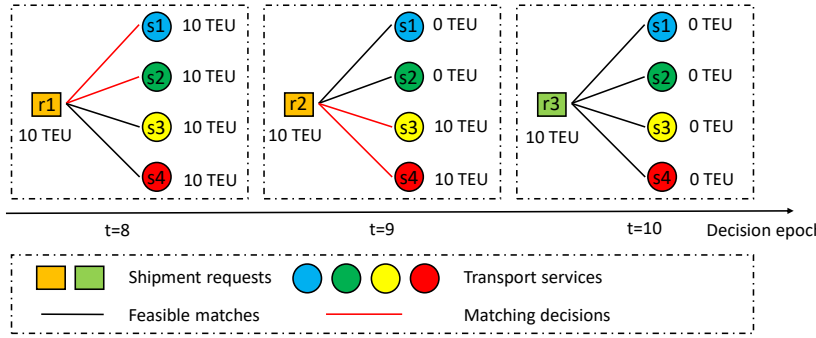

r1: {dry (container type), Shanghai (origin terminal), Duisburg (destination terminal), 10 TEU (container volume), 8 (announce time), 10 (release time), 970 (due time), 1800 € /TEU (freight rate), 9 €/TEU-h (delay cost)};
r2: {dry, Shanghai, Duisburg, 10 TEU, 9, 12, 852, 2400, 12};
r3:{reefer, Shanghai, Duisburg, 10 TEU, 10, 12, 612, 3400, 17};
s1: {ship (mode), Shanghai (origin terminal), Rotterdam (destination terminal), 10 TEU (reefer slots), 20 (departure time), 750 (arrival time), 1000 € /TEU (transport cost)};
s2: {barge, Rotterdam, Duisburg, 10 TEU, 800, 817, 50};
s3: {train, Chongqing, Duisburg, 10 TEU, 240, 600, 2000};
s4: {truck, Shanghai, Chongqing, 10 TEU, 22, 1800};

Figure 6.3: Illustrative example of online matching processes under the FCFS strategy.

$$\tilde{T}D_s \sim N(TD_v^{'} + \sum_{j\in\{1\ldots n-1\}} \mu_{I_v^j} + \sum_{j\in\{1\ldots n-1\}} 2lt_{d_{I_v^j}}^{MT_v^{'}}, \sum_{j\in\{1\ldots n-1\}} \sigma_{I_v^j}^2),$$

where $TD_v^{'}$ is the departure time of vehicle v from its origin terminal, $MT_v^{'}$ is the mode of vehicle v. We denote $\tilde{T}D_s \sim N(\mu_s^+, \sigma_s^{+2})$. Similarly, the arrival time of service $s = I_v^n$ follows normal distribution given by:

$$\tilde{T}A_s \sim N(TD_v^{'} + \sum_{j\in\{1\ldots n\}} \mu_{I_v^j} + \sum_{j\in\{1\ldots n-1\}} 2lt_{d_{I_v^j}}^{MT_v^{'}}, \sum_{j\in\{1\ldots n\}} \sigma_{I_v^j}^2).$$

We denote $\tilde{T}A_s \sim N(\mu_s^-, \sigma_s^{-2})$.

6.3.4 Objectives and infeasible transshipments

The objective of the platform is to maximize total profits over the planning horizon T by dynamically optimizing acceptance and matching decisions over a global synchromodal network. In practice, the first come first served (FCFS) strategy has been widely adopted in the container industry [61]. Under such a strategy, decisions are made based on deterministic information only. An illustrative example of online matching processes under the FCFS strategy is shown in Figure 6.3. At decision epoch $t = 8$, the platform accepts request r1, and matches r1 with ship service s1 and barge service s2 which are the cheapest services. At decision epoch $t = 9$, the platform accepts request r2, and matches r2 with rail service s3 and truck service s4. At decision epoch $t = 10$, the platform receives reefer request r3 which is very profitable. However, the platform has to reject request r3 since no capacity is available. To make better decisions over the planning horizon, the platform needs to consider the stochastic information of future requests.

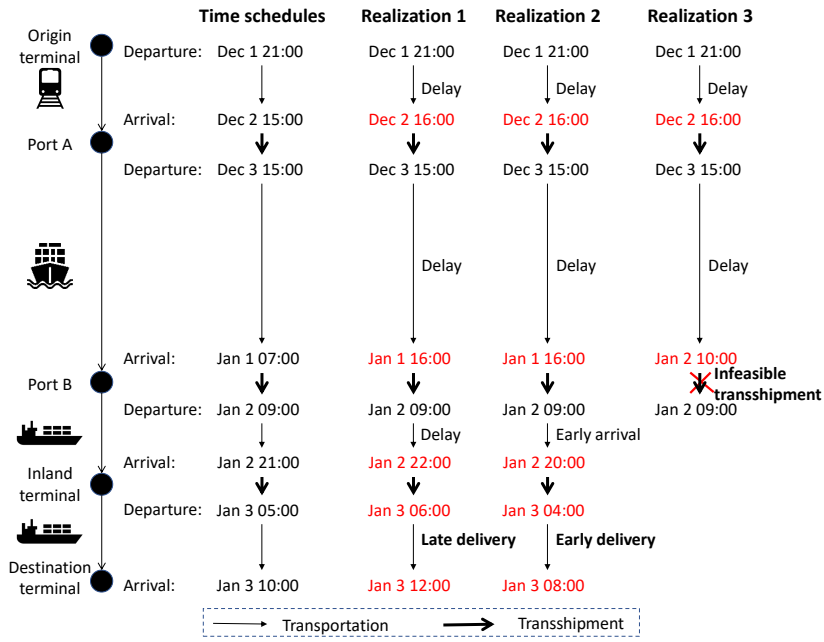

Figure 6.4: Possible outcomes of travel time uncertainty in global transport.

On the other hand, travel time uncertainty of services in a global synchromodal network may lead to infeasible transshipments in addition to the commonly studied outcome of late or early delivery at destinations [e.g., 51, 80]. An illustrative example is shown in Figure 6.4. A shipment is planned to be transported by a train service from its origin terminal to port A, by a ship service from port A to port B, and by two barge services from port B to its destination terminal according to fixed time schedules. The outcomes of travel time uncertainty in global synchromodal transportation include late delivery at destination terminal under realization 1 which causes delayed costs, early delivery at destination terminal under realization 2 which causes storage costs, and infeasible transshipment at port B under realization 3 which requires reoptimization.

6.4 Markov decision process model

In this section, we formulate a Markov decision process (MDP) model for the problem under study. There are seven fundamental elements in the MDP model: decision epochs, state variables, exogenous information, decision variables, transition functions, profits, and objective functions [70]. A brief summary of these elements is as follows:

- **Decision epochs**. We define t as the points in time at which decisions are made, referred to as the decision epoch, $t \in \{0, 1, ..., T\}$. Therefore, the planning horizon is divided into T consecutive time intervals.
- **State variables**. The state $\mathbf{F}^t$ of the global synchromodal matching system contains all the information that is necessary and sufficient to model the system at decision epoch

t. We distinguish between the initial state $\mathbf{F}^0$ and the dynamic state $\mathbf{F}^t$ for $t > 0$. The initial state contains all the deterministic sets and parameters $\{N, R^0, V, S, T, c^{\text{emission}}\}$, initial values of dynamic parameters $U^0 = \left[U_s^{0k}\right]_{\forall s \in S, k \in K}$, and probability distributions of random variables $\left[\tilde{T}D_s\right]_{\forall s \in S \setminus S^{\text{truck}}}$, $\left[\tilde{T}A_s\right]_{\forall s \in S \setminus S^{\text{truck}}}$, $[\tilde{t}_s]_{\forall s \in S}$, $\{\tilde{R}^t\}_{\forall t \in \{1,\ldots T\}}$. The dynamic state $\mathbf{F}^t$ contains the information that is evolving over time, i.e., the set of free capacity of services at decision epoch t, $\mathbf{F}^t = U^t$.

- **Exogenous information**. The exogenous information $\mathbf{W}^t$ consists of all the new information that first becomes known at decision epoch t. We define $\mathbf{W}^t = [\bar{T}D_s]_{s \in S^{+t}} \cup [\bar{T}A_s]_{s \in S^{-t}} \cup R^t \cup \bar{R}^t$, where $S^{+t} = \{s \in S | t-1 < \bar{T}D_s \leq t\}$ is the set of services departing their origin terminals during time interval $(t-1, t]$, $t > 0$; $S^{-t} = \{s \in S | t-1 < \bar{T}A_s \leq t\}$ is the set of services arriving their destination terminals during time interval $(t-1, t]$, $t > 0$; $R^t = \{r | t-1 < \mathbb{T}_r^{\text{announce}} \leq t\}$ is the set of requests received during time interval $(t-1, t]$, $t > 0$; $\bar{R}^t$ is the set of accepted requests that require reoptimization at decision epoch t due to infeasible transshipments. An infeasible transshipment happens in two situations: first, the accepted shipment r just arrived terminal i, the matched service $s \in \{S^{+1} \cup \ldots \cup S^{+t} | x_{rs} = 1, o_s = i\}$ has already departed; second, the accepted shipment r has already arrived terminal i, and the matched service $s \in \{S^{+t} | x_{rs} = 1, o_s = i\}$ just departed from terminal i, but the remaining time is not enough for transshipments.
- **Decision variables**. At decision epoch t, the platform needs to decide on acceptance y^t for requests R^t and matching x^t for requests $R^t \cup \bar{R}^t$. The decisions are restricted by the time-spatial compatibility between requests and services, and free capacities of services at decision epoch t. Let y_r^t be the binary variable which is 1 if request $r \in R^t$ is accepted, 0 otherwise. We use the binary variable x_{rs}^t to represent the match between request $r \in R^t \cup \bar{R}^t$ and service $s \in S$. The decision vectors y^t, x^t consist of all the decisions at decision epoch t as seen in (6.1-6.2), subject to constraints (6.3-6.21), which define the feasible decision space.

$$y^t = \left[y_r^t\right]_{\forall r \in R^t} \tag{6.1}$$

$$x^t = \left[x_{rs}^t\right]_{\forall r \in R^t \cup \bar{R}^t, s \in S} \tag{6.2}$$

subject to

$$y_r^t \leq \sum_{s \in S_{or}^+} x_{rs}^t, \quad \forall r \in R^t, \tag{6.3}$$

$$y_r^t \leq \sum_{s \in S_{dr}^-} x_{rs}^t, \quad \forall r \in R^t, \tag{6.4}$$

$$\sum_{s \in S_{or}^+} x_{rs}^t \leq 1, \quad \forall r \in R^t, \tag{6.5}$$

$$\sum_{s \in S_{dr}^-} x_{rs}^t \leq 1, \quad \forall r \in R^t, \tag{6.6}$$

$$\sum_{s \in S_{or}^+} x_{rs}^t = 1, \quad \forall r \in \bar{R}^t, \tag{6.7}$$

$$\sum_{s \in S_{dr}^-} x_{rs}^t = 1, \quad \forall r \in \bar{R}^t, \tag{6.8}$$

$$\sum_{s\in S_{or}^{-}} x_{rs}^{t} \le 0, \quad \forall r \in R^{t} \cup \bar{R}^{t}, \tag{6.9}$$

$$\sum_{s\in S_{dr}^{+}} x_{rs}^{t} \le 0, \quad \forall r \in R^{t} \cup \bar{R}^{t}, \tag{6.10}$$

$$\sum_{s\in S_{i}^{-}} x_{rs}^{t} \le 1, \quad \forall r \in R^{t} \cup \bar{R}^{t}, i \in N\backslash\{o_r, d_r\}, \tag{6.11}$$

$$\sum_{s\in S_{i}^{+}} x_{rs}^{t} \le 1, \quad \forall r \in R^{t} \cup \bar{R}^{t}, i \in N\backslash\{o_r, d_r\}, \tag{6.12}$$

$$\sum_{s\in S_{i}^{+}} x_{rs}^{t} = \sum_{s\in S_{i}^{-}} x_{rs}^{t}, \quad \forall r \in R^{t} \cup \bar{R}^{t}, i \in N\backslash\{o_r, d_r\}, \tag{6.13}$$

$$\sum_{r\in R^{t}\cup\bar{R}^{t}} x_{rs}^{t} u_r \le U_s^{t}, \quad \forall s \in S, \tag{6.14}$$

$$\sum_{r\in R^{tk}\cup\bar{R}^{tk}} x_{rs}^{t} u_r \le U_s^{tk}, \quad \forall s \in S, k = \text{reefer}, \tag{6.15}$$

$$\mathbb{T}_r^{\text{release}} + lt_{o_r}^{MT_s} \le TD_{rs} + \mathbf{M}(1 - x_{rs}^{t}), \quad \forall r \in R^{t} \cup \bar{R}^{t}, s \in S_{o_r}^{+\text{truck}}, \tag{6.16}$$

$$\mathbb{T}_r^{\text{release}} + lt_{o_r}^{MT_s} \le \tilde{T}D_s + \mathbf{M}(1 - x_{rs}^{t}), \quad \forall r \in R^{t} \cup \bar{R}^{t}, s \in S_{o_r}^{+}\backslash S_{o_r}^{+\text{truck}}, \tag{6.17}$$

$$\begin{aligned}\tilde{T}A_s + lt_i^{MT_s} + lt_i^{MT_q} \le \tilde{T}D_q + \mathbf{M}(1 - x_{rs}^{t}) + \mathbf{M}(1 - x_{rq}^{t}), \quad \forall r \in R^{t} \cup \bar{R}^{t}, \\ i \in N\backslash\{o_r, d_r\}, s \in S_i^{-}\backslash S_i^{-\text{truck}}, q \in S_i^{+}\backslash S_i^{+\text{truck}},\end{aligned} \tag{6.18}$$

$$\begin{aligned}TD_{rs} + \tilde{t}_s + lt_i^{MT_s} + lt_i^{MT_q} \le \tilde{T}D_q + \mathbf{M}(1 - x_{rs}^{t}) + \mathbf{M}(1 - x_{rq}^{t}), \quad \forall r \in R^{t} \cup \bar{R}^{t}, \\ i \in N\backslash\{o_r, d_r\}, s \in S_i^{-\text{truck}}, q \in S_i^{+}\backslash S_i^{+\text{truck}},\end{aligned} \tag{6.19}$$

$$\begin{aligned}\tilde{T}A_s + lt_i^{MT_s} + lt_i^{MT_q} \le TD_{rq} + \mathbf{M}(1 - x_{rs}^{t}) + \mathbf{M}(1 - x_{rq}^{t}), \quad \forall r \in R^{t} \cup \bar{R}^{t}, \\ i \in N\backslash\{o_r, d_r\}, s \in S_i^{-}\backslash S_i^{-\text{truck}}, q \in S_i^{+\text{truck}},\end{aligned} \tag{6.20}$$

$$\begin{aligned}TD_{rs} + \tilde{t}_s + lt_i^{MT_s} + lt_i^{MT_q} \le TD_{rq} + \mathbf{M}(1 - x_{rs}^{t}) + \mathbf{M}(1 - x_{rq}^{t}), \quad \forall r \in R^{t} \cup \bar{R}^{t}, \\ i \in N\backslash\{o_r, d_r\}, s \in S_i^{-\text{truck}}, q \in S_i^{+\text{truck}}.\end{aligned} \tag{6.21}$$

Constraints (6.3-6.4) ensure that new request $r \in R^t$ will not be accepted by the platform if there is no matching possibilities. Constraints (6.5-6.6) ensure that at most one service transports new request $r \in R^t$ departing from its origin or arriving to its destination. Constraints (6.7-6.8) ensure that reoptimization request $r \in \bar{R}^t$ must be transported by one service departing from its origin and by one service arriving to its destination. Constraints (6.9-6.12) are designed to eliminate subtours. Constraints (6.13) ensure flow conservation. Constraints (6.14) ensure that the total container volumes of requests matched with service s do not exceed its free capacity. Constraints (6.15) ensure that the total volumes of reefer containers matched with service s cannot exceed its free capacity on reefer slots. In practice, dry containers can use reefer slots, but reefer containers cannot use dry slots. Constraints (6.16-6.17) ensure that the departure time of service s minus loading time must be earlier than the release time of request r, if request r will be transported by service s depart its origin terminal. Here, $\mathbf{M}$ is a large number used for binary constraints. Constraints (6.18-6.21) ensure that the arrival time of service $s \in S_i^-$ plus loading and unloading time must be earlier than the departure time of service $q \in S_i^+$ if request r will be transported by service s entering terminal i and by service q leaving terminal i.

- **Transition function**. Following decision x^t from state $\mathbf{F}^t$ with exogenous information $\mathbf{W}^t$, the system transitions to a new state. We denote the transition function by $\mathbf{F}^{t+1} = f(\mathbf{F}^t, \mathbf{W}^t, x^t)$. Specifically, the free capacity of service $s \in S$ at stage $t+1$ is decided by the free capacity of service s at decision epoch t, the cancellation of bookings from reoptimization requests $\bar{R}^t$ which includes service s in its planned itinerary IR_r, and the matching decisions made for requests $R^t \cup \bar{R}^t$, as shown in (6.22-6.23).

$$U_s^{t+1} = U_s^t + \sum_{r \in \bar{R}^t, s \in IR_r} u_r - \sum_{r \in R^t \cup \bar{R}^t} u_r x_{rs}^t, \quad \forall s \in \{S | TD_s > t\}, \tag{6.22}$$

$$U_s^{(t+1)k} = U_s^{tk} + \sum_{r \in \bar{R}^{tk}, s \in IR_r} u_r - \sum_{r \in R^{tk} \cup \bar{R}^{tk}} u_r x_{rs}^t, \quad \forall s \in \{S | TD_s > t\}, k = \text{reefer}. \tag{6.23}$$

- **Profits**. Based on the state $\mathbf{F}^t$, the exogenous information $\mathbf{W}^t$, and the decision $[y^t, x^t]$, the profits at decision epoch t can be defined as a function of $\mathbf{F}^t$, $\mathbf{W}^t$ and $[y^t, x^t]$, as shown in (6.24). Due to the time gap between the acceptance and the transportation of the same request, while the freight rate of request $r \in R^t$ is charged by the platform at current time stage, the cost for request r happens in future time stages. Due to the possibility of infeasible transshipments, the actual costs generated by accepted requests are also uncertain and hard to estimate. We use $\tilde{\mathbf{C}}_r(\mathbf{F}^t, \mathbf{W}^t, [y^t, x^t])$ to denote the total costs generated for request $r \in R^t$.

$$\mathbf{P}^t(\mathbf{F}^t, \mathbf{W}^t, \left[y^t, x^t\right]) = \sum_{r \in R^t} p_r u_r y_r^t - \sum_{r \in R^t} \tilde{\mathbf{C}}_r(\mathbf{F}^t, \mathbf{W}^t, \left[y^t, x^t\right]). \tag{6.24}$$

- **Objective functions**. Due to future request uncertainty and the capacity limitation of transport services, decisions made for current requests affect the decisions for future requests. Therefore, the objective of the MDP model is to maximize the expected profits over the planning horizon given as follows:

$$\max_{y^{1\ldots T}, x^{0\ldots T}} \mathbb{E}_{\mathbf{F}^0} \mathbb{E}_{\mathbf{W}^1, \ldots, \mathbf{W}^T | \mathbf{F}^0} \{ \sum_{t=0}^{T} \mathbf{P}^t(\mathbf{F}^t, \mathbf{W}^t, \left[y^t, x^t\right]) | \mathbf{F}^0 \} \tag{6.25}$$

We refer to the objective function in (6.25) as the cumulative formulation. Using Bellman's principle of optimality, the optimal profits can be computed through a set of recursive equations, as seen in (6.26).

$$\begin{aligned} \textbf{P0} \quad Q^t(\mathbf{F}^t, \mathbf{W}^t, \left[y^t, x^t\right]) = & \max_{y^t, x^t} \sum_{r \in R^t} p_r u_r y_r^t \\ & - \sum_{r \in R^t} \mathbb{E}\{\tilde{\mathbf{C}}_r(\mathbf{F}^t, \mathbf{W}^t, \left[y^t, x^t\right])\} \\ & + \mathbb{E}_{\Omega^t}\{Q^{t+1}(\mathbf{F}^{t+1}, \mathbf{W}^{t+1}, \left[y^{t+1}, x^{t+1}\right])\}, \end{aligned} \tag{6.26}$$

where $\mathbb{E}\{\tilde{C}_r\}$ represents the expected total costs generated for request r, $\mathbb{E}_{\Omega^t}$ represents the expected total profits for requests received after decision epoch t, Ω^t represents the set of requests received after t.

6.5 Hybrid stochastic approach

The recursive formulation (6.26) requires enumerating all states, exogenous information, and decisions in the future time stages which are known as the three curses of dimensionality [70]. In this section, we develop a hybrid stochastic approach (HSA) to solve the DSGSM problem. Specially, we design a rolling horizon framework (RHF) to update input parameters and to react to infeasible transshipments; we design a chance-constrained programming (CCP) model to set confidence level of chance constraints regarding infeasible transshipments, and define the approximation of $\mathbb{E}\{\tilde{C}_r\}$; we use a sample average approximation (SAA) method to approximate $\mathbb{E}_{\Omega^t}$ by sampling requests appeared in prediction horizon H under Γ scenarios. After that, due to the computational complexity, we design a preprocessing-based heuristic algorithm (P-HA) to solve the optimization problem at each decision epoch.

6.5.1 Rolling horizon framework

RHF is known as an efficient periodic reoptimization approach that has been applied in many fields, such as routing problems [6] and scheduling problems [84]. The RHF can handle multiple dynamic events that appear in a system simultaneously, which is quite common in global synchromodal transport. The RHF solves the DSGSM problem iteratively by updating the input parameters and reacting to infeasible transshipments at each decision epoch as given by Algorithm 6.1. At decision epoch $t \in \{0,...,T\}$, the RHA updates the new information received during time interval $(t-1,t]$, including requests R^t, actual departure times $[\bar{T}D_s]_{\forall s \in S^{+t} \setminus S^{\text{truck}}}$ and arrival times $[\bar{T}A_s]_{\forall s \in S^{-t} \setminus S^{\text{truck}}}$ of ship, barge, and train services, and actual departure times $[\bar{T}D_{rs}]_{\forall s \in S^{+t} \cap S^{\text{truck}}}$ and arrival times $[\bar{T}A_{rs}]_{\forall s \in S^{-t} \cap S^{\text{truck}}}$ of truck services. Based on the actual arrival and departure times of matched services $\{s \in S | x_{rs} = 1\}$ of accepted request $r \in \{R^0 \cup ... \cup R^{t-1} | y_r = 1\}$, the RHA checks which requests need reoptimization due to infeasible transshipments. The platform thus cancels the capacity bookings on the matched services which depart after decision epoch t for reoptimization request $r \in \bar{R}^t$. The RHA then updates the free capacity regarding dry and reefer slots of these services. After that, the RHA generates sample requests based on Monte Carlo Simulation. The optimization model that used in each iteration is developed based on the CCP (presented in Section 6.5.2) and SAA (presented in Section 6.5.3). The RHA uses the P-HA (presented in Section 6.5.4) to generate acceptance and matching decisions based on the input parameters and the optimization model. The platform thus books capacities on the matched services based on the matching decisions. After that, the RHA updates free capacities of services and itineraries of requests, and calculates the planning profits $\mathbf{P}^t$ based on transport plans and actual profits $\mathbf{AP}^t$ caused in transport processes. At the end of the planning horizon, the RHA calculates the total planned profit and the total actual profit generated over planning horizon T.

6.5.2 Chance-constrained programming model

In the literature, different techniques have been developed to deal with travel time uncertainty: deterministic, stochastic, and robust programming [80]. While deterministic programming considers average travel times and robust programming considers minimum and maximum travel times, stochastic programming takes into account the probability distribu-

Algorithm 6.1 Rolling horizon framework.

Input: Terminals N; contractual requests R^0; services S; free capacity $\left[U_s^{0k}\right]_{\forall s\in S,k\in K}$; length of planning horizon T; probability distributions of spot requests and travel times; confidence level α; length of prediction horizon H, and number of scenarios Γ.

Output: Acceptance decision $[y_r^t]_{\forall r\in R^t,t\in\{1,\ldots,T\}}$; matching decision $[x_{rs}^t]_{\forall r\in R^t\cup\bar{R}^t,s\in S,t\in\{0,\ldots,T\}}$; itinerary $\{IR_r\}_{r\in R}$; number of infeasible transshipments $N^{\text{infeasible}}$; planned profits $[\mathbf{P}^t]_{t\in\{0,\ldots,T\}}$; actual profits $\left[\mathbf{AP}^t\right]_{t\in\{0,\ldots,T\}}$.

Initialize: Let $R^t\leftarrow\emptyset$, $\bar{R}^t\leftarrow\emptyset$, $U_s^t\leftarrow 0$, $IR_r\leftarrow\emptyset$, $N^{\text{infeasible}}\leftarrow 0$, $\mathbf{P}^t\leftarrow 0$, $\mathbf{AP}^t\leftarrow 0$.

for decision epoch $t\in\{0,1,\ldots,T\}$ **do**
  receive requests R^t, actual departure time $\bar{T}D_s$ of service $s\in S^{+t}\backslash S^{\text{truck}}$, actual arrival time $\bar{T}A_s$ of service $s\in S^{-t}\backslash S^{\text{truck}}$, actual departure time $\bar{T}D_{rs}$ of service $s\in S^{+t}\cap S^{\text{truck}}$, and actual arrival time $\bar{T}A_{rs}$ of service $s\in S^{-t}\cap S^{\text{truck}}$
  for request $r\in R^0\cup\ldots\cup R^{t-1}$ **do**
    if $IR_r=\emptyset$ **then**
      go to $r=r+1$
    else
      for terminal $i\in N$ **do**
        if request r just arrived terminal i, service $s\in\{S^{+1}\cup\ldots\cup S^{+t}|o_s=i\}$ has already departed; or request r has already arrived terminal i, service $s\in\{S^{+t}|o_s=i\}$ just departed, but the time for transshipment operations is not enough **then**
          update reoptimization requests $\bar{R}^t\leftarrow\bar{R}^t\cup\{r\}$
          update number of infeasible transshipments $N^{\text{infeasible}}\leftarrow N^{\text{infeasible}}+1$
          update free capacity $U_s^t\leftarrow U_s^t+u_r$ for $s\in\{IR_r|TD_s>t\}$
          if $CT_r=$ reefer **then**
            update free capacity $U_s^{tk}\leftarrow U_s^{tk}+u_r$ for $s\in\{IR_r|TD_s>t\},k=$ reefer
  generate sample requests $\leftarrow$ *Monte Carlo Simulation*
  get optimization model $\leftarrow$ ***CCP+SAA***
  obtain acceptance and matching decision $[y^t,x^t]\leftarrow$ ***P-HA***
  update free capacity $U_s^{t+1}\leftarrow U_s^t-\sum_{r\in R^t\cup\bar{R}^t}u_rx_{rs}^t$ for $s\in S$
  update free capacity $U_s^{(t+1)k}\leftarrow U_s^{tk}-\sum_{r\in R^{tk}\cup\bar{R}^{tk}}u_rx_{rs}^t$ for $s\in S,k=$ reefer
  update itinerary $\{IR_r\}$ for $r\in R$
  calculate planned profits $\mathbf{P}^t$ and actual profits $\mathbf{AP}^t$
calculate total planned profit and actual profit in planning horizon T

tions of travel times. In general, stochastic programming can be either formulated as a CCP model or a stochastic programming model with recourse (SPR) [51]. While CCP models ensure the feasibility of stochastic constraints, SPR models define recourse actions to induce an expected penalty cost on objective functions. Typically, SPR models define a delay cost for late delivery, a storage cost for early delivery, and a large penalty cost for infeasible transshipments without the consideration of reoptimization after disturbances. Since the extra costs caused by reoptimization procedures at later stages are hard to estimate, we develop a CCP model to approximate stochastic constraints (6.17-6.21) and to approximate the expected cost $\mathbb{E}\{\bar{C}_r\}$ for request r in model **P0**. The CCP model does not take into account the correction costs caused by the reoptimization of requests.

Under CCP, stochastic constraints (6.17-6.21) will hold at least with probability α, where α is referred to as the confidence level provided as an approximate safety margin by the platform. A high α means the matches have a low probability causing infeasible

transshipments. The confidence level α also controls the problems' tightness and computational complexity. When $\alpha = 0.5$, the CCP model becomes a deterministic model; when $\alpha = 1$, the CCP model becomes a robust model. The objective is to maximize expected total profits while ensuring that the probability of feasible transshipments exceed α. The formulation of the CCP model at decision epoch t is:

$$\begin{aligned}\textbf{P1}\ \ Q^t(\mathbf{F}^t,\mathbf{W}^t,[y^t,x^t]) = \max_{y^t,x^t} & \sum_{r\in R^t} p_r u_r y_r^t - \Bigg(\sum_{r\in R^t\cup\bar{R}^t}\sum_{s\in S} c_s x_{rs}^t u_r + \sum_{r\in R^t\cup\bar{R}^t}\sum_{i\in N} f_{ri}u_r \\ & + \sum_{r\in R^t\cup\bar{R}^t}\sum_{i\in N} c_i^{\text{storage}}\mathbb{E}(\tilde{w}_{ri})u_r + \sum_{r\in R^t\cup\bar{R}^t} c_r^{\text{delay}}\mathbb{E}(\tilde{\mathbb{T}}_r^{\text{delay}})u_r \\ & + \sum_{k\in K}\sum_{r\in R^{tk}\cup\bar{R}^{tk}}\sum_{s\in S} c^{\text{emission}} e_s^k x_{rs}^t u_r \Bigg) \\ & + E_{\Omega^t}\left[Q^{t+1}(\mathbf{F}^{t+1},\mathbf{W}^{t+1},[y^{t+1},x^{t+1}])\right].\end{aligned} \tag{6.27}$$

subject to constraints (6.3-6.16),

$$\mathrm{P}\{\mathbb{T}_r^{\text{release}} + lt_{o_r}^{MT_s} \le \tilde{T}D_s + \mathbf{M}(1-x_{rs}^t)\} \ge \alpha, \forall r\in R^t\cup\bar{R}^t, s\in S_{o_r}^+\backslash S_{o_r}^{+\text{truck}}, \tag{6.28}$$

$$\begin{aligned}\mathrm{P}\{\tilde{T}A_s + lt_i^{MT_s} + lt_i^{MT_q} \le \tilde{T}D_q + \mathbf{M}(1-x_{rs}^t) + \mathbf{M}(1-x_{rq}^t)\} \ge \alpha, \\ \forall r\in R^t\cup\bar{R}^t, i\in N\backslash\{o_r,d_r\}, s\in S_i^-\backslash S_i^{-\text{truck}}, q\in S_i^+\backslash S_i^{+\text{truck}},\end{aligned} \tag{6.29}$$

$$\begin{aligned}\mathrm{P}\{TD_{rs} + \tilde{t}_s + lt_i^{MT_s} + lt_i^{MT_q} \le \tilde{T}D_q + \mathbf{M}(1-x_{rs}^t) + \mathbf{M}(1-x_{rq}^t)\} \ge \alpha, \\ \forall r\in R^t\cup\bar{R}^t, i\in N\backslash\{o_r,d_r\}, s\in S_i^{-\text{truck}}, q\in S_i^+\backslash S_i^{+\text{truck}},\end{aligned} \tag{6.30}$$

$$\begin{aligned}\mathrm{P}\{\tilde{T}A_s + lt_i^{MT_s} + lt_i^{MT_q} \le TD_{rq} + \mathbf{M}(1-x_{rs}^t) + \mathbf{M}(1-x_{rq}^t)\} \ge \alpha, \\ \forall r\in R^t\cup\bar{R}^t, i\in N\backslash\{o_r,d_r\}, s\in S_i^-\backslash S_i^{-\text{truck}}, q\in S_i^{+\text{truck}},\end{aligned} \tag{6.31}$$

$$\begin{aligned}\mathrm{P}\{TD_{rs} + \tilde{t}_s + lt_i^{MT_s} + lt_i^{MT_q} \le TD_{rq} + \mathbf{M}(1-x_{rs}^t) + \mathbf{M}(1-x_{rq}^t)\} \ge \alpha, \\ \forall r\in R^t\cup\bar{R}^t, i\in N\backslash\{o_r,d_r\}, s\in S_i^{-\text{truck}}, q\in S_i^{+\text{truck}},\end{aligned} \tag{6.32}$$

$$f_{ri} = \sum_{s\in S_i^+} x_{rs}^t lc_i^{MT_s}, \quad \forall r\in R^t\cup\bar{R}^t, i=o_r, \tag{6.33}$$

$$f_{ri} = \sum_{s\in S_i^-} x_{rs}^t lc_i^{MT_s}, \quad \forall r\in R^t\cup\bar{R}^t, i=d_r, \tag{6.34}$$

$$f_{ri} = \sum_{s\in S_i^+}\sum_{q\in S_i^-}\left(lc_i^{MT_s} + lc_i^{MT_q}\right) z_{rsq}^t l_{sq}, \quad \forall r\in R^t\cup\bar{R}^t, i\in N\backslash\{o_r,d_r\}, \tag{6.35}$$

$$z_{rsq}^t \le x_{rs}^t, \quad \forall r\in R^t\cup\bar{R}^t, s\in S, q\in S, \tag{6.36}$$

$$z_{rsq}^t \le x_{rq}^t, \quad \forall r\in R^t\cup\bar{R}^t, s\in S, q\in S, \tag{6.37}$$

$$z_{rsq}^t \ge x_{rs}^t + x_{rq}^t - 1, \quad \forall r\in R^t\cup\bar{R}^t, s\in S, q\in S, \tag{6.38}$$

$$\mathbb{E}(\tilde{w}_{ro_r}) \ge \mathbb{E}(\tilde{T}D_s) - lt_{o_r}^{MT_s} - \mathbb{T}_r^{\text{release}} + \mathbf{M}(x_{rs}^t - 1),\ \forall r\in R^t\cup\bar{R}^t, s\in S_{o_r}^+\backslash S_{o_r}^{+\text{truck}}, \tag{6.39}$$

$$\mathbb{E}(\tilde{w}_{ro_r}) \ge TD_{rs} - lt_{o_r}^{MT_s} - \mathbb{T}_r^{\text{release}} + \mathbf{M}(x_{rs}^t - 1),\ \forall r\in R^t\cup\bar{R}^t, s\in S_{o_r}^{+\text{truck}}, \tag{6.40}$$

$$\mathbb{E}(\tilde{w}_{ri}) \geq \mathbb{E}(\tilde{T}D_q) - \mathbb{E}(\tilde{T}A_s) - lt_i^{MT_s} - lt_i^{MT_q} + \mathbf{M}(x_{rs}^t - 1) + \mathbf{M}(x_{rq}^t - 1), \quad \forall r \in R^t \cup \bar{R}^t, i \in N \backslash \{o_r, d_r\}, s \in S_i^- \backslash S_i^{-\text{truck}}, q \in S_i^+ \backslash S_i^{+\text{truck}}, \tag{6.41}$$

$$\mathbb{E}(\tilde{w}_{ri}) \geq \mathbb{E}(\tilde{T}D_q) - TD_{rs} - \mathbb{E}(\tilde{t}_s) - lt_i^{MT_s} - lt_i^{MT_q} + \mathbf{M}(x_{rs}^t - 1) + \mathbf{M}(x_{rq}^t - 1), \quad \forall r \in R^t \cup \bar{R}^t, i \in N \backslash \{o_r, d_r\}, s \in S_i^{-\text{truck}}, q \in S_i^+ \backslash S_i^{+\text{truck}}, \tag{6.42}$$

$$\mathbb{E}(\tilde{w}_{ri}) \geq TD_{rq} - \mathbb{E}(\tilde{T}A_s) - lt_i^{MT_s} - lt_i^{MT_q} + \mathbf{M}(x_{rs}^t - 1) + \mathbf{M}(x_{rq}^t - 1), \quad \forall r \in R^t \cup \bar{R}^t, i \in N \backslash \{o_r, d_r\}, s \in S_i^- \backslash S_i^{-\text{truck}}, q \in S_i^{+\text{truck}}, \tag{6.43}$$

$$\mathbb{E}(\tilde{w}_{ri}) \geq TD_{rq} - TD_{rs} - \mathbb{E}(\tilde{t}_s) - lt_i^{MT_s} - lt_i^{MT_q} + \mathbf{M}(x_{rs}^t - 1) + \mathbf{M}(x_{rq}^t - 1), \quad \forall r \in R^t \cup \bar{R}^t, i \in N \backslash \{o_r, d_r\}, s \in S_i^{-\text{truck}}, q \in S_i^{+\text{truck}}, \tag{6.44}$$

$$\mathbb{E}(\tilde{w}_{rd_r}) \geq \mathbb{T}_r^{\text{due}} - \mathbb{E}(\tilde{T}A_s) - lt_{d_r}^{MT_s} + \mathbf{M}(x_{rs}^t - 1), \ \forall r \in R^t \cup \bar{R}^t, s \in S_{d_r}^- \backslash S_{d_r}^{-\text{truck}}, \tag{6.45}$$

$$\mathbb{E}(\tilde{w}_{rd_r}) \geq \mathbb{T}_r^{\text{due}} - TD_{rs} - \mathbb{E}(\tilde{t}_s) - lt_{d_r}^{MT_s} + \mathbf{M}(x_{rs}^t - 1), \ \forall r \in R^t \cup \bar{R}^t, s \in S_{d_r}^{-\text{truck}}, \tag{6.46}$$

$$\mathbb{E}(\tilde{\mathbb{T}}_r^{\text{delay}}) \geq \mathbb{E}(\tilde{T}A_s) + lt_{d_r}^{MT_s} - \mathbb{T}_r^{\text{due}} + \mathbf{M}(x_{rs}^t - 1), \ \forall r \in R^t \cup \bar{R}^t, s \in S_{d_r}^- \backslash S_{d_r}^{-\text{truck}}, \tag{6.47}$$

$$\mathbb{E}(\tilde{\mathbb{T}}_r^{\text{delay}}) \geq TD_{rs} + \mathbb{E}(\tilde{t}_s) + lt_{d_r}^{MT_s} - \mathbb{T}_r^{\text{due}} + \mathbf{M}(x_{rs}^t - 1), \ \forall r \in R^t \cup \bar{R}^t, s \in S_{d_r}^{-\text{truck}}, \tag{6.48}$$

where f_{ri} is the planned loading and unloading cost of request r at terminal i; $\mathbb{E}(\tilde{w}_{ri})$ is the estimated storage time of request r at terminal i; $\mathbb{E}(\tilde{\mathbb{T}}_r^{\text{delay}})$ is the estimated delay in delivery of request r at destination terminal d_r; P is the probability measure; z_{rsq}^t is a binary variable which equals to 1 if request r has to transfer between service s and q, 0 otherwise; $\mathbb{E}(\tilde{T}D_s) = \mu_s^+$, $\mathbb{E}(\tilde{T}A_s) = \mu_s^-$, $\mathbb{E}(\tilde{t}_s) = \mu_s$.

The objective function **P1** is to maximize the total profits which consist of the planned profits at decision epoch t including freight rates, travel costs, transfer costs, storage costs, delay costs and carbon tax, and estimated profits generated after decision epoch t. Constraints (6.28-6.32) ensure that the possibility of feasible transshipment at terminals will be higher than the confidence level α. Constraints (6.33-6.35) calculate the loading costs at origin terminals, the unloading costs at destination terminals, and the loading and unloading costs at transshipment terminals. Constraints (6.36-6.38) ensure that binary variable z_{rsq}^t equals to 1 if $x_{rs}^t = 1$ and $x_{rq}^t = 1$, 0 otherwise. Constraints (6.39-6.46) calculate the storage time at origin, transshipment, and destination terminals. Constraints (6.47-6.48) calculate delay in deliveries at destination terminals. Based on the properties of normal distributions, constraints (6.28-6.32) can be linearized as:

$$\frac{\mathbb{T}_r^{\text{release}} + lt_{o_r}^{MT_s} + \mathbf{M}(x_{rs}^t - 1) - \mu_s^+}{\sigma_s^+} \leq \phi^{-1}(1-\alpha), \forall r \in R^t \cup \bar{R}^t, s \in S_{o_r}^+ \backslash S_{o_r}^{+\text{truck}}, \tag{6.49}$$

$$\frac{lt_i^{MT_s} + lt_i^{MT_q} + \mathbf{M}(x_{rs}^t - 1) + \mathbf{M}(x_{rq}^t - 1) - (\mu_q^+ - \mu_s^-)}{\sqrt{(\sigma_q^+)^2 + (\sigma_s^-)^2}} \leq \phi^{-1}(1-\alpha), \quad \forall r \in R^t \cup \bar{R}^t, i \in N \backslash \{o_r, d_r\}, s \in S_i^- \backslash S_i^{-\text{truck}}, q \in S_i^+ \backslash S_i^{+\text{truck}}, \tag{6.50}$$

$$\frac{TD_{rs} + lt_i^{MT_s} + lt_i^{MT_q} + \mathbf{M}(x_{rs}^t - 1) + \mathbf{M}(x_{rq}^t - 1) - (\mu_q^+ - \mu_s)}{\sqrt{(\sigma_q^+)^2 + (\sigma_s)^2}} \leq \phi^{-1}(1-\alpha), \quad \forall r \in R^t \cup \bar{R}^t, i \in N \backslash \{o_r, d_r\}, s \in S_i^{-\text{truck}}, q \in S_i^+ \backslash S_i^{+\text{truck}}, \tag{6.51}$$

$$\frac{TD_{rq} - lt_i^{MT_s} - lt_i^{MT_q} + \mathbf{M}(1-x_{rs}^t) + \mathbf{M}(1-x_{rq}^t) - \mu_s^-}{\sigma_s^-} \geq \phi^{-1}(\alpha), \quad \forall r \in R^t \cup \bar{R}^t, i \in N \backslash \{o_r, d_r\}, s \in S_i^- \backslash S_i^{-\text{truck}}, q \in S_i^{+\text{truck}}, \tag{6.52}$$

$$\frac{TD_{rq} - TD_{rs} - lt_i^{MT_s} - lt_i^{MT_q} + \mathbf{M}(1-x_{rs}^t) + \mathbf{M}(1-x_{rq}^t) - \mu_s}{\sigma_s} \geq \phi^{-1}(\alpha), \quad \forall r \in R^t \cup \bar{R}^t, i \in N \backslash \{o_r, d_r\}, s \in S_i^{-\text{truck}}, q \in S_i^{+\text{truck}}, \tag{6.53}$$

where $\phi^{-1}(\alpha)$ is the inverse function of standardized normal distributions.

6.5.3 Sample average approximation method

In this section, we present the SAA method that approximates the expected profits E_{Ω_t} generated after decision epoch t in model **P1**. At decision epoch t, a sample $\{\omega^1, ..., \omega^\gamma, ..., \omega^\Gamma\}$ of Γ scenarios is generated according to the probability distributions of shipment requests $\{\pi_{CT}, \pi_o, \pi_d, \pi_u, \pi_{\mathbb{T}^{\text{announce}}}, \pi_{\mathbb{T}^{\text{release}}}, \pi_{\mathbb{T}^{\text{due}}}, \pi_p, \pi_{c^{\text{delay}}}\}$. Each scenario includes a prediction of spot requests arrived between stage $t+1$ and stage $t+H$, $\omega^\gamma = \{\omega^{\gamma(t+1)}, \omega^{\gamma(t+2)}, ..., \omega^{\gamma(t+H)}\}$. Here, H is the prediction horizon that is just long enough to obtain good decisions at decision epoch t. The expected cost E_{Ω^t} in (6.27) is approximated by the sample average function $\Gamma^{-1}\sum_{\gamma=1}^{\Gamma}$. Let $\hat{y}_r^{\gamma h}$ be the binary variable which equals to 1 if sample request $r \in \omega^{\gamma h}$ is accepted, and $\hat{x}_{rs}^{\gamma h}$ be the binary variable which equals to 1 if sample request $r \in \omega^{\gamma h}$ is matched with service $s \in S$ under scenario $\gamma \in \{1, .., \Gamma\}$ at stage $h \in \mathbb{H} = \{t+1, ..., \max\{T, t+H\}\}$. We define $\hat{f}_{ri}$ as the loading and unloading cost and $\hat{\mathbb{E}}(\tilde{w}_{ri})$ as the waiting time of sample request $r \in \omega^{\gamma h}$ at terminal i, $\hat{\mathbb{E}}(\tilde{\mathbb{T}}_r^{\text{delay}})$ as the delay in delivery of sample request r. The formulation of the DSGSM problem at decision epoch t changes to:

$$\begin{aligned}
\textbf{P2}\quad Q^t(\mathbf{F}^t, \mathbf{W}^t, [y^t, x^t]) = \max_{y^t, x^t, \hat{y}^t, \hat{x}^t} & \sum_{r \in R^t} p_r u_r y_r^t - \Bigg(\sum_{r \in R^t \cup \bar{R}^t} \sum_{s \in S} c_s x_{rs}^t u_r \\
& + \sum_{r \in R^t \cup \bar{R}^t} \sum_{i \in N} f_{ri} u_r + \sum_{r \in R^t \cup \bar{R}^t} \sum_{i \in N} c_i^{\text{storage}} \mathbb{E}(\tilde{w}_{ri}) u_r \\
& + \sum_{r \in R^t \cup \bar{R}^t} c_r^{\text{delay}} \mathbb{E}(\tilde{\mathbb{T}}_r^{\text{delay}}) u_r \\
& + \sum_{k \in K} \sum_{r \in R^{tk} \cup \bar{R}^{tk}} \sum_{s \in S} c^{\text{emission}} e_s^k x_{rs}^t u_r \Bigg) \\
& + \frac{1}{\Gamma} \sum_{\gamma=1}^{\Gamma} \sum_{h \in \mathbb{H}} \Bigg[\sum_{r \in \omega^{\gamma h}} p_r u_r \hat{y}_r^{\gamma h} - \Bigg(\sum_{r \in \omega^{\gamma h}} \sum_{s \in S} c_s \hat{x}_{rs}^{\gamma h} u_r \\
& + \sum_{r \in \omega^{\gamma h}} \sum_{i \in N} \hat{f}_{ri} u_r + \sum_{r \in \omega^{\gamma h}} \sum_{i \in N} c_i^{\text{storage}} \hat{\mathbb{E}}(\tilde{w}_{ri}) u_r \\
& + \sum_{r \in \omega^{\gamma h}} c_r^{\text{delay}} \hat{\mathbb{E}}(\tilde{\mathbb{T}}_r^{\text{delay}}) u_r \\
& + \sum_{k \in K} \sum_{r \in \omega^{\gamma h k}} \sum_{s \in S} c^{\text{emission}} e_s^k \hat{x}_{rs}^{\gamma h} u_r \Bigg) \Bigg]
\end{aligned} \tag{6.54}$$

subject to constraints (6.3-6.13,6.16,6.33-6.53) for $r \in R^t \cup \bar{R}^t \cup \omega^{\gamma h}, \gamma \in \{1,...,\Gamma\}, h \in \mathbb{H}$,

$$\sum_{r \in R^t \cup \bar{R}^t} x^t_{rs} u_r + \sum_{h \in \mathbb{H}} \sum_{r \in \omega^{\gamma h}} \hat{x}^{\gamma h}_{rs} u_r \leq U^t_s, \quad \forall s \in S, \gamma \in \{1,...,\Gamma\}, \tag{6.55}$$

$$\sum_{r \in R^{tk} \cup \bar{R}^{tk}} x^t_{rs} u_r + \sum_{h \in \mathbb{H}} \sum_{r \in \omega^{\gamma hk}} \hat{x}^{\gamma h}_{rs} u_r \leq U^{tk}_s, \quad \forall s \in S, k = \text{reefer}, \gamma \in \{1,...,\Gamma\}. \tag{6.56}$$

Constraints (6.55-6.56) ensure that the total container volumes of new requests, reoptimization requests, and sample requests matched with service s do not exceed its free capacity at decision epoch t.

6.5.4 Preprocessing-based heuristic algorithm

Due to the computational complexity, we design the P-HA to solve model **P2** at each decision epoch. The P-HA is adapted from the heuristic algorithm designed by Guo et al. [37] in which travel times are considered deterministic. The P-HA consists of three steps: preprocessing of feasible paths, preprocessing of feasible matches, and binary integer linear programming.

Preprocessing of feasible paths

We define a path p as a combination of services in sequence. A path p is feasible only if the services inside a combination satisfy time-spatial compatibility. Specifically, for two consecutive services s_i, s_{i+1} within path p, the destination of service s_i must be the same as the origin of service s_{i+1}; the arrival time of service s_i plus unloading time must be earlier than the departure time of service s_{i+1} minus loading time at transshipment terminal d_{s_i} with confidence level α. We define L as the largest number of services in a path. Let P denotes the set of feasible paths, and P^l_{ij} represents the set of feasible paths with l services that depart from terminal i, and arrive at terminal j.

The pseudocode of preprocessing of feasible paths is shown in Algorithm 6.2. The algorithm starts with determining the feasible paths for each OD pair with just one service, and subsequently combines these paths with a single service to create feasible paths with two services, three services, and so on. To examine whether a new path $[s_1,...,s_{l-1},s] \in P^l_{ij}$ consisting of feasible path $p = [s_1,...,s_{l-1}] \in P^{l-1}_{io_s}$ and service $s \in S^-_j$ is feasible, we check the transshipment feasibility between service s_{l-1} and service s by using constraints (6.50-6.53) with $x_{rs_{l-1}} = 1, x_{rs} = 1$. After that, we check whether feasible path $p \in P$ has subtours, and remove paths with subtours.

Preprocessing of feasible matches

A match between request $r \in R$ and path $p = [s_1,...,s_l] \in P$ is feasible if it satisfies time-spatial compatibility. Specifically, the origin terminal of shipment request r should be the same as the origin of service s_1; the destination of request r should be the same as the destination of service s_l. The release time of request r should be earlier than the departure time of service s_1 minus loading time at origin terminal o_r with confidence level α. We denote N^{match} as the maximum number of feasible matches. Let Φ_r be the set of feasible paths for request r, and c_{rp} be the total costs of matching request r with path p including travel costs, transfer costs, storage costs, delay costs, and carbon tax.

Algorithm 6.2 Feasible path generation algorithm.

Input: Terminals N, services S, the largest number of services in a path L, index $l \in \{1,2,...,L\}$.
Output: Feasible paths $\{P_{ij}^l\}_{i\in N, j\in N, l\in\{1,...,L\}}$.
Initialize: Let $P \leftarrow \emptyset, l \leftarrow 1$.

for terminal $i \in N$, terminal $j \in N$ **do**
  for service $s \in S$ **do**
    if origin $o_s = i$ and destination $d_s = j$ **then**
      $P_{ij}^l \leftarrow P_{ij}^l \cup \{[s]\}$
$l \leftarrow l+1$
while $l \leq L$ **do**
  for terminal $i \in N$, terminal $j \in N$ **do**
    for service $s \in S$ **do**
      if origin $o_s \neq i$ and destination $d_s = j$ **then**
        for feasible path $p = [s_1,...,s_{l-1}] \in P_{io_s}^{l-1}$ **do**
          if P{feasible transshipment between service s_{l-1} and s} $\geq \alpha$ **then**
            $P_{ij}^l \leftarrow P_{ij}^l \cup \{[s_1,...,s_{l-1},s]\}$
  $l \leftarrow l+1$
for terminal $i \in N$, terminal $j \in N$, index $l \in \{1,...,L\}$ **do**
  for path $p \in P_{ij}^l$ **do**
    for service $s \in p$ **do**
      if $d_s = i$ or $o_s = j$ **then**
        $P_{ij}^l \leftarrow P_{ij}^l \setminus \{p\}$
    for service $s \in p, q \in p$ **do**
      if $o_s = o_q$ **then**
        $P_{ij}^l \leftarrow P_{ij}^l \setminus \{p\}$

Algorithm 6.3 Feasible match generation algorithm.

Input: Feasible paths P, requests $R = R^t \cup \bar{R}^t \cup \{\omega^{\gamma h}\}_{\forall\gamma\in\{1,...,\Gamma\}, h\in\mathbb{H}}$, the largest number of services in a path L, the maximum number of feasible matches N^{match}, objective function (6.54).
Output: Feasible matches $\{\Phi_r\}_{\forall r\in R}$, total costs $\left[c_{rp}\right]_{\forall r\in R, p\in P}$.
Initialize: Let $\Phi \leftarrow \emptyset, l \leftarrow 1$.

for request $r \in R$ **do**
  for $l \in \{1,2,...,L\}$ **do**
    for feasible path $p = [s_1,s_2,...,s_l] \in P_{o_r d_r}^l$ **do**
      if P{feasible transshipment at origin terminal o_r} $\geq \alpha$ **then**
        $\Phi_r \leftarrow \Phi_r \cup \{p\}$
        $c_{rp} \leftarrow$ Calculate the objective function
  if the number of feasible matches in $\Phi_r > N^{\text{match}}$ **then**
    $\Phi_r \leftarrow$ the N^{match} cheapest matches in Φ_r

The pseudocode of preprocessing of feasible matches is shown in Algorithm 6.3. For request r and path $p = [s_1,...,s_l] \in P_{o_r d_r}^l$, the transshipment feasibility between r and p is checked by using constraints (6.16) and (6.49) with $x_{rs_1} = 1$. For each request r, if the number of feasible matches in Φ_r exceeds N^{match}, Φ_r will be replaced by the set of N^{match} cheapest matches.

Binary integer programming model

Based on the above preprocessing procedures, the objective function is updated to maximize the total profits for the matching of requests with feasible paths. Let z_{rp}^t be a binary variable equal to 1 if request $r \in R^t \cup \bar{R}^t$ is matched with path $p \in P$, and 0 otherwise. Let $\hat{z}_{rp}^{\gamma h}$ be the binary variable equal to 1 if request $r \in \omega^{\gamma h}, \gamma \in \{1,...,\Gamma\}, h \in \mathbb{H}$ is matched with path $p \in P$, and 0 otherwise. Model $P2$ will be translated into a binary integer programming (BIP) model:

$$\begin{aligned} \textbf{P3}\ \ Q^t(\mathbf{F}^t, \mathbf{W}^t, [y^t, z^t]) = \max_{y^t, z^t, \hat{y}^t, \hat{z}^t} & \sum_{r \in R^t} p_r u_r y_r^t - \sum_{r \in R^t \cup \bar{R}^t} \sum_{p \in \Phi_r} c_{rp} z_{rp}^t \\ & + \frac{1}{\Gamma} \sum_{\gamma=1}^{\Gamma} \sum_{h \in \mathbb{H}} \Big(\sum_{r \in \omega^{\gamma h}} p_r u_r \hat{y}_r^{\gamma h} - \sum_{r \in \omega^{\gamma h}} \sum_{p \in \Phi_r} c_{rp} \hat{z}_{rp}^{\gamma h} \Big) \end{aligned} \tag{6.57}$$

subject to

$$y_r^t \le \sum_{p \in \Phi_r} z_{rp}^t, \quad \forall r \in R^t, \tag{6.58}$$

$$\sum_{p \in \Phi_r} z_{rp}^t \le 1, \quad \forall r \in R^t, \tag{6.59}$$

$$\sum_{p \in \Phi_r} z_{rp}^t = 1, \quad \forall r \in \bar{R}^t, \tag{6.60}$$

$$\hat{y}_r^{\gamma h} \le \sum_{p \in \Phi_r} \hat{z}_{rp}^{\gamma h}, \quad \forall \gamma \in \{1,...,\Gamma\}, h \in \mathbb{H}, r \in \omega^{\gamma h}, \tag{6.61}$$

$$\sum_{p \in \Phi_r} \hat{z}_{rp}^{\gamma h} \le 1, \quad \forall \gamma \in \{1,...,\Gamma\}, h \in \mathbb{H}, r \in \omega^{\gamma h}, \tag{6.62}$$

$$\sum_{r \in R^t \cup \bar{R}^t} \sum_{p \in \Phi_{rs}} u_r z_{rp}^t + \sum_{h \in \mathbb{H}} \sum_{r \in \omega^{\gamma h}} \sum_{p \in \Phi_{rs}} u_r \hat{z}_{rp}^{\gamma h} \le U_s^t, \quad \forall \gamma \in \{1,...,\Gamma\}, s \in S, \tag{6.63}$$

$$\sum_{r \in R^{tk} \cup \bar{R}^{tk}} \sum_{p \in \Phi_{rs}} u_r z_{rp}^t + \sum_{h \in \mathbb{H}} \sum_{r \in \omega^{\gamma hk}} \sum_{p \in \Phi_{rs}} u_r \hat{z}_{rp}^{\gamma h} \le U_s^{tk}, \ \forall \gamma \in \{1,...,\Gamma\}, s \in S, k = \text{reefer}, \tag{6.64}$$

$$y_r^t, z_{rp}^t, \hat{y}_r^{\gamma h}, \hat{z}_{rp}^{\gamma h} \in \{0,1\}, \quad \forall \gamma \in \{1,...,\Gamma\}, h \in \mathbb{H}, r \in R^t \cup \bar{R}^t \cup \omega^{\gamma h}, p \in \Phi, \tag{6.65}$$

where $\Phi_{rs} = \{p \in \Phi_r | s \in p\}$.

Constraints (6.58-6.59) ensure that at most one feasible path will be assigned to each new request $r \in R^t$ if r is accepted. Constraints (6.60) ensure that one feasible path will be assigned to each reoptimization request $r \in \bar{R}^t$. Constraints (6.61-6.62) ensure that at most one feasible path will be assigned to each sample request $r \in \omega^{\gamma h}$ if r is accepted. Constraints (7.58-6.64) ensure that the total container volumes of requests assigned to service $s \in S$ does not exceed its free capacity regarding total slots and reefer slots.

6.6 Numerical experiments

In this section, we evaluate the performance of the HSA on the DSGSM problem in comparison to a deterministic approach (DA) which does not consider future requests and uses average travel times (i.e., $\alpha = 0.5,\ H = 0,\ \Gamma = 0$) and a robust approach (RA) which does

not consider future requests and considers the maximum and minimum travel times (i.e., $\alpha = 1,\ H = 0,\ \Gamma = 0$). The DA is a risk neutral approach in which decision makers are indifferent to uncertainties, and the RA is a risk averse approach that seeks sureness. The performance of the HSA will be tested under the impact of different confidence levels, numbers of scenarios, and lengths of the prediction horizon. The approaches are implemented in MATLAB, and all experiments are executed on 3.70 GHz Intel Xeon processors with 32 GB of RAM. The optimization problems are solved with CPLEX 12.6.3.

Unless otherwise stated, the benchmark values of coefficients are set as follows: planning horizon (unit: hours) $T = 1400$; the length of time intervals is one hour; loading cost (unit: €/TEU) $lc_i^{\text{ship}} = 18$, $lc_i^{\text{barge}} = 18$, $lc_i^{\text{train}} = 12$, $lc_i^{\text{truck}} = 12$ for $i \in N$; loading time (unit: hours) $lt_i^{\text{ship}} = 12$, $lt_i^{\text{barge}} = 4$, $lt_i^{\text{train}} = 2$, $lt_i^{\text{truck}} = 1$ for $i \in N$; storage cost (unit: €/TEU-h) $c_i^{\text{storage}} = 1$ for $i \in N$; carbon tax (unit: €/kg) $c^{\text{emission}} = 0.07$; delay cost (unit: €/TEU-h) $c_r^{\text{delay}} = 0.005 * p_r$ for $r \in R$; mean of travel times $\mu_s = t_s$ for $s \in S$; standard deviation of travel times $\sigma_s = 0.1 * t_s$ for $s \in S \backslash S^{\text{truck}}$, $\sigma_s = 0.5 * t_s$ for $s \in S^{\text{truck}}$. Regarding the HSA, the default settings are as follows: confidence level $\alpha = 0.7$; prediction horizon $H = 10$, number of scenarios $\Gamma = 12$; the largest number of services in a path $L = 7$, the maximum number of feasible matches for each request $N^{\text{match}} = 300$.

6.6.1 A small network

We first consider a small network $G1$ to test the impact of different objective functions and different policies in global synchromodal transport. The topology of network $G1$ is shown in Figure 6.5. It consists of two terminals in Europe and three terminals in Asia that are connected by Suez Canal Route (SCR), Northern Sea Route (NSR), and Eurasia Land Bridge (ELB). Compared with the SCR, the NSR has a shorter travel time but a higher travel cost caused by ice-breaking fees [53]. With the implementation of IMO 2020 regulations, shipping liner companies are required to use low-sulfur fuels on the sea, which in turn increases about 60% of travel costs in the SCR and the NSR [52]. As an alternative, the ELB becomes more and more competitive thanks to its shortest travel time. However, without subsidies from governments, the ELB is still the most expensive route.

We design 18 services for network G1: 8 in Asia, 6 in Europe and 4 connecting Asia and Europe as presented in Table 6.1. The travel costs are designed under the consideration of ice-breaking fees in the NSR, IMO 2020 regulations in the SCR and the NSR, and without subsidies from governments. We consider 6 contractual requests received by the system before the planning horizon. The detailed request data is shown in Table 6.2. Compared with reefer shipments (requests 1, 3, 5), dry shipments (requests 2, 4, 6) have longer lead times, lower freight rates, and lower delay costs. We use $G1 - n_1 - n_2$ to represent an instance under network $G1$ with n_1 contractual requests and n_2 spot requests.

Effects of objective functions and policies

The effects of objective functions and policies are tested under instance G1-6-0 without spot requests and travel time uncertainties, i.e., $\mu_s = t_s, \sigma_s = 0,\ \forall s \in S,\ R^t = \emptyset,\ \forall t \in \{1, ..., T\}$. Therefore, we set $\alpha = 0.5, H = 0, \Gamma = 0$.

The results generated under different objective functions are shown in Table 6.3. Comparing case 6 with cases 1 to 5, the total profit is the highest. It means that considering

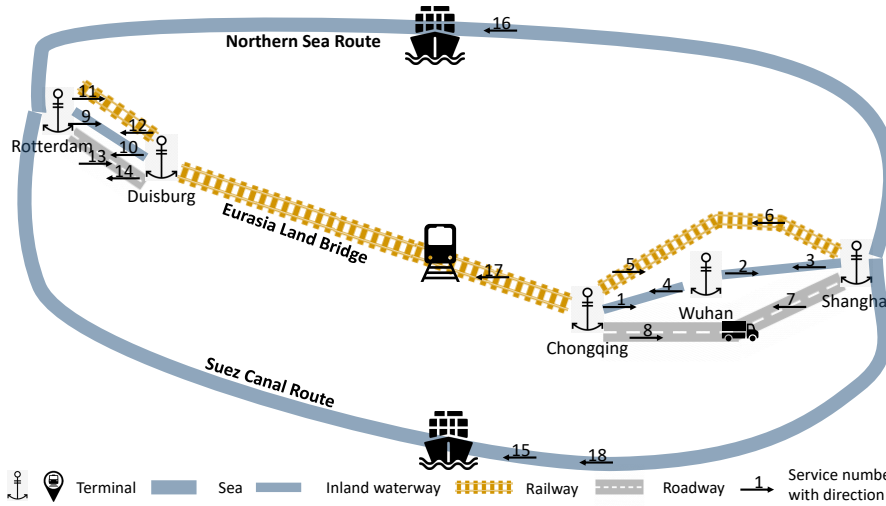

Figure 6.5: The topology of global synchromodal network G1.

Table 6.1: Service data of network G1.

Service. ID	Mode	Origin	Destination	Total capacity (TEU)	Reefer slots (TEU)	Departure time	Arrival time	Travel time (h)	Travel cost (€)	Carbon emissions-dry (kg)	Carbon emissions-reefer (kg)	Preceding service	Succeeding service
1	barge	Chongqing	Wuhan	160	50	144	235	91	192	313	940		2
2	barge	Wuhan	Shanghai	160	50	243	328	85	178	291	874	1	
3	barge	Shanghai	Wuhan	160	50	144	229	85	178	291	874		4
4	barge	Wuhan	Chongqing	160	50	237	328	91	192	313	940	3	
5	train	Chongqing	Shanghai	90	30	144	181	37	269	526	1578		
6	train	Shanghai	Chongqing	90	30	144	181	37	269	526	1578		
7	truck	Shanghai	Chongqing	200	60			22	1823	1489	4466		
8	truck	Chongqing	Shanghai	200	60			22	1823	1489	4466		
9	barge	Rotterdam	Duisburg	160	30	1010	1027	17	35	57	170		
10	barge	Duisburg	Rotterdam	160	30	750	767	17	35	57	170		
11	train	Rotterdam	Duisburg	90	30	910	917	7	48	92	276		
12	train	Duisburg	Rotterdam	90	30	750	757	7	48	92	276		
13	truck	Rotterdam	Duisburg	200	60			3	334	219	658		
14	truck	Duisburg	Rotterdam	200	60			3	334	219	658		
15	ship	Shanghai	Rotterdam	200	50	350	988	638	1441	2161	6483		
16	ship	Shanghai	Rotterdam	200	50	350	900	550	2240	1631	4894		
17	train	Chongqing	Duisburg	90	30	350	723	373	2007	3517	10551		
18	ship	Shanghai	Rotterdam	200	50	518	1156	638	1441	2161	6483		

Table 6.2: Request data of instance G1-6-0.

Requests	Container type	Origin	Destination	Container volume (TEU)	Announce time	Release time	Lead time (h)	Freight rate (€/TEU)	Delay cost (€/TEU-h)
1	reefer	Shanghai	Rotterdam	5	0	100	720	4000	20
2	dry	Shanghai	Rotterdam	5	0	100	840	3500	17.5
3	reefer	Wuhan	Rotterdam	5	0	100	600	4500	22.5
4	dry	Wuhan	Rotterdam	5	0	100	960	3000	15
5	reefer	Chongqing	Duisburg	5	0	100	480	5000	25
6	dry	Chongqing	Duisburg	5	0	100	1080	2500	12.5

the trade-off among logistics costs, delays, and emissions is very important. While cases 1 to 6 are designed to minimize different costs, case 7 aims to maximize the total profit that consists of revenue and total costs. Compared with cases 1 to 6, the total profit is significant higher under case 7. Comparing case 6 and case 7 shows that it may be necessary to reject the requests that are not profitable.

Table 6.3: Impact of different objective functions under instance G1-6-0.

Cases	Objective function	Total profits	Revenue	Travel costs	Transfer costs	Storage costs	Delay costs	Carbon tax	Number of rejections	Delay (TEU-h)	Emission (kg)
1	Travel costs	-67978	112500	**48061**	2040	6914	113163	10300	0	4945	147146
2	Transfer costs	-34695	112500	50677	**1320**	8890	74925	11383	0	3416	162611
3	Storage costs	-47333	112500	59413	2400	**4814**	81063	12144	0	3482	173483
4	Delay costs	1590	112500	63648	1560	9317	**21439**	14947	0	**873**	213529
5	Carbon tax	-67375	112500	72030	2040	8367	89363	**8076**	0	3773	**115366**
6	Total costs	4946	112500	63282	2100	5983	21439	14750	**0**	873	210711
7	Total profits	**13107**	87500	53249	1980	4743	3364	11057	**1**	150	157957

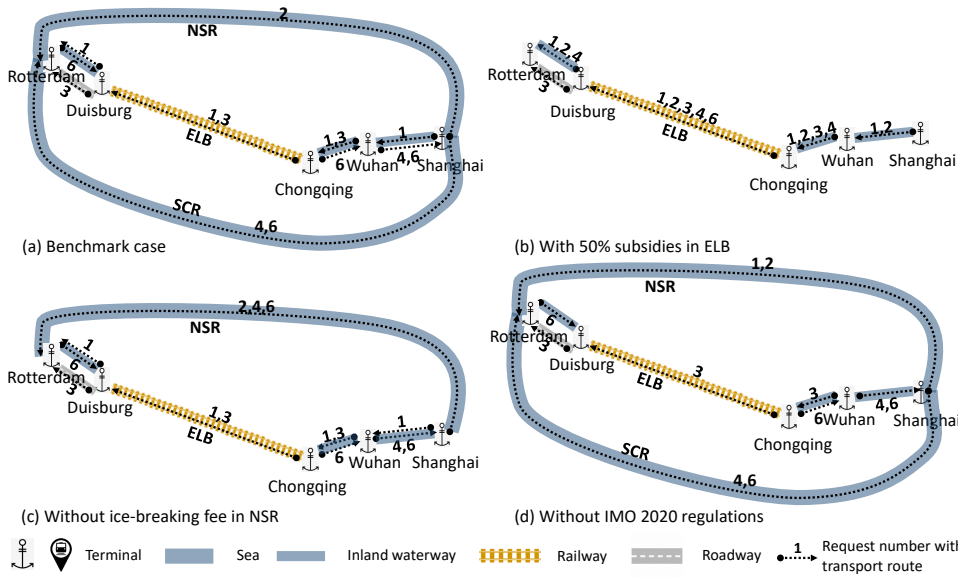

Figure 6.6: The itineraries of requests under different policies.

To investigate the impact of different policies on acceptance and matching decisions, we design three other scenarios in comparison to benchmark case 7: (i) with subsidies in the ELB, where the travel cost of service 17 reduces by 50%; (ii) without ice-breaking fee in the NSR, where the travel cost of service 16 reduces by 1152.24 €; (iii) without IMO 2020 regulations that reduces the costs of services 15, 16, 18 by 60%. Figure 6.6 shows that the itineraries of requests are quite sensitive to different policies. Global decision makers need to consider these policies in the light of the potential impacts on the usage of different transport alternatives and on the generation of logistics costs, delays, and carbon emissions. Under the benchmark case, request 5 is rejected; requests 1 and 3 with reefer shipments are assigned to the ELB; requests 2, 4, 6 with dry shipments are assigned to the SCR and the NSR. With 50% subsidies in the ELB, requests 2, 4 and 6 switch from the SCR and NSR to the ELB; without ice-breaking fee in the NSR, requests 4 and 6 switch from the SCR to the NSR; without the IMO 2020 regulations, request 1 switches from the ELB to the NSR.

Table 6.4: The realization of travel times.

Service. ID	1	2	3	4	5	6	7	8	9	10	11	12	13	14	15	16	17	18
Actual travel time	98	99	89	101	40	36	23	21	18	15	7	7	3	4	631	537	384	657
Actual departure time	144	250	144	241	144	144			1010	750	910	750			350	350	350	518
Actual arrival time	242	349	233	342	184	180			1028	765	917	757			981	887	734	1175

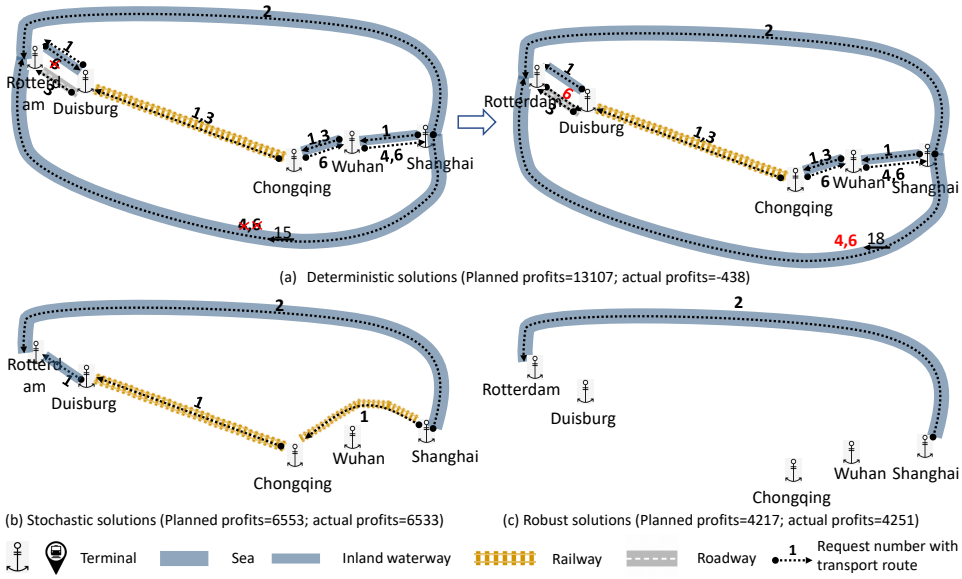

Figure 6.7: Comparison of deterministic, stochastic and robust solutions.

Comparing deterministic, stochastic, and robust approaches

To investigate the differences between solutions generated by the HSA (i.e., $\alpha = 0.7$), the DA (i.e., $\alpha = 0.5$), and the RA (i.e., $\alpha = 1$), we use instance G1-6-0 with the realization of travel time uncertainties, as shown in Table 6.4. Under this realization, barge service 2 is delayed, the transfers between barge service 2 and ship service 15 and 16 are therefore becoming infeasible. Due to travel time uncertainty, the planned profits obtained before the actual travel time realization are different from the actual profits. Figure 6.7 shows that the deterministic solutions have the highest planned profits but have the lowest actual profits due to infeasible transshipments at Shanghai Port for requests 4 and 6. In comparison, the stochastic solutions have the highest actual profits by rejecting requests 4 and 6 and choosing a train service instead of barge services for request 1. Compared with the deterministic solutions and the stochastic solutions, the robust solutions are the most conservative solutions with the highest number of rejections and without infeasible transshipments.

6.6.2 A realistic network

In this section, we test the behavior of the methodologies under a realistic network $G2$ with 8 terminals and 106 services. The topology of network $G2$ is shown in Figure 6.8. We generate several instances to represent different characteristics of requests under network

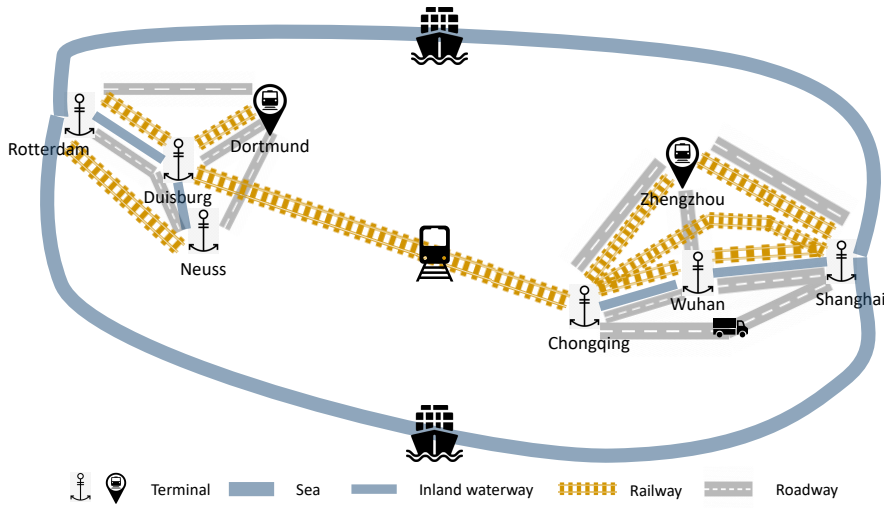

Figure 6.8: The topology of global synchromodal network G2.

Table 6.5: Probability distributions of spot requests.

Parameters	Value	Probability
Container type	{dry,reefer}	{0.9,0.1}
Origin	{Shanghai,Zhengzhou,Wuhan,Chongqing}	Uniform distribution
Destination	{Rotterdam,Duisburg,Neuss,Dortmund}	Uniform distribution
Container volume	{1,2,...,9}	Uniform distribution
$\Delta T1$	{0,1,2,...}	Poisson distribution with mean 24 minutes
Announce time	$\mathbb{T}_{r+1}^{\text{announce}} = \mathbb{T}_{r}^{\text{announce}} + \Delta T1$	
$\Delta T2$	{1,2,...,24}	Uniform distribution
Release time	$\mathbb{T}_{r}^{\text{release}} = \lceil \mathbb{T}_{r}^{\text{announce}} \rceil + \Delta T2$	
Lead time	{480,600,720,840,960,1080}	
Freight rate	{5000,4500,4000,3500,3000,2500}	{0.15,0.15,0.2,0.2,0.15,0.15}
Delay cost	{25,22.5,20,17.5,15,12.5}	

$G2$. The probability distributions of spot requests are shown in Table 6.5. We use $G2-n_1-n2$ to represent an instance under network $G2$ with n_1 contractual requests and n_2 spot requests. The service and request data used in this chapter is available at http://doi.org/10.4121/uuid:512169a0-5a69-43a9-a85b-105dd351cc74.

Performance of the CCP for travel time uncertainties

In this section, we aim to investigate the performance of the CCP in addressing travel time uncertainties. The CCP is worked together with the RHF and the P-HA to generate solutions at each decision epoch without the consideration of stochastic information on spot requests, namely, $\Gamma = 0$, $H = 0$. The performance of the CCP is tested under the impact of different confidence levels, delay costs, and travel time deviations.

To investigate the impact of different confidence levels, we use instance G2-150-150 under 20 realizations of travel times. The realizations of travel times are generated based on Monte Carlo Simulation by sampling their probability distributions with a fixed lower

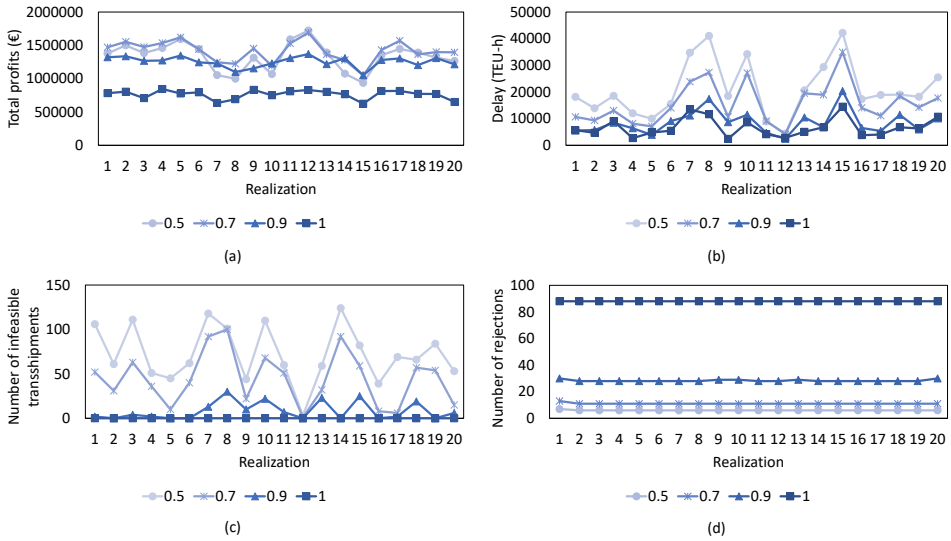

Figure 6.9: The impact of different confidence levels on instance G2-150-150.

bound of $0.9 * t_s$ for $s \in S$. Figure 6.9 shows that with the same confidence level, different solutions are generated under different realizations of travel times. From Figure 6.9(a), we can see that on average, the CCP has the best performance in total profits when $\alpha = 0.7$ and the worst when $\alpha = 1$. Figure 6.9(b) shows that in general, the higher the confidence level, the lower the delays in deliveries. Figure 6.9(c) shows that the higher the confidence level, the lower the number of infeasible transshipments. When $\alpha = 1$, the solutions are robust without infeasible transshipments under all the realizations. Figure 6.9(d) shows that the higher the confidence level, the higher the number of rejections.

To understand the differences in online decision processes under different confidence levels, we analyze the solutions generated under travel time realization 14. We denote 'CPP' as cumulated planned profits, and 'CAP' as the cumulated actual profits. Figure 6.10 shows that the higher the confidence level, the lower the cumulated planned profits. The reason is that with a higher confidence level, the system will choose 'suboptimal' decisions that have lower probabilities of infeasible transshipments. After the realization of actual travel times over the planning horizon, the total actual profits are higher than the total planned profits with confidence level 0.9 and 1 (which are very conservative), but lower than the planned profits with confidence level 0.5 and 0.7 (which take risks of infeasible transshipments). In comparison, the total actual profit is the highest with confidence level 0.9.

To investigate the influence of confidence level on instances with different degrees of dynamism (DODs), we design the following four instances: G2-225-75, G2-150-150, G2-75-225, G2-0-300. We define DOD as the ratio between the number of spot requests and the number of total requests. We use confidence level 0.5 as the benchmark and denote 'gaps' as the gaps in total actual profits, i.e., gaps=$\frac{\text{Total profits}(\alpha)-\text{Total profits}(0.5)}{\text{Total profits}(0.5)}$. Besides, we present the average results generated under 20 realizations of travel times. Table 6.6 shows that for all the instances, the CCP has the best performance in total profits with confidence level 0.7. The robust solutions (with confidence level 1) were worse than the deterministic solutions

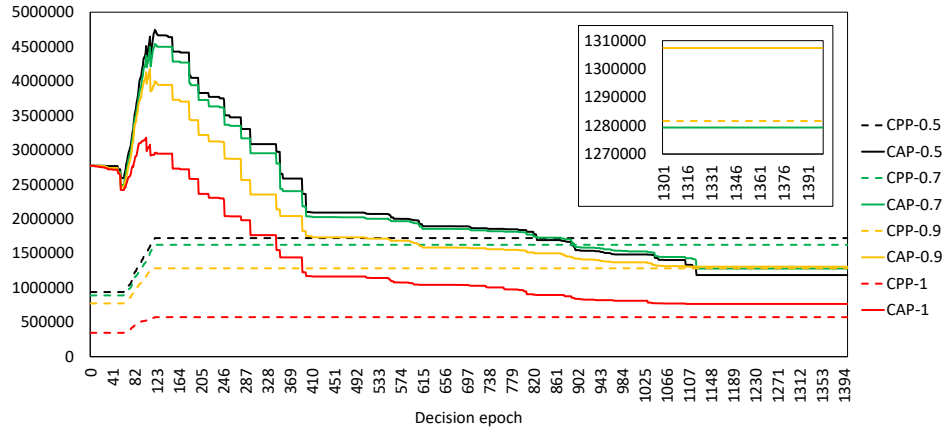

Figure 6.10: Online decision processes with different confidence levels.

Table 6.6: Impact of different confidence level on instances with different DOD.

Instances	Degree of dynamism	Confidence level	Total profits (€)	Infeasible transshipments	Rejections	CPU (seconds)	Gaps (%)
G2-225-75	25%	0.50	1443321	75	4	0.22	0.00
		0.70	1469731	45	9	0.18	**1.83**
		0.90	1334829	9	25	0.13	-7.52
		1.00	784627	0	59	0.10	-45.64
G2-150-150	50%	0.50	1334025	72	6	0.43	0.00
		0.70	1413988	44	11	0.39	**5.99**
		0.90	1253208	8	28	0.32	-6.06
		1.00	763565	0	88	0.24	-42.76
G2-75-225	75%	0.50	1328131	77	6	0.69	0.00
		0.70	1364769	50	12	0.62	**2.76**
		0.90	1247088	8	31	0.50	-6.10
		1.00	861556	0	90	0.41	-35.13
G2-0-300	100%	0.50	1256014	75	20	0.96	0.00
		0.70	1276508	52	25	0.86	**1.63**
		0.90	1263179	10	33	0.75	0.57
		1.00	848616	0	108	0.58	-32.44

(with confidence level 0.5) in all the instances. With confidence level 0.7, the CCP has the largest improvements in total profits under instance G2-150-150 with 50% DOD. It is also interesting to see that for all the instances, the higher the confidence level, the lower the number of infeasible transshipments and the higher the number of rejections. Furthermore, the computational complexity decreases with the increasing confidence level.

To test the impact of different delay costs and standard deviations of travel times, we set $\alpha = 0.7$ and use average results generated based on 20 realizations of actual travel times. Let 'gaps' be the gaps in total profits between the CCP and the DA ($\alpha = 0.5$). Table 6.7 shows that increasing the delay cost coefficients, the total profits, delays, and the number of infeasible transshipments will decrease and the number of rejections will increase in all the instances. Besides, the performance of the CCP becomes better in improving total profits with higher delay cost coefficients under all the instances. Interestingly, it is observed that with different delay cost coefficients, the CCP has the best performance under instances

Table 6.7: Impact of different delay costs.

Instances	Delay cost coefficients (*benchmark value)	Total profits (€)	Infeasible transshipments	Rejections	Delay (TEU-h)	Gaps (%)
	0.5	1600755	52	5	24648	0.17
G2-225-75	1.0	1469731	45	9	14013	1.83
	2.0	1251323	42	15	9324	**9.52**
	0.5	1549203	48	6	29518	1.25
G2-150-150	1.0	1413988	44	11	15673	5.99
	2.0	1173366	44	13	11243	**7.36**
	0.5	1541888	53	9	25822	1.32
G2-75-225	1.0	1364769	50	12	16247	2.76
	2.0	1141062	48	16	11687	**5.38**
	0.5	1512624	53	13	27338	-1.25
G2-0-300	1.0	1276508	52	25	15388	1.63
	2.0	1053527	51	31	11254	**4.49**

Table 6.8: Impact of different standard deviations.

Instances	Standard deviation coefficients (*benchmark value)	Total profits (€)	Infeasible transshipments	Rejections	Delay (TEU-h)	Gaps (%)
	1.0	1469731	45	9	14013	1.83
G2-225-75	1.5	1348739	25	19	13834	17.80
	2.0	895563	39	26	30761	**26.96**
	1.0	1413988	44	11	15673	5.99
G2-150-150	1.5	1262171	25	21	16735	19.89
	2.0	866506	35	28	31336	**42.04**
	1.0	1364769	50	12	16247	2.76
G2-75-225	1.5	1253172	27	25	16953	26.65
	2.0	866958	35	33	30925	**67.85**
	1.0	1276508	52	25	15388	1.63
G2-0-300	1.5	1220973	27	30	17437	28.61
	2.0	852891	34	37	31538	**60.61**

with different DODs. On the other hand, Table 6.8 shows that travel time deviations have a large impact on the performance of the CCP in increasing total profits. The larger the standard deviation, the better the performance of the CCP in comparison to the DA. This is reasonable since with higher standard deviations, the variability in travel times is very high and the estimations are not as accurate. In comparison, instance G2-75-225 has the best performance in improving the total profits that achieves 67.85% with standard deviations $\sigma_s = 0.2 * t_s$ for $s \in S \backslash S^{\text{truck}}$ and $\sigma_s = t_s$ for $s \in S^{\text{truck}}$.

Performance of the SAA for spot request uncertainties

In this section, we aim to investigate the performance of the SAA in addressing spot request uncertainties. The SAA is also worked together with the RHF and the P-HA without the consideration of stochastic information about travel times, namely, $\alpha = 0.5$. The performance of the SAA is tested under the impact of different numbers of scenarios and lengths of the prediction horizon. We use the DA ($\Gamma = 0$, $H = 0$) as the benchmark. Let 'gaps in total profits'$=\frac{\text{Total profits}(\Gamma,H)-\text{Total profits}(0,0)}{\text{Total profits}(0,0)}$. The total profits are the average total profits generated under 20 realizations of travel times. In case of sample requests instability, we replicate the optimization process 10 times for all instances. Figure 6.11(a) shows that under instance G2-150-150, the performance of the SAA in total profits increases as the number

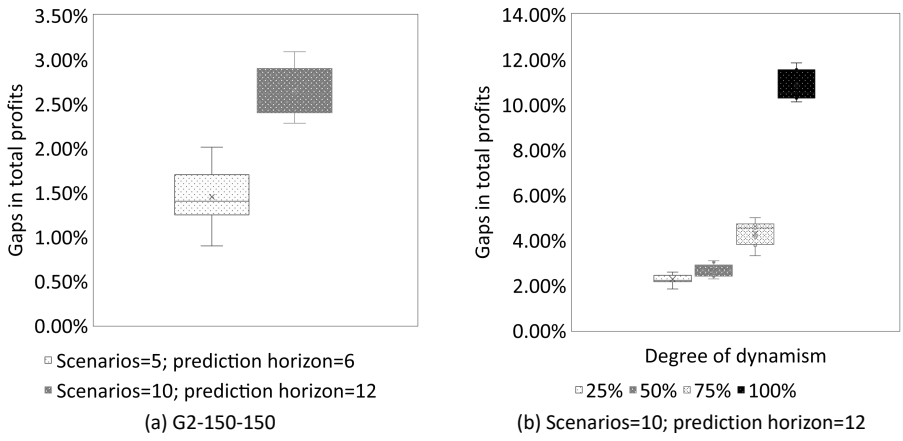

Figure 6.11: Performance of the sample average approximation method.

of scenarios and the length of the prediction horizon grow up. We set $\Gamma = 10$, $H = 12$. Figure 6.11(b) shows that the SAA outperforms the DA in all the instances, and the gap between the SAA and the DA grows with the increasing DOD.

Performance of the HSA for travel time and spot request uncertainties

To investigate the benefits of incorporating the stochastic information of both travel times and spot requests, we use the HSA which consists of the CCP and SAA together with the RHF and P-HA. We set $\alpha = 0.7$, $\Gamma = 10$, $H = 12$ for the HSA and use the DA ($\alpha = 0.5$, $\Gamma = 0$, $H = 0$), the CCP ($\alpha = 0.7$, $\Gamma = 0$, $H = 0$), and the SAA ($\alpha = 0.5$, $\Gamma = 10$, $H = 12$) as the benchmarks. We generate the average results under 20 realizations of travel times and 10 samples of spot requests. Table 6.9 shows that the HSA has better performance in total profits than the DA in all the instances and than the CCP and SAA in instances with higher DODs. Furthermore, the number of rejections increases with the increasing DOD and achieves the highest under instance G2-0-300 which has no contractual requests. This is reasonable since the system cannot reject contractual requests. Moreover, we observe that the HSA has the best performance in instance G2-0-300 which has a 100% DOD as stochastic information pays off when it is highly dynamic. It is also interesting to note that incorporating the stochastic information of spot requests, the number of rejections increases in all the instances except in instance G2-0-300. We define 'gaps in cumulated profits' as the gaps between the cumulated profits under the DA and SAA. Figure 6.12 shows that under the SAA, the system might reject current requests to reserve capacities for sample requests that are predicted to be more profitable. The higher the DOD, the larger the number of cumulated rejections and therefore the larger the free capacity at later stages. We observe that in instance G2-0-300, under the SAA, the system has more capacity to accept requests that arrive later thanks to the large number of cumulated rejections in earlier stages. Besides, Table 6.9 shows that increasing the confidence level, the computational complexity will decrease thanks to the chance constraints. However, increasing the number of scenarios and the length of the prediction horizon, the computational complexity will increase dramatically caused by the increasing size of sample requests.

Table 6.9: Performance of the hybrid stochastic approach.

Instances	α	Γ	H	Total profits (€)	Infeasible transshipments	Rejections	Delay (TEU-h)	Emission (kg)	CPU (seconds)	Gaps (%)
G2-225-75	0.5	0	0	1443321	75	4	18026	5768862	0.22	0.00
	0.7	0	0	1469731	45	9	14013	5717070	0.18	1.83
	0.5	10	12	1476023	71	6	16824	5680165	43.22	2.27
	0.7	10	12	1459075	44	14	13531	5632343	38.24	**1.09**
G2-150-150	0.5	0	0	1334025	72	6	21049	5742178	0.43	0.00
	0.7	0	0	1413988	44	11	15673	5637143	0.39	5.99
	0.5	10	12	1369395	69	11	19679	5582664	86.58	2.65
	0.7	10	12	1424060	43	15	14572	5558380	77.78	**6.75**
G2-75-225	0.5	0	0	1328131	77	6	21277	5681453	0.69	0.00
	0.7	0	0	1364769	50	12	16247	5596631	0.62	2.76
	0.5	10	12	1385221	70	12	19842	5527160	334.68	4.30
	0.7	10	12	1414896	46	15	15192	5536685	175.26	**6.53**
G2-0-300	0.5	0	0	1256014	75	20	19734	5408196	0.96	0.00
	0.7	0	0	1276508	52	25	15388	5222779	0.86	1.63
	0.5	10	12	1391737	70	14	19599	5455597	454.64	10.81
	0.7	10	12	1428613	47	16	15018	5486612	186.35	**13.74**

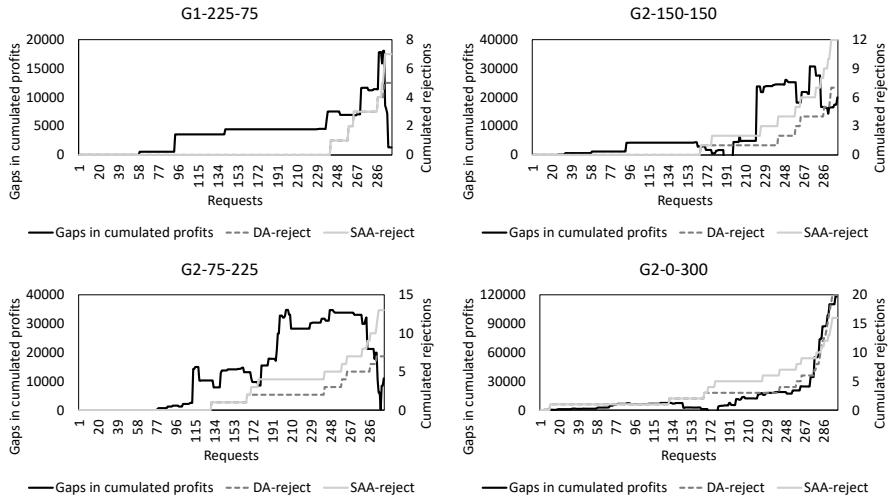

Figure 6.12: Differences in matching processes between instances with different DODs.

Performance of the P-HA

The P-HA is based on preprocessing procedures which may lead to suboptimal solutions. To test the computational performance and solution quality of the P-HA, we use an exact approach as the benchmark in which optimization model **P2** is solved by CPLEX directly. We denote 'N.var' as the number of variables, 'N.con' as the number of constraints, 'Obj' as the total profits, and 'CPU' as the computation time in seconds. Let $\alpha = 0.5, \Gamma = 0, H = 0$. Table 6.10 shows that the exact approach can only solve the first three small instances within 24 hours. Increasing the largest number of services in a path to 7 and the maximum number of feasible matches to 300, the P-HA can get optimal solutions for these instances within 183.14 seconds. Under the same setting, the P-HA can generate feasible solutions within 15 minutes for large instances. By using the P-HA, the system has the flexibility to choose proper L and N^{match} values to achieve the trade-off between computational complexity and solution quality.

Table 6.10: Performance of the preprocessing-based heuristic algorithm.

Instances	Exact approach				P-HA (L=3, N^{match}=100)				P-HA (L=7, N^{match}=300)			
	N.var	N.con	Obj	CPU	N.var	N.con	Obj	CPU	N.var	N.con	Obj	CPU
G1-6-0	2268	6540	13107	40.44	58	42	12838	0.52	76	46	13107	0.29
G1-10-0	3780	10840	26114	181.36	95	48	25400	0.50	121	52	26114	0.29
G2-1-0	11466	35994	23127	7417.06	45	24	23127	1.23	297	53	23127	183.14
G2-5-0	57330	181852			303	86	30672	1.22	1501	134	32738	192.64
G2-10-0	114660	362164			532	107	57805	1.30	2996	162	62090	219.75
G2-100-0	1146600	3612428	above 24 hours		6581	333	501344	4.29	29576	391	545749	349.85
G2-200-0	2293200	7224988			12918	535	1255557	7.81	58895	592	1331016	503.60
G2-300-0	3439800	10846452			18891	735	1800835	16.33	88389	792	1889476	680.40
G2-400-0	4586400	14439116			26182	936	2195048	26.27	118197	991	2253709	894.98

6.7 Conclusions

This chapter answers research question **RQ4** by investigating a dynamic and stochastic shipment matching problem in global synchromodal transport. The problem is dynamic since the global synchromodal matching platform receives real-time information on spot requests and travel times. The problem is stochastic since the uncertainties in requests and travel times are incorporated. We formulated a Markov decision process to model the problem. Due to the curse of dimensionality, we developed a hybrid stochastic approach (HSA) to solve the problem. The HSA uses a chance-constrained programming model to address travel time uncertainty, a sample average approximation method to address spot request uncertainty, and a preprocessing-based heuristic algorithm to generate solutions at each decision epoch of a rolling horizon framework.

We conducted extensive experiments to validate the performance of the HSA in comparison to a deterministic approach (DA) in which decisions are made based on estimated travel times and a robust approach (RA) in which decisions are made based on maximum and minimum travel times. The experimental results indicate that the performance of the HSA is highly affected by the settings of the confidence level, the number of scenarios, and the length of the prediction horizon, and they need to be studied closely for the problem at hand. In this chapter, the HSA outperforms the DA and RA under various scenarios of the global synchromodal matching system.

This research can be extended in several promising directions. First, in this chapter, we considered a centralized platform that provides integrated decisions for global shipments. However, in practice, a large number of entities are involved in global container transport and they may not all be willing to give authority to a centralized platform. The coordination mechanism among them and incentives to stimulate cooperation are part of future research. This is the subject of Chapter 7. Second, we assumed that the platform publishes fixed fare classes for container bookings. Future research can consider dynamic pricing strategies for online platforms to realize the balance between supply and demand.

Chapter 7

Dynamic, stochastic, and coordinated global shipment matching

In Chapter 6, a centralized platform is proposed to support global synchromodal transport planning. However, in practice, multiple operators are present and they may not all be willing to give authority to a centralized platform. This chapter investigates distributed optimization approaches that stimulate cooperation among local operators under dynamic and stochastic environments.

This chapter is structured as follows. Section 7.1 introduces the distributed nature of global synchromodal transport systems. In Section 7.2, a detailed problem description is provided. Section 7.3 presents the mathematical formulation of coordinated global synchromodal shipment matching. In Section 7.4, three distributed optimization approaches are developed to handle interconnecting constraints, followed by a heuristic algorithm design in Section 7.5. Section 7.6 conducts numerical experiments to investigate the performance of the proposed approaches. Finally, the conclusions are given in Section 7.7.

Parts of this chapter have been submitted to a journal: "W. Guo, B. Atasoy, W. Beelaerts van Blokland, and R. R. Negenborn. Distributed approaches for coordinated global synchromodal shipment matching with travel time uncertainty. Submitted to a journal, 2020."

7.1 Introduction

Global synchromodal transportation, as discussed in Chapter 6, is the provision of efficient, reliable, flexible, and sustainable services through integrated planning for all the shipments involved in a global network under the control of a centralized platform [99]. However, in practice, the operators of a global synchromodal transport system are often geographically distributed, which makes it very difficult to apply a central controller to manage the whole system [25]. For example, the hinterland transportation from Chongqing terminal to Shanghai Port is managed by China Railway Container Transport, the maritime transportation from Shanghai port to Rotterdam port is organized by COSCO Shipping Lines, and the hin-

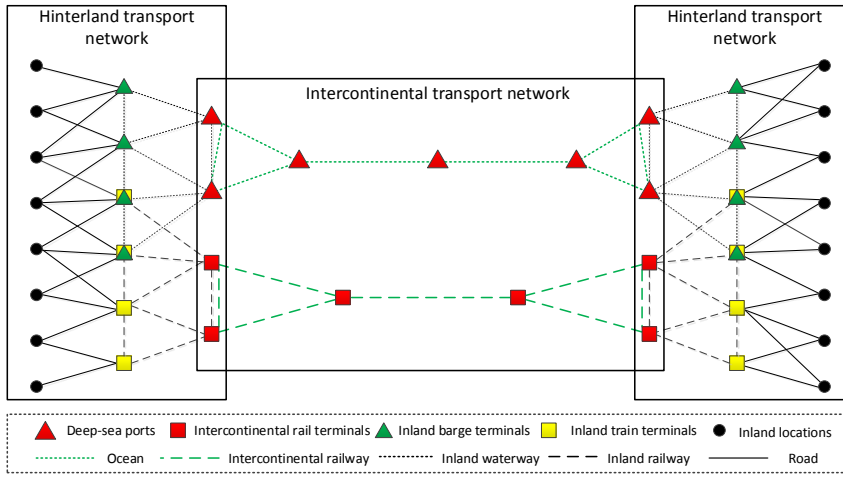

Figure 7.1: Topology of a distributed global transport network.

terland transportation from Rotterdam port to Duisburg terminal is controlled by European Gateway Services. These local operators typically operate in different but interconnected service areas, as shown in Figure 7.1.

If players are not willing to give authority to a central controller, *distributed approaches* are needed to stimulate the cooperation among local operators [65]. Under such approaches, local operators have independent planning authority in their service networks and cooperate to achieve a common goal, such as increasing total profits, reducing the number of infeasible transshipments at export/import terminals, reducing delays in deliveries at destination terminals. Therefore, they operate under local constraints as well as under those imposed by the interconnection among local operators [25]. Thanks to the development of information and communication technologies and intelligent transport systems, local operators can not only make online decisions but also exchange information in real-time [50].

In this chapter, we investigate a coordinated global synchromodal shipment matching problem in which a platform owned by a global operator receives real-time shipment requests from shippers and exchanges relevant information with local operators, as shown in Figure 7.2. Under such a platform, the global operator acts as an intermediary between shippers and local operators, to connect transport demand and supply without having direct control over these entities. Specifically, the global operator sends relative information of shipment requests to local operators and leaves the matching decisions with transport services to local operators. To stimulate local operators choosing the 'optimal' matching decisions that benefit the common goal, distributed approaches that handle interconnecting constraints need to be designed. After achieving consistency in matching decisions, the global operator combines the matched services into itineraries to provide an integrated transport plan for each shipment request. The coordination goal is hereby to maximize the total profits for accepting and matching shipment requests. The profit gain as a result of the collaboration needs to be shared among all the stakeholders to guarantee a win-win situation and fairness [28]. This chapter focuses on the cooperative transport planning problem and leaves the profit sharing mechanism design to future research.

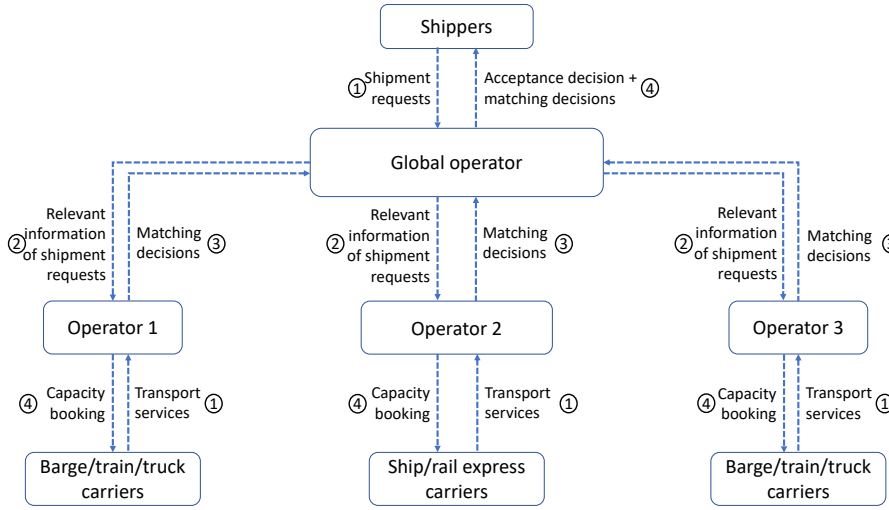

Figure 7.2: Business model of coordinated global synchromodal shipment matching.

Although distributed approaches have been applied in many fields, such as Power distribution networks [66], railway traffic management [44], vehicle platoons [116], intermodal freight transport chains [25], and hinterland synchromodal container flow control [50], it is still challenging for global synchromodal shipment matching which has different interconnecting constraints from above studies. In the literature, the work of Li et al. [50] is the most similar to this chapter. Li et al. [50] investigated a coordinated model predictive container flow control problem among multiple hinterland operators in different but interconnected service areas. These operators coordinate to reach an agreement on the volumes of container flows that each operator will hand over to other operators. Different from the work of Li et al. [50], this chapter focuses on shipment requests that have specific time windows instead of container flows. Therefore, the interconnecting constraints include not only spatial compatibility but also time compatibility at export/import terminals. Furthermore, most of the distributed studies assume all the input information are deterministic without uncertainties. However, in global synchromodal transportation, travel time uncertainty is quite common resulting from weather conditions and traffic congestion [18]. As discussed in Chapter 6, ignoring travel time uncertainty in global synchromodal shipment matching might result in suboptimal or even infeasible solutions. To the best of our knowledge, none of the existing studies in the literature investigated dynamic, stochastic, and coordinated synchromodal transport planning problems.

The contributions of this chapter are given as follows: (i) we introduce a dynamic, stochastic, and coordinated global shipment matching problem; (ii) we develop mathematical models and interconnecting constraints to describe the problem; (iii) we develop three distributed approaches combined with a rolling horizon approach and a chance-constrained programming approach to support dynamic and stochastic coordination among local operators; (iv) we design a heuristic algorithm to generate timely solutions at each iteration; (v) we evaluate the performance of the proposed approaches under a comprehensive set of experiments.

7.2 Problem description

We consider a coordinated global synchromodal shipment matching problem in which a global operator and three local operators cooperate to make acceptance and matching decisions for shipment requests. These operators play as agents that can make online decisions and exchange information in real-time. Each operator employs a rolling horizon framework [37] to handle real-time shipment requests. The global operator receives requests from shippers and makes acceptance or rejection decisions for each request. Each local operator receives part or all of the information of requests from the global operator and receives transport services from local carriers. Based on the local constraints (i.e., capacity limitation, time-spatial compatibility at transshipment terminals) and the interconnecting constraints (i.e., time-spatial compatibility at export/import terminals), local operators make matching decisions at each decision epoch. After achieving consistency in matching decisions, each local operator books capacity on matched services from local carriers. The global operator combines the matched services into itineraries for each accepted shipment request.

Let $O = \{1,2,3\}$ be the set of local operators. Operator 1 is the hinterland operator in the export continent, operator 2 is the intercontinental operator, and operator 3 is the hinterland operator in the import continent.

Let $N = N^1 \cup N^2 \cup N^3$ be the set of terminals. Here, N^1 is associated with the export hinterland network that belongs to operator 1; N^2 corresponds to the intercontinental transport network; N^3 is the set of terminals in the import hinterland network that belongs to operator 3. Let N^{exp} be the set of export terminals, $N^{\text{exp}} = N^1 \cap N^2$; let N^{imp} be the set of import terminals, $N^{\text{imp}} = N^2 \cap N^3$. Let lt_i^m be the loading/unloading time with mode $m \in M = \{\text{ship, barge, train, truck}\}$ at terminal $i \in N$. We make a common assumption that the loading/unloading and storage capacity at terminals are unlimited [18].

Let $S = S^1 \cup S^2 \cup S^3$ be the set of transport services. Here, S^o is the set of services belongs to operator o. Each service $s \in S^o$ is characterized by its mode $MT_s \in M$, origin terminal o_s, destination terminal d_s, free capacity U_s^t at decision epoch t, scheduled departure time TD_s, scheduled arrival time TA_s, estimated travel time t_s, and travel cost c_s. Let $\bar{t}_s$, $\bar{T}D_s$ and $\bar{T}A_s$ be the actual travel, departure and arrival time of service s which are unknown before their realization. We consider ship, barge and train services as line services, namely, different services with the same mode might be operated by the same vehicle. We define l_{sq} equals to 0 if service s is the preceding service of service q, otherwise equals to 1. We consider each truck service as a fleet of trucks that have flexible departure times. We define TD_{rs} as a variable that indicates the departure time of service $s \in S^{\text{truck}}$ with shipment $r \in R$. Same as Chapter 6, we assume the travel times $[\tilde{t}_s]_{\forall s \in S}$ are continuous random variables following normal distributions $\tilde{t}_s \sim N(\mu_s, \sigma_s^2)$. Here, μ_s is the mean travel time between terminal o_s and terminal d_s, and σ_s is the corresponding standard deviation. The departure time of service $s \in S \backslash S^{\text{truck}}$ follows normal distribution $\tilde{T}D_s \sim N(\mu_s^+, \sigma_s^{+2})$. The arrival time of service $s \in S \backslash S^{\text{truck}}$ follows normal distribution $\tilde{T}A_s \sim N(\mu_s^-, \sigma_s^{-2})$.

Let R be the set of shipment requests. Each request $r \in R$ is characterized by its origin terminal $o_r \in N$, destination terminal $d_r \in N$, container volume u_r, announce time $\mathbb{T}_r^{\text{announce}}$ (i.e., the time when global operator receives the request), release time $\mathbb{T}_r^{\text{release}}$ (i.e., the time when the shipment is available for transport process), and fare class including freight rate p_r, lead time LD_r, and delay cost c_r^{delay}. The due time of request r is represented as, $\mathbb{T}_r^{\text{due}} = \mathbb{T}_r^{\text{release}} + LD_r$. Let $R^t = \{r \in R | t-1 < \mathbb{T}_r^{\text{announce}} \leq t\}$ be the set of new requests received

during time interval $(t-1,t]$; let $\bar{R}^t$ be the set of accepted requests that need reoptimization at decision epoch t due to infeasible transshipments caused by travel time variations.

While the objective of the global operator is to maximize revenues by accepting requests, the objectives of local operators are to minimize total costs for matching requests with services. The coordinated common goal is to maximize the total profits that include total revenues and total costs.

7.3 Coordinated global synchromodal shipment matching

Same as Chapter 6, we use chance constraints to deal with travel time uncertainties. In this section, we first present the formulations for the global operator and local operators. After that, we discuss the interconnecting constraints among multiple operators. Finally, we present the common goal of coordinated synchromodal global shipment matching.

7.3.1 Mathematical model for the global operator

Let y_r^t be the binary variable which equals to 1 if new request $r \in R^t$ is accepted at decision epoch t, 0 otherwise. The objective of the global operator is to maximize total revenues received from shippers through acceptance decisions, presented as follows:

$$\textbf{P0-0} \quad \max_{y^t} \sum_{r \in R^t} p_r u_r y_r^t \tag{7.1}$$

7.3.2 Mathematical model for operator o

Let x_{rs}^t be the binary variable which is 1 if request $r \in R^t \cup \bar{R}^t$ is matched with service $s \in S$. Let $\mathbb{T}_r^o$ be the delay of request r at its destination terminal $d_r \in N^o$. Let t_{ri}^- and t_{ri}^+ be the arrival and departure time of request r at terminal $i \in N^{\exp} \cup N^{\text{imp}} \backslash \{o_r, d_r\}$. The objective of each local operator is to minimize total costs which consists of transportation costs and delay costs. The formulation for operator o is presented as follows:

$$\textbf{P0-}o \quad \min_{x^t} \sum_{r \in R^t \cup \bar{R}^t} \sum_{s \in S^o} c_s x_{rs}^t u_r + \sum_{r \in R^t \cup \bar{R}^t} c_r^{\text{delay}} \mathbb{T}_r^o u_r \tag{7.2}$$

subject to

$$\sum_{s \in S_i^{o-}} x_{rs}^t \leq 1, \quad \forall r \in R^t \cup \bar{R}^t, i \in N^o \backslash \{o_r\}, \tag{7.3}$$

$$\sum_{s \in S_i^{o+}} x_{rs}^t \leq 1, \quad \forall r \in R^t \cup \bar{R}^t, i \in N^o \backslash \{d_r\}, \tag{7.4}$$

$$\sum_{s \in S_{or}^{o-}} x_{rs}^t \leq 0, \quad \forall r \in R^t \cup \bar{R}^t, \tag{7.5}$$

$$\sum_{s \in S_{dr}^{o+}} x_{rs}^t \leq 0, \quad \forall r \in R^t \cup \bar{R}^t, \tag{7.6}$$

$$\sum_{s \in S_i^{o+}} x_{rs}^t = \sum_{s \in S_i^{o-}} x_{rs}^t, \quad \forall r \in R^t \cup \bar{R}^t, i \in N^o \backslash \{\{o_r\}, \{d_r\}, N^{\exp}, N^{\text{imp}}\}, \tag{7.7}$$

$$\sum_{r\in R^t\cup\bar{R}^t} x^t_{rs}u_r \le U^t_s, \quad \forall s\in S^o, \tag{7.8}$$

$$\mathbb{T}^{\text{release}}_r + lt^{MT_s}_{o_r} \le TD_{rs} + \mathbf{M}(1-x^t_{rs}), \quad \forall r\in R^t\cup\bar{R}^t, s\in S^{o+\text{truck}}_{o_r}, \tag{7.9}$$

$$\mathrm{P}\{\mathbb{T}^{\text{release}}_r + lt^{MT_s}_{o_r} \le \tilde{T}D_s + \mathbf{M}(1-x^t_{rs})\} \ge \alpha,\ \forall r\in R^t\cup\bar{R}^t, s\in S^{o+}_{o_r}\backslash S^{o+\text{truck}}_{o_r}, \tag{7.10}$$

$$\begin{aligned}&\mathrm{P}\{\tilde{T}A_s + lt^{MT_s}_i + lt^{MT_q}_i \le \tilde{T}D_q + \mathbf{M}(1-x^t_{rs}) + \mathbf{M}(1-x^t_{rq})\} \ge \alpha,\\ &\forall r\in R^t\cup\bar{R}^t, i\in N^o\backslash\{o_r,d_r\}, s\in S^{o-}_i\backslash S^{o-\text{truck}}_i, q\in S^{o+}_i\backslash S^{o+\text{truck}}_i, l_{sq}=1,\end{aligned} \tag{7.11}$$

$$\begin{aligned}&\mathrm{P}\{TD_{rs} + \tilde{t}_s + lt^{MT_s}_i + lt^{MT_q}_i \le \tilde{T}D_q + \mathbf{M}(1-x^t_{rs}) + \mathbf{M}(1-x^t_{rq})\} \ge \alpha,\\ &\forall r\in R^t\cup\bar{R}^t, i\in N^o\backslash\{o_r,d_r\}, s\in S^{o-\text{truck}}_i, q\in S^{o+}_i\backslash S^{o+\text{truck}}_i,\end{aligned} \tag{7.12}$$

$$\begin{aligned}&\mathrm{P}\{\tilde{T}A_s + lt^{MT_s}_i + lt^{MT_q}_i \le TD_{rq} + \mathbf{M}(1-x^t_{rs}) + \mathbf{M}(1-x^t_{rq})\} \ge \alpha,\\ &\forall r\in R^t\cup\bar{R}^t, i\in N^o\backslash\{o_r,d_r\}, s\in S^{o-}_i\backslash S^{o-\text{truck}}_i, q\in S^{o+\text{truck}}_i,\end{aligned} \tag{7.13}$$

$$\begin{aligned}&\mathrm{P}\{TD_{rs} + \tilde{t}_s + lt^{MT_s}_i \le TD_{rq} + \mathbf{M}(1-x^t_{rs}) + \mathbf{M}(1-x^t_{rq})\} \ge \alpha,\\ &\forall r\in R^t\cup\bar{R}^t, i\in N^o\backslash\{o_r,d_r\}, s\in S^{o-\text{truck}}_i, q\in S^{o+\text{truck}}_i,\end{aligned} \tag{7.14}$$

$$\mathbb{T}^o_r \ge \tilde{T}A_s + lt^{MT_s}_{d_r} - \mathbb{T}^{\text{due}}_r + \mathbf{M}(x^t_{rs}-1), \quad \forall r\in R^t\cup\bar{R}^t, s\in S^{k-}_{d_r}\backslash S^{k-\text{truck}}_{d_r}, \tag{7.15}$$

$$\mathbb{T}^o_r \ge TD_{rs} + t_s + lt^{MT_s}_{d_r} - \mathbb{T}^{\text{due}}_r + \mathbf{M}(x^t_{rs}-1), \quad \forall r\in R^t\cup\bar{R}^t, s\in S^{k-\text{truck}}_{d_r}, \tag{7.16}$$

$$\begin{aligned}&t^-_{ri} \ge \mu^-_s + \phi^{-1}(\alpha)\sigma^-_s + lt^{MT_s}_i + \mathbf{M}(x^t_{rs}-1),\ \forall r\in R^t\cup\bar{R}^t,\\ &i\in N^{\text{exp}}\cup N^{\text{imp}}\backslash\{o_r,d_r\}, s\in S^{o-}_i\backslash S^{o-\text{truck}}_i,\end{aligned} \tag{7.17}$$

$$\begin{aligned}&t^-_{ri} \ge TD_{rs} + \mu_s + \phi^{-1}(\alpha)\sigma_s + lt^{MT_s}_i + \mathbf{M}(x^t_{rs}-1), \forall r\in R^t\cup\bar{R}^t,\\ &i\in N^{\text{exp}}\cup N^{\text{imp}}\backslash\{o_r,d_r\}, s\in S^{o-\text{truck}}_i,\end{aligned} \tag{7.18}$$

$$\begin{aligned}&t^+_{ri} \le \mu^+_q - \phi^{-1}(\alpha)\sigma^+_q - lt^{MT_q}_i + \mathbf{M}(1-x^t_{rq}),\ \forall r\in R^t\cup\bar{R}^t,\\ &i\in N^{\text{exp}}\cup N^{\text{imp}}\backslash\{o_r,d_r\}, q\in S^{o+}_i\backslash S^{o+\text{truck}}_i,\end{aligned} \tag{7.19}$$

$$\begin{aligned}&t^+_{ti} \le TD_{rq} - lt^{MT_q}_i + \mathbf{M}(1-x^t_{rq}), \quad \forall r\in R^t\cup\bar{R}^t, i\in N^{\text{exp}}\cup N^{\text{imp}}\backslash\{o_r,d_r\},\\ &q\in S^{o+\text{truck}}_i.\end{aligned} \tag{7.20}$$

Constraints (7.3-7.6) eliminate subtours. Constraints (7.7) ensure flow conservation at transshipment terminals. Constraints (7.8) represent capacity limitations. Constraints (7.9-7.14) ensure that the probability of feasible transshipments at terminals will be higher than confidence level α. Constraints (7.15-7.16) calculate delay in deliveries of request r at destination terminal. Constraints (7.17-7.18) calculate the arrival time at export and import terminals. Constraints (7.19-7.20) calculate the depart time at export and import terminals.

The linearization of probability constraints (7.10-7.14) are presented as follows:

$$\frac{\mathbb{T}^{\text{release}}_r + lt^{MT_s}_{o_r} + \mathbf{M}(x^t_{rs}-1) - \mu^+_s}{\sigma^+_s} \le \phi^{-1}(1-\alpha), \forall r\in R^t\cup\bar{R}^t, s\in S^{o+}_{o_r}\backslash S^{o+\text{truck}}_{o_r}, \tag{7.21}$$

$$\begin{aligned}&\frac{lt^{MT_s}_i + lt^{MT_q}_i + \mathbf{M}(x^t_{rs}-1) + \mathbf{M}(x^t_{rq}-1) - (\mu^+_q - \mu^-_s)}{\sqrt{(\sigma^+_q)^2 + (\sigma^-_s)^2}} \le \phi^{-1}(1-\alpha),\\ &\forall r\in R^t\cup\bar{R}^t, i\in N^o\backslash\{o_r,d_r\}, s\in S^{o-}_i\backslash S^{o-\text{truck}}_i, q\in S^{o+}_i\backslash S^{o+\text{truck}}_i, l_{sq}=1\end{aligned} \tag{7.22}$$

$$\frac{TD_{rs}+lt_i^{MT_s}+lt_i^{MT_q}+\mathbf{M}(x_{rs}^t-1)+\mathbf{M}(x_{rq}^t-1)-(\mu_q^+-\mu_s)}{\sqrt{(\sigma_q^+)^2+(\sigma_s)^2}} \leq \phi^{-1}(1-\alpha), \quad \forall r \in R^t \cup \bar{R}^t, i \in N^o \backslash \{o_r, d_r\}, s \in S_i^{o-\text{truck}}, q \in S_i^{o+} \backslash S_i^{o+\text{truck}}, \tag{7.23}$$

$$\frac{TD_{rq}-lt_i^{MT_s}-lt_i^{MT_q}+\mathbf{M}(1-x_{rs}^t)+\mathbf{M}(1-x_{rq}^t)-\mu_s^-}{\sigma_s^-} \geq \phi^{-1}(\alpha), \quad \forall r \in R^t \cup \bar{R}^t, i \in N^o \backslash \{o_r, d_r\}, s \in S_i^{o-} \backslash S_i^{o-\text{truck}}, q \in S_i^{o+\text{truck}}, \tag{7.24}$$

$$\frac{TD_{rq}-TD_{rs}-lt_i^{MT_s}-lt_i^{MT_q}+\mathbf{M}(1-x_{rs}^t)+\mathbf{M}(1-x_{rq}^t)-\mu_s}{\sigma_s} \geq \phi^{-1}(\alpha), \quad \forall r \in R^t \cup \bar{R}^t, i \in N^o \backslash \{o_r, d_r\}, s \in S_i^{o-\text{truck}}, q \in S_i^{o+\text{truck}}. \tag{7.25}$$

where $\phi^{-1}(\alpha)$ is the inverse function of standardized normal distribution, $\phi^{-1}(\alpha) = -\phi^{-1}(1-\alpha)$, $\phi^{-1}(0.5) = 0$.

7.3.3 Interconnecting constraints

To ensure the feasibility of transport plan for each shipment, following interconnecting constraints must be met:

$$y_r^t \leq \sum_{s \in S_{or}^{1+}} x_{rs}^t + \sum_{s \in S_{or}^{2+}} x_{rs}^t + \sum_{s \in S_{or}^{3+}} x_{rs}^t, \quad \forall r \in R^t, \tag{7.26}$$

$$y_r^t \leq \sum_{s \in S_{dr}^{1-}} x_{rs}^t + \sum_{s \in S_{dr}^{2-}} x_{rs}^t + \sum_{s \in S_{dr}^{3-}} x_{rs}^t, \quad \forall r \in R^t, \tag{7.27}$$

$$\sum_{s \in S_{or}^{1+}} x_{rs}^t + \sum_{s \in S_{or}^{2+}} x_{rs}^t + \sum_{s \in S_{or}^{3+}} x_{rs}^t = 1, \quad \forall r \in \bar{R}^t, \tag{7.28}$$

$$\sum_{s \in S_{dr}^{1-}} x_{rs}^t + \sum_{s \in S_{dr}^{2-}} x_{rs}^t + \sum_{s \in S_{dr}^{3-}} x_{rs}^t = 1, \quad \forall r \in \bar{R}^t, \tag{7.29}$$

$$\sum_{s \in S_i^{1-}} x_{rs}^t + \sum_{s \in S_i^{2-}} x_{rs}^t = \sum_{s \in S_i^{1+}} x_{rs}^t + \sum_{s \in S_i^{2+}} x_{rs}^t, \ \forall r \in R^t \cup \bar{R}^t, i \in N^{\text{exp}} \backslash \{o_r, d_r\}, \tag{7.30}$$

$$\sum_{s \in S_i^{2-}} x_{rs}^t + \sum_{s \in S_i^{3-}} x_{rs}^t = \sum_{s \in S_i^{2+}} x_{rs}^t + \sum_{s \in S_i^{3+}} x_{rs}^t, \ \forall r \in R^t \cup \bar{R}^t, i \in N^{\text{imp}} \backslash \{o_r, d_r\}, \tag{7.31}$$

$$t_{ri}^- \leq t_{ri}^+, \quad \forall r \in R^t \cup \bar{R}^t, i \in N^{\text{exp}} \backslash \{o_r, d_r\}, \tag{7.32}$$

$$t_{ri}^- \leq t_{ri}^+, \quad \forall r \in R^t \cup \bar{R}^t, i \in N^{\text{imp}} \backslash \{o_r, d_r\}. \tag{7.33}$$

Constraints (7.26-7.27) ensure that new request $r \in R^t$ will be accepted by global operator only if there have services depart from its origin terminal o_r and services arrive to its destination terminal d_r. Constraints (7.28-7.29) ensure that reoptimization request $r \in \bar{R}^t$ will be transported by one service departing from its origin terminal o_r and by one service arriving to its destination terminal d_r. Constraints (7.30-7.31) ensure flow conservation at import and export terminal for request $r \in R^t \cup \bar{R}^t$. Constraints (7.32)-(7.33) ensure the arrival time at export and import terminals will be earlier than the departure time for each request $r \in R^t \cup \bar{R}^t$.

7.3.4 Coordinated global synchromodal shipment matching

The coordinated common goal is to maximize total profits which consists of revenues received from shippers, transport costs paid to carriers, and delay costs paid to shippers. The formulation of coordinated global synchromodal shipment matching at decision epoch t is presented as follows:

$$\mathbf{P0}\ \ \mathbf{Z0} = \max_{y^t, x^t} \sum_{r \in R^t} p_r u_r y_r^t - \sum_{o \in \{1,2,3\}} \left(\sum_{r \in R^t \cup \bar{R}^t} \sum_{s \in S^o} c_s x_{rs}^t u_r + \sum_{r \in R^t \cup \bar{R}^t} c_r^{\text{delay}} \mathbb{T}_r^o u_r \right) \tag{7.34}$$

subject to local constraints (7.3-7.9,7.15-7.25) for $o \in \{1,2,3\}$, and interconnecting constraints (7.26-7.33).

Since matching decisions are made by local operators independently with local information, model **P0** cannot be solved directly. To ensure the decisions made by local operators meet interconnecting constraints, distributed approaches are required.

7.4 Distributed approaches

We develop three distributed approaches: Lagrangian relaxation method (LR), Augmented Lagrangian relaxation method (ALR), and alternating direction method of multipliers algorithm (ADMM). The main idea of these distributed approaches is to relax interconnecting constraints by bringing them into the objective function **Z0** with associated *Lagrangian multipliers* [65]. In this way, the original problem can be decomposed into four subproblems that relate to each operator. At each iteration, the global operator creates acceptance decisions based on the relaxed model and receives matching decisions from three local operators. If the interconnecting constraints cannot be met, the Lagrangian multipliers will be updated based on the proposed approaches. The process will be repeated until achieving a consistency on interconnecting constraints. The main difference among these three distributed approaches is the way to relax the original problem.

7.4.1 Lagrangian relaxation method

The LR approach is a relaxation method which penalizes violations of interconnecting constraints using a Lagrange multiplier, which imposes a cost on violations [48]. These added costs are used instead of the strict interconnecting constraints in the optimization. Specifically, we introduce Lagrangian multipliers $\lambda 1_r$, $\lambda 2_r$, $\lambda 3_r$, $\lambda 4_r$, $\lambda 5_{ri}$, $\lambda 6_{ri}$, $\lambda 7_{ri}$, $\lambda 8_{ri}$ to dualize interconnecting constraints (7.26), (7.27), (7.28), (7.29), (7.30), (7.31), (7.32), (7.33), respectively. Here, $\lambda 1_r$, $\lambda 2_r$, $\lambda 7_{ri}$, $\lambda 8_{ri}$ are positive values. The multipliers $\lambda 1_r$ and $\lambda 3_r$ can be interpreted as the prices paid to local operators for departing shipments from origin terminals. The multipliers $\lambda 2_r$ and $\lambda 4_r$ can be interpreted as the costs paid for delivering shipments to destination terminals. The multipliers $\lambda 5_{ri}$ and $\lambda 6_{ri}$ play as the penalty costs charged from local operators due to the violation of spatial compatibility at export/import terminals. The multipliers $\lambda 7_{ri}$ and $\lambda 8_{ri}$ play as the penalty costs charged from local operators due to the violation of time compatibility at export/import terminals. The formulation of the relaxed model is presented as follows:

$$
\begin{aligned}
\textbf{P1 Z1} = \max_{y^t, x^t} & \sum_{r\in R^t} p_r u_r y_r^t - \sum_{o\in\{1,2,3\}} \left(\sum_{r\in R^t\cup\bar{R}^t} \sum_{s\in S^o} c_s x_{rs}^t u_r + \sum_{r\in R^t\cup\bar{R}^t} c_r^{\text{delay}} \mathbb{T}_r^o u_r \right) \\
& + \sum_{r\in R^t} \lambda 1_r \Big(\sum_{s\in S_{or}^{1+}} x_{rs}^t + \sum_{s\in S_{or}^{2+}} x_{rs}^t + \sum_{s\in S_{or}^{3+}} x_{rs}^t - y_r^t \Big) \\
& + \sum_{r\in R^t} \lambda 2_r \Big(\sum_{s\in S_{dr}^{1-}} x_{rs}^t + \sum_{s\in S_{dr}^{2-}} x_{rs}^t + \sum_{s\in S_{dr}^{3-}} x_{rs}^t - y_r^t \Big) \\
& + \sum_{r\in \bar{R}^t} \lambda 3_r \Big(\sum_{s\in S_{or}^{1+}} x_{rs}^t + \sum_{s\in S_{or}^{2+}} x_{rs}^t + \sum_{s\in S_{or}^{3+}} x_{rs}^t - 1 \Big) \\
& + \sum_{r\in \bar{R}^t} \lambda 4_r \Big(\sum_{s\in S_{dr}^{1-}} x_{rs}^t + \sum_{s\in S_{dr}^{2-}} x_{rs}^t + \sum_{s\in S_{dr}^{3-}} x_{rs}^t - 1 \Big) \\
& + \sum_{r\in R^t\cup\bar{R}^t} \sum_{i\in N^{\text{exp}}\setminus\{o_r,d_r\}} \lambda 5_{ri} \left(\sum_{s\in S_i^{1+}} x_{rs}^t + \sum_{s\in S_i^{2+}} x_{rs}^t - \sum_{s\in S_i^{1-}} x_{rs}^t - \sum_{s\in S_i^{2-}} x_{rs}^t \right) \\
& + \sum_{r\in R^t\cup\bar{R}^t} \sum_{i\in N^{\text{imp}}\setminus\{o_r,d_r\}} \lambda 6_{ri} \left(\sum_{s\in S_i^{2+}} x_{rs}^t + \sum_{s\in S_i^{3+}} x_{rs}^t - \sum_{s\in S_i^{2-}} x_{rs}^t - \sum_{s\in S_i^{3-}} x_{rs}^t \right) \\
& + \sum_{r\in R^t\cup\bar{R}^t} \sum_{i\in N^{\text{exp}}\setminus\{o_r,d_r\}} \lambda 7_{ri} \left(t_{ri}^+ - t_{ri}^- \right) \\
& + \sum_{r\in R^t\cup\bar{R}^t} \sum_{i\in N^{\text{imp}}\setminus\{o_r,d_r\}} \lambda 8_{ri} \left(t_{ri}^+ - t_{ri}^- \right)
\end{aligned}
\tag{7.35}
$$

subject to Constraints (7.3-7.9,7.15-7.25) for $o \in \{1,2,3\}$.

Model **P1** is easy to be decomposed into following four operator-based subproblems:

- LR-based model for global operator.

$$
\textbf{P1-0} \ \max_{y^t} \sum_{r\in R^t} p_r u_r y_r^t - \sum_{r\in R^t} \lambda 1_r y_r^t - \sum_{r\in R^t} \lambda 2_r y_r^t \tag{7.36}
$$

- LR-based model for operator 1.

$$
\begin{aligned}
\textbf{P1-1} \ \min_{x^t} & \sum_{r\in R^t\cup\bar{R}^t} \sum_{s\in S^1} c_s x_{rs}^t u_r + \sum_{r\in R^t\cup\bar{R}^t} c_r^{\text{delay}} \mathbb{T}_r^1 u_r \\
& - \sum_{r\in R^t} \lambda 1_r \sum_{s\in S_{or}^{1+}} x_{rs}^t - \sum_{r\in R^t} \lambda 2_r \sum_{s\in S_{dr}^{1-}} x_{rs}^t - \sum_{r\in \bar{R}^t} \lambda 3_r \sum_{s\in S_{or}^{1+}} x_{rs}^t \\
& - \sum_{r\in \bar{R}^t} \lambda 4_r \sum_{s\in S_{dr}^{1-}} x_{rs}^t - \sum_{r\in R^t\cup\bar{R}^t} \sum_{i\in N^{\text{exp}}\setminus\{o_r,d_r\}} \lambda 5_{ri} \left(\sum_{s\in S_i^{1+}} x_{rs}^t - \sum_{s\in S_i^{1-}} x_{rs}^t \right) \\
& + \sum_{r\in R^t\cup\bar{R}^t} \sum_{i\in N^{\text{exp}}\setminus\{o_r,d_r\}} \lambda 7_{ri} t_{ri}^-
\end{aligned}
\tag{7.37}
$$

subject to Constraints (7.3-7.9,7.15-7.25) for $o = 1$.

- LR-based model for operator 2.

$$\begin{aligned}
\textbf{P1-2}\ \min_{x^t} & \sum_{r\in R^t\cup\bar{R}^t}\sum_{s\in S^2} c_s x^t_{rs}u_r + \sum_{r\in R^t\cup\bar{R}^t} c^{\text{delay}}_r \mathbb{T}^2_r u_r \\
& - \sum_{r\in R^t}\lambda 1_r \sum_{s\in S^{2+}_{or}} x^t_{rs} - \sum_{r\in R^t}\lambda 2_r \sum_{s\in S^{2-}_{d_r}} x^t_{rs} - \sum_{r\in \bar{R}^t}\lambda 3_r \sum_{s\in S^{2+}_{or}} x^t_{rs} \\
& - \sum_{r\in \bar{R}^t}\lambda 4_r \sum_{s\in S^{2-}_{d_r}} x^t_{rs} - \sum_{r\in R^t\cup\bar{R}^t}\sum_{i\in N^{\text{exp}}\setminus\{o_r,d_r\}} \lambda 5_{ri}\left(\sum_{s\in S^{2+}_i} x^t_{rs} - \sum_{s\in S^{2-}_i} x^t_{rs}\right) \\
& - \sum_{r\in R^t\cup\bar{R}^t}\sum_{i\in N^{\text{imp}}\setminus\{o_r,d_r\}} \lambda 6_{ri}\left(\sum_{s\in S^{2+}_i} x^t_{rs} - \sum_{s\in S^{2-}_i} x^t_{rs}\right) \\
& - \sum_{r\in R^t\cup\bar{R}^t}\sum_{i\in N^{\text{exp}}\setminus\{o_r,d_r\}} \lambda 7_{ri} t^+_{ri} + \sum_{r\in R^t\cup\bar{R}^t}\sum_{i\in N^{\text{imp}}\setminus\{o_r,d_r\}} \lambda 8_{ri} t^-_{ri}
\end{aligned} \tag{7.38}$$

  subject to Constraints (7.3-7.9,7.15-7.25) for $o = 2$.

- LR-based model for operator 3.

$$\begin{aligned}
\textbf{P1-3}\ \min_{x^t} & \sum_{r\in R^t\cup\bar{R}^t}\sum_{s\in S^3} c_s x^t_{rs}u_r + \sum_{r\in R^t\cup\bar{R}^t} c^{\text{delay}}_r \mathbb{T}^3_r u_r \\
& - \sum_{r\in R^t}\lambda 1_r \sum_{s\in S^{3+}_{or}} x^t_{rs} - \sum_{r\in R^t}\lambda 2_r \sum_{s\in S^{3-}_{d_r}} x^t_{rs} - \sum_{r\in \bar{R}^t}\lambda 3_r \sum_{s\in S^{3+}_{or}} x^t_{rs} \\
& - \sum_{r\in \bar{R}^t}\lambda 4_r \sum_{s\in S^{3-}_{d_r}} x^t_{rs} - \sum_{r\in R^t\cup\bar{R}^t}\sum_{i\in N^{\text{imp}}\setminus\{o_r,d_r\}} \lambda 6_{ri}\left(\sum_{s\in S^{3+}_i} x^t_{rs} - \sum_{s\in S^{3-}_i} x^t_{rs}\right) \\
& - \sum_{r\in R^t\cup\bar{R}^t}\sum_{i\in N^{\text{imp}}\setminus\{o_r,d_r\}} \lambda 8_{ri} t^-_{ri}
\end{aligned} \tag{7.39}$$

  subject to Constraints (7.3-7.9,7.15-7.25) for $o = 3$.

We assume (y^*, x^*) as the optimal solution of the original problem **P0**, (y^{**}, x^{**}) as the optimal solution of dual problem **P1**. However, the optimal solution of the dual problem might be infeasible to the original problem. Therefore, we transform the infeasible solution to a feasible solution by setting $y_r = 0, [x_{rs}] = [0]$ for request r, and define (y, x) as the transformed feasible solution of the original problem. Based on the properties of Lagrangian relaxation, we can get $\mathbf{Z0}(y,x) \le \mathbf{Z0}(y^*,x^*) \le \mathbf{Z1}(y^*,x^*) \le \mathbf{Z1}(y^{**},x^{**})$. We define $LB = \mathbf{Z0}(y,x)$ as the lower bound of the original problem, and define $UB = \mathbf{Z1}(y^{**},x^{**})$ as the upper bound of the original problem. In convex problems, when $UB = LB$, the obtained solution is the optimal solution to the original problem. Due to the existence of binary variables, the original problem is not convex. Therefore, we can not prove the optimality of the solution when $UB = LB$ for the original problem. However, this solution will be the best solution that we can find under the LR approach. Therefore, the objective of the LR is to find the optimum Lagrangian multipliers that satisfy $UB = LB$.

Since the dual problem **P1** is not differentiable everywhere due to the existence of binary variables, a standard subgradient method is used to update the Lagrangian multipliers,

shown as follows:

$$\lambda 1_r^{n+1} = \max\{0, \lambda 1_r^n + \rho 1_r^n (y_r^t - \sum_{s \in S_{or}^{1+}} x_{rs}^t - \sum_{s \in S_{or}^{2+}} x_{rs}^t - \sum_{s \in S_{or}^{3+}} x_{rs}^t)\}, \quad \forall r \in R^t, \tag{7.40}$$

$$\lambda 2_r^{n+1} = \max\{0, \lambda 2_r^n + \rho 2_r^n (y_r^t - \sum_{s \in S_{dr}^{1-}} x_{rs}^t - \sum_{s \in S_{dr}^{2-}} x_{rs}^t - \sum_{s \in S_{dr}^{3-}} x_{rs}^t)\}, \quad \forall r \in R^t, \tag{7.41}$$

$$\lambda 3_r^{n+1} = \lambda 3_r^n + \rho 3_r^n (1 - \sum_{s \in S_{or}^{1+}} x_{rs}^t - \sum_{s \in S_{or}^{2+}} x_{rs}^t - \sum_{s \in S_{or}^{3+}} x_{rs}^t), \quad \forall r \in \bar{R}^t, \tag{7.42}$$

$$\lambda 4_r^{n+1} = \lambda 2_r^n + \rho 4_r^n (1 - \sum_{s \in S_{dr}^{1-}} x_{rs}^t - \sum_{s \in S_{dr}^{2-}} x_{rs}^t - \sum_{s \in S_{dr}^{3-}} x_{rs}^t)\}, \quad \forall r \in \bar{R}^t, \tag{7.43}$$

$$\lambda 5_{ri}^{n+1} = \lambda 5_{ri}^n + \rho 5_r^n \left(\sum_{s \in S_i^{1-}} x_{rs}^t + \sum_{s \in S_i^{2-}} x_{rs}^t - \sum_{s \in S_i^{1+}} x_{rs}^t - \sum_{s \in S_i^{2+}} x_{rs}^t \right), \quad \forall r \in R^t \cup \bar{R}^t, i \in N^{\exp} \backslash \{o_r, d_r\}, \tag{7.44}$$

$$\lambda 6_{ri}^{n+1} = \lambda 6_{ri}^n + \rho 6_r^n \left(\sum_{s \in S_i^{2-}} x_{rs}^t + \sum_{s \in S_i^{3-}} x_{rs}^t - \sum_{s \in S_i^{2+}} x_{rs}^t - \sum_{s \in S_i^{3+}} x_{rs}^t \right), \quad \forall r \in R^t \cup \bar{R}^t, i \in N^{\text{imp}} \backslash \{o_r, d_r\}, \tag{7.45}$$

$$\lambda 7_{ri}^{n+1} = \max\{0.0001, \lambda 7_{ri}^n + \rho 7_{ri}^n (t_{ri}^- - t_{ri}^+)\}, \quad \forall r \in R^t \cup \bar{R}^t, i \in N^{\exp} \backslash \{o_r, d_r\}, \tag{7.46}$$

$$\lambda 8_{ri}^{n+1} = \max\{0.00015, \lambda 8_{ri}^n + \rho 8_{ri}^n (t_{ri}^- - t_{ri}^+)\}, \quad \forall r \in R^t \cup \bar{R}^t, i \in N^{\text{imp}} \backslash \{o_r, d_r\}, \tag{7.47}$$

where the superscript n is the iteration index used in the dual updating process; ρ^n is the step size at iteration n. To mitigate the issues of slow convergence, early stopping, and possible traps in local optimality, the step size parameters are updated as following strategy: $\rho^{n+1} = \theta 1 * \rho^n$ if $\lambda^{n+1} > \lambda^n$; $\rho^{n+1} = \theta 2 * \rho^n$ if $\lambda^{n+1} < \lambda^n$; $\theta 1 > 1$, $0 < \theta 2 < 1$; $\rho^{\min}$ is the minimum value of ρ; $\rho^{\max}$ is the maximum value. Regarding the minimum value of $\lambda 7_{ri}$ and $\lambda 8_{rj}$, the reason we give different positive values is to avoid the traps in generating the same infeasible departure/arrival times at export/import terminals by model **P1-2** when $s \in S^2, x_{rs} = 1$, $o_s = i$, $d_s = j$.

The solution framework of the LR approach is presented in Algorithm 7.1. At the modification step, in addition to the updating procedure of Lagrangian multipliers, we set lower bounds of departure time of truck service s with shipment r and lower bounds of departure time at export and import terminals. These lower bounds are updated based on infeasible solutions received at the current iteration. In this way, time variables can avoid the infeasible loop that when the Lagrangian multiplier is a positive value, the minimum value is always chosen as departure times; when the Lagrangian multiplier is a negative value, the maximum value is always chosen as departure times.

7.4.2 Augmented Lagrangian relaxation method

In this section, we develop the ALR method to deal with interconnecting constraints (7.32) and (7.33). The ALR method was first proposed by Hestenes [40] and Powell [69] to eliminate the duality gap between the equality constrained problem and its Lagrangian dual prob-

Algorithm 7.1 LR-based solution framework.

1: **Initialization**. Set iteration number $n = 0$; maximum iteration number $N^{\text{iteration}}$; Lagrangian multipliers $\lambda^n = [0]$; positive parameters ρ^0; assign small positive numbers to $\theta 1$, $\theta 2$, $\xi 1$, $\xi 2$, $a1$, $a2$; lower bounds of departure times of service $s \in S^{3+\text{truck}}$ $[lb_{rs}] = [0]$; lower bound of departure time at export and import terminals $[lb_{ri}] = [0]$; number of infeasible transshipments $[N^{\text{Inf}}] = [0]$;

2: **Optimization**. Solve **P1-0** - **P1-3** in parallel, and obtain solution $[y_r^t]$, $[x_{rs}^t]$, $[\mathbb{T}_r]$, $[t_{ri}^+]$, and $[t_{ri}^-]$ for the nth iteration.

3: **Modification**. Update the Lagrangian multiplier λ^{n+1} based on equations (7.40-7.47); update the lower bounds for departure time of truck services lb_{rs} for $r \in R^t \cup \bar{R}^t, s \in S_i^{3+\text{truck}}$: $lb_{rs} = t_{ri}^- + lt_i^{MT_s}$; for $r \in R^t \cup \bar{R}^t, i \in N^{\text{exp}} \backslash \{o_r, d_r\}$, if $t_{ri}^+ < t_{ri}^-$, $N_{ri}^{\text{Inf}} = N^{\text{Inf}} + 1$; if $N^{\text{Inf}} > a1$, update lower bounds of departure time at export terminal: $lb_{ri} = t_{ri}^+ + 1$. If $t_{ri}^+ < t_{ri}^-$ for $r \in R^t \cup \bar{R}^t, i \in N^{\text{imp}} \backslash \{o_r, d_r\}$, $N_{ri}^{\text{Inf}} = N^{\text{Inf}} + 1$; if $N^{\text{Inf}} > a2$, $lb_{ri} = t_{ri}^+ + 1$.

4: **Calculation**. Calculate lower bound LB: for $r \in R^t \cup \bar{R}^t$, if y_r^t, $[x_{rs}^t]$ are infeasible solutions, reject request r, $y_r^t \leftarrow 0$, $[x_{rs}^t] \leftarrow [0]$; calculate upper bound UB: the Lagrangian objective function.

5: **Termination**. Terminate if either of the following criteria is satisfied:

- $|\lambda^{n+1} - \lambda^n| \leq \xi 1$;
- $|UB - LB|/UB \leq \xi 2$;
- $n > N^{\text{iteration}}$.

6: $n \leftarrow n + 1$, and go to step (2).

lem. This method was later extended by Rockafellar [78] to deal with inequality constraints. Similar to the LR approach, the ALR approach relaxes the interconnecting constraints by adding a linear penalty term to the objective function **Z0**. The difference is that the ALR approach adds an additional quadratic terms to mimic a Lagrangian multiplier [57]. We use $Q(y^t, x^t, \lambda 1, \lambda 2, \lambda 3, \lambda 4, \lambda 5, \lambda 6)$ to represent the relaxed objective function including interconnecting constraints (7.26-7.31). The ALR-based model is defined as:

$$\begin{aligned}
\textbf{P2 Z2} = \max_{y^t, x^t} & Q(y^t, x^t, \lambda 1, \lambda 2, \lambda 3, \lambda 4, \lambda 5, \lambda 6) \\
& - \sum_{r \in R^t \cup \bar{R}^t} \sum_{i \in N^{\text{exp}} \backslash \{o_r, d_r\}} \lambda 7_{ri} \Delta t_{ri} - \sum_{r \in R^t \cup \bar{R}^t} \sum_{i \in N^{\text{exp}} \backslash \{o_r, d_r\}} \frac{\rho 7_{ri}}{2} \Delta t_{ri}^2 \\
& - \sum_{r \in R^t \cup \bar{R}^t} \sum_{i \in N^{\text{imp}} \backslash \{o_r, d_r\}} \lambda 8_{ri} \Delta t_{ri} - \sum_{r \in R^t \cup \bar{R}^t} \sum_{i \in N^{\text{imp}} \backslash \{o_r, d_r\}} \frac{\rho 8_{ri}}{2} \Delta t_{ri}^2
\end{aligned} \tag{7.48}$$

where $\Delta t_{ri} = \max\{0, t_{ri}^- - t_{ri}^+\}$, ρ is a penalty parameter.

The quadratic term in the ALR formulation is non-separable which preventing us from decomposing the dual problem to local operator-related subproblems. Therefore, we introduce a parallel scheme to approximate it. The parallel scheme applies the auxiliary problem principle to decouple the quadratic terms, as shown in model **P2-0**-**P2-3**:

- ALR-based model for global operator: **P2-0** = **P1-0**.

- ALR-based model for operator 1.

$$
\begin{aligned}
\textbf{P2-1}\ \min_{x^t} & \sum_{r\in R^t\cup\bar{R}^t}\sum_{s\in S^1} c_s x^t_{rs} u_r + \sum_{r\in R^t\cup\bar{R}^t} c^{\text{delay}}_r \mathbb{T}^1_r u_r \\
& - \sum_{r\in\bar{R}^t}\lambda 1_r \sum_{s\in S^{1+}_{or}} x^t_{rs} - \sum_{r\in R^t}\lambda 2_r \sum_{s\in S^{1-}_{d_r}} x^t_{rs} - \sum_{r\in\bar{R}^t}\lambda 3_r \sum_{s\in S^{1+}_{or}} x^t_{rs} \\
& - \sum_{r\in\bar{R}^t}\lambda 4_r \sum_{s\in S^{1-}_{d_r}} x^t_{rs} - \sum_{r\in R^t\cup\bar{R}^t}\sum_{i\in N^{\text{exp}}\setminus\{o_r,d_r\}} \lambda 5_{ri}\left(\sum_{s\in S^{1+}_i} x^t_{rs} - \sum_{s\in S^{1-}_i} x^t_{rs}\right) \\
& + \sum_{r\in R^t\cup\bar{R}^t}\sum_{i\in N^{\text{exp}}\setminus\{o_r,d_r\}} \lambda 7_{ri}\Delta t1_{ri} + \sum_{r\in R^t\cup\bar{R}^t}\sum_{i\in N^{\text{exp}}\setminus\{o_r,d_r\}} \frac{\rho 7_{ri}}{2}\Delta t1^2_{ri} \\
& + \sum_{r\in R^t\cup\bar{R}^t}\sum_{i\in N^{\text{exp}}\setminus\{o_r,d_r\}} \frac{b7_{ri}-\rho 7_{ri}}{2}\left(t^-_{ri} - t^{-(n-1)}_{ri}\right)^2
\end{aligned}
\tag{7.49}
$$

subject to Constraints (7.3-7.9,7.15-7.25) for $o = 1$, where $\Delta t1_{ri} = \max\{0, t^-_{ri} - t^{+(n-1)}_{ri}\}$.

- ALR-based model for operator 2.

$$
\begin{aligned}
\textbf{P2-2}\ \min_{x^t} & \sum_{r\in R^t\cup\bar{R}^t}\sum_{s\in S^2} c_s x^t_{rs} u_r + \sum_{r\in R^t\cup\bar{R}^t} c^{\text{delay}}_r \mathbb{T}^2_r u_r \\
& - \sum_{r\in R^t}\lambda 1_r \sum_{s\in S^{2+}_{or}} x^t_{rs} - \sum_{r\in R^t}\lambda 2_r \sum_{s\in S^{2-}_{d_r}} x^t_{rs} \\
& - \sum_{r\in\bar{R}^t}\lambda 3_r \sum_{s\in S^{2+}_{or}} x^t_{rs} - \sum_{r\in\bar{R}^t}\lambda 4_r \sum_{s\in S^{2-}_{d_r}} x^t_{rs} \\
& - \sum_{r\in R^t\cup\bar{R}^t}\sum_{i\in N^{\text{exp}}\setminus\{o_r,d_r\}} \lambda 5_{ri}\left(\sum_{s\in S^{2+}_i} x^t_{rs} - \sum_{s\in S^{2-}_i} x^t_{rs}\right) \\
& - \sum_{r\in R^t\cup\bar{R}^t}\sum_{i\in N^{\text{imp}}\setminus\{o_r,d_r\}} \lambda 6_{ri}\left(\sum_{s\in S^{2+}_i} x^t_{rs} - \sum_{s\in S^{2-}_i} x^t_{rs}\right) \\
& + \sum_{r\in R^t\cup\bar{R}^t}\sum_{i\in N^{\text{exp}}\setminus\{o_r,d_r\}} \lambda 7_{ri}\Delta t21_{ri} + \sum_{r\in R^t\cup\bar{R}^t}\sum_{i\in N^{\text{exp}}\setminus\{o_r,d_r\}} \frac{\rho 7_{ri}}{2}\Delta t21^2_{ri} \\
& + \sum_{r\in R^t\cup\bar{R}^t}\sum_{i\in N^{\text{exp}}\setminus\{o_r,d_r\}} \frac{b7_{ri}-\rho 7_{ri}}{2}\left(t^+_{ri} - t^{+(n-1)}_{ri}\right)^2 \\
& + \sum_{r\in R^t\cup\bar{R}^t}\sum_{i\in N^{\text{imp}}\setminus\{o_r,d_r\}} \lambda 8_{ri}\Delta t22_{ri} + \sum_{r\in R^t\cup\bar{R}^t}\sum_{i\in N^{\text{imp}}\setminus\{o_r,d_r\}} \frac{\rho 8_{ri}}{2}\Delta t22^2_{ri} \\
& + \sum_{r\in R^t\cup\bar{R}^t}\sum_{i\in N^{\text{imp}}\setminus\{o_r,d_r\}} \frac{b8_{ri}-\rho 8_{ri}}{2}\left(t^-_{ri} - t^{-(n-1)}_{ri}\right)^2
\end{aligned}
\tag{7.50}
$$

subject to Constraints (7.3-7.9,7.15-7.25) for $o = 2$, where $\Delta t21_{ri} = \max\{0, t^{-(n-1)}_{ri} - t^+_{ri}\}$, $\Delta t22_{ri} = \max\{0, t^-_{ri} - t^{+(n-1)}_{ri}\}$.

- ALR-based model for operator 3.

$$
\begin{aligned}
\textbf{P2-3}\ \min_{x^t} & \sum_{r\in R^t\cup\bar{R}^t}\sum_{s\in S^3} c_s x^t_{rs} u_r + \sum_{r\in R^t\cup\bar{R}^t} c^{\text{delay}}_r \mathbb{T}^3_r u_r \\
& - \sum_{r\in R^t} \lambda 1_r \sum_{s\in S^{3+}_{or}} x^t_{rs} - \sum_{r\in R^t} \lambda 2_r \sum_{s\in S^{3-}_{dr}} x^t_{rs} \\
& - \sum_{r\in \bar{R}^t} \lambda 3_r \sum_{s\in S^{3+}_{or}} x^t_{rs} - \sum_{r\in \bar{R}^t} \lambda 4_r \sum_{s\in S^{3-}_{dr}} x^t_{rs} \\
& - \sum_{r\in R^t\cup\bar{R}^t}\sum_{i\in N^{\text{exp}}\setminus\{o_r,d_r\}} \lambda 5_{ri}\left(\sum_{s\in S^{3+}_i} x^t_{rs} - \sum_{s\in S^{3-}_i} x^t_{rs}\right) \\
& - \sum_{r\in R^t\cup\bar{R}^t}\sum_{i\in N^{\text{imp}}\setminus\{o_r,d_r\}} \lambda 6_{ri}\left(\sum_{s\in S^{3+}_i} x^t_{rs} - \sum_{s\in S^{3-}_i} x^t_{rs}\right) \\
& + \sum_{r\in R^t\cup\bar{R}^t}\sum_{i\in N^{\text{imp}}\setminus\{o_r,d_r\}} \lambda 8_{ri}\Delta t3_{ri} + \sum_{r\in R^t\cup\bar{R}^t}\sum_{i\in N^{\text{imp}}\setminus\{o_r,d_r\}} \frac{\rho 8_{ri}}{2}\Delta t3^2_{ri} \\
& + \sum_{r\in R^t\cup\bar{R}^t}\sum_{i\in N^{\text{imp}}\setminus\{o_r,d_r\}} \frac{b8_{ri}-\rho 8_{ri}}{2}\left(t^+_{ri} - t^{+(n-1)}_{ri}\right)^2
\end{aligned}
\tag{7.51}
$$

subject to Constraints (7.3-7.9,7.15-7.25) for $o = 3$, where $\Delta t3 = \max\{0, t^{-(n-1)}_{ri} - t^+_{ri}\}$.

To find the optimum Lagrangian multipliers, we apply the same subgradient method to update Lagrangian multipliers $\lambda 1$ to $\lambda 6$, shown in equations (7.40-7.45). Lagrangian multipliers $\lambda 7$ and $\lambda 8$ are iteratively updated by

$$\lambda 7^{n+1}_{ri} = \lambda 7^n_{ri} + \rho 7^n_{ri}\Delta t_{ri}, \forall r \in R^t \cup \bar{R}^t, i \in N^{\text{exp}}\setminus\{o_r, d_r\}, \tag{7.52}$$

$$\lambda 8^{n+1}_{ri} = \lambda 8^n_{ri} + \rho 8^n_{ri}\Delta t_{ri},\ \forall r \in R^t \cup \bar{R}^t, i \in N^{\text{imp}}\setminus\{o_r, d_r\}, \tag{7.53}$$

where $\Delta t_{ri} = \max\{0, t^-_{ri} - t^+_{ri}\}$.

The solution framework of the ALR approach is shown in Algorithm 7.2 The ALR framework is similar to the LR framework, except the optimization model and Lagrangian multipliers updating equations.

7.4.3 Alternating directing method of multipliers

In this section, we develop the ADMM method to handle interconnecting constraints (7.32)-(7.33). The ADMM method is a variant of the ALR method that uses partial updates for the dual variables [115]. The relaxed model is the same as the ALR model, namely **P3** = **P2**. Under the ADMM, operator-related problems are optimized in serial, as shown in model **P3-0**-**P3-3**.

- ADMM-based model for global operator: **P3-0** = **P1-0**

Algorithm 7.2 ALR-based solution framework.

1: **Initialization**. Set iteration number $n = 0$; maximum iteration number $N^{\text{iteration}}$; Lagrangian multipliers $\lambda^n = [0]$; positive parameters ρ^0 and b^0; assign small positive numbers to $\theta 1$, $\theta 2$, $\xi 1$, $\xi 2$, $a1$, $a2$; lower bounds of departure times of service $s \in S^{3+\text{truck}}$ $[lb_{rs}] = [0]$; lower bound of departure time at export and import terminals $[lb_{ri}] = [0]$; number of infeasible transshipment $[N^{\text{Inf}}] = [0]$;

2: **Optimization**. Solve **P2-0** - **P2-3** in parallel, and obtain solution $[y_r^t]$, $[x_{rs}^t]$, $[\mathbb{T}_r]$, $[t_{ri}^+]$, and $[t_{ri}^-]$ for the nth iteration.

3: **Modification**. Update the Lagrangian multiplier λ^{n+1} based on equations (7.40-7.45), (7.52-7.53); update the lower bounds for departure time of truck services lb_{rs} for $r \in R^t \cup \bar{R}^t, s \in S_i^{3+\text{truck}}$: $lb_{rs} = t_{ri}^- + lt_i^{MT_s}$; for $r \in R^t \cup \bar{R}^t, i \in N^{\text{exp}} \backslash \{o_r, d_r\}$, if $t_{ri}^+ < t_{ri}^-$, $N_{ri}^{\text{Inf}} = N^{\text{Inf}} + 1$; if $N^{\text{Inf}} > a1$, update lower bounds of departure time at export terminal: $lb_{ri} = t_{ri}^+ + 1$. If $t_{ri}^+ < t_{ri}^-$ for $r \in R^t \cup \bar{R}^t, i \in N^{\text{imp}} \backslash \{o_r, d_r\}$, $N_{ri}^{\text{Inf}} = N^{\text{Inf}} + 1$; if $N^{\text{Inf}} > a2$, $lb_{ri} = t_{ri}^+ + 1$.

4: **Calculation**. Calculate lower bound LB: for $r \in R^t \cup \bar{R}^t$, if y_r^t, $[x_{rs}^t]$ are infeasible solutions, reject request r, $y_r^t \leftarrow 0$, $[x_{rs}^t] \leftarrow [0]$; calculate upper bound UB: the Lagrangian objective function.

5: **Termination**. Terminate if either of the following criteria is satisfied:

- $|\lambda^{n+1} - \lambda^n| \le \xi 1$;
- $|UB - LB|/UB \le \xi 2$;
- $n > N^{\text{iteration}}$.

6: $n \leftarrow n + 1$, and go to step (2).

- ADMM-based model for operator 1.

$$
\begin{aligned}
\textbf{P3-1} \min_{x^t} & \sum_{r \in R^t \cup \bar{R}^t} \sum_{s \in S^1} c_s x_{rs}^t u_r + \sum_{r \in R^t \cup \bar{R}^t} c_r^{\text{delay}} \mathbb{T}_r^1 u_r \\
& - \sum_{r \in R^t} \lambda 1_r \sum_{s \in S_{o_r}^{1+}} x_{rs}^t - \sum_{r \in R^t} \lambda 2_r \sum_{s \in S_{d_r}^{1-}} x_{rs}^t \\
& - \sum_{r \in \bar{R}^t} \lambda 3_r \sum_{s \in S_{o_r}^{1+}} x_{rs}^t - \sum_{r \in \bar{R}^t} \lambda 4_r \sum_{s \in S_{d_r}^{1-}} x_{rs}^t \\
& - \sum_{r \in R^t \cup \bar{R}^t} \sum_{i \in N^{\text{exp}} \backslash \{o_r, d_r\}} \lambda 5_{ri} \left(\sum_{s \in S_i^{1+}} x_{rs}^t - \sum_{s \in S_i^{1-}} x_{rs}^t \right) \\
& + \sum_{r \in R^t \cup \bar{R}^t} \sum_{i \in N^{\text{exp}} \backslash \{o_r, d_r\}} \lambda 7_{ri} \Delta t 1_{ri} + \sum_{r \in R^t \cup \bar{R}^t} \sum_{i \in N^{\text{exp}} \backslash \{o_r, d_r\}} \frac{\rho 7_{ri}}{2} \Delta t 1_{ri}^2
\end{aligned}
\tag{7.54}
$$

subject to Constraints (7.3-7.9,7.15-7.25) for $o = 1$, where $\Delta t 1_{ri} = \max\{0, t_{ri}^- - t_{ri}^{+(n-1)}\}$.

- ADMM-based model for operator 2.

$$
\begin{aligned}
\textbf{P3-2}\ \min_{x^t} & \sum_{r\in R^t\cup\bar{R}^t}\sum_{s\in S^2} c_s x^t_{rs} u_r + \sum_{r\in R^t\cup\bar{R}^t} c^{\text{delay}}_r \mathbb{T}^2_r u_r \\
& - \sum_{r\in\bar{R}^t}\lambda 1_r \sum_{s\in S^{2+}_{or}} x^t_{rs} - \sum_{r\in R^t}\lambda 2_r \sum_{s\in S^{2-}_{dr}} x^t_{rs} - \sum_{r\in\bar{R}^t}\lambda 3_r \sum_{s\in S^{2+}_{or}} x^t_{rs} \\
& - \sum_{r\in\bar{R}^t}\lambda 4_r \sum_{s\in S^{2-}_{dr}} x^t_{rs} - \sum_{r\in R^t\cup\bar{R}^t}\sum_{i\in N^{\text{exp}}\setminus\{o_r,d_r\}} \lambda 5_{ri}\left(\sum_{s\in S^{2+}_i} x^t_{rs} - \sum_{s\in S^{2-}_i} x^t_{rs}\right) \\
& - \sum_{r\in R^t\cup\bar{R}^t}\sum_{i\in N^{\text{imp}}\setminus\{o_r,d_r\}} \lambda 6_{ri}\left(\sum_{s\in S^{2+}_i} x^t_{rs} - \sum_{s\in S^{2-}_i} x^t_{rs}\right) \\
& + \sum_{r\in R^t\cup\bar{R}^t}\sum_{i\in N^{\text{exp}}\setminus\{o_r,d_r\}} \lambda 7_{ri}\Delta t21_{ri} + \sum_{r\in R^t\cup\bar{R}^t}\sum_{i\in N^{\text{exp}}\setminus\{o_r,d_r\}} \frac{\rho 7_{ri}}{2}\Delta t21^2_{ri} \\
& + \sum_{r\in R^t\cup\bar{R}^t}\sum_{i\in N^{\text{imp}}\setminus\{o_r,d_r\}} \lambda 8_{ri}\Delta t22_{ri} + \sum_{r\in R^t\cup\bar{R}^t}\sum_{i\in N^{\text{imp}}\setminus\{o_r,d_r\}} \frac{\rho 8_{ri}}{2}\Delta t22^2_{ri}
\end{aligned}
\tag{7.55}
$$

subject to Constraints (7.3-7.9,7.15-7.25) for $o=2$, where $\Delta t21_{ri}=\max\{0,t^{-(n)}_{ri}-t^{+}_{ri}\}$, $\Delta t22_{ri}=\max\{0,t^{-}_{ri}-t^{+(n-1)}_{ri}\}$.

- ADMM-based model for operator 3.

$$
\begin{aligned}
\textbf{P3-3}\ \min_{x^t} & \sum_{r\in R^t\cup\bar{R}^t}\sum_{s\in S^3} c_s x^t_{rs} u_r + \sum_{r\in R^t\cup\bar{R}^t} c^{\text{delay}}_r \mathbb{T}^3_r u_r \\
& - \sum_{r\in\bar{R}^t}\lambda 1_r \sum_{s\in S^{3+}_{or}} x^t_{rs} - \sum_{r\in R^t}\lambda 2_r \sum_{s\in S^{3-}_{dr}} x^t_{rs} - \sum_{r\in\bar{R}^t}\lambda 3_r \sum_{s\in S^{3+}_{or}} x^t_{rs} \\
& - \sum_{r\in\bar{R}^t}\lambda 4_r \sum_{s\in S^{3-}_{dr}} x^t_{rs} - \sum_{r\in R^t\cup\bar{R}^t}\sum_{i\in N^{\text{exp}}\setminus\{o_r,d_r\}} \lambda 5_{ri}\left(\sum_{s\in S^{3+}_i} x^t_{rs} - \sum_{s\in S^{3-}_i} x^t_{rs}\right) \\
& - \sum_{r\in R^t\cup\bar{R}^t}\sum_{i\in N^{\text{imp}}\setminus\{o_r,d_r\}} \lambda 6_{ri}\left(\sum_{s\in S^{3+}_i} x^t_{rs} - \sum_{s\in S^{3-}_i} x^t_{rs}\right) \\
& + \sum_{r\in R^t\cup\bar{R}^t}\sum_{i\in N^{\text{imp}}\setminus\{o_r,d_r\}} \lambda 8_{ri}\Delta t3_{ri} + \sum_{r\in R^t\cup\bar{R}^t}\sum_{i\in N^{\text{imp}}\setminus\{o_r,d_r\}} \frac{\rho 8_{ri}}{2}\Delta t3^2_{ri}
\end{aligned}
\tag{7.56}
$$

subject to constraints (7.3-7.9,7.15-7.25) for $o=3$, where $\Delta t3=\max\{0,t^{-(n)}_{ri}-t^{+}_{ri}\}$.

The Lagrangian multipliers are updated by using equations (7.40-7.45), (7.52-7.53).

The solution framework of the ADMM approach is very similar to the ALR approach, except the optimization models **P3-1**-**P3-3** are solved in serial.

7.5 Preprocessing-based heuristic algorithm

Due to the computational complexity of the optimization models discussed above, in this section, we present a preprocessing-based heuristic algorithm to generate timely solutions at each iteration. The algorithm is adapted from the work of Guo et al. [35]. Different from [35], the heuristic designed in this chapter aims to find the set of feasible paths within each local network instead of global paths. It mainly consists of three steps: preprocessing of feasible paths; preprocessing of feasible matches; path-based mathematical models.

Preprocessing of feasible paths. We define a path p as a combination of one or more services in sequence. A path p is feasible if the services inside a combination satisfy time-spatial compatibility. Specifically, for two consecutive services s_i, s_{i+1} within path p, the destination of service s_i must be the same as the origin of service s_{i+1}; the arrival time of service s_i must be earlier than the departure time of service s_{i+1} minus loading and unloading time and travel time variations at transshipment terminal d_{s_i}. Let L be the maximum number of services within a path. The set $P = \{P^1, P^2, P^3\}$ denotes the collection of feasible paths, and P^i denotes the set of feasible paths in the local network of operator i.

Preprocessing of feasible matches. A match $\langle r, p\rangle$ means shipment r will be transported by path p from its origin to destination. A match between request $r \in R$ and path $p = [s_1, ..., s_l] \in P$ is feasible if it satisfies time compatibility: the release time of request r should be earlier than the departure time of service s_1 minus loading time and travel time variations at origin terminal o_{s_1}. Let Φ_r^o be the set of feasible paths within network o for request r, and let c_p denote the transport costs of path p. Let TD_{rp} denote the departure time of request r with path p; let TA_{rp} be the arrival time of request r with path p; let t_{rp} be the transport time of request r with path p.

Mathematical model. Based on the above preprocessing procedures, the objective function is updated to maximize the total profits for the acceptance and matching of requests with feasible paths. We denote z_{rp}^t as a binary variable which is 1 if request $r \in R^t \cup \bar{R}^t$ is matched with path $p \in P = \{P^1, P^2, P^3\}$, and 0 otherwise. Model **P0** changes to:

$$\textbf{P4}\ \ \textbf{Z4} = \max_{y^t, z^t} \sum_{r \in R^t} p_r u_r y_r^t - \sum_{o \in \{1,2,3\}} \left(\sum_{r \in R^t \cup \bar{R}^t} \sum_{p \in \Phi_r^o} c_p z_{rp}^t u_r + \sum_{r \in R^t \cup \bar{R}^t} c_r^{\text{delay}} \mathbb{T}_r^o u_r \right) \tag{7.57}$$

subject to for $o \in \{1,2,3\}$,

$$\sum_{r \in R} \sum_{p \in \Phi_{rs}^o} u_r z_{rp}^t \le U_s^t, \quad \forall s \in S^o, \tag{7.58}$$

$$\mathbb{T}_r^o \ge TA_{rp} - \mathbb{T}_r^{\text{due}} + \mathbf{M}(z_{rp}^t - 1), \quad \forall r \in R^t \cup \bar{R}^t, p \in \{P^o | d_p = d_r\}, \tag{7.59}$$

$$\mathbb{T}_r^o \ge t_{ri}^+ + t_{rp} - \mathbb{T}_r^{\text{due}} + \mathbf{M}(z_{rp}^t - 1), \quad \forall r \in R^t \cup \bar{R}^t, p \in \{P^{o\text{truck}} | o_p = i, d_p = d_r\}, \tag{7.60}$$

$$t_{ri}^- \ge TA_{rp} + \mathbf{M}(z_{rp}^t - 1), \forall r \in R^t \cup \bar{R}^t, i \in N^{\text{exp}} \cup N^{\text{imp}} \backslash \{o_r, d_r\}, p \in \{P^o | d_p = i\}, \tag{7.61}$$

$$t_{ri}^+ \le TD_{rp} + \mathbf{M}(1 - z_{rp}^t), \forall r \in R^t \cup \bar{R}^t, i \in N^{\text{exp}} \cup N^{\text{imp}} \backslash \{o_r, d_r\}, p \in \{P^o | o_p = i\}, \tag{7.62}$$

where $\Phi_{rs} = \{p \in \Phi_r | s \in p\}$, $P^{o\text{truck}} = \{p = [s_1, ..., s_L] \in P^o | MT_{s_1} = \text{truck}\}$.

Interconnecting constraints change to:

$$y_r^t \leq \sum_{o\in\{1,2,3\}} \sum_{p\in\{P^o|o_p=o_r\}} z_{rp}^t, \quad \forall r \in R^t, \tag{7.63}$$

$$y_r^t \leq \sum_{o\in\{1,2,3\}} \sum_{p\in\{P^o|d_p=d_r\}} z_{rp}^t, \quad \forall r \in R^t, \tag{7.64}$$

$$\sum_{o\in\{1,2,3\}} \sum_{p\in\{P^o|o_p=o_r\}} z_{rp}^t = 1, \quad \forall r \in \bar{R}^t, \tag{7.65}$$

$$\sum_{o\in\{1,2,3\}} \sum_{p\in\{P^o|d_p=d_r\}} z_{rp}^t = 1, \quad \forall r \in \bar{R}^t, \tag{7.66}$$

$$\sum_{p\in\{P^2|o_p=i\}} z_{rp}^t = \sum_{p\in\{P^1|d_p=i\}} z_{rp}^t, \ \forall r \in R^t \cup \bar{R}^t, i \in N^{\text{exp}} \backslash \{o_r, d_r\} \tag{7.67}$$

$$\sum_{p\in\{P^3|o_p=i\}} z_{rp}^t = \sum_{p\in\{P^2|d_p=i\}} z_{rp}^t, \ \forall r \in R^t \cup \bar{R}^t, i \in N^{\text{imp}} \backslash \{o_r, d_r\} \tag{7.68}$$

$$t_{ri}^- \leq t_{ri}^+, \quad \forall r \in R^t \cup \bar{R}^t, i \in N^{\text{exp}} \backslash \{o_r, d_r\}, \tag{7.69}$$

$$t_{ri}^- \leq t_{ri}^+, \quad \forall r \in R^t \cup \bar{R}^t, i \in N^{\text{imp}} \backslash \{o_r, d_r\}. \tag{7.70}$$

These interconnecting constraints will be relaxed based on the same distributed approach. Here, we only present the relaxed objective function under the LR method as follows:

$$\begin{aligned}
\textbf{P5 Z5} = \max_{y^t, z^t} & \sum_{r\in R^t} p_r u_r y_r^t - \sum_{o\in\{1,2,3\}} \left(\sum_{r\in R^t\cup\bar{R}^t} \sum_{p\in P^o} c_p z_{rp}^t u_r + \sum_{r\in R^t\cup\bar{R}^t} c_r^{\text{delay}} \mathbb{T}_r^o u_r \right) \\
& + \sum_{r\in R^t} \lambda 1_r \Big(\sum_{o\in\{1,2,3\}} \sum_{p\in\{P^o|o_p=o_r\}} z_{rp}^t - y_r^t \Big) \\
& + \sum_{r\in R^t} \lambda 2_r \Big(\sum_{o\in\{1,2,3\}} \sum_{p\in\{P^o|d_p=d_r\}} z_{rp}^t - y_r^t \Big) \\
& + \sum_{r\in \bar{R}^t} \lambda 3_r \Big(\sum_{o\in\{1,2,3\}} \sum_{p\in\{P^o|o_p=o_r\}} z_{rp}^t - 1 \Big) \\
& + \sum_{r\in \bar{R}^t} \lambda 4_r \Big(\Big(\sum_{o\in\{1,2,3\}} \sum_{p\in\{P^o|d_p=d_r\}} z_{rp}^t - 1 \Big) \\
& + \sum_{r\in R^t\cup\bar{R}^t} \sum_{i\in N^{\text{exp}}\backslash\{o_r,d_r\}} \lambda 5_{ri} \left(\sum_{p\in\{P^2|o_p=i\}} z_{rp}^t - \sum_{p\in\{P^1|d_p=i\}} z_{rp}^t \right) \\
& + \sum_{r\in R^t\cup\bar{R}^t} \sum_{i\in N^{\text{imp}}\backslash\{o_r,d_r\}} \lambda 6_{ri} \left(\sum_{p\in\{P^3|o_p=i\}} z_{rp}^t - \sum_{p\in\{P^2|d_p=i\}} z_{rp}^t \right) \\
& + \sum_{r\in R^t\cup\bar{R}^t} \sum_{i\in N^{\text{exp}}\backslash\{o_r,d_r\}} \lambda 7_{ri} \left(t_{ri}^+ - t_{ri}^- \right) \\
& + \sum_{r\in R^t\cup\bar{R}^t} \sum_{i\in N^{\text{imp}}\backslash\{o_r,d_r\}} \lambda 8_{ri} \left(t_{ri}^+ - t_{ri}^- \right)
\end{aligned} \tag{7.71}$$

subject to Constraints (7.58-7.62) for $o \in \{1,2,3\}$.

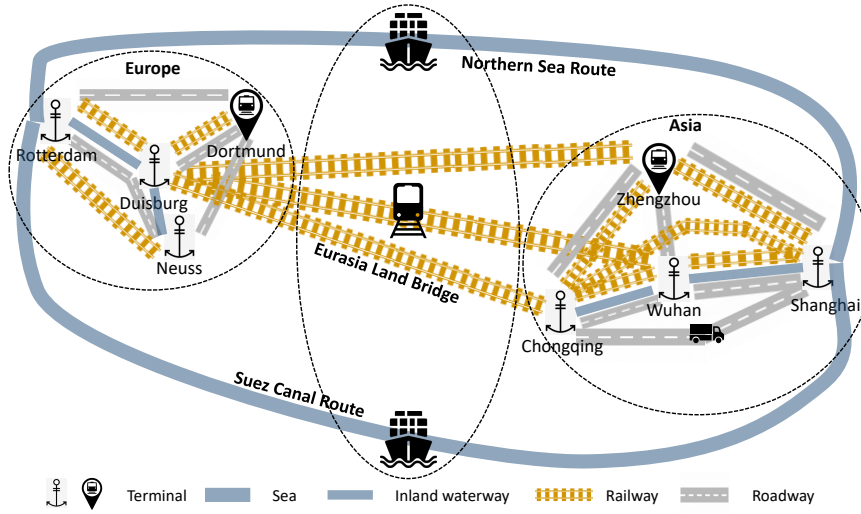

Figure 7.3: Topology of a global synchromodal network.

7.6 Numerical experiments

We evaluate the performance of the proposed three distributed approaches (i.e., LR, ALR, and ADMM) in comparison to the centralized approach (CA) proposed in Chapter 6. The approaches are implemented in MATLAB, and all experiments are executed on 3.70 GHz Intel Xeon processors with 32 GB of RAM. The optimization problems are solved with CPLEX 12.6.3.

We use a global synchromodal network which includes three subnetworks: a hinterland network in Asia, an intercontinental network connecting Asia and Europe, and a hinterland network in Europe, as shown in Figure 7.3. The Asian network includes one deep-sea port (i.e., Shanghai port) and three inland terminals (i.e., Zhengzhou, Wuhan, Chongqing); the European network includes one deep-sea port (i.e., Rotterdam port) and three inland terminals (i.e, Duisburg, Neuss, and Dortmund). The intercontinental network connects Asia and Europe by three routes: Northern Sea Route, Eurasia Land Bridge, and Suez Canal Route. We design 40 services of the Asian network, 52 services of the European network, and 14 services of the intercontinental network. The detailed data of services is presented in Appendix 7.A. At each terminal, the loading/unloading times (unit: hours) are set as follows: $lt_i^{\text{ship}} = 12$, $lt_i^{\text{barge}} = 4$, $lt_i^{\text{train}} = 2$, $lt_i^{\text{truck}} = 1$ for $i \in N$.

We generate several instances to represent different characteristics of shipment requests. We use G-n_1-n_2 to represent an instance with n_1 static requests and n_2 dynamic requests under the given distributed global network.

Unless otherwise stated, the benchmark values of coordination parameters are set as follows: $[\rho 1] = [\rho 2] = [\rho 3] = [\rho 4] = [\rho 5] = [\rho 6] = [2500]$, $[\rho 7] = [\rho 8] = [0.001]$, $[b7] = [b8] = [0.003]$, $[\rho 1^{\min}] = [\rho 2^{\min}] = [\rho 3^{\min}] = [\rho 4^{\min}] = [\rho 5^{\min}] = [\rho 6^{\min}] = 10$, $[\rho 7^{\min}] = [\rho 8^{\min}] = [0.0001]$, $[\rho 7^{\max}] = [\rho 8^{\max}] = [0.01]$, $\theta 1 = 1$, $\theta 2 = 0.5$, $\xi 1 = 0.003$, $\xi 2 = 0$, $a1 = 0$, $a2 = 10$, $N^{\text{iteration}} = 1000$; the benchmark scenario is set as static and deterministic, namely $R^t \cup \bar{R}^t = \emptyset$ for $t > 0$, $\sigma_s = 0$ for $s \in S$, $\alpha = 0.5$; $\mathbf{M} = 1400$.

Table 7.1: Demand data G-5-0.

Requests	Origin	Destination	Container volume (TEU)	Announce time	Release time	Due time	Delay cost (€/TEU-h)	Freight rate (€/TEU)
1	Chongqing	Rotterdam	9	0	89	569	25	5000
2	Wuhan	Dortmund	9	0	23	1103	12.5	2500
3	Zhengzhou	Dortmund	2	0	60	1140	12.5	2500
4	Chongqing	Neuss	1	0	119	1199	12.5	2500
5	Chongqing	Neuss	4	0	92	692	22.5	4500

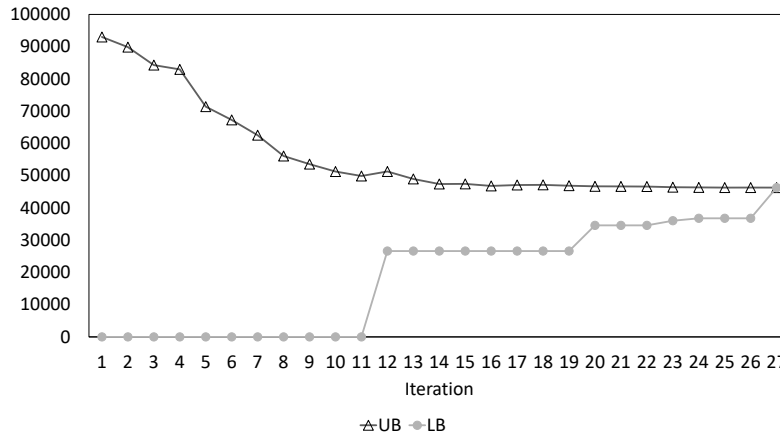

Figure 7.4: Evolution of lower and upper bounds of instance G-5-0 under the LR approach.

7.6.1 Coordination process illustration

To analyze the coordination process of the LR approach, we design a small instance G-5-0. The data of requests in instance G-5-0 is shown in Table 7.1.

Figure 7.4 shows the evolution of the lower and the upper bound of the objective function in **P0** under the LR approach. It is easy to see that since all the initial Lagrangian multipliers are set as 0, the gap between the upper and lower bounds in the early is relatively large. However, it reduces rather quickly. At iteration 27, the upper bound equals the lower bound, which means the optimal solution under the LR approach has been found for instance G-5-0. The evolution of requests' itineraries is shown in Appendix 7.A.

Regarding interconnecting constraints, we choose request 3 to analyze the coordination process. Figure 7.5 (a) shows that at initial iteration, when the Lagrangian multiplier $\lambda 1_3$ is 0, the global operator chooses to accept request 3, local operators do not arrange any services to transport request 3 leaving its origin terminal. Thus, conflicts happen between global and local operators. At iteration 2, the global operator increases the value of $\lambda 1_3$ to 2500. With this incentive, local operators arrange a service to transport request *r* leaving its origin terminal. Thereafter, the decisions made by the global operator and local operators always keep consistent. Therefore, the global operator does not increase the price of $\lambda 1_3$ anymore. Similarly, Figure 7.5 (b) shows that after five iterations, the decision made by the global operator and local operators achieve consistency. The global operator chooses to accept request 3, local operators arrange a service to deliver request 3 to its destination terminal.

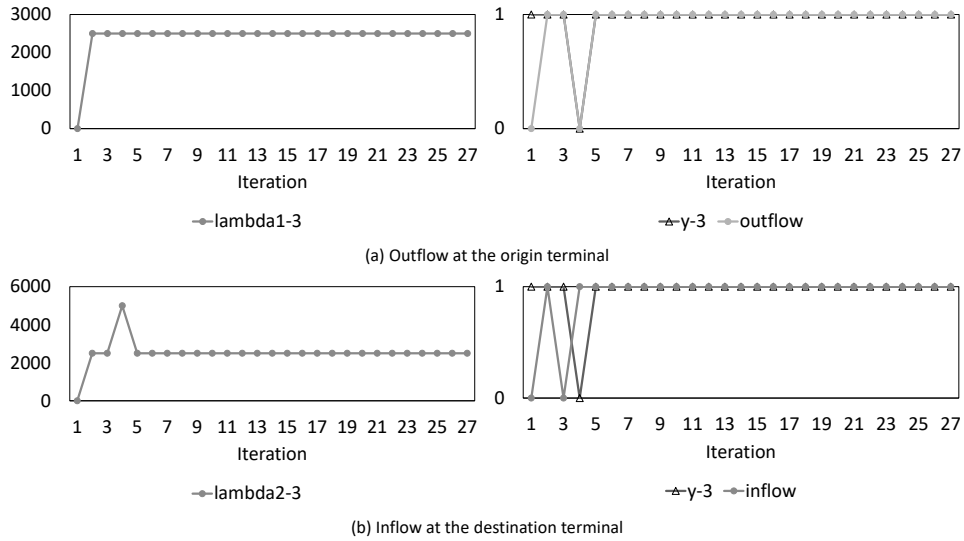

Figure 7.5: Coordination process of Lagrangian multipliers ($\lambda 1_3$ and $\lambda 2_3$, left side) and interconnecting variables (acceptance decision y_3, outflow at the origin terminal, and inflow at destination terminal, right side) of request 3 under the LR.

Figure 7.6(a) shows the evolution of the Lagrangian multiplier $\lambda 5$ and the differences between the value of inflow and outflow for request 3 at the export terminal. It is interesting to note that when the value of inflow is higher than the value of outflow at the current iteration, the global operator increases the value of Lagrangian multiplier $\lambda 5$ at the next iteration; when the value of inflow is lower than the value of outflow out at the current iteration, the global operator decreases the values of Lagrangian multiplier $\lambda 5$ at the next iteration. It is also worth to note that the updates of Lagrangian multipliers become smaller as the iterations advance since the value of penalty parameter $\rho 5$ decreases when $\lambda 5^{n+1} > \lambda 5^{n}$. After 18 iterations, the value of inflow and outflow at Shanghai port achieves consistency. The similar trend is shown in Figure 7.6 (b). The consistency of inflow and outflow at the import terminal achieves at iteration 23.

Figure 7.7 (a) shows the evolution of Lagrangian multiplier $\lambda 7$ and the differences between the departure and arrival time at the export terminal. We notice that the value of Lagrangian multiplier $\lambda 7$ will be increased only when the value of the departure time is higher than the value of the arrival time at Shanghai port. After 19 iterations, the consistency on time compatibility at the export terminal is realized. Similarly, the consistency on time compatibility at the import terminal is achieved after 23 iterations.

Compare Figure 7.5, Figure 7.6, and Figure 7.7, it is interest to find that the value of decision variables is not only influenced by corresponding Lagrangian multipliers but also affected by other variables. That is the reason why when the value of the Lagrangian multiplier stays the same, the value of corresponding decision variables might still change.

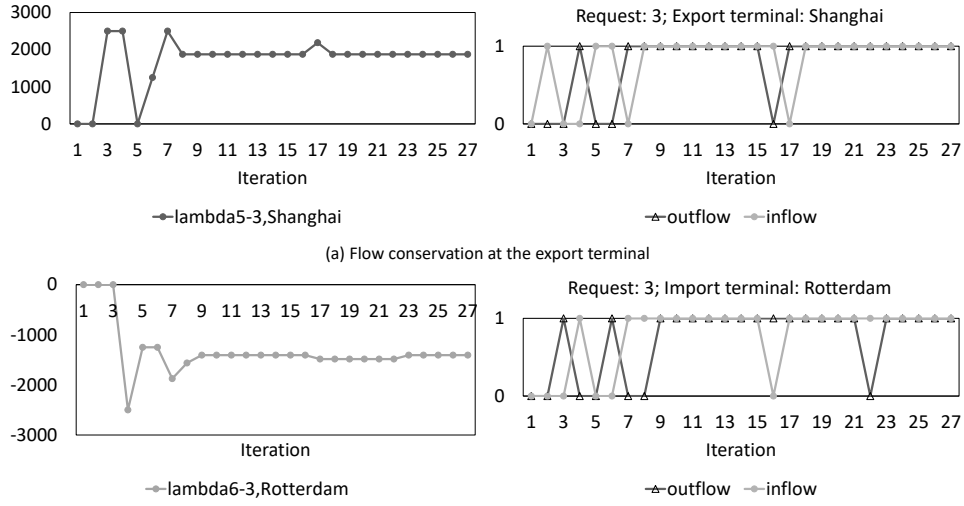

Figure 7.6: Coordination process of Lagrangian multipliers ($\lambda 5_{3,\text{Shanghai}}$ and $\lambda 6_{3,\text{Rotterdam}}$, left side) and interconnecting variables (inflow and outflow at Shanghai and Rotterdam terminal, right side) of request 3 under the LR.

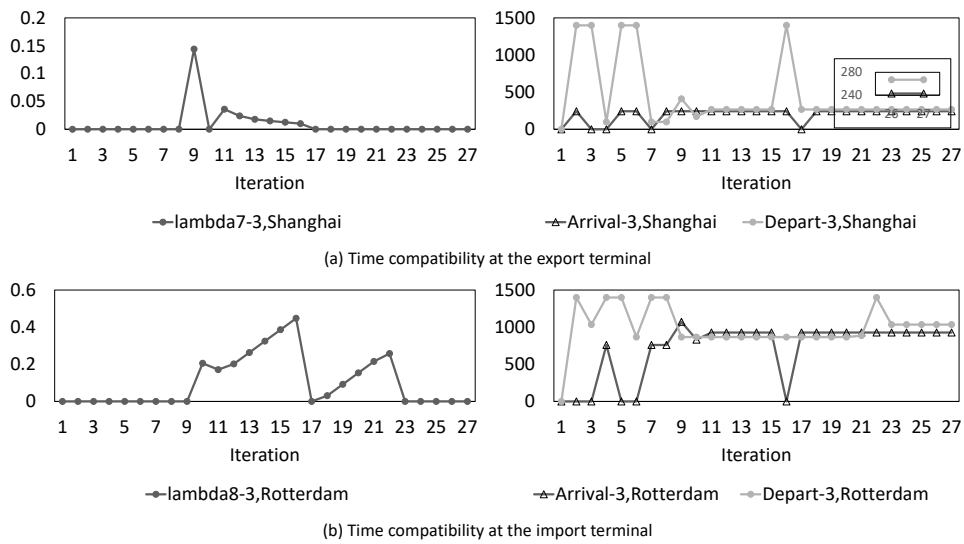

Figure 7.7: Coordination process of Lagrangian multipliers ($\lambda 7_{3,\text{Shanghai}}$ and $\lambda 8_{3,\text{Rotterdam}}$, left side) and interconnecting variables (Arrival time t^{-}_{3i} and departure time t^{+}_{3i} at Shanghai and Rotterdam terminal, right side) of request 3 under the LR.

Table 7.2: Sensitivity analysis of penalty parameters under the LR approach.

Cases	ρ1	ρ2	ρ5	ρ6	ρ7	ρ8	Number of iterations	Total profits (€)	Rejection
1	1000	1000	1000	1000	0.001	0.001	62	46293.04	0
2	2000	2000	2000	2000	0.001	0.001	34	46293.04	0
3	2500	2500	2500	2500	0.001	0.001	27	46293.04	0
4	3000	3000	3000	3000	0.001	0.001	100	44856.80	1
5	4000	4000	4000	4000	0.001	0.001	100	44856.80	1
6	2500	2500	2500	2500	0.000001	0.000001	25	46293.04	0
7	2500	2500	2500	2500	0.00001	0.00001	25	46293.04	0
8	2500	2500	2500	2500	0.0001	0.0001	27	46293.04	0
9	2500	2500	2500	2500	0.001	0.001	27	46293.04	0
10	2500	2500	2500	2500	0.01	0.01	31	46293.04	0

7.6.2 Sensitivity analysis of penalty parameters

To analyze the sensitivity of penalty parameters under the LR approach, we vary the value of ρ1, ρ2, ρ5, and ρ6 from 1000 to 4000 and vary the value of ρ7 and ρ8 from 0.000001 to 0.01 under instance G-5-0. We set the maximum number of iterations to 100. Table 7.2 shows that increasing the value of penalty parameters ρ1, ρ2, ρ5, and ρ6 from 1000 to 2500, the number of iterations decreases from 62 to 27. However, further increasing their values, the performance of the LR approach becomes worse even with rejections due to infeasible solutions. On the other hand, increasing the value of penalty parameters ρ7 and ρ8 from 0.000001 to 0.01, the number of iterations increases from 25 to 31. Table 7.2 shows that the spatial penalty parameters are more sensitive than the time penalty parameters.

7.6.3 Comparison between the LR, the ALR, and the ADMM approach

To compare the performance of the LR, the ALR, and the ADMM approach, we use four instances: G-5-0, G-10-0, G-20-0, G-30-0. The solutions generated by the CA are the optimal solutions to model **P0**. We consider two performance indicators: total profits (unit: €) and computation time (unit: seconds). While the CPU of the CA is the time of solving the centralized model (see Chapter 6), the CPU of the LR and the ALR is the summation of the maximum CPU generated by local operators at each iteration, the CPU of the ADMM is the summation of all the CPUs generated by local operators at each iteration since the optimization models of operator 1, 2, and 3 are implemented in serial instead of parallel.

Table 7.3 shows that for all the instances, the ADMM has the worst performance in total profits and computation time, the ALR can generate solutions that with higher profits than the LR but mostly with a higher CPU. The reason is that the ALR model **P2** is a mixed integer quadratic model while the LR model **P1** is a mixed integer linear programming model. Specifically, for instance G-5-0, the LR, the ALR, and the ADMM can both obtain optimal solutions. Compared with the ALR and the ADMM, the LR has the lowest number of iterations and the lowest computation time. For instance G-10-0 and G-20-0, the ALR generates higher profits than the LR but with higher CPUs. For instance G-30-0, while the ADMM converges at iteration 607, both the LR and the ALR cannot achieve convergence until the maximum number of iterations. However, the profits generated by the LR and the ALR are still higher than the profits generated by the ADMM. This further proves the theory that when the problem is non-convex, the solution obtained at the convergent point under distributed approaches might be suboptimal.

Table 7.3: Comparison between the LR, the ALR, and the ADMM approach.

Instances	CA			LR			ALR			ADMM	
	Profits	CPU (s)	Iterations	Profits	CPU (s)	Iterations	Profits	CPU (s)	Iterations	Profits	CPU (s)
G-5-0	46293.04	31.18	27	46293.04	122.96	28	46293.04	142.08	46	46293.04	240.62
G-10-0	84437.12	102.70	79	82821.51	1188.16	136	84437.12	2170.25	200	82412.82	3645.18
G-20-0	165582.77	2943.28	331	158676.63	61890.08	302	162564.93	78070.61	1000*	131389.17	330686.12
G-30-0	247182.02	4574.51	1000*	231232.04	843611.26	1000*	232302.54	825054.60	607	208874.02	646286.00

* The maximum number of iterations is 1000

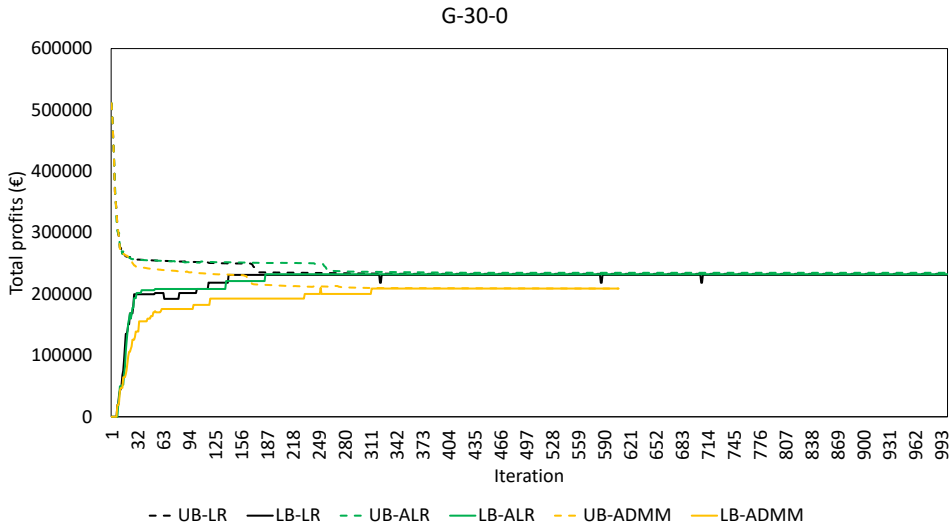

Figure 7.8: Evolution of lower and upper bounds under the LR, the ALR, and the ADMM.

From Table 7.3, we can see that the CPU of the LR, the ALR, and the ADMM increases dramatically with the increasing size of instances. It is therefore very difficult to apply these distributed approaches under dynamic scenarios that require getting solutions within a quite short time. One way to reduce the CPUs of the distributed approaches is to relax the termination criteria. Figure 7.8 shows that the upper and lower bounds converge very fast at the beginning of iterations, after a certain rounds of communication, the changes become quite small before the final convergence. Therefore, we can terminate the optimization when the gaps between the lower bound and upper bound achieve a certain level. For example, for instance G-30-0, we set termination criteria $\xi 2 = 0.1$. Figure 7.9 shows that the LR and the ALR can obtain the same profits as the results presented in Table 7.3 but with a lower CPU. However, the CPUs are still quite high which are unacceptable for dynamic scenarios. A heuristic algorithm that can generate timely solutions is required.

7.6.4 Performance of the preprocessing-based heuristic algorithm

We use the same instances presented above to test the performance of the preprocessing-based heuristic algorithm. About the heuristic, we set the maximum number of services in a path to 1 (LR-heuristic-1) and 2 (LR-heuristic-2), respectively. The results generated by the heuristics are compared with the results generated by the exact approach (i.e., solving model

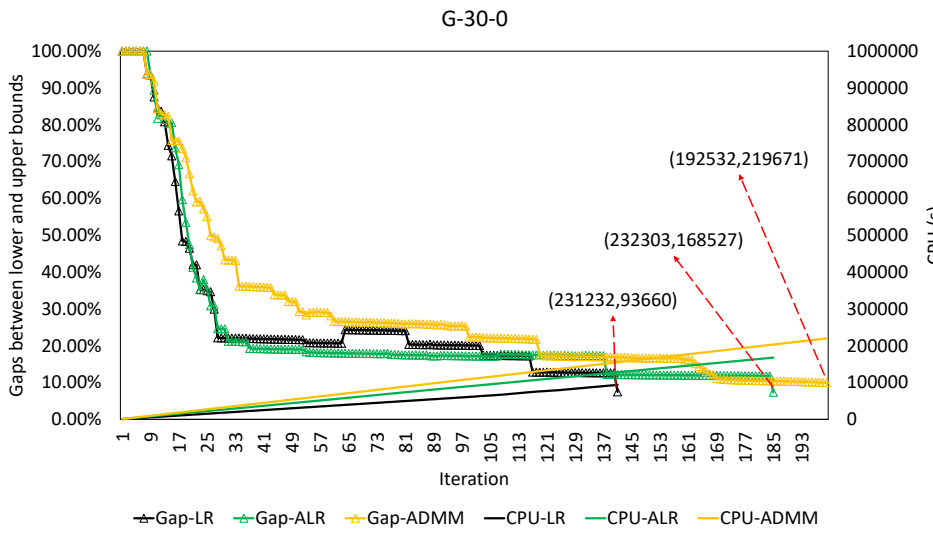

Figure 7.9: Gaps between the lower and upper bounds under the proposed approach.

Table 7.4: Performance of the preprocessing-based heuristic algorithm.

Instances	LR-exact			LR-heuristic-2			LR-heuristic-1		
	Iterations	Total profits	CPU (s)	Iterations	Total profits	CPU (s)	Iterations	Total profits	CPU (s)
G-5-0	27	46293.04	122.96	41	46293.04	27.02	22	42589.93	0.82
G-10-0	79	82821.51	1188.16	85	82821.51	182.49	34	79118.40	3.47
G-20-0	331	158676.63	61890.08	143	154113.57	3528.13	141	150893.92	18.63
G-30-0	1000*	231232.04	843611.26	121	232302.54	10452.45	103	230775.99	42.95

* The maximum number of iterations is 1000

P1 directly by using CPLEX) under the LR framework. Table 7.4 shows that for instance G-5-0 and G-10-0, LR-heuristic-2 can generate the same profits as LR-exact but with a quite lower CPU. For instance G-20-0, the performance of LR-heuristic-2 in profits is a bit lower than LR-exact, but the CPU reduces from 61890 to 3528 seconds. It is interesting to note that for instance G-30-0, LR-heuristic-2 has better performance than LR-exact not only in the CPU but also in the total profits. The reason is that for instance G-30-0, LR-exact cannot converge within the maximum number of iterations (i.e., 1000). Therefore, the solution generated by LR-exact is not the best solution under the LR framework. However, LR-heuristic-2 converges at iteration 121 and finds the best solution. Interestingly, the profits generated by LR-heuristic-2 is the same as the profits generated by the ALR presented in Table 7.3.

We notice that for instance with above 30 requests, the CPU under the LR-heuristic-2 is higher than 1 hour. To further reduce the computation time, we reduce the maximum number of services in a path L from 2 to 1. Table 7.4 shows that under LR-heuristic-1, all the instances can be solved within 1 min. The gaps between LR-exact and LR-heuristic-1 are within 8%. The experiment results show that with the proposed heuristic algorithm, decision-makers have the flexibility to choose proper L values to achieve the trade-off between computational complexity and solution quality.

Table 7.5: Performance of the LR under instance G-0-300.

Approaches	Confidence level	Planned profits	Actual profits	Rejection	Infeasible transshipments	Delay	CPU (s)	Gaps1	Gaps2
	0.5	2420045	1868594	13	106	10823	7		
	0.7	2205024	1879882	26	106	5825	6		
CA-heuristic	0.75	2053775	1857981	27	25	7053	6		
	0.9	1882434	1808298	42	0	3282	4		
	0.5	2053228	1771023	42	46	8376	12	-15.16%	-5.22%
	0.7	1971107	1813868	45	47	5809	15	-10.61%	-3.51%
LR-heuristic	0.75	1934313	1827904	49	28	5138	15	-5.82%	-1.62%
	0.9	1824334	1784273	61	5	3394	12	-3.09%	-1.33%

7.6.5 Dynamic and stochastic scenarios

Based on the proposed heuristic algorithm, we further test the performance of the LR approach under dynamic and stochastic scenarios. We set the mean of travel times $\mu_s = t_s$ for $s \in S$; standard deviation of travel times $\sigma_s = 0.1 * t_s$ for $s \in S \backslash S^{\text{truck}}$, $\sigma_s = 0.5 * t_s$ for $s \in S^{\text{truck}}$. The actual departure, arrival, and travel times under five realizations are presented in Appendix 7.A. We set the planning horizon (unit: hours) $T = 1400$, the length of time intervals to one hour. Regarding the heuristic, we set the largest number of services in a path for static requests to 1 and for dynamic requests to 2.

Due to travel time variations, the planned profits might be different from the actual profits for each instance. We consider two indicators: gaps1 representing the gaps between the planned profits generated by the CA-heuristic (see Chapter 6) and the LR-heuristic; gaps2 representing the gaps between the actual profits generated by the CA-heuristic and the LR-heuristic. Table 7.5 shows that the gaps in actual profits between the LR-heuristic and the CA-heuristic are within 5%. The higher the confidence level, the lower the gaps between these two approaches. It is also interesting to observe that increasing the confidence level, the number of rejections will increase, and the number of infeasible transshipments generally decreases. While the CA-heuristic has the best performance when $\alpha = 0.7$, the LR-heuristic has the best performance when $\alpha = 0.75$.

To analyze the relationship between the confidence level and the characteristics of instances, we use four instances with different degrees of dynamism: G-225-75, G-150-150, G-75-225, and G-0-300. In practice, since the static requests are received before the planning horizon, the required computation time is not as strict as dynamic requests. However, considering the time limitation of simulation for this work, we set the maximum number of services in a path to 1 for static requests and 2 for dynamic requests. Table 7.6 shows that the LR-heuristic has the best performance in actual profits when $\alpha = 0.75$ for instances with a higher degree of dynamism. For each instance, the planned profits decrease with the increase of the confidence level. The reason is that with a higher confidence level, the system will choose 'suboptimal' decisions that have a lower possibility of infeasible transshipments. It is also interesting to note that for each instance, the higher the confidence level, the large the number of rejections. The number of infeasible transshipments shows the opposite trend. Besides, we observe that under the confidence level, in general, increasing the degree of dynamism of instances, the number of rejections will reduce and the number of infeasible transshipments will grow. The computation time also typically rises with the increase of degree of dynamism.

Table 7.6: Comparison between instances with different degrees of dynamism.

Instance	Degree of dynamism	Confidence level	LR-heuristic					
			Planned profits	Actual profits	Rejection	Infeasible transshipments	Delay	CPU (s)
G-225-75	25%	0.5	1875293	**1674542**	60	27	5462	10
		0.7	1678736	1571433	80	18	3303	11
		0.75	1598911	1476257	89	10	3173	11
		0.9	1489710	1402580	97	3	3190	10
		0.9999	1201142	1116293	125	1	3124	11
G-150-150	50%	0.5	2002916	1776948	45	39	6635	15
		0.7	1880998	1779845	53	25	4270	16
		0.75	1866351	**1801584**	55	12	3750	11
		0.9	1756861	1673247	65	4	4116	9
		0.9999	1308564	1221987	111	2	3350	9
G-75-225	75%	0.5	2081806	1843619	40	43	7563	15
		0.7	1956186	1835534	44	28	5466	15
		0.75	1950500	**1866161**	49	15	4553	27
		0.9	1847305	1747697	59	9	4449	25
		0.9999	1254534	1234626	109	4	3061	17
G-0-300	100%	0.5	2053228	1835628	42	42	7177	12
		0.7	1968135	1846296	45	34	5458	27
		0.75	1931342	**1863937**	49	20	4460	26
		0.9	1824334	1772727	61	7	3702	25
		0.9999	1264306	1234570	110	1	2625	16

7.7 Conclusions

This chapter answers research question **RQ5** by developing and evaluating a dynamic, stochastic, and coordinated shipment matching problem in global synchromodal transportation. Three distributed approaches were developed to stimulate the coordination between a global operator and three local operators. The differences among the Lagrangian relaxation method (LR), the augmented Lagrangian relaxation method (ALR), and the alternating direction method of multipliers (ADMM) lie in the relaxed objective functions and the iteration process. While the optimization models under the LR and the ALR are implemented in parallel, the optimization runs in serial under the ADMM. Due to the computational complexity, a preprocessing-based heuristic algorithm was designed to generate timely solutions at each iteration.

We used four instances to compare the performance of these three approaches in total profits and computation time. The experiment results showed that on average, the ALR has the best performance in total profits, the LR has the best performance in computation time, and the ADMM has the worst performance in both. However, the computation times generated by the distributed approaches were unacceptable under dynamic and stochastic scenarios. We used the same instances to test the performance of the designed heuristic algorithm. The experiment results showed that with the proposed heuristic, all the instances can be solved within 1 min, and the gaps between the exact solutions and heuristic solutions are within 8%. After that, we used a dynamic and stochastic instance to investigate the performance of the LR combined with the heuristic algorithm. The experiment results showed that the gaps between the profits generated by the centralized approach and the LR are within 5%. Finally, we investigated the relationship between the confidence level and the degree of dynamism of instances under the LR framework. The experiment results showed that the LR approach has the best performance when the confidence level is 0.75 for instances with a higher degree of dynamism.

In conclusion, with the proposed distributed approaches, global transport planning that requires coordination among different operators and synchronization in operations to achieve a common goal (e.g., increasing total profits) can be realized; with the proposed heuristic, decision makers can decide on the trade-off between solution quality and computational efficiency.

Our future research will focus on the following three major aspects: (1) investigating the performance of the LR, the ALR and the ADMM under larger networks; (2) designing profit distribution mechanisms that ensure the fairness among stakeholders; (3) considering the collaboration among operators in the same level of the global transport chain, such as the collaboration between a barge carrier and a truck company in hinterland transportation.

Appendix 7.A

Table 7.7: Service data of the export hinterland network.

Service. ID	Mode	Origin	Destination	Capacity (TEU)	Scheduled departure time	Scheduled arrival time	Transport time (h)	Distance (km)	Transport cost (€/TEU)	Preceding service	Succeeding service
1	Barge	Chongqing	Wuhan	160	72.0	163.3	91.3	1370	191.80		2
2	Barge	Wuhan	Shanghai	160	171.3	256.3	84.9	1274	178.36	1	
3	Barge	Chongqing	Wuhan	160	144.0	235.3	91.3	1370	191.80		4
4	Barge	Wuhan	Shanghai	160	243.3	328.3	84.9	1274	178.36	3	
5	Barge	Shanghai	Wuhan	160	72.0	156.9	84.9	1274	178.36		6
6	Barge	Wuhan	Chongqing	160	164.9	256.3	91.3	1370	191.80	5	
7	Barge	Shanghai	Wuhan	160	144.0	228.9	84.9	1274	178.36		8
8	Barge	Wuhan	Chongqing	160	236.9	328.3	91.3	1370	191.80	7	
9	Train	Chongqing	Shanghai	90	51.0	88.2	37.2	1672	269.05		
10	Train	Chongqing	Shanghai	90	219.0	256.2	37.2	1672	269.05		
11	Train	Shanghai	Chongqing	90	51.0	88.2	37.2	1672	269.05		
12	Train	Shanghai	Chongqing	90	219.0	256.2	37.2	1672	269.05		
13	Train	Wuhan	Shanghai	90	99.0	117.0	18.0	811	131.29		
14	Train	Wuhan	Shanghai	90	267.0	285.0	18.0	811	131.29		
15	Train	Shanghai	Wuhan	90	99.0	117.0	18.0	811	131.29		
16	Train	Shanghai	Wuhan	90	267.0	285.0	18.0	811	131.29		
17	Train	Zhengzhou	Shanghai	90	51.0	72.9	21.9	986	159.29		
18	Train	Zhengzhou	Shanghai	90	219.0	240.9	21.9	986	159.29		
19	Train	Shanghai	Zhengzhou	90	51.0	72.9	21.9	986	159.29		
20	Train	Shanghai	Zhengzhou	90	219.0	240.9	21.9	986	159.29		
21	Train	Chongqing	Wuhan	90	74.0	94.0	20.0	900	145.53		
22	Train	Chongqing	Wuhan	90	242.0	262.0	20.0	900	145.53		
23	Train	Wuhan	Chongqing	90	123.0	143.0	20.0	900	145.53		
24	Train	Wuhan	Chongqing	90	291.0	311.0	20.0	900	145.53		
25	Train	Chongqing	Zhengzhou	90	15.0	45.8	30.8	1385	223.13		
26	Train	Chongqing	Zhengzhou	90	183.0	213.8	30.8	1385	223.13		
27	Train	Zhengzhou	Chongqing	90	79.0	109.8	30.8	1385	223.13		
28	Train	Zhengzhou	Chongqing	90	247.0	277.8	30.8	1385	223.13		
29	Truck	Shanghai	Zhengzhou	1000			12.7	954	1068.56		
30	Truck	Shanghai	Wuhan	1000			11.2	839	948.96		
31	Truck	Shanghai	Chongqing	1000			22.4	1679	1822.56		
32	Truck	Zhengzhou	Shanghai	1000			12.7	954	1068.56		
33	Truck	Zhengzhou	Wuhan	1000			6.8	510	606.80		
34	Truck	Zhengzhou	Chongqing	1000			16.0	1200	1324.40		
35	Truck	Wuhan	Shanghai	1000			11.2	839	948.96		
36	Truck	Wuhan	Zhengzhou	1000			6.8	510	606.80		
37	Truck	Wuhan	Chongqing	1000			11.7	878	989.52		
38	Truck	Chongqing	Shanghai	1000			22.4	1679	1822.56		
39	Truck	Chongqing	Zhengzhou	1000			16.0	1200	1324.40		
40	Truck	Chongqing	Wuhan	1000			11.7	878	989.52		

Table 7.8: Service data of the interconnected network.

Service. ID	Mode	Origin	Destination	Capacity (TEU)	Scheduled departure time	Scheduled arrival time	Transport time (h)	Distance (km)	Transport cost (€/TEU)	Preceding service	Succeeding service
41	Barge	Rotterdam	Duisburg	160	775	791.5	16.5	247.5	34.65		42
42	Barge	Duisburg	Neuss	160	799.5	802	2.5	37.5	5.25	41	
43	Barge	Rotterdam	Duisburg	160	871	887.5	16.5	247.5	34.65		44
44	Barge	Duisburg	Neuss	160	895.5	898	2.5	37.5	5.25	43	
45	Barge	Rotterdam	Duisburg	160	943	959.5	16.5	247.5	34.65		46
46	Barge	Duisburg	Neuss	160	967.5	970	2.5	37.5	5.25	45	
47	Barge	Rotterdam	Duisburg	160	1039	1055.5	16.5	247.5	34.65		48
48	Barge	Duisburg	Neuss	160	1063.5	1066	2.5	37.5	5.25	47	
49	Barge	Neuss	Duisburg	160	496	498.5	2.5	37.5	5.25		50
50	Barge	Duisburg	Rotterdam	160	506.5	523	16.5	247.5	34.65	49	
51	Barge	Neuss	Duisburg	160	592	594.5	2.5	37.5	5.25		52
52	Barge	Duisburg	Rotterdam	160	602.5	619	16.5	247.5	34.65	51	
53	Barge	Neuss	Duisburg	160	664	666.5	2.5	37.5	5.25		54
54	Barge	Duisburg	Rotterdam	160	674.5	691	16.5	247.5	34.65	53	
55	Barge	Neuss	Duisburg	160	760	762.5	2.5	37.5	5.25		56
56	Barge	Duisburg	Rotterdam	160	770.5	787	16.5	247.5	34.65	55	
57	Train	Rotterdam	Duisburg	90	720.0	726.5	6.5	292.5	48.33		
58	Train	Rotterdam	Duisburg	90	816.0	822.5	6.5	292.5	48.33		
59	Train	Rotterdam	Duisburg	90	888.0	894.5	6.5	292.5	48.33		
60	Train	Rotterdam	Duisburg	90	984.0	990.5	6.5	292.5	48.33		
61	Train	Duisburg	Rotterdam	90	454.0	460.5	6.5	292.5	48.33		
62	Train	Duisburg	Rotterdam	90	574.0	580.5	6.5	292.5	48.33		
63	Train	Duisburg	Rotterdam	90	694.0	700.5	6.5	292.5	48.33		
64	Train	Duisburg	Rotterdam	90	814.0	820.5	6.5	292.5	48.33		
65	Train	Rotterdam	Neuss	90	775.0	780.5	5.5	247.5	41.13		
66	Train	Rotterdam	Neuss	90	871.0	876.5	5.5	247.5	41.13		
67	Train	Rotterdam	Neuss	90	943.0	948.5	5.5	247.5	41.13		
68	Train	Rotterdam	Neuss	90	1039.0	1044.5	5.5	247.5	41.13		
69	Train	Neuss	Rotterdam	90	376.0	381.5	5.5	247.5	41.13		
70	Train	Neuss	Rotterdam	90	544.0	549.5	5.5	247.5	41.13		
71	Train	Neuss	Rotterdam	90	712.0	717.5	5.5	247.5	41.13		
72	Train	Neuss	Rotterdam	90	880.0	885.5	5.5	247.5	41.13		
73	Train	Duisburg	Dortmund	90	429.0	429.8	0.8	37.5	7.53		
74	Train	Duisburg	Dortmund	90	597.0	597.8	0.8	37.5	7.53		
75	Train	Duisburg	Dortmund	90	765.0	765.8	0.8	37.5	7.53		
76	Train	Duisburg	Dortmund	90	933.0	933.8	0.8	37.5	7.53		
77	Train	Dortmund	Duisburg	90	430.0	430.8	0.8	37.5	7.53		
78	Train	Dortmund	Duisburg	90	598.0	598.8	0.8	37.5	7.53		
79	Train	Dortmund	Duisburg	90	766.0	766.8	0.8	37.5	7.53		
80	Train	Dortmund	Duisburg	90	934.0	934.8	0.8	37.5	7.53		
81	Truck	Rotterdam	Duisburg	1000			3.3	247.5	333.80		
82	Truck	Rotterdam	Neuss	1000			3.6	270	357.20		
83	Truck	Rotterdam	Dortmund	1000			4.2	315	404.00		
84	Truck	Duisburg	Rotterdam	1000			3.3	247.5	333.80		
85	Truck	Duisburg	Neuss	1000			0.5	37.5	115.40		
86	Truck	Duisburg	Dortmund	1000			0.9	67.5	146.60		
87	Truck	Neuss	Rotterdam	1000			3.6	270	357.20		
88	Truck	Neuss	Duisburg	1000			0.5	37.5	115.40		
89	Truck	Neuss	Dortmund	1000			1.0	76.1	155.54		
90	Truck	Dortmund	Rotterdam	1000			4.2	315	404.00		
91	Truck	Dortmund	Duisburg	1000			0.9	67.5	146.60		
92	Truck	Dortmund	Neuss	1000			0.5	37.5	115.40		

Table 7.9: Service data of the import hinterland network.

Service. ID	Mode	Origin	Destination	Capacity (TEU)	Scheduled departure time	Scheduled arrival time	Transport time (h)	Distance (km)	Transport cost (€/TEU)	Preceding service	Succeeding service
93	Ship	Shanghai	Rotterdam	200	111	749	638	18890.40	1441.34		
94	Ship	Shanghai	Rotterdam	200	183	821	638	18890.40	1441.34		
95	Ship	Shanghai	Rotterdam	200	279	917	638	18890.40	1441.34		
96	Ship	Shanghai	Rotterdam	200	351	989	638	18890.40	1441.34		
97	Ship	Shanghai	Rotterdam	200	351	901	550	14260.40	2240.31		
98	Ship	Shanghai	Rotterdam	1000	423	1061	638	18890.40	1441.34		
99	Train	Chongqing	Duisburg	90	56	429	373	11179	2006.63		
100	Train	Chongqing	Duisburg	90	104	477	373	11179	2006.63		
101	Train	Chongqing	Duisburg	90	152	525	373	11179	2006.63		
102	Train	Chongqing	Duisburg	90	200	573	373	11179	2006.63		
103	Train	Chongqing	Duisburg	90	248	621	373	11179	2006.63		
104	Train	Chongqing	Duisburg	90	296	669	373	11179	2006.63		
105	Train	Chongqing	Duisburg	90	344	717	373	11179	2006.63		
106	Train	Chongqing	Duisburg	90	392	765	373	11179	2006.63		
107	Ship	Shanghai	Rotterdam	1000	600	1238	638	18890.40	1441.34		

Table 7.10: Actual departure, arrival, and travel times of the export hinterland network.

Services	Realization 1			Realization 2			Realization 3			Realization 4			Realization 5		
	Actual departure time	Actual arrival time	Actual travel time	Actual departure time	Actual arrival time	Actual travel time	Actual departure time	Actual arrival time	Actual travel time	Actual departure time	Actual arrival time	Actual travel time	Actual departure time	Actual arrival time	Actual travel time
1	72.00	160.08	88.08	72.00	174.81	102.81	72.00	158.62	86.62	72.00	172.32	100.32	72.00	177.18	105.18
2	168.08	249.23	81.15	182.81	275.12	92.30	166.62	250.67	84.06	180.32	266.21	85.89	185.18	278.05	92.87
3	144.00	253.62	109.62	144.00	229.25	85.25	144.00	235.68	91.68	144.00	237.13	93.13	144.00	249.27	105.27
4	261.62	350.68	89.05	237.25	330.30	93.05	243.68	323.64	79.96	245.13	331.79	86.66	257.27	340.66	83.39
5	72.00	166.20	94.20	72.00	151.94	79.94	72.00	163.32	91.32	72.00	164.74	92.74	72.00	157.29	85.29
6	174.20	267.95	93.74	159.94	246.16	86.22	171.32	262.43	91.11	172.74	261.24	88.50	165.29	260.97	95.68
7	144.00	234.59	90.59	144.00	225.58	81.58	144.00	221.54	77.54	144.00	231.66	87.66	144.00	230.40	86.40
8	242.59	327.66	85.07	233.58	316.86	83.28	229.54	322.10	92.55	239.66	323.69	84.02	238.40	350.88	112.48
9	51.00	89.40	38.40	51.00	88.13	37.13	51.00	87.45	36.45	51.00	91.95	40.95	51.00	88.41	37.41
10	219.00	256.19	37.19	219.00	254.78	35.78	219.00	256.51	37.51	219.00	254.32	35.32	219.00	256.67	37.67
11	51.00	89.82	38.82	51.00	87.19	36.19	51.00	85.92	34.92	51.00	87.12	36.12	51.00	87.08	36.08
12	219.00	252.50	33.50	219.00	257.75	38.75	219.00	256.75	37.75	219.00	254.19	35.19	219.00	257.60	38.60
13	99.00	116.42	17.42	99.00	118.31	19.31	99.00	118.50	19.50	99.00	115.47	16.47	99.00	118.02	19.02
14	267.00	287.11	20.11	267.00	285.76	18.76	267.00	286.91	19.91	267.00	283.97	16.97	267.00	286.01	19.01
15	99.00	119.64	20.64	99.00	115.40	16.40	99.00	117.09	18.09	99.00	118.17	19.17	99.00	118.14	19.14
16	267.00	285.71	18.71	267.00	286.54	19.54	267.00	285.25	18.25	267.00	284.89	17.89	267.00	286.83	19.83
17	51.00	73.23	22.23	51.00	74.20	23.20	51.00	73.64	22.64	51.00	76.09	25.09	51.00	71.22	20.22
18	219.00	242.96	23.96	219.00	241.44	22.44	219.00	241.33	22.33	219.00	241.39	22.39	219.00	242.14	23.14
19	51.00	71.76	20.76	51.00	77.70	26.70	51.00	76.22	25.22	51.00	74.59	23.59	51.00	74.24	23.24
20	219.00	242.27	23.27	219.00	246.50	27.50	219.00	241.08	22.08	219.00	240.57	21.57	219.00	239.94	20.94
21	74.00	93.96	19.96	74.00	96.86	22.86	74.00	97.50	23.50	74.00	96.30	22.30	74.00	93.95	19.95
22	242.00	263.38	21.38	242.00	263.01	21.01	242.00	261.86	19.86	242.00	262.86	20.86	242.00	260.37	18.37
23	123.00	143.97	20.97	123.00	144.88	21.88	123.00	142.37	19.37	123.00	146.26	23.26	123.00	143.78	20.78
24	291.00	310.00	19.00	291.00	312.77	21.77	291.00	312.25	21.25	291.00	309.58	18.58	291.00	310.32	19.32
25	15.00	47.44	32.44	15.00	45.48	30.48	15.00	45.53	30.53	15.00	45.51	30.51	15.00	51.68	36.68
26	183.00	211.49	28.49	183.00	221.49	38.49	183.00	215.46	32.46	183.00	218.09	35.09	183.00	215.21	32.21
27	79.00	110.75	31.75	79.00	107.15	28.15	79.00	107.26	28.26	79.00	108.75	29.75	79.00	108.84	29.84
28	247.00	280.05	33.05	247.00	277.01	30.01	247.00	282.73	35.73	247.00	277.11	30.11	247.00	275.54	28.54
29			15.40			18.97			18.08			14.83			14.15
30			14.52			10.85			13.35			11.98			12.49
31			24.09			23.37			27.04			30.02			31.15
32			12.90			12.73			11.62			22.10			15.30
33			10.22			11.73			11.09			6.28			6.56
34			17.38			25.08			15.57			27.16			25.68
35			14.02			14.18			19.10			13.90			11.57
36			6.18			9.51			13.91			12.85			7.90
37			21.04			11.10			12.63			15.04			19.03
38			32.58			21.70			27.49			23.32			27.53
39			25.43			15.23			17.77			15.79			24.53
40			18.43			26.98			12.09			18.51			18.38

Table 7.11: Actual departure, arrival, and travel times of the import hinterland network.

Services	Realization 1			Realization 2			Realization 3			Realization 4			Realization 5		
	Actual departure time	Actual arrival time	Actual travel time	Actual departure time	Actual arrival time	Actual travel time	Actual departure time	Actual arrival time	Actual travel time	Actual departure time	Actual arrival time	Actual travel time	Actual departure time	Actual arrival time	Actual travel time
41	775.00	791.08	16.08	775.00	792.16	17.16	775.00	790.61	15.61	775.00	791.34	16.34	775.00	792.55	17.55
42	799.08	801.90	2.81	800.16	802.45	2.29	798.61	801.11	2.50	799.34	802.09	2.75	800.55	803.72	3.17
43	871.00	886.66	15.66	871.00	886.89	15.89	871.00	888.59	17.59	871.00	888.53	17.53	871.00	886.11	15.11
44	894.66	897.65	2.99	894.89	897.58	2.70	896.59	899.30	2.72	896.53	899.06	2.53	894.11	896.68	2.57
45	943.00	959.97	16.97	943.00	960.33	17.33	943.00	958.74	15.74	943.00	960.23	17.23	943.00	958.75	15.75
46	967.97	970.33	2.36	968.33	971.04	2.71	966.74	969.17	2.43	968.23	970.50	2.28	966.75	969.37	2.62
47	1039.00	1055.26	16.26	1039.00	1058.83	19.83	1039.00	1057.72	18.72	1039.00	1056.37	17.37	1039.00	1055.63	16.63
48	1063.26	1065.89	2.63	1066.83	1069.36	2.54	1065.72	1068.31	2.59	1064.37	1067.28	2.92	1063.63	1066.35	2.71
49	496.00	498.27	2.27	496.00	498.36	2.36	496.00	498.35	2.35	496.00	498.81	2.81	496.00	498.41	2.41
50	506.27	525.09	18.82	506.36	522.35	16.00	506.35	521.64	15.29	506.81	523.87	17.06	506.41	521.54	15.12
51	592.00	594.73	2.73	592.00	594.34	2.34	592.00	594.40	2.40	592.00	594.62	2.62	592.00	594.58	2.58
52	602.73	618.58	15.85	602.34	617.80	15.46	602.40	620.45	18.05	602.62	619.09	16.47	602.58	621.21	18.63
53	664.00	666.48	2.48	664.00	666.37	2.37	664.00	666.54	2.54	664.00	666.25	2.25	664.00	666.81	2.81
54	674.48	691.42	16.94	674.37	690.11	15.74	674.54	690.21	15.67	674.25	689.59	15.33	674.81	691.74	16.92
55	760.00	762.70	2.70	760.00	762.53	2.53	760.00	762.66	2.66	760.00	762.28	2.28	760.00	762.35	2.35
56	770.70	786.34	15.63	770.53	787.33	16.80	770.66	788.21	17.55	770.28	786.01	15.73	770.35	788.15	17.81
57	720.00	725.99	5.99	720.00	726.83	6.83	720.00	726.35	6.35	720.00	727.16	7.16	720.00	726.75	6.75
58	816.00	822.95	6.95	816.00	822.52	6.52	816.00	823.96	7.96	816.00	823.19	7.19	816.00	822.13	6.13
59	888.00	895.08	7.08	888.00	894.22	6.22	888.00	894.75	6.75	888.00	895.40	7.40	888.00	894.34	6.34
60	984.00	990.20	6.20	984.00	990.44	6.44	984.00	989.97	5.97	984.00	990.90	6.90	984.00	990.55	6.55
61	454.00	460.80	6.80	454.00	460.14	6.14	454.00	460.29	6.29	454.00	461.29	7.29	454.00	460.00	6.00
62	574.00	580.42	6.42	574.00	580.87	6.87	574.00	581.19	7.19	574.00	580.54	6.54	574.00	580.06	6.06
63	694.00	700.56	6.56	694.00	701.25	7.25	694.00	700.27	6.27	694.00	701.29	7.29	694.00	700.32	6.32
64	814.00	820.53	6.53	814.00	820.01	6.01	814.00	820.89	6.89	814.00	820.07	6.07	814.00	820.13	6.13
65	775.00	780.00	5.00	775.00	780.44	5.44	775.00	780.43	5.43	775.00	781.07	6.07	775.00	781.26	6.26
66	871.00	875.98	4.98	871.00	876.21	5.21	871.00	876.49	5.49	871.00	876.99	5.99	871.00	876.63	5.63
67	943.00	948.58	5.58	943.00	948.37	5.37	943.00	948.33	5.33	943.00	948.25	5.25	943.00	948.82	5.82
68	1039.00	1044.72	5.72	1039.00	1044.33	5.33	1039.00	1044.31	5.31	1039.00	1044.03	5.03	1039.00	1045.69	6.69
69	376.00	381.84	5.84	376.00	382.41	6.41	376.00	381.45	5.45	376.00	381.33	5.33	376.00	381.30	5.30
70	544.00	549.03	5.03	544.00	550.03	6.03	544.00	549.92	5.92	544.00	549.38	5.38	544.00	549.34	5.34
71	712.00	718.14	6.14	712.00	717.05	5.05	712.00	718.05	6.05	712.00	717.57	5.57	712.00	717.76	5.76
72	880.00	885.37	5.37	880.00	886.19	6.19	880.00	885.10	5.10	880.00	885.35	5.35	880.00	885.23	5.23
73	429.00	429.79	0.79	429.00	429.88	0.88	429.00	429.82	0.82	429.00	429.87	0.87	429.00	429.77	0.77
74	597.00	597.91	0.91	597.00	597.75	0.75	597.00	597.80	0.80	597.00	597.82	0.82	597.00	597.89	0.89
75	765.00	765.82	0.82	765.00	765.92	0.92	765.00	765.76	0.76	765.00	765.80	0.80	765.00	765.97	0.97
76	933.00	933.84	0.84	933.00	933.85	0.85	933.00	933.96	0.96	933.00	933.82	0.82	933.00	933.94	0.94
77	430.00	430.87	0.87	430.00	430.98	0.98	430.00	430.85	0.85	430.00	430.78	0.78	430.00	430.89	0.89
78	598.00	598.77	0.77	598.00	598.77	0.77	598.00	598.83	0.83	598.00	598.79	0.79	598.00	598.80	0.80
79	766.00	766.85	0.85	766.00	766.86	0.86	766.00	767.00	1.00	766.00	766.85	0.85	766.00	767.02	1.02
80	934.00	934.87	0.87	934.00	934.83	0.83	934.00	934.86	0.86	934.00	934.86	0.86	934.00	934.90	0.90
81			4.49			3.31			3.28			4.42			6.60
82			4.66			3.57			4.06			3.28			5.36
83			5.89			4.87			8.07			5.57			5.00
84			5.45			3.54			5.06			3.98			5.83
85			0.59			0.63			0.71			0.67			0.51
86			1.26			1.29			1.49			1.43			0.95
87			5.70			3.61			4.31			4.78			4.81
88			0.55			0.92			0.55			1.01			0.45
89			1.15			1.85			1.47			0.98			1.66
90			4.81			4.41			4.49			6.54			5.66
91			1.64			0.87			1.43			2.21			1.54
92			0.48			0.53			0.49			0.54			0.79

Table 7.12: Actual departure, arrival, and travel times of the intercontinental network.

Services	Realization 1			Realization 2			Realization 3			Realization 4			Realization 5		
	Actual departure time	Actual arrival time	Actual travel time	Actual departure time	Actual arrival time	Actual travel time	Actual departure time	Actual arrival time	Actual travel time	Actual departure time	Actual arrival time	Actual travel time	Actual departure time	Actual arrival time	Actual travel time
93	111.00	821.76	710.76	111.00	835.94	724.94	111.00	768.07	657.07	111.00	712.19	601.19	111.00	806.09	695.09
94	183.00	858.45	675.45	183.00	807.47	624.47	183.00	873.27	690.27	183.00	881.84	698.84	183.00	876.43	693.43
95	279.00	943.15	664.15	279.00	954.33	675.33	279.00	945.87	666.87	279.00	882.69	603.69	279.00	892.04	613.04
96	351.00	1006.73	655.73	351.00	962.88	611.88	351.00	1046.19	695.19	351.00	999.58	648.58	351.00	1031.00	680.00
97	351.00	912.85	561.85	351.00	915.81	564.81	351.00	903.99	552.99	351.00	887.56	536.56	351.00	949.43	598.43
98	399.00	1071.58	672.58	399.00	1036.03	637.03	399.00	1034.97	635.97	399.00	1081.84	682.84	399.00	1100.90	701.90
99	56.00	446.26	390.26	56.00	455.34	399.34	56.00	458.88	402.88	56.00	528.40	472.40	56.00	406.83	350.83
100	104.00	520.65	416.65	104.00	506.44	402.44	104.00	465.49	361.49	104.00	472.78	368.78	104.00	506.60	402.60
101	152.00	534.76	382.76	152.00	514.97	362.97	152.00	597.18	445.18	152.00	490.81	338.81	152.00	551.94	399.94
102	200.00	540.51	340.51	200.00	574.60	374.60	200.00	607.79	407.79	200.00	552.52	352.52	200.00	604.43	404.43
103	248.00	587.82	339.82	248.00	623.91	375.91	248.00	630.62	382.62	248.00	600.69	352.69	248.00	588.09	340.09
104	296.00	728.04	432.04	296.00	669.17	373.17	296.00	654.96	358.96	296.00	645.45	349.45	296.00	699.62	403.62
105	344.00	700.64	356.64	344.00	750.96	406.96	344.00	726.02	382.02	344.00	795.81	451.81	344.00	731.31	387.31
106	392.00	734.69	342.69	392.00	787.90	395.90	392.00	802.09	410.09	392.00	765.30	373.30	392.00	791.57	399.57

Table 7.13: Evolution of requests' itineraries of instance G-5-0 under the LR approach.

Iteration	Itinerary 1	Itinerary 2	Itinerary 3	Itinerary 4	Itinerary 5
1	[]	[]	[]	[]	[]
2	[10,50]	[13,76]	[18,76]	[10,101,48]	[10,85]
3	[]	[23,47]	[27,47]	93	47
4	[10,50]	76	[93,76]	[10,47,48]	[10,85]
5	[]	[13,76]	[18,76]	[47,48]	[94,85]
6	[10,50]	[23,76]	[18,100,43,76]	[10,101,48]	[10,100,82]
7	[]	[43,76]	[27,93,76]	94	[10,85]
8	[10,50]	[13,76]	[18,93,76]	[47,48]	[93,85]
9	100	[23,47]	[18,98,43,76]	[47,48]	[10,100,85]
10	50	76	[18,94,43,76]	[10,48]	[93,85]
11	[10,100,50]	[13,76]	[18,95,43,76]	[93,101,47]	[10,100,82]
12	[100,50]	[23,93,76]	[18,95,43,76]	[10,48]	82
13	[100,50]	[13,43,76]	[18,95,43,76]	[93,48]	[10,82]
14	[100,50]	[13,93,43,76]	[18,95,43,76]	[10,47,48]	[93,82]
15	[100,50]	[13,98,43,76]	[18,95,43,76]	[47,48]	[10,100,85]
16	[100,50]	[13,94,43,76]	[18,43,76]	[10,48]	[10,93,85]
17	[100,50]	[13,94,43,76]	[27,95,43,76]	[10,93,101,47,48]	85
18	[100,50]	[13,94,43,76]	[18,95,43,76]	48	[10,100,85]
19	[100,50]	[13,94,43,76]	[18,95,43,76]	[94,47,48]	[94,85]
20	[100,50]	[13,94,43,76]	[18,95,43,76]	[10,47,48]	[10,100,85]
21	[100,50]	[13,94,43,76]	[18,95,59,76]	[10,94,48]	[94,85]
22	[100,50]	[13,94,43,76]	[18,95,76]	[10,101,47,48]	[10,85]
23	[100,50]	[13,94,43,76]	[18,95,47,86]	[95,47,48]	[10,100,85]
24	[100,50]	[13,94,43,76]	[18,95,47,86]	[10,95,47,48]	[94,85]
25	[100,50]	[13,94,43,76]	[18,95,47,86]	[10,95,47,48]	85
26	[100,50]	[13,94,43,76]	[18,95,47,86]	[10,95,47,48]	[10,100,85]
27	[100,50]	[13,94,43,76]	[18,95,47,86]	[10,95,47,48]	[100,85]

Chapter 8

Conclusions and future research

This thesis is dedicated to developing methodologies that support the decision-making processes of synchromodal matching platforms under dynamic, stochastic, and distributed environments, so that the transport plans become more efficient, effective, reliable, flexible, and sustainable. This chapter presents the main conclusions and gives the future research directions.

8.1 Conclusions

The main research question proposed in this thesis is: "How to develop methodologies that support the decision-making processes of synchromodal matching platforms under dynamic, stochastic, and distributed environments?". Under this main question, five sub-questions were defined which are answered through Chapters 3-7. The answers to these questions are summarized as follows:

- How to model shipment matching with time-dependent travel times in hinterland synchromodal transportation?

  In Chapter 3, a mixed integer linear programming model was developed for hinterland synchromodal shipment matching with time-dependent travel times. The model formulates binary variables to represent the matches between shipment requests and transport services, introduces time-dependent travel time functions for truck services, and assigns different weights for different objectives to represent multi-objective functions. Thanks to the developed model, shipment requests with different time windows can be matched with transport services with different modes and time schedules considering the influences on logistics costs, emissions, and transportation time. Compared with a time-constant model, the time-dependent model shows to have total cost savings from 0.38% to 2.81% when the traffic congestion coefficient increases from 2 to 4.5.

- How to deal with real-time shipment requests in hinterland synchromodal transportation?

In Chapter 4, a rolling horizon approach was developed to handle real-time shipment requests in hinterland synchromodal transportation. Under this approach, decisions are made at fixed time points for all active requests including newly received requests at the current time interval and the requests received at previous time intervals which have not expired yet. The decisions are fixed only when the response for the request cannot be further postponed. Due to the computational complexity of the optimization model, a heuristic algorithm was designed to generate timely solutions at each decision epoch. The algorithm transforms the optimization model to a binary integer programming model by generating feasible paths and matches. The experiment results demonstrate the solution accuracy and computational efficiency of the heuristic algorithm in comparison to an exact algorithm. The proposed rolling horizon approach outperforms a greedy approach from practice in total costs up to 4% under various scenarios of the synchromodal matching platform. Thanks to the proposed methodologies, decision makers can provide online matches for real-time shipment requests considering the trade-off between logistics costs, delays, and emissions.

- How to address spot request uncertainties in hinterland synchromodal shipment matching?

  In Chapter 5, an anticipatory approach was developed to handle spot request uncertainty in dynamic shipment matching processes by incorporating stochastic information of random variables. Due to the curse of dimensionality, this approach uses a sample average approximation method to approximate expected objective functions and a progressive hedging algorithm to generate solutions at each decision epoch of a rolling horizon framework. Under the sample average approximation method, the expected objective function is approximated by a sample average estimate derived from a random sample. Under the progressive hedging algorithm, the optimization model is decomposed into scenario-based subproblems which are iteratively solved in parallel until meeting the non-anticipativity constraints. With the proposed approach, decision makers can consider a large set of scenarios to more accurately represent the stochasticity of future requests and in turn achieves better performance in total costs. Compared with a myopic approach, the anticipatory approach is shown to have total cost savings up to 6.5% under various scenarios of the synchromodal matching platform.

- How to address travel time uncertainties in global synchromodal shipment matching?

  In Chapter 6, a hybrid stochastic approach is developed to solve spot request and travel time uncertainties simultaneously in global synchromodal transportation. This approach integrates a rolling horizon framework that handles real-time shipment requests, a sample average approximation method that addresses spot request uncertainty, a chance-constrained programming (CCP) model that addresses travel time uncertainty, and a preprocessing-based heuristic algorithm that generates timely solutions at each decision epoch. The CCP model addresses travel time uncertainty by ensuring the feasibility of stochastic constraints to be at a certain level, called confidence level. A high confidence level means the matching decisions have a low probability causing infeasible transshipments but the decisions might be suboptimal at the current stage. Compared with a deterministic approach, the hybrid stochastic

approach shows to have better performance in total profits with minimum 1.09%, average 7.03%, maximum 13.74% under various scenarios of the global synchromodal transport system. Besides, with the proposed approach, decision makers have the flexibility to choose the trade-off between total profits, the number of request rejections, and the number of infeasible transshipments.

- How to design coordinated mechanisms that facilitate cooperative planning in global synchromodal transport?

  In Chapter 7, three distributed approaches are proposed to stimulate the cooperation between a global operator and three local operators in global synchromodal transportation, including the Lagrangian relaxation method (LR), the augmented Lagrangian relaxation method (ALR), and the alternated direction method of multipliers (ADMM). The distributed approaches relax the interconnecting constraints which connect the independent operators by bringing them into the objective function of the original problem with associated Lagrangian multipliers. In this way, the original problem can be decomposed into operator-related subproblems. These subproblems are solved iteratively until achieving consistency in interconnecting constraints. Different distributed approach applies different iteration processes. The experiment results show that on average, the ALR has the best performance in total profits, the LR has the best performance in computation time, and the ADMM has the worst performance in both. Due to the computational complexity of the optimization problems, a heuristic algorithm is designed to generate timely solutions at each iteration. The experiment requests show that instances that require above 24 hours to be solved under an exact algorithm can be solved within 1 min under the heuristic algorithm. Briefly, with the proposed distributed approaches, global transport planning that requires coordination among local operators can be realized; with the proposed heuristic, decision makers have the flexibility to choose the trade-off between solution quality and computational efficiency.

8.2 Managerial insights

From the theoretical perspective, this thesis contributes to the Operations Research discipline by developing advanced methodologies in the field of synchromodal transportation. From a practical perspective, this thesis provides managerial insights for managers and policy-makers to improve practice operations. The main managerial insights are listed as follows:

- Companies running on networks with heavy traffic congestion are highly recommended to use the time-dependent model developed in Chapter 3 to reduce costs and infeasible transshipments;

- Companies running on a larger percentage of spot requests are expected to benefit more from the rolling horizon approach proposed in Chapter 4 by effectively managing the utilization of barges, trains, and trucks with the consideration of the time-sensitivity of shipments;

- Thanks to the developed anticipatory approach in Chapter 5, companies running on instances with a higher degree of dynamism are expected to benefit more from the stochastic information of future requests;

- Companies that have spot requests and travel time uncertainties simultaneously are highly recommended to adopt the hybrid stochastic approach designed in Chapter 6 to achieve better performance in total profits, infeasible transshipments, and delays;

- With the developed distributed approaches in Chapter 7, companies that running on local networks can achieve a global goal by sharing limited information.

8.3 Future research directions

In this section, several future research directions are given as follows:

- This thesis tested the performance of the proposed dynamic, stochastic, and coordinated approaches in a European hinterland network with 10 terminals and a Eurasia global network with 4 terminals in each continent. Future research should further test the performance of the proposed approaches in larger and more complex networks.

- In this thesis, we considered truck services as a fleet of trucks that have flexible departure times but fixed routes. Future models should consider flexible routes of truck services to increase their flexibility, and in turn reduce empty miles and traffic congestion. On the other hand, this thesis considers that all the services are known in advance and based on fixed contracts. However, in practice, the number of trucks available to the system is quite dynamic considering the excess capacity of services from other systems. Investigating the benefits of incorporating ad hoc truck services in synchromodal shipment matching is an interest research direction.

- In this thesis, we used the same stochastic information of random variables in the whole optimization processes. To better describe the random variables under the current context, learning algorithms that learn from real-time information and adapt distributions over time deserve further research. On the other hand, this thesis adopts a rolling horizon framework to implement the optimization process based on real-time information at each decision epoch. With the help of learning algorithms, decision makers can learn from past decisions and give priorities to different services for different requests. In this way, decision makers can provide faster and better decisions for newly received requests based on their characteristics.

- In this thesis, we considered the cooperation among operators in different levels of the global transport chain, namely vertical collaboration. The collaboration is based on limited information exchange among operators. Carriers located in the same subnetwork are assumed under the control of a central operator. However, in practice, the carriers might not all be willing to give authority to a central operator. The cooperation among carriers in the same level of the supply chain is different from the vertical collaboration. The coordination mechanism might be not only information exchange

but also request exchange and capacity exchange. How to design horizontal cooperation among operators in global synchromodal transportation is a promising research area.

- To attract shippers towards mode-free booking, dynamic pricing strategies that set different prices to the same route with different services considering the dynamics in demand and supply are essential. While dynamic pricing strategies have been well adopted in the airline industry, these techniques have not yet been well adopted in the container transport industry [61]. The reason is that decision-makers under the current container transport system do not have the ability to publish real-time prices. However, under the proposed synchromodal matching platforms, shippers can request container booking online, and decisions can be made in real-time. Dynamic pricing strategies for synchromodal transportation become possible and necessary.

- To ensure the win-win situation and fairness, an important aspect of cooperative planning is to share the profit gain among all the stakeholders. In the literature, the majority of the studies in cooperative transportation use sharing methods based on cooperative game theory [32], such as Shapley values and proportional methods. However, different problems might have different characteristics and different forms of cooperation, and the definition of fairness might also be different. How to design a proper profit sharing mechanism for coordinated global synchromodal transportation is a promising research direction. On the other hand, considering the dynamic and stochastic nature of the global synchromodal transport planning problem in practice, the contribution from each entity to the cooperation may also change over time with uncertainties. Hence, it is also interesting to investigate how to share profits based on dynamic and stochastic games and contracts.

Bibliography

[1] N. A. Agatz, A. L. Erera, M. W. Savelsbergh, and X. Wang. Dynamic ride-sharing: A simulation study in metro atlanta. *Transportation Research Part B: Methodological*, 45(9):1450–1464, 2011.

[2] R. Akkerman, P. Farahani, and M. Grunow. Quality, safety and sustainability in food distribution: a review of quantitative operations management approaches and challenges. *OR Spectrum*, 32(4):863–904, 2010.

[3] M. Albareda-Sambola, E. Fernández, and G. Laporte. The dynamic multiperiod vehicle routing problem with probabilistic information. *Computers & Operations Research*, 48:31–39, 2014.

[4] J. Alonso-Mora, S. Samaranayake, A. Wallar, E. Frazzoli, and D. Rus. On-demand high-capacity ride-sharing via dynamic trip-vehicle assignment. *Proceedings of the National Academy of Sciences*, 114(3):462–467, 2017.

[5] T. Ambra, A. Caris, and C. Macharis. Towards freight transport system unification: reviewing and combining the advancements in the physical internet and synchromodal transport research. *International Journal of Production Research*, 57(6):1606–1623, 2018.

[6] A. M. Arslan, N. Agatz, L. Kroon, and R. Zuidwijk. Crowdsourced delivery—a dynamic pickup and delivery problem with ad hoc drivers. *Transportation Science*, 53(1):222–235, 2019.

[7] B. Ayar and H. Yaman. An intermodal multicommodity routing problem with scheduled services. *Computational Optimization and Applications*, 53(1):131–153, 2011.

[8] C. Barnhart and H. D. Ratliff. Modeling intermodal routing. *Journal of Business Logistics*, 14(1):205, 1993.

[9] B. Behdani, Y. Fan, B. Wiegmans, and R. Zuidwijk. Multimodal schedule design for synchromodal freight transport systems. *SSRN Electronic Journal*, pages 424–444, 2014.

[10] A. Bhattacharya, S. A. Kumar, M. Tiwari, and S. Talluri. An intermodal freight transport system for optimal supply chain logistics. *Transportation Research Part C: Emerging Technologies*, 38:73–84, 2014.

[11] I. C. Bilegan, L. Brotcorne, D. Feillet, and Y. Hayel. Revenue management for rail container transportation. *EURO Journal on Transportation and Logistics*, 4(2):261–283, 2014.

[12] T. S. Chang. Best routes selection in international intermodal networks. *Computers & Operations Research*, 35(9):2877–2891, 2008.

[13] J. H. Cho, H. S. Kim, and H. R. Choi. An intermodal transport network planning algorithm using dynamic programming—a case study: from busan to rotterdam in intermodal freight routing. *Applied Intelligence*, 36(3):529–541, 2010.

[14] T. G. Crainic, P. Dell'Olmo, N. Ricciardi, and A. Sgalambro. Modeling dry-port-based freight distribution planning. *Transportation Research Part C: Emerging Technologies*, 55:518–534, 2015.

[15] T. G. Crainic, M. Hewitt, and W. Rei. Scenario grouping in a progressive hedging-based meta-heuristic for stochastic network design. *Computers & Operations Research*, 43:90–99, 2014.

[16] T. G. Crainic and K. H. Kim. Chapter 8 intermodal transportation. In *Transportation*, pages 467–537. Elsevier, 2007.

[17] T. G. Crainic, G. Perboli, and M. Rosano. Simulation of intermodal freight transportation systems: a taxonomy. *European Journal of Operational Research*, 270(2):401–418, 2018.

[18] E. Demir, W. Burgholzer, M. Hrušovský, E. Arıkan, W. Jammernegg, and T. van Woensel. A green intermodal service network design problem with travel time uncertainty. *Transportation Research Part B: Methodological*, 93:789–807, 2016.

[19] E. Demir, M. Hrušovský, W. Jammernegg, and T. van Woensel. Green intermodal freight transportation: bi-objective modelling and analysis. *International Journal of Production Research*, 57(19):6162–6180, 2019.

[20] J. X. Dong, C. Y. Lee, and D. P. Song. Joint service capacity planning and dynamic container routing in shipping network with uncertain demands. *Transportation Research Part B: Methodological*, 78:404–421, 2015.

[21] J. F. Ehmke, A. M. Campbell, and T. L. Urban. Ensuring service levels in routing problems with time windows and stochastic travel times. *European Journal of Operational Research*, 240(2):539–550, 2015.

[22] A. L. Erera, J. C. Morales, and M. Savelsbergh. Global intermodal tank container management for the chemical industry. *Transportation Research Part E: Logistics and Transportation Review*, 41(6):551–566, 2005.

[23] Eurostat. Modal split of freight transport. Available at: https://ec.europa.eu/eurostat/databrowser/view/t2020_rk320/default/table?lang=en

[24] S. Fazi, J. C. Fransoo, and T. van Woensel. A decision support system tool for the transportation by barge of import containers: A case study. *Decision Support Systems*, 79:33–45, 2015.

[25] A. D. Febbraro, N. Sacco, and M. Saeednia. An agent-based framework for cooperative planning of intermodal freight transport chains. *Transportation Research Part C: Emerging Technologies*, 64:72–85, 2016.

[26] A. Frémont and P. Franc. Hinterland transportation in europe: Combined transport versus road transport. *Journal of Transport Geography*, 18(4):548–556, 2010.

[27] D. Gade, G. Hackebeil, S. M. Ryan, J. P. Watson, R. J. B. Wets, and D. L. Woodruff. Obtaining lower bounds from the progressive hedging algorithm for stochastic mixed-integer programs. *Mathematical Programming*, 157(1):47–67, 2016.

[28] M. Gansterer and R. F. Hartl. Collaborative vehicle routing: A survey. *European Journal of Operational Research*, 268(1):1–12, 2018.

[29] M. Gendreau, O. Jabali, and W. Rei. 50th anniversary invited article—future research directions in stochastic vehicle routing. *Transportation Science*, 50(4):1163–1173, 2016.

[30] R. Giusti, D. Manerba, G. Bruno, and R. Tadei. Synchromodal logistics: An overview of critical success factors, enabling technologies, and open research issues. *Transportation Research Part E: Logistics and Transportation Review*, 129:92–110, 2019.

[31] J. C. Goodson, J. W. Ohlmann, and B. W. Thomas. Rollout policies for dynamic solutions to the multivehicle routing problem with stochastic demand and duration limits. *Operations Research*, 61(1):138–154, 2013.

[32] M. Guajardo and M. Rönnqvist. A review on cost allocation methods in collaborative transportation. *International Transactions in Operational Research*, 23(3):371–392, 2015.

[33] W. Guo, B. Atasoy, W. B. van Blokland, and R. R. Negenborn. Anticipatory approach for dynamic and stochastic shipment matching in hinterland synchromodal transportation.

[34] W. Guo, B. Atasoy, W. B. van Blokland, and R. R. Negenborn. Distributed approaches for coordinated global synchromodal shipment matching with travel time uncertainty.

[35] W. Guo, B. Atasoy, W. B. van Blokland, and R. R. Negenborn. Global synchromodal transport with dynamic and stochastic shipment matching.

[36] W. Guo, B. Atasoy, W. B. van Blokland, and R. R. Negenborn. Dynamic and stochastic shipment matching problem in multimodal transportation. *Transportation Research Record: Journal of the Transportation Research Board*, 2674(2):262–273, 2020.

[37] W. Guo, B. Atasoy, W. B. van Blokland, and R. R. Negenborn. A dynamic shipment matching problem in hinterland synchromodal transportation. *Decision Support Systems*, 134:113289, 2020.

[38] W. Guo, W. B. van Blokland, and G. Lodewijks. Survey on characteristics and challenges of synchromodal transportation in global cold chains. In *Lecture Notes in Computer Science*, pages 420–434. Springer International Publishing, 2017.

[39] W. Guo, W. B. van Blokland, G. Lodewijks, and R. R. Negenborn. Multi-commodity multi-service matching design for container transportation systems. In *Proceedings of the 97th Annual meeting of the Transportation Research Board*, number 18-04314, 2018.

[40] M. R. Hestenes. Multiplier and gradient methods. *Journal of Optimization Theory and Applications*, 4(5):303–320, 1969.

[41] M. Hrušovský, E. Demir, W. Jammernegg, and T. van Woensel. Hybrid simulation and optimization approach for green intermodal transportation problem with travel time uncertainty. *Flexible Services and Manufacturing Journal*, 30(3):486–516, 2016.

[42] S. Ichoua, M. Gendreau, and J. Y. Potvin. Vehicle dispatching with time-dependent travel times. *European Journal of Operational Research*, 144(2):379–396, 2003.

[43] ITF. Intermodal freight transport. Available at: https://www.itf-oecd.org/benchmarking-intermodal-freight-transport

[44] B. Kersbergen, T. van den Boom, and B. D. Schutter. Distributed model predictive control for railway traffic management. *Transportation Research Part C: Emerging Technologies*, 68:462–489, 2016.

[45] R. Konings, E. Kreutzberger, and V. Maraš. Major considerations in developing a hub-and-spoke network to improve the cost performance of container barge transport in the hinterland: the case of the port of rotterdam. *Journal of Transport Geography*, 29:63–73, 2013.

[46] C. Y. Lee and D. P. Song. Ocean container transport in global supply chains: Overview and research opportunities. *Transportation Research Part B: Methodological*, 95:442–474, 2017.

[47] L. Lee, E. Chew, and M. Sim. A revenue management model for sea cargo. *International Journal of Operational Research*, 6(2):195, 2009.

[48] C. Lemaréchal. Lagrangian relaxation. In *Lecture Notes in Computer Science*, pages 112–156. Springer Berlin Heidelberg, 2001.

[49] L. Li, R. R. Negenborn, and B. D. Schutter. Intermodal freight transport planning – a receding horizon control approach. *Transportation Research Part C: Emerging Technologies*, 60:77–95, 2015.

[50] L. Li, R. R. Negenborn, and B. D. Schutter. Distributed model predictive control for cooperative synchromodal freight transport. *Transportation Research Part E: Logistics and Transportation Review*, 105:240–260, 2017.

[51] X. Li, P. Tian, and S. C. Leung. Vehicle routing problems with time windows and stochastic travel and service times: Models and algorithm. *International Journal of Production Economics*, 125(1):137–145, 2010.

[52] F. Lian, Y. He, and Z. Yang. Competitiveness of the china-europe railway express and liner shipping under the enforced sulfur emission control convention. *Transportation Research Part E: Logistics and Transportation Review*, 135:101861, 2020.

[53] D. Y. Lin and Y. T. Chang. Ship routing and freight assignment problem for liner shipping: Application to the northern sea route planning problem. *Transportation Research Part E: Logistics and Transportation Review*, 110:47–70, 2018.

[54] X. Lin, R. R. Negenborn, and G. Lodewijks. Towards quality-aware control of perishable goods in synchromodal transport networks. *IFAC-PapersOnLine*, 49(16):132–137, 2016.

[55] Z. Liu, Q. Meng, S. Wang, and Z. Sun. Global intermodal liner shipping network design. *Transportation Research Part E: Logistics and Transportation Review*, 61:28–39, 2014.

[56] J. Long, W. Tan, W. Szeto, and Y. Li. Ride-sharing with travel time uncertainty. *Transportation Research Part B: Methodological*, 118:143–171, 2018.

[57] H. Luo, X. Sun, and H. Wu. Convergence properties of augmented lagrangian methods for constrained global optimization. *Optimization Methods and Software*, 23(5):763–778, 2008.

[58] N. Masoud and R. Jayakrishnan. A decomposition algorithm to solve the multi-hop peer-to-peer ride-matching problem. *Transportation Research Part B: Methodological*, 99:1–29, 2017.

[59] Q. Meng, S. Wang, H. Andersson, and K. Thun. Containership routing and scheduling in liner shipping: Overview and future research directions. *Transportation Science*, 48(2):265–280, 2014.

[60] Q. Meng, S. Wang, and Z. Liu. Network design for shipping service of large-scale intermodal liners. *Transportation Research Record: Journal of the Transportation Research Board*, 2269(1):42–50, 2012.

[61] Q. Meng, H. Zhao, and Y. Wang. Revenue management for container liner shipping services: Critical review and future research directions. *Transportation Research Part E: Logistics and Transportation Review*, 128:280–292, 2019.

[62] M. R. K. Mes and M. E. Iacob. Synchromodal transport planning at a logistics service provider. In *Logistics and Supply Chain Innovation*, pages 23–36. Springer International Publishing, 2015.

[63] L. Moccia, J. F. Cordeau, G. Laporte, S. Ropke, and M. P. Valentini. Modeling and solving a multimodal transportation problem with flexible-time and scheduled services. *Networks*, 57(1):53–68, 2010.

[64] A. Najmi, D. Rey, and T. H. Rashidi. Novel dynamic formulations for real-time ride-sharing systems. *Transportation Research Part E: Logistics and Transportation Review*, 108:122–140, 2017.

[65] R. Negenborn, B. D. Schutter, and J. Hellendoorn. Multi-agent model predictive control for transportation networks: Serial versus parallel schemes. *Engineering Applications of Artificial Intelligence*, 21(3):353–366, 2008.

[66] R. R. Negenborn. *Multi-agent model predictive control with applications to power networks*. phdthesis, 2007.

[67] S. Pfoser, H. Treiblmaier, and O. Schauer. Critical success factors of synchromodality: Results from a case study and literature review. *Transportation Research Procedia*, 14:1463–1471, 2016.

[68] V. Pillac, M. Gendreau, C. Guéret, and A. L. Medaglia. A review of dynamic vehicle routing problems. *European Journal of Operational Research*, 225(1):1–11, 2013.

[69] M. J. D. Powell. Algorithms for nonlinear constraints that use lagrangian functions. *Mathematical Programming*, 14(1):224–248, 1978.

[70] W. B. Powell. A unified framework for stochastic optimization. *European Journal of Operational Research*, 275(3):795–821, 2019.

[71] C. Puettmann and H. Stadtler. A collaborative planning approach for intermodal freight transportation. *OR Spectrum*, 32(3):809–830, 2010.

[72] W. Qu, J. Rezaei, Y. Maknoon, and L. Tavasszy. Hinterland freight transportation replanning model under the framework of synchromodality. *Transportation Research Part E: Logistics and Transportation Review*, 131:308–328, 2019.

[73] Y. Qu, T. Bektaş, and J. Bennell. Sustainability SI: Multimode multicommodity network design model for intermodal freight transportation with transfer and emission costs. *Networks and Spatial Economics*, 16(1):303–329, 2014.

[74] V. Reis. Should we keep on renaming a 35-year-old baby? *Journal of Transport Geography*, 46:173–179, 2015.

[75] U. Ritzinger, J. Puchinger, and R. F. Hartl. A survey on dynamic and stochastic vehicle routing problems. *International Journal of Production Research*, 54(1):215–231, 2015.

[76] A. E. P. Rivera and M. R. Mes. Anticipatory freight selection in intermodal long-haul round-trips. *Transportation Research Part E: Logistics and Transportation Review*, 105:176–194, 2017.

[77] A. P. Rivera and M. Mes. Service and transfer selection for freights in a synchromodal network. In *Lecture Notes in Computer Science*, pages 227–242. Springer International Publishing, 2016.

[78] R. T. Rockafellar. The multiplier method of hestenes and powell applied to convex programming. *Journal of Optimization Theory and Applications*, 12(6):555–562, 1973.

[79] R. T. Rockafellar and R. J. B. Wets. Scenarios and policy aggregation in optimization under uncertainty. *Mathematics of Operations Research*, 16(1):119–147, 1991.

[80] F. Rodrigues, A. Agra, M. Christiansen, L. M. Hvattum, and C. Requejo. Comparing techniques for modelling uncertainty in a maritime inventory routing problem. *European Journal of Operational Research*, 277(3):831–845, 2019.

[81] A. Ruszczyński and A. Shapiro. Stochastic programming models. In *Handbooks in Operations Research and Management Science*, pages 1–64. Elsevier, 2003.

[82] M. Schilde, K. Doerner, and R. Hartl. Metaheuristics for the dynamic stochastic dial-a-ride problem with expected return transports. *Computers & Operations Research*, 38(12):1719–1730, 2011.

[83] Y. Shi, T. Boudouh, O. Grunder, and D. Wang. Modeling and solving simultaneous delivery and pick-up problem with stochastic travel and service times in home health care. *Expert Systems with Applications*, 102:218–233, 2018.

[84] J. Silvente, G. M. Kopanos, E. N. Pistikopoulos, and A. Espuña. A rolling horizon optimization framework for the simultaneous energy supply and demand planning in microgrids. *Applied Energy*, 155:485–501, 2015.

[85] P. Singh, M. van Sinderen, and R. Wieringa. Synchromodal transport: pre-requisites, activities and effects. In *Ils conference*, pages 1–4, 2016.

[86] D. P. Song and J. X. Dong. Cargo routing and empty container repositioning in multiple shipping service routes. *Transportation Research Part B: Methodological*, 46(10):1556–1575, 2012.

[87] M. SteadieSeifi, N. Dellaert, W. Nuijten, T. van Woensel, and R. Raoufi. Multimodal freight transportation planning: A literature review. *European Journal of Operational Research*, 233(1):1–15, 2014.

[88] M. SteadieSeifi. *Multimodal transportation for perishable products*. phdthesis, Technische Universiteit Eindhoven, 2017.

[89] M. Stiglic, N. Agatz, M. Savelsbergh, and M. Gradisar. The benefits of meeting points in ride-sharing systems. *Transportation Research Part B: Methodological*, 82:36–53, 2015.

[90] P. Sun, L. P. Veelenturf, S. Dabia, and T. van Woensel. The time-dependent capacitated profitable tour problem with time windows and precedence constraints. *European Journal of Operational Research*, 264(3):1058–1073, 2018.

[91] P. Sun, L. P. Veelenturf, M. Hewitt, and T. van Woensel. The time-dependent pickup and delivery problem with time windows. *Transportation Research Part B: Methodological*, 116:1–24, 2018.

[92] Y. Sun, M. Hrušovský, C. Zhang, and M. Lang. A time-dependent fuzzy programming approach for the green multimodal routing problem with rail service capacity uncertainty and road traffic congestion. *Complexity*, 2018:1–22, 2018.

[93] Y. Sun and M. Lang. Modeling the multicommodity multimodal routing problem with schedule-based services and carbon dioxide emission costs. *Mathematical Problems in Engineering*, 2015:1–21, 2015.

[94] Y. Sun, M. Lang, and D. Wang. Optimization models and solution algorithms for freight routing planning problem in the multi-modal transportation networks: A review of the state-of-the-art. *The Open Civil Engineering Journal*, 9(1):714–723, 2015.

[95] L. Tavasszy, B. Behdani, and R. Konings. Intermodality and synchromodality. In *Ports and Networks*, pages 251–266. Routledge, 2017.

[96] N. K. Tran, H. D. Haasis, and T. Buer. Container shipping route design incorporating the costs of shipping, inland/feeder transport, inventory and CO2 emission. *Maritime Economics & Logistics*, 19(4):667–694, 2017.

[97] UNCTAD. Review of maritime transport, 2019. Available at: https://unctad.org/en/PublicationsLibrary/rmt2019_en.pdf

[98] W. J. A. van Heeswijk, M. R. K. Mes, J. M. J. Schutten, and W. H. M. Zijm. Freight consolidation in intermodal networks with reloads. *Flexible Services and Manufacturing Journal*, 30(3):452–485, 2016.

[99] B. van Riessen, R. R. Negenborn, and R. Dekker. Synchromodal container transportation: An overview of current topics and research opportunities. In *Lecture Notes in Computer Science*, pages 386–397. Springer International Publishing, 2015.

[100] B. van Riessen, R. R. Negenborn, and R. Dekker. Real-time container transport planning with decision trees based on offline obtained optimal solutions. *Decision Support Systems*, 89:1–16, 2016.

[101] B. van Riessen, R. R. Negenborn, and R. Dekker. The cargo fare class mix problem for an intermodal corridor: revenue management in synchromodal container transportation. *Flexible Services and Manufacturing Journal*, 29(3-4):634–658, 2017.

[102] B. van Riessen, R. R. Negenborn, R. Dekker, and G. Lodewijks. Service network design for an intermodal container network with flexible transit times and the possibility of using subcontracted transport. *International Journal of Shipping and Transport Logistics*, 7(4):457, 2015.

[103] B. van Riessen, R. R. Negenborn, G. Lodewijks, and R. Dekker. Impact and relevance of transit disturbances on planning in intermodal container networks using disturbance cost analysis. *Maritime Economics & Logistics*, 17(4):440–463, 2014.

[104] B. Verweij, S. Ahmed, A. J. Kleywegt, G. Nemhauser, and A. Shapiro. The sample average approximation method applied to stochastic routing problems: A computational study. *Computational Optimization and Applications*, 24(2/3):289–333, 2003.

[105] H. Wang, X. Wang, and X. Zhang. Dynamic resource allocation for intermodal freight transportation with network effects: Approximations and algorithms. *Transportation Research Part B: Methodological*, 99:83–112, 2017.

[106] X. Wang. Optimal allocation of limited and random network resources to discrete stochastic demands for standardized cargo transportation networks. *Transportation Research Part B: Methodological*, 91:310–331, 2016.

[107] X. Wang. Static and dynamic resource allocation models for single-leg transportation markets with service disruptions. *Transportation Research Part E: Logistics and Transportation Review*, 103:87–108, 2017.

[108] Y. Wang, Q. Meng, and Y. Du. Liner container seasonal shipping revenue management. *Transportation Research Part B: Methodological*, 82:141–161, 2015.

[109] Y. Wang, I. C. Bilegan, T. G. Crainic, and A. Artiba. A revenue management approach for network capacity allocation of an intermodal barge transportation system. In *Lecture Notes in Computer Science*, pages 243–257. Springer International Publishing, 2016.

[110] J. P. Watson and D. L. Woodruff. Progressive hedging innovations for a class of stochastic mixed-integer resource allocation problems. *Computational Management Science*, 8(4):355–370, 2010.

[111] H. Wei and M. Dong. Import-export freight organization and optimization in the dry-port-based cross-border logistics network under the belt and road initiative. *Computers & Industrial Engineering*, 130:472–484, 2019.

[112] M. Xu, Y. Cui, M. Hu, X. Xu, Z. Zhang, S. Liang, and S. Qu. Supply chain sustainability risk and assessment. *Journal of Cleaner Production*, 225:857–867, 2019.

[113] D. Yang, K. Pan, and S. Wang. On service network improvement for shipping lines under the one belt one road initiative of china. *Transportation Research Part E: Logistics and Transportation Review*, 117:82–95, 2018.

[114] J. Yang, P. Jaillet, and H. Mahmassani. Real-time multivehicle truckload pickup and delivery problems. *Transportation Science*, 38(2):135–148, 2004.

[115] Y. Yao, X. Zhu, H. Dong, S. Wu, H. Wu, L. C. Tong, and X. Zhou. ADMM-based problem decomposition scheme for vehicle routing problem with time windows. *Transportation Research Part B: Methodological*, 129:156–174, 2019.

[116] Y. Zheng, S. E. Li, K. Li, F. Borrelli, and J. K. Hedrick. Distributed model predictive control for heterogeneous vehicle platoons under unidirectional topologies. *IEEE Transactions on Control Systems Technology*, 25(3):899–910, 2017.

[117] R. A. Zuidwijk and A. W. Veenstra. The value of information in container transport. *Transportation Science*, 49(3):675–685, 2015.

[118] S. Zurheide and K. Fischer. A revenue management slot allocation model for liner shipping networks. *Maritime Economics & Logistics*, 14(3):334–361, 2012.

[119] S. Zurheide and K. Fischer. Revenue management methods for the liner shipping industry. *Flexible Services and Manufacturing Journal*, 27(2-3):200–223, 2014.

Samenvatting

Met het toenemende volume containers in de wereldhandel wordt het belangrijker om het transport van containers efficient te plannen. Om de concurrerendheid in wereldwijde logistieke ketens te verbeteren werken betrokken partijen samen, zowel op hetzelfde niveau als op verschillende niveaus: het zogenaamde synchromodale transport. Synchromodaliteit is het gebruik van efficiente, effectieve en duurzame transportplannen voor alle transportbewegingen in een geïntegreerd netwerk, met behulp van geavanceerde informatietechnologie. Het besluitvormingsproces in een synchromodaal transportsysteem is evenwel erg complex. 1. Er moet rekening worden gehouden met variabele reistijden door congestie in het verkeer. 2. Er is een dynamische aanpak nodig die real-time rekening houdt nieuwe transportvraag in het netwerk. 3. De vraag van de spotmarkt is niet van te voren bekend. 4. Tot nu toe wordt in wereldwijde synchromodale transportnetwerken geen rekening gehouden met onzekerheid in reistijden. 5. Er zijn op dit moment nog steeds geen methoden die de samenwerking bevorderen tussen de verschillende betrokken partijen in het wereldwijde containertransport.

In dit proefschrift worden de hiervoor genoemde uitdagingen aangepakt met dynamische, stochastische en gecoordineerde modellen. In het bijzonder is onderzoek gedaan naar de volgende vijf onderwerpen:

- Synchromodale transportplanning met variabele reistijden (Hoofdstuk 3)

  De planning van het synchromodale achterlandtransport is onderzocht aan de hand van een netwerkoperator die probeert een optimale balans te vinden tussen transportopdrachten met harde tijdvensters en mutimodaal transportaanbod met tijdvensters, waarbij rekening wordt gehouden met congestie in het wegverkeer. Voor de oplossing van het probleem wordt een matching model met variabele reistijden geformuleerd. Het experiment laat zien dat het matching model met variable reistijden lagere totale kosten geeft dan een model met constante reistijden, in het bijzonder in scenarios met veel congestie.

- Dynamische transportplanning (Hoofdstuk 4)

  Er is een online synchromodaal planningsprobleem onderzocht waarin een overlegplatform probeert om een optimale afstemming te vinden tussen real-time vraag naar transport en multimodaal aanbod. Er wordt een benadering met een glijdende horizon voorgesteld om nieuwe vraag naar transport te verwerken. Er is een heuristische algoritme ontwikkeld om voor elke tijdstap een oplossing te genereren. De resultaten van het experiment tonen de nauwkeurigheid van de oplossing en de efficientie van

de berekeningen met het heuristische algoritme in vergelijking met een exact algoritme. Het voorgestelde algoritme met een glijdende horizon geeft veel lagere totale kosten dan de greedy methode uit de praktijk, onder verschillende scenarios voor het synchromodale platform. Met de voorgestelde methode kunnen binnenvaartschepen, treinen en trucks efficienter worden ingezet, rekening houdend met de invloed op logistieke kosten, vertragingen en emissies en de tijdsvensters van de transportopdrachten.

- Dynamische en stochastische transportplanning (Hoofdstuk 5)

  Er is een dynamisch en stochastisch transportplanningsprobleem onderzocht met onzekerheid in de toekomstige vraag. Voor de oplossing van het probleem wordt een anticiperende aanpak voorgesteld waarbij gebruik wordt gemaakt van een benadering van de waarde van de objectfunctie en een progressief hedge-algoritme om voor elk tijdstap over een glijdende horizon een oplossing te genereren. Er zijn uitgebreide numerieke experimenten uitgevoerd om deze aanpak te evalueren. In vergelijking met een korte termijn aanpak geeft de anticiperende aanpak in de bestudeerde situaties een kostenbesparing tot 6.5%. De resultaten van de experimenten laten ook zien dat het belangrijk is om stochastische informatie mee te nemen in het beslissingsproces van het overlegplatform voor de planning van het synchromodale transport naar het achterland.

- Dynamische en stochastische wereldwijde transportplanning (Hoofdstuk 6)

  Er is een dynamisch en stochastisch wereldwijd transportplanningprobleem bestudeerd, met incidentele vraag (spotmarkt) en onzekerheid in transporttijden. Voor de oplossing van het probleem is een hybride stochastische benadering ontwikkeld, bestaande uit een glijdende horizon voor de verwerking van real-time informatie, een chance-constrained programmeringsmodel voor de verwerking van onzekerheid in de transporttijden, een benadering van de vraag van de sportmarkt en een heuristisch preprocessing algoritme dat steeds voor elke tijdstap een oplossing genereert. De experimentele resultaten laten zien dat de resultaten van de hybride stochastische methode sterk worden beinvloed door het betrouwbaarheidsniveau, het aantal scenarios en de lengte van de horizon. Met een gedetailleerde analyse van deze parameters presteert de hybride stochastische methode veel beter dan een deterministische methode onder verschillende scenarios voor het overlegplatform.

- Dynamische, stochastische en gecoordineerde wereldwijde transportplanning (Hoofdstuk 7)

  In dit onderdeel wordt voor wereldwijd synchromodaal transport een dynamische, stochastische en gecoordineerde planning geintroduceerd. Er worden drie benaderingen ontwikkeld voor de behandeling van relaties tussen een globale operator en drie locale operators: de Lagrange relaxatiemethode, de verbeterde Lagrange relaxatiemethode en de alternating direction methode met multiplicatoren. In verband met de complexiteit van de berekeningen in de optimaliseringsmodellen is voor het genereren van oplossingen in elke iteratie een heuristisch preprocessing algoritme ontworpen. De experimentele resultaten laten zien dat met de voorgestelde gedistribueerde benaderingen een oplossing kan worden gevonden voor transportplanningsproblemen

waarin coordinatie tussen verschillende operatoren nodig is voor het bereiken van een gemeenschappelijk doel. Daarbij kan middels de ontworpen heuristiek een afweging worden gemaakt tussen de kwaliteit van de oplossing en de efficientie van de berekeningen.

Samenvattend: In dit proefschrift worden methoden ontwikkeld voor ondersteuning van beslissingen van overlegplatforms voor de planning van synchromodaal transport onder dynamische, stochastische en gedistribueerde omstandigheden. Doel is betere transportplannen met lagere logistieke kosten, minder vertragingen en minder CO2-emissies.

Summary

With the increasing volumes of containers in global trade, efficient global container transport planning becomes more and more important. To improve the competitiveness in global supply chains, stakeholders turn to collaborate with each other at vertical as well as horizontal level, namely synchromodal transportation. Synchromodality is the provision of efficient, effective, and sustainable transport plans for all the shipments involved in an integrated network driven by advanced information technologies. However, the decision-making processes of a global synchromodal transport system is very complex. First, time-dependent travel times caused by traffic congestion need to be considered. Second, a dynamic approach that handles real-time shipment requests in a synchromodal network is required. Third, spot requests received from spot markets are unknown in advance. Fourth, travel time uncertainty is not handled yet for global synchromodal transport networks. Fifth, distributed approaches that stimulate cooperation among multiple stakeholders involved in global container transportation are still missing.

This thesis addresses the above-mentioned challenges with dynamic, stochastic, and coordinated models. Specifically, the following five topics have been studied:

- Synchromodal shipment matching with time-dependent travel times (Chapter 3)

  A hinterland synchromodal shipment matching problem is investigated where a network operator aims to provide optimal matches between shipments with hard time windows and multimodal services with time schedules considering the existence of road traffic congestion. A matching model with time-dependent travel times is formulated to solve the problem. The experiment results show that the matching model with time-dependent travel times has better performance than the model with time-constant travel times in total costs, especially under heavily congested scenarios.

- Dynamic shipment matching (Chapter 4)

  An online synchromodal matching problem is investigated where a platform aims to provide optimal matches between real-time shipment requests and multimodal services. A rolling horizon approach is proposed to handle newly arrived shipment requests. A heuristic algorithm is developed to generate timely solutions at each decision epoch. The experiment results demonstrate the solution accuracy and computational efficiency of the heuristic algorithm in comparison to an exact algorithm. The proposed rolling horizon approach outperforms a greedy approach from practice in total costs under various scenarios of the synchromodal matching platform. With the proposed approaches, the use of barges, trains, and trucks can be managed more

effectively taking into account their impact on logistics cost, delays, and emissions together with different time sensitivities of shipments.

- Dynamic and stochastic shipment matching (Chapter 5)

  A dynamic and stochastic shipment matching problem is investigated under future request uncertainty. An anticipatory approach is proposed to solve the problem which uses a sample average approximation method to approximate expected objective functions and a progressive hedging algorithm to generate solutions at each decision epoch of a rolling horizon framework. Extensive numerical experiments have been conducted to verify the performance of the approach. Compared with a myopic approach, the anticipatory approach is shown to have total cost savings up to 6.5% under the designed instances. The experimental results highlight the benefits of incorporating stochastic information in online decision-making processes of the hinterland synchromodal matching platform.

- Dynamic and stochastic global shipment matching (Chapter 6)

  A dynamic and stochastic global shipment matching problem is investigated under spot request and travel time uncertainties. To solve the problem, a hybrid stochastic approach is developed which consists of a rolling horizon framework that handles real-time information, a chance-constrained programming model that deals with travel time uncertainty, a sample average approximation method that addresses spot request uncertainty, and a preprocessing-based heuristic algorithm that generates timely solutions at each decision epoch. The experimental results indicate that the performance of the hybrid stochastic approach is highly affected by the confidence level, the number of scenarios, and the length of the prediction horizon. With a detailed analysis of these parameters, the hybrid stochastic approach outperforms a deterministic approach and a robust approach under various scenarios of the global synchromodal matching platform.

- Dynamic, stochastic, and coordinated global shipment matching (Chapter 7)

  This topic introduces a dynamic, stochastic, and coordinated shipment matching problem in global synchromodal transportation. Three distributed approaches are developed to handle interconnecting constraints between a global operator and three local operators, including the Lagrangian relaxation method, the augmented Lagrangian relaxation method, and the alternating direction method of multipliers. Due to the computation complexity of the optimization models, a preprocessing-based heuristic algorithm is designed to generate timely solutions at each iteration. The experiment results show that with the proposed distributed approaches, global transport planning that requires coordination among different operators to achieve a common goal can be realized; with the designed heuristic, decision makers can decide on the trade-off between solution quality and computational efficiency.

In short, this thesis develops methodologies to support decision-making processes of synchromodal matching platforms under dynamic, stochastic, and distributed environments, aiming at achieving a better performance of transport plans in logistics costs, delays, and carbon emissions.

Curriculum vitae

Wenjing Guo was born on October 14, 1991 in Qianjiang, Hubei, China. She received her BSc degree in Mathematics and Applied Mathematics from Wuhan Textile University in 2013. In the same year, she started her master study in Traffic and Transportation Engineering at Wuhan University of Technology, under the supervision of Prof. Wenfeng Li. After receiving her MSc degree in 2016, she joined the Department of Maritime Technology and Transport at Delft University of Technology as a PhD researcher. Her PhD project on Dynamic, Stochastic, and Coordinated Optimization for Synchromodal Matching Platforms is funded by the China Scholarship Council, under the supervision of Prof. Rudy R. Negenborn, Dr. Wouter Beelaerts van Blokland, and Dr. Bilge Atasoy.

Her research interests include operations research, intermodal transportation, dynamic optimization, stochastic optimization, and distributed optimization. Her main ambition is to combine advanced approaches with practical applications considering the trend towards sustainability, ecommerce, automation, and digitalization in freight transportation.

Publications

1. W. Guo, B. Atasoy, W. Beelaerts van Blokland, and R. R. Negenborn. Distributed approaches for coordinated global synchromodal shipment matching with travel time uncertainty. Submitted to a journal, 2020.

2. W. Guo, B. Atasoy, W. Beelaerts van Blokland, and R. R. Negenborn. Global synchromodal transport with dynamic and stochastic shipment matching. Submitted to a journal, 2020.

3. W. Guo, B. Atasoy, W. Beelaerts van Blokland, and R. R. Negenborn. Anticipatory approach for dynamic and stochastic shipment matching in hinterland synchromodal transportation. Submitted to a journal, 2020.

4. W. Guo, B. Atasoy, W. Beelaerts van Blokland, and R. R. Negenborn. Dynamic and stochastic shipment matching problem in multimodal transportation. *Transportation Research Record*, 2674(2): 262-273, 2020.

5. W. Guo, B. Atasoy, W. Beelaerts van Blokland, and R. R. Negenborn. A dynamic shipment matching problem in hinterland synchromodal transportation. *Decision Support Systems*, 134:113289, 2020.

6. W. Guo, B. Atasoy, W. Beelaerts van Blokland, and R. R. Negenborn. A coordinated shipment matching problem in global intermodal transportation. Accepted for *the 100th Annual Meeting of the Transportation Research Board*, 2021.

7. W. Guo, B. Atasoy, W. Beelaerts van Blokland, and R. R. Negenborn. A global intermodal shipment matching problem under travel time uncertainty. In *proceedings the 11th International Conference on Computational Logistics*, pages 553-568, Enschede, the Netherlands, 2020.

8. W. Guo, W. Beelaerts van Blokland, and R. R. Negenborn. A many-to-one algorithm to solve a many-to-many matching problem for routing. In *Proceedings of the 9th International Conference on Computational Logistics*, pages 279-294, Salerno, Italy, 2018.

9. W. Guo, W. Beelaerts van Blokland, G. Lodewijks, and R. R. Negenborn. Multi-commodity multi-service matching design for container transportation systems. In *Proceedings of the 97th Annual Meeting of the Transportation Research Board*, Washington, DC, 2018.

10. W. Guo, W. Beelaerts van Blokland, G. Lodewijks. Survey on characteristics and challenges of synchromodal transportation in global cold chains. In *Proceedings of the 8th International Conference on Computational Logistics*, pages 420-434, Southampton, UK, 2017.

TRAIL Thesis Series

The following list contains the most recent dissertations in the TRAIL Thesis Series. For a complete overview of more than 200 titles see the TRAIL website: www.rsTRAIL.nl.
The TRAIL Thesis Series is a series of the Netherlands TRAIL Research School on transport, infrastructure and logistics.

Guo, W., *Dynamic, Stochastic, and Coordinated Optimization for Synchromodal Matching Platforms*, T2020/16, November 2020, TRAIL Thesis Series, the Netherlands

Narayan, J., *Design and Analysis of On-Demand Mobility Systems*, T2020/15, October 2020, TRAIL Thesis Series, the Netherlands

Gong, X., *Using Social Media to Characterise Crowds in City Events for Crowd Management*, T2020/14, September 2020, TRAIL Thesis Series, the Netherlands

Rijal, A., *Managing External Temporal Constraints in Manual Warehouses*, T2020/13, September 2020, TRAIL Thesis Series, the Netherlands

Alonso Gonzalez, M.J., *Demand for Urban Pooled On-Demand Services: Attitudes, preferences and usage*, T2020/12, July 2020, TRAIL Thesis Series, the Netherlands

Alwosheel, A.S.A., *Trustworthy and Explainable Artificial Neural Networks for choice Behaviour Analysis*, T2020/11, July 2020, TRAIL Thesis Series, the Netherlands

Zeng, Q., *A New Composite Indicator of Company Performance Measurement from Economic and Environmental Perspectives for Motor Vehicle Manufacturers*, T2020/10, May 2020, TRAIL Thesis Series, the Netherlands

Mirzaei, M., *Advanced Storage and Retrieval Policies in Automated Warehouses*, T2020/9, April 2020, TRAIL Thesis Series, the Netherlands

Nordhoff, S., *User Acceptance of Automated Vehicles in Public Transport*, T2020/8, April 2020, TRAIL Thesis Series, the Netherlands

Winter, M.K.E., *Providing Public Transport by Self-Driving Vehicles: User preferences, fleet operation, and parking management*, T2020/7, April 2020, TRAIL Thesis Series, the Netherlands

Mullakkal-Babu, F.A., *Modelling Safety Impacts of Automated Driving Systems in Multi-Lane Traffic*, T2020/6, March 2020, TRAIL Thesis Series, the Netherlands

Krishnakumari, P.K., *Multiscale Pattern Recognition of Transport Network Dynamics and*

its Applications: A bird?s eye view on transport, T2020/5, February 2020, TRAIL Thesis Series, the Netherlands

Wolbertus, *Evaluating Electric Vehicle Charging Infrastructure Policies*, T2020/4, February 2020, TRAIL Thesis Series, the Netherlands

Yap, M.D., Measuring, *Predicting and Controlling Disruption Impacts for Urban Public Transport*, T2020/3, February 2020, TRAIL Thesis Series, the Netherlands

Luo, D., *Data-driven Analysis and Modeling of Passenger Flows and Service Networks for Public Transport Systems*, T2020/2, February 2020, TRAIL Thesis Series, the Netherlands

Erp, P.B.C. van, *Relative Flow Data: New opportunities for traffic state estimation*, T2020/1, February 2020, TRAIL Thesis Series, the Netherlands

Zhu, Y., *Passenger-Oriented Timetable Rescheduling in Railway Disruption Management*, T2019/16, December 2019, TRAIL Thesis Series, the Netherlands

Chen, L., *Cooperative Multi-Vessel Systems for Waterborne Transport*, T2019/15, November 2019, TRAIL Thesis Series, the Netherlands

Kerkman, K.E., *Spatial Dependence in Travel Demand Models: Causes, implications, and solutions*, T2019/14, October 2019, TRAIL Thesis Series, the Netherlands

Liang, X., *Planning and Operation of Automated Taxi Systems*, T2019/13, September 2019, TRAIL Thesis Series, the Netherlands

Ton, D., *Unravelling Mode and Route Choice Behaviour of Active Mode Users*, T2019/12, September 2019, TRAIL Thesis Series, the Netherlands

Shu, Y., *Vessel Route Choice Model and Operational Model Based on Optimal Control*, T2019/11, September 2019, TRAIL Thesis Series, the Netherlands

Luan, X., *Traffic Management Optimization of Railway Networks*, T2019/10, July 2019, TRAIL Thesis Series, the Netherlands

Hu, Q., *Container Transport inside the Port Area and to the Hinterland*, T2019/9, July 2019, TRAIL Thesis Series, the Netherlands

Andani, I.G.A., *Toll Roads in Indonesia: transport system, accessibility, spatial and equity impacts, T2019/8, June 2019, TRAIL Thesis Series*, the Netherlands

Ma, W., *Sustainability of Deep Sea Mining Transport Plans*, T2019/7, June 2019, TRAIL Thesis Series, the Netherlands

Alemi, A., *Railway Wheel Defect Identification*, T2019/6, January 2019, TRAIL Thesis Series, the Netherlands

Liao, F., *Consumers, Business Models and Electric Vehicles*, T2019/5, May 2019, TRAIL Thesis Series, the Netherlands

Tamminga, G., *A Novel Design of the Transport Infrastructure for Traffic Simulation Models*, T2019/4, March 2019, TRAIL Thesis Series, the Netherlands

Lin, X., *Controlled Perishable Goods Logistics: Real-time coordination for fresher products*, T2019/3, January 2019, TRAIL Thesis Series, the Netherlands